The Use of Translational Sub-molecular Motion in the Synthesis of Novel [2]Rotaxanes

By

Jeffrey S. Hannam

Degree of Doctor of Philosophy

Department of Chemistry

University of Edinburgh

March 2004

For my Parents John and Rita

Table of Contents

List of Figures

2.00 Å, 162.1°.

HN11/O40A–HN11A 1.92 Å, 156.4°.

List of Schemes

containing up to fourteen methylene groups between the two templating sites.

Scheme 4.1. Schematic preparation of an otherwise difficult or impossible to obtain rotaxane using a second generation mechanically interlocking auxiliary: (a) attach substrate to auxiliary; (b) formation of rotaxane about template; (c) isomerization ($E{\rightarrow}Z$); (d) open gate; (e) shuttle macrocycle from template to substrate; (f) close gate; (g) cleave auxiliary.

Scheme 4.2. Synthesis of rotaxane **1**: (a) 1-(3-dimethylaminopropyl)-3-ethyl-carbodiimide hydrochloride, 4-DMAP, CH_2Cl_2, 93 %; (b) isophthaloyl dichloride, *p*-xylylenediamine, Et_3N, $CHCl_3$, 62 %; (c) hυ 254nm, 20 min, 49 %; (d) *tetra*-butylammonium fluoride, THF, 98 %; (e) *tert*-butylphenylsilyl chloride, imidazole, 4-DMAP, DMSO, 78 %; (f) 3,3-diphenylpropanol, potassium *tert*-butoxide (5 mol %), 81 %.

Scheme 4.3. Preparation of Rotaxane **1**. a) benzyl chloroformate, Et_3N, CH_2Cl_2, 70 %; b) *tert*-butyldiphenysilyl chloride, imidazole, 4-DMAP, CH_2Cl_2, 91%; c) $NaBH_4$, LiCl, MeOH, THF, 99 %; d) 5 % Pd/C, NH_4CHO, MeOH, 98 %; e) 2,2-diphenylethylamine, EDCI, HOBt, Et_3N, CH_2Cl_2, 93 %; f) NaOH, THF, H_2O, 98 %; g) **S4**, EDCI, HOBt, Et_3N, CH_2Cl_2, 93 %; h) 3,5-di-*tert*-butylphenol, K_2CO_3, NaI, 2-butanone, 91 %; i) NaOH, EtOH, H_2O, 96 %; j) **3**, EDCI, DMAP, CH_2Cl_2, 87 %; k) isophthaloyl dichloride, *p*-xylylene diamine, Et_3N, $CHCl_3$, 62 %; l) hυ 254nm, 20 min, 49 %; m) TBAF, THF, 98 %; n) *tert*-butylphenylsilyl chloride, imidazole, 4-DMAP, DMSO, 74 %; o) 3,3-diphenylpropanol, potassium *tert*-butoxide (5 mol %), 81 %.. Full experimental procedures are described below.

List of Tables

Abstract

This thesis is concerned with the synthesis of the class of interlocked molecular architectures called rotaxanes. Currently rotaxanes can be synthesized in high yields by exploiting noncovalent interactions between reacting fragments. The success of these supramolecular approaches are detailed in Chapter 1 and are contrasted with early attempts at their synthesis, which were low yielding. The novel properties of interlocked molecular architectures are also elaborated, emphasizing their potential as molecular level machines. Chapter 2 contains a detailed study of the hydrogen bond-directed synthesis of benzylic amide macrocycle-containing [2]rotaxanes. This task is performed by structural variation of the linear thread component in the standard five-component clipping reaction. The introduction of flexibility, non-optimal binding motifs, and the removal of key noncovalent interactions provide an insight into this remarkable process. In addition to analysis of the resulting yields of the [2]rotaxanes, the interlocked products are characterized by X-ray crystallography and ^{1}H NMR spectroscopy affording further insights into the specific structural requirements needed for subsequent interlocking.

After a detailed study of this hydrogen bond-directed interlocking process, in Chapter 3 we synthesize a rotaxane, in high yield, whose components bear no formal recognition elements. To enable this task, we exploit solvent dependent translational isomerism observed in peptide-based amphiphilic rotaxanes in the form of a so-called mechanically interlocking auxiliary (MIA). The MIA is used to mechanically interlock a macrocycle around a suitable template (driven by the hydrogen bond-directed process studied in Chapter 2), followed by translation of the ring to a position over the desired substrate and, finally, cleavage of the auxiliary to leave a rotaxane with no designed noncovalent interactions between macrocycle and thread. The use of ^{1}H NMR spectroscopy allows us to characterize the products by indicating the relative position of the macrocycle over the thread component. Analysis of the final product by X-ray crystallography shows the consequences forcing such unnatural spatial arrangements on submolecular fragments.

In Chapter 4 we extend the concept of a MIA by demonstrating the function of a second-generation MIA based on a fumaramide template. The advantages of the

fumaramide-based MIA are seen in the increased yield obtained for the benzylic amide-containing macrocycle rotaxane, but are slightly offset by the inclusion of a necessary photoisomerization step. Again, ^{1}H NMR spectroscopy is used to determine the position of the macrocycle on the thread component in the rotaxanes synthesized.

Declaration

The scientific work described in this thesis was carried out in the Department of Chemistry at University of Warwick between October 1999 and September 2001 and in the Department of Chemistry at University of Edinburgh between October 2001 and December 2003. Unless otherwise stated, it is the work of the author and has not been submitted in whole or in support of an application for another degree or qualification of this or any other University or institute of learning.

Acknowledgements

List of Abbreviations

Å	Angstrom
δ	chemical shift
$\Delta G°$	Gibbs energy
ATP	adenosine triphosphate
Boc	butyloxycarbonyl
Calcd.	calculated
CD	Circular Dichroism
$CDCl_3$	deutero-chloroform
CD_3CN	deutero-acetonitrile
COSY	Correlation Spectroscopy
CPK	Corey-Pauling-Koltun
DB24C8	dibenzo-24-crown-8
DEAD	diethyldiazodicarboxylate
DIBAL	diisobutylaluminium hydride
4-DMAP	4-dimethylaminopyridine
DMF	*N,N'*-dimethylformamide
DMSO	dimethylsulphoxide
E	*trans* isomer
EDCI	1-(3-dimethylaminopropyl)-3-ethyl-carbodiimide hydrochloride
EDTA	ethylenediamine tetraacetic acid
en	ethylenediamine
equiv	equivalents
Et_3N	triethylamine
EtOH	ethanol
FAB	Fast Atom Bombardment
g	grams
h	hours
HMBC	Heteronuclear Multiple-Bond Correlation
HMQC	Heteronuclear Multiple-Quantum Correlation
HOBt	1-hydroxybenzotriazole

HRMS	High Resolution Mass Spectrometry
LRMS	Low Resolution Mass Spectrometry
IR	Infra Red
k	rate constant
m-CPBA	*meta*-chloroperoxy benzoic acid
m-NBA	*meta*-nitrobenzoic acid
MeOH	methanol
MeCN	acetonitrile
mg	milligram
MHz	Mega hertz
min	minutes
mL	millilitres
mmol	millimole
m.p.	melting point
m/z	Mass-to-charge ratio
nm	nanometres
NMR	Nuclear Magnetic Resonance
PhSeH	benzeneselenol
ppm	part per million
RNA	ribonucleic acid
TBAF	tetrabutylammonium fluoride
THF	tetrahydrofuran
THIOG	thioglycerol
THYME	tetrahydroxymethylethylene
TFA	trifluoroacetic acid
TLC	Thin Layer Chromatography
TTF	tetrathiafulvalene
VT	Variable Temperature
Z	*cis* isomer

Note: When a standard chemical formula (i.e., one containing symbols only representing chemical elements and not functional group abbreviations) is used to describe a compound in this Thesis, the formula is not reproduced in the table above.

Comments on Presentation of Data

All the melting points (m.p.) were determined using a Electrothermal 9100 melting point apparatus and are uncorrected. ^1H (400 MHz) and ^{13}C (100 MHz) NMR spectra were recorded on a Bruker DPX 400 MHz spectrometer using dilute solution in $CDCl_3$, d_6-DMSO, $C_2D_2Cl_4$ without any internal reference and referenced to the residual solvent signal as internal standard ($CHCl_3$ at $\delta H = 7.27$, s; $\delta C = 77.0$, t; d_6-DMSO at $\delta H = 2.52$, m; $\delta C = 39.8$, m; $C_2D_2Cl_4$ at $\delta H = 5.96$, s; $\delta C = 78.0$, t) and the chemical shifts are reported in part per million (ppm) from low to high field. All the ^1H and ^{13}C NMR spectra were recorded at 298K unless otherwise stated. The FIDs were processed by the software WinNMR. ^1H NMR are reported as follows: br = broad, s = singlet, d = doublet, dd = doublet of doublets, t = triplet, dt doublet of triplets, q = quartet, m = multiplet,. ^{13}C NMR are reported as follows: Ar$\underline{C}$ (ipso) = quaternary aromatic, Ar$\underline{C}$H = non quaternary aromatic, s = quaternary carbon-C, d = $\underline{C}$H, t = $\underline{C}$H$_2$, q = $\underline{C}$H$_3$. H-H COSY, HMQC, HMBC, 2D were also recorded for some compounds to enable more detailed assignment of ^1H and ^{13}C signals. Column chromatography was carried out using Kiesegel C60 (Merck) as stationary phase. TLC detection was performed on silica gel plates (0.25 mm thick, 60 F254, Merck, Germany). The TLC plates were observed under UV light or visualized using 8% sulfuric acid. Mass spectrometry and HRMS analyses were performed by the University of Edinburgh mass spectrometry service using fast atom bombardment (FAB) from m-nitrobenzyl alcohol matrix unless otherwise stated. Elemental analyses were performed by the University of Warwick elemental analysis service. Photo-isomerizations were carried out in quartz vessels using a multilamp photoreactor model MLU18 manufactured by Photochemical Reactors Ltd, Reading UK. Reagents and anhydrous solvents used for the reactions were purchased from Aldrich and were in general used without further purification. Isophthaloyl dichloride was routinely recrystallized from hexane and p-xylylenediamine was distilled under reduced pressure. Anhydrous chloroform used for the rotaxane formation reactions was stabilized with amylenes, not ethanol. For the presentation of crystal structures the carbon atoms of the macrocycle are shown in blue and those of the thread in yellow;

oxygen atoms are red, nitrogen atoms dark blue, sulphur in green and amide hydrogen atoms are white. Non-amide hydrogen atoms are omitted for clarity.

CHAPTER ONE

The Synthesis of Interlocked Molecular Architectures and the Supramolecular Age

"What I cannot create I do not understand"
Richard P. Feynman

1.0 Introduction

The natural world is a rich source of primary and secondary metabolites whose chemical structures engage the minds and challenge the skills of the chemists involved in their synthesis.[1] In addition to this, the synthesis of unnatural products with the hope of improving the quality of life for humankind, e.g., pharmaceuticals[2] are also desired goals within the framework of synthetic chemistry. The ability to successfully pursue any of these endeavours is dependent on the synthetic and analytical methods available. This is true of research into interlocked molecular architectures and early efforts were characterized by ingenious approaches limited by the inadequate synthetic methodology available. This early research was also driven by theoretical considerations of the arrangement and relative spatial orientation of interlocked and intertwined rings, which is often referred to as topological stereochemistry.[3]

The explosion in research activity relating to interlocked architectures has occurred ostensibly in the past 15-20 years and has resulted in access to structures hitherto confined to the imaginations of synthetic chemists.[4] This is due, primarily to the development of supramolecular chemistry, in the late 1970's, which Lehn[5] described as the "chemistry of molecular assemblies and of the intermolecular bond". These seminal advances were recognized in 1987 with the award of the Nobel prize to Lehn,[6] Cram[7] and Pedersen.[8] Supramolecular chemistry can trace its roots however to concepts discussed at the turn of the century, such as Paul Ehrlich's receptor idea, Alfred Werner's coordination chemistry and Emil Fischer's lock-and-key principle. In the interim period a greater understanding of the function and mechanisms of biological processes and their reliance on noncovalent forces and self-assembly phenomena has inspired chemists to transfer these principles to the synthetic arena. Hence, the development of host-guest chemistry, molecular recognition,[9] self-assembly[10] and template-directed synthesis[11] have all shaped the highly interdisciplinary field we call supramolecular chemistry. These factors, along with concomitant advances in analytical chemistry and synthetic methodology have allowed the preparation, characterisation and analysis of interlocked molecular architectures and their associated non-interlocked precursors.

This introductory chapter aims to detail the syntheses of interlocked molecular architectures from early attempts to those invoking supramolecular assistance in their construction. The unique properties that are bestowed on such molecules as a result of interlocking are also emphasized and highlight the transition of interlocked molecular architectures from laboratory curiosities to forerunners in the burgeoning field of smart materials and molecular-scale devices.[12,13]

1.1 Nomenclature and Terminology Associated with Interlocked Molecular Architectures

Before the beginning of our journey through of the world of interlocked molecular architectures, it is sensible to detail some of the terminology associated with interlocked molecular architectures and their synthesis.
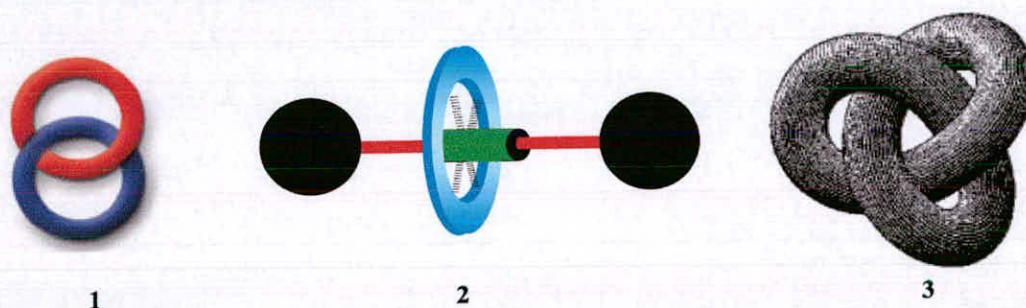
Figure 1.1. Cartoon representations of commonly encountered interlocked molecular architectures

In Figure 1.1 the three most common interlocked molecular architectures are depicted in cartoon format. The first is the catenane comprised of two or more interlocked rings, which derives its name from the Latin *catena* meaning chain. The rings comprising a catenane are inseparable unless a covalent bond is broken. Rotaxanes are comprised of a macrocyclic component encircling a dumbbell-shaped molecule in the form of a 'linear' thread with two bulky stopper groups that maintain the macrocyclic component on the thread moiety. The name rotaxane is again derived from the Latin *rota* meaning wheel, and *axis* meaning axle. The nomenclature employed for these systems involves placing (in square brackets) the number of interlocked components involved in the compound in question. Hence, a [2]catenane **1** is comprised of two interlocked macrocycles and a [2]rotaxane **2** is

comprised of a dumbbell component and a macrocycle. The remaining interlocked architecture in Figure 1.1 is a knotted structure, named a trefoil knot **3** as it has three crossing points within its structure. The nomenclature associated with knots and other more complicated molecular entanglements is more nebulous and will not be discussed any further here.[14,15]
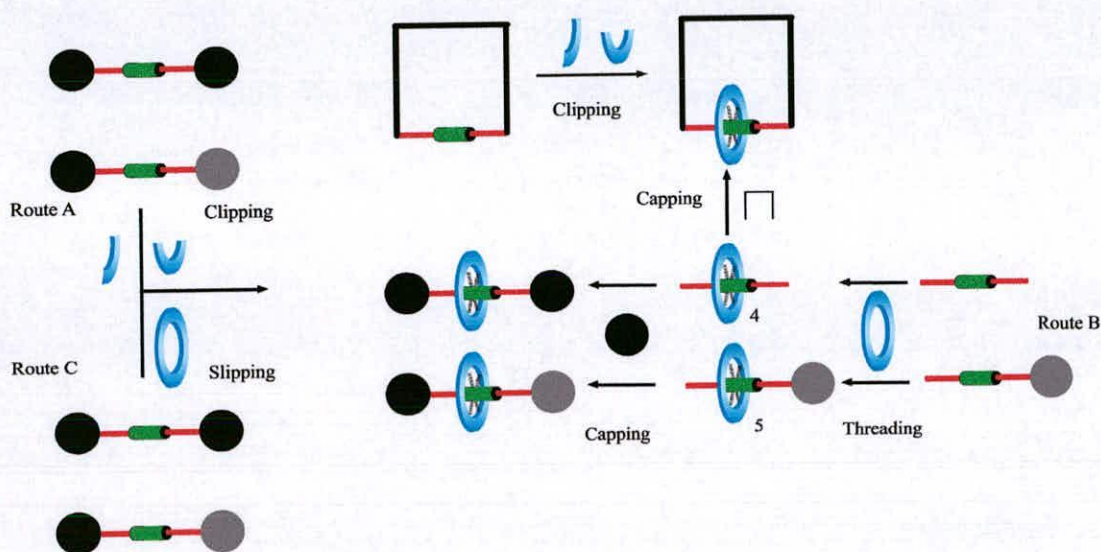
Scheme 1.1. Possible synthetic strategies towards interlocked molecular architectures.

In strategic terms there are three general methods for synthesizing interlocked molecular architectures. (Scheme 1.1) Route A involves the elaboration of a macrocycle around a preformed dumbbell shaped thread molecule and is called *clipping*. Route B relies on the threading of a macrocycle on a linear component to form a pseudorotaxane **4**[16] or semirotaxane **5**, subsequent reaction with a bulky stopper group affords rotaxane and is called *capping*. Route C involves the *slipping* of a macrocycle over a preformed dumbbell at elevated temperature (or pressure). A key criterion for success in this approach is that the stoppers and macrocycle are of complementary sizes for the given system. Catenanes can be assembled through dual capping of a pseudorotaxane intermediate **4** or clipping around a preformed macrocycle. Each of the principles associated with the synthesis of interlocked molecular architectures will be emphasised during this overview of the world of catenanes, rotaxanes and knots.

1.2 Early Attempts at the Chemical Synthesis of Interlocked Molecular Architectures

1.2.1 Statistical Approaches

Although mentioned as long ago as 1912 by Willtstäter, it was not until the 1960's that successful syntheses were published. In 1960 Wasserman[17] reported the successful synthesis of a [2]catenane **6** (Scheme 1.2) based on what has become known as the 'statistical' approach. This relies on the chance *threading* of a macrocyclic precursor through another macrocycle (to form a pseudorotaxane) and subsequent cyclisation to form the catenane product. In this example, the preformed macrocycle was in the form of a pentadeuterated C_{34} cycloalkane **7**. An acyloin condensation of C_{34} diester in the presence of the pentadeuterated macrocycle formed the interlocked catenane in less than 1 %. The interlocked nature of the catenane was determined by cleavage of the acyloin ring to obtain pentadeuterated macrocycle **7**, which was argued could only be as a result of prior interlocking. The very low yield of Wassermann's synthesis is an indication of the inherent problems with statistical approaches, in that there is no driving force for the formation of intermediary pseudorotaxanes.
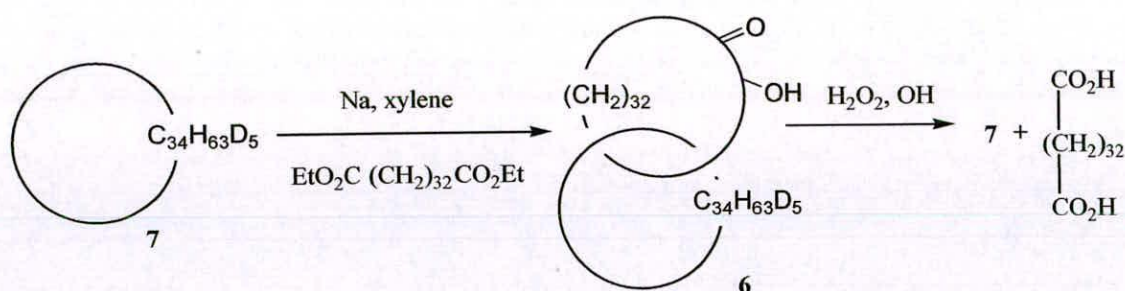
Scheme 1.2. The preparation of the first [2]catenane **6** by the statistical approach

In 1967 Harrison and Harrison reported the first synthesis of a [2]rotaxane **8** (called Hooplane by the authors).[18] An acyloin macrocycle was attached *via* a succinic acid spacer to a solid support resin contained within a column and repeatedly treated with trityl chloride and 1,10-decandiol (Scheme 1.3). The rings were cleaved from the resin and the rotaxane **8** was isolated in 6 % yield, after purification. Again, the

interlocked nature of the isolated rotaxane was determined by IR spectroscopy, in combination with degradation studies. Harrison in later studies reported the *slipping* of variable-sized hydrocarbon macrocycles onto preformed hydrocarbon linear threads with trityl stoppers using both thermal[19] and reversible bond formation.[20] The maximum yield obtained by these methods was 1.2 %.
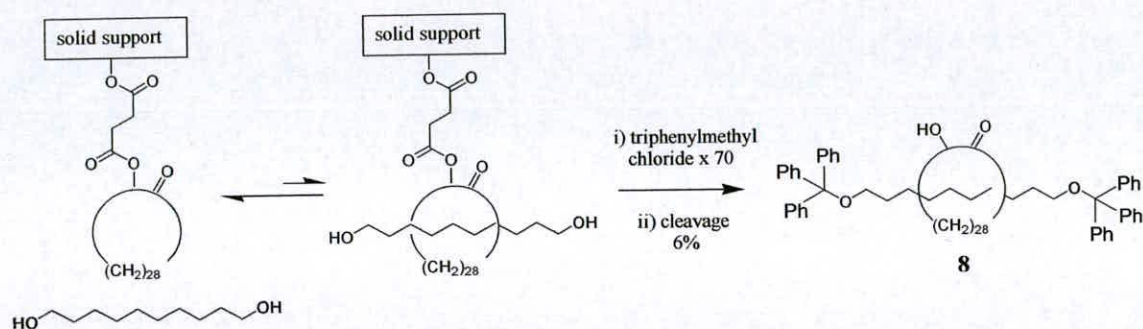
Scheme 1.3. First synthesis of a [2]rotaxane by tethering to a solid support

Several research groups have reported the detection of catenanes by the so-called Möbius strip approach in conjunction with olefin metathesis.[21] This observation was questioned by Bickelhaupt and co-workers who showed the mechanism invoked in the earlier studies was incorrect and the generally accepted mechanism no longer support the formation of catenanes.[22] Walba and co-workers have successfully applied the Möbius strip approach with tetrahydroxymethylethylene (THYME) polyethers to prepare a number of interlocked molecular architectures and also the formation of the first molecular Möbius strip.[23]

1.2.2 Covalent-Directed Approaches in the Synthesis of Interlocked Molecular Architectures

Another strategy to access interlocked molecular architectures is the use of so-called covalent directed methods. The key strategic element in directed syntheses is the use of auxiliary covalent bonds to orientate reacting fragments, such that interlocking is promoted. The directed approach was pioneered by Schill in the 1960s and he has made a number of different interlocked architectures by this method.[24] The first catenane synthesis *via* directed methods was reported in 1964 by Schill and

Lüttringhaus (Scheme 1.4).[25] The cyclisaton of key intermediate **9** *via* intramolecular alkylation of the amine is constrained by the tetrahedral geometry of the acetal precursor **9**. Subsequent acetal hydrolysis and cleavage of the aryl-nitrogen bond afforded the [2]catenane **10**.
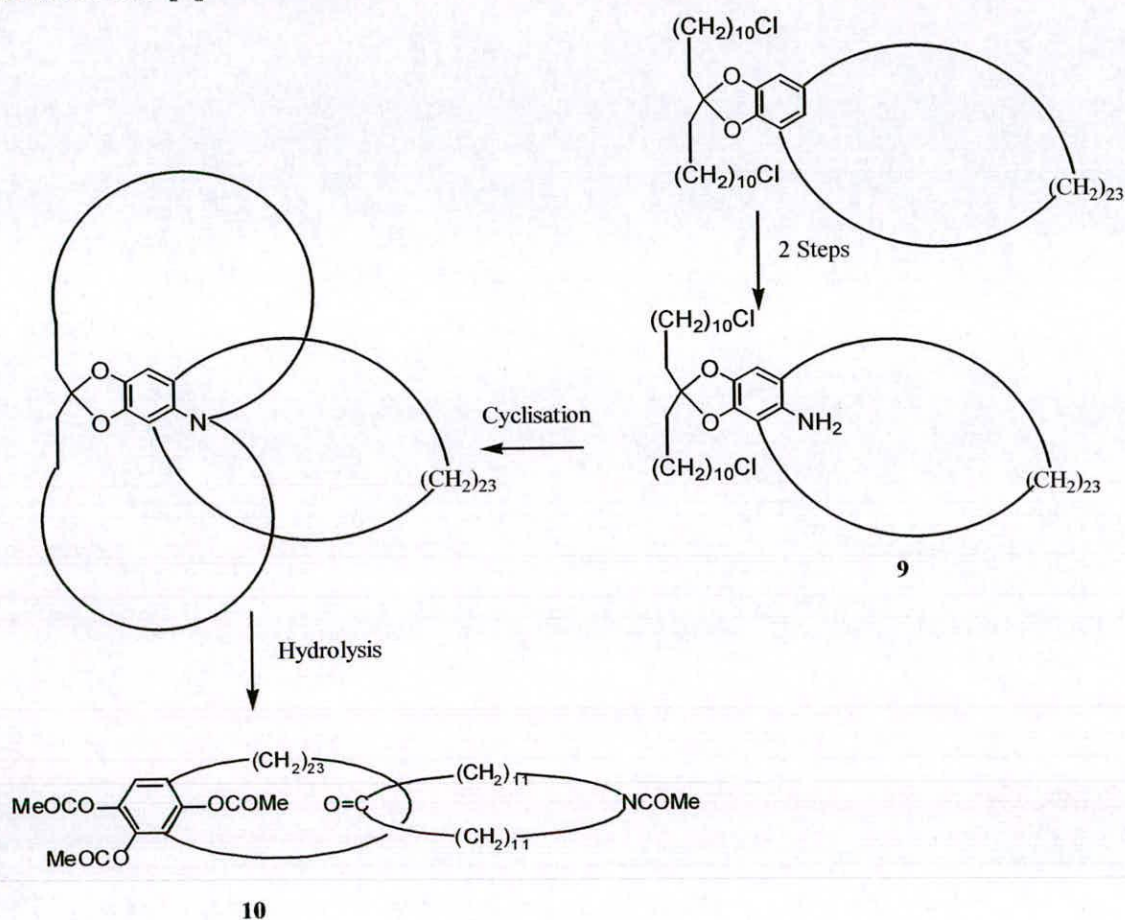
Scheme 1.4. The synthesis of a [2]catenane by covalent-directed methods

The inherent problem with covalent-directed approaches is the synthetic sequences are characterised by many technically demanding steps and as a consequence, low overall yields. The covalent directed approach is an ingenious synthetic strategy limited by the lack of thermodynamic driving force promoting the key cyclisation reactions. This thermodynamic driving force was later provided by invoking noncovalent interactions between reacting fragments, which will be detailed in the remainder of this introductory chapter.

1.3 The Synthesis of Interlocked Molecular Architectures Invoking Supramolecular Assistance

1.3.1 The Synthesis of Interlocked Molecular Architectures Using a Transition Metal Template

The ability of transition metals to predispose ligands in a predictable spatial orientation during crucial bond formations has led to their widespread use as templates in the synthesis of macrocyclic products.[26] The discovery that transition metals act as templates in the synthesis of macrocycles was first reported by Curtis in the 1961.[27] This discovery sparked a great interest in metals as templates in the rational synthesis of macrocycles, which was pioneered in the main by the efforts of Busch and co-workers.[28] Many of the examples invoking transition metal 'templates' are often two-dimensional in their *modus operandi*, however there are comparatively fewer examples whereby the transitional metal positions the ligands in a truly three-dimensional manner.[29]

Although mooted in the chemical literature for many years,[30] Sauvage and Dietrich-Buchecker provided the key breakthrough in using transition metal/ organic ligand systems to access interlocked molecular architectures.[31,32] The seminal example relies on the psuedo-tetrahedral geometry of Cu^{I} centres with two bidentate phenanthroline ligands which are held in a mutually orthogonal manner as complex **11** as shown in Scheme 1.5.[33] Two approaches were attempted to afford the desired catenate. Firstly a preformed macrocycle **12** containing one bidentate phenanthroline ligand was treated with $Cu(MeCN)_4BF_4$ and a diphenolic phenanthroline ligand **13** to afford complex **14** (route A). This was then reacted with pentaethyleneglycol diiodide to provide the requisite catenate **15** in 42 % yield. The second and more direct approach involved treating the *bis*-phenanthroline complex **11**, with pentaethyleneglycol dibromibe to give catenate **15** in a 27 % yield (route B). This direct approach became the method of choice for the synthesis of such symmetrical systems. The word catenate was chosen to name such compounds as it indicates the presence of a transition metal ion complex.

7
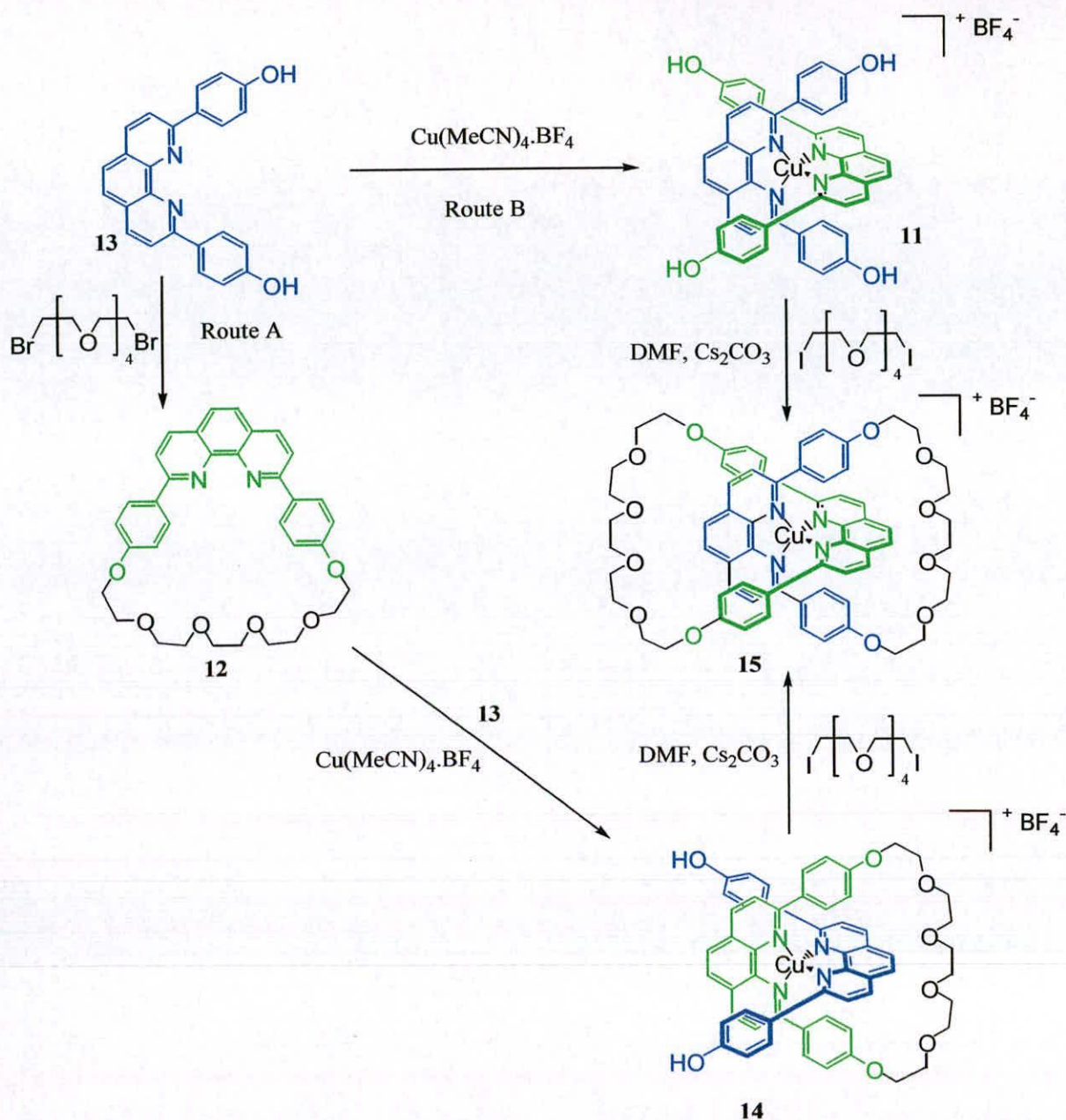
Scheme 1.5. The synthesis of Cu^I-based catenate **15**.

The metal can be removed by treatment of catenate **15** with KCN to give the demetallated catenate **16** (Scheme 1.6), which according to convention is called a catenand.[34] The consequences of demetallation are profound. In the presence of the metal the catenate provides a compact structure through coordination to the copper and π-π stacking between units. Removal of the metal causes the two rings to move in such a way to minimise unfavourable interactions between the phenanthroline

units and provides a much more flexible overall structure. Interestingly such catenates are remarkably stable to demetallation as compared to analogous non-interlocked ligand systems. This can be attributed to the topological confinement of the ligating moieties within the interlocked superstructure and this phenomena is the called the catenand effect.[35]
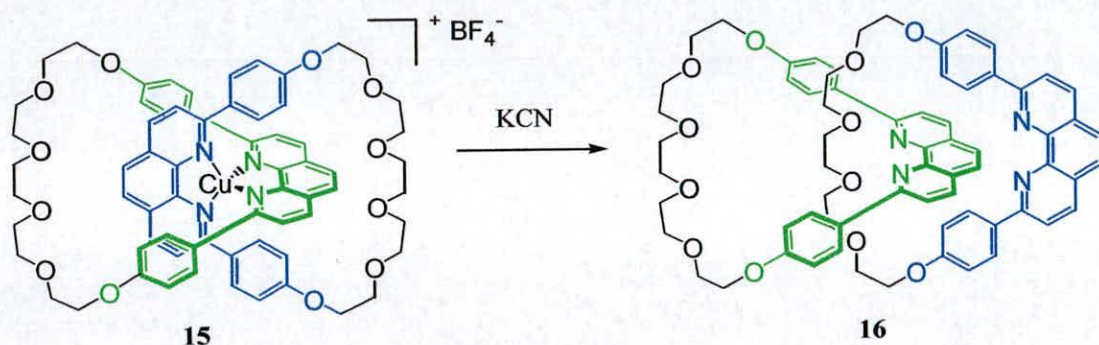
Scheme 1.6. Demetallation of catenate **15** to afford corresponding catenand **16**

In the late 1990's ring-closing alkene metathesis was used by Sauvage and Grubbs to obtain [2]catenates in high yields.[36] Although alkene metathesis was used in one of the earliest syntheses of catenanes,[21] Grubbs had recently developed a isolable catalyst which had high activity and an excellent range of functional group tolerance.[37] Again the Cu^I/ phenanthroline transition metal/ ligand system was used to construct the central core of the catenate system, but incorporating terminal alkene units in the pendant arms. Thus, complex **17** was treated with Grubbs' catalyst to give the corresponding [2]catenate **18** in an excellent 92 % yield.
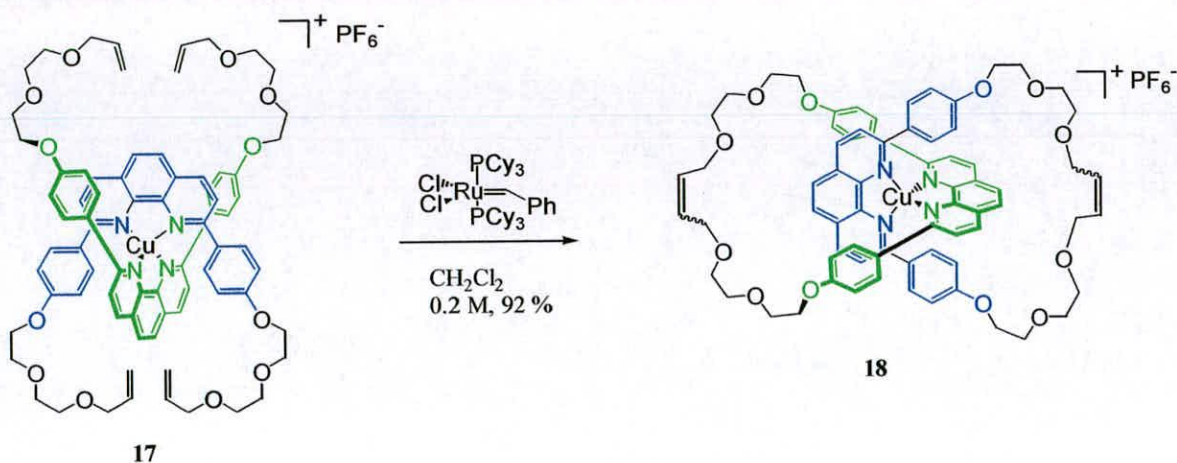
Scheme 1.7. High-yielding synthesis of Cu^I catenates by ring closing metathesis

The basic catenate assembly system of Sauvage, based on a tetrahedral Cu[I] metal template/ phenanthroline ligand system has remained largely unchanged since its inception. However, in 2001, Leigh and co workers reported a simple, general and efficient synthesis of catenates with octahedral coordination geometry.[38] The ligating moieties were based on benzylic 2,6-diiminopyridine pioneered by Busch and co-workers.[39] Treatment of a range of metal-diiminopyridine octahedral complexes **19a-d** were treated with Grubbs' catalyst afforded catenates **20a-d** in good to excellent yields. Demetallation of the octahedral catenates **20a-d** initially proved problematic as treatment with an excess of EDTA resulted in recovery of starting materials. This illustrates an exceptional kinetic stability inferred by the interlocked nature of the molecule. This problem was circumvented by reduction of the imines with $NaBH_4$ followed by treatment with EDTA to give amine-based catenand **21**.

19a M = Mn, X = ClO_4
19b M = Zn, X = BPh_4
19c M = Cd, X = ClO_4
19d M = Co, X = BPh_4

1 $NaBH_4$, EtOH

2 EDTA, disodium salt

78 %

21

20a M = Mn, X = ClO_4, 63 %
20b M = Zn, X = BPh_4, 81 %
20c M = Cd, X = ClO_4, 70 %
20d M = Co, X = BPh_4, 41 %
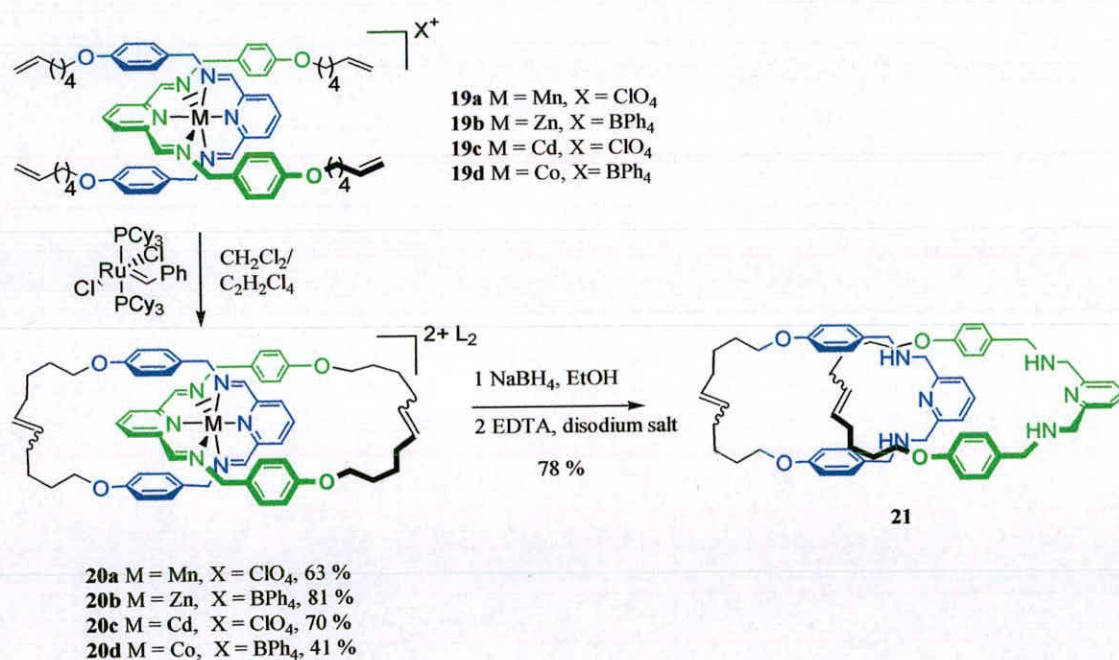
Scheme 1.8. Synthesis of octahedral catenates by ring closing metathesis.

The first synthesis of a rotaxane based on transition metal ion/ ligand interactions was reported by Gibson and co-workers who elaborated on the Sauvage phenanthroline/ Cu[I] core.[40] The pseudorotaxane precursor **14** was treated with a

trityl-terminated alkyl halide and subsequently demetallated with an acidic resin to give **22** in a 42 % yield.
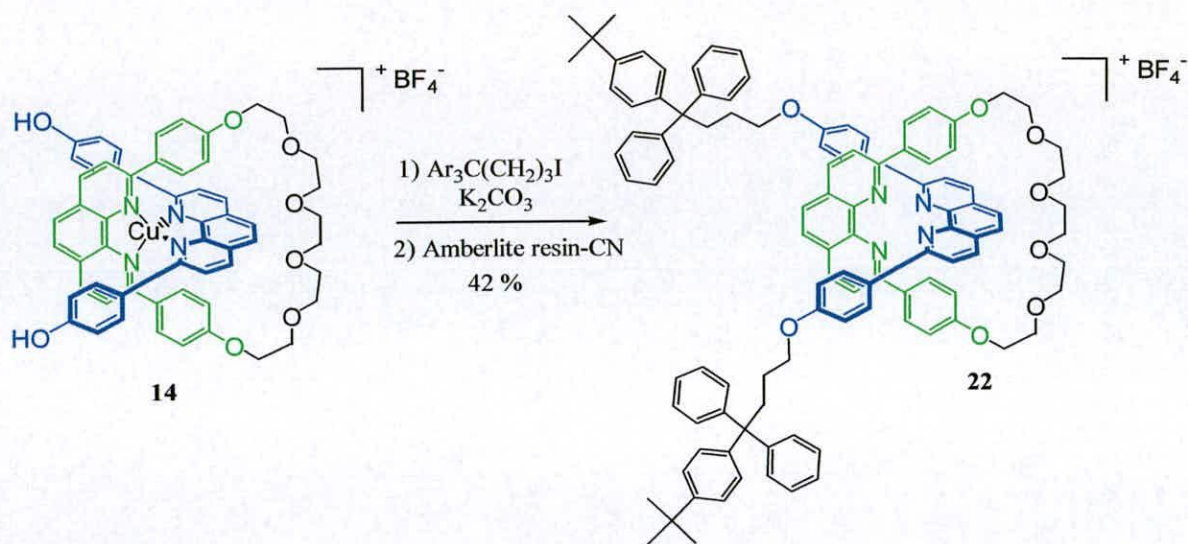
Scheme 1.9. Synthesis of a [2]rotaxane using a Cu^I template

Sauvage in contemporaneous studies made a series of transition metal-based rotaxanes incorporating porphyrins as stoppers in attempts to mimic the array of tetrapyrrolic chromophores, found at the heart of bacterial photosynthetic reaction centres.[41]

The synthesis of molecular knots has been most successfully achieved through the use of transition metal ions. Indeed, strategies towards the synthesis of knots, using transition metal ions as anchors were discussed in the literature before the fruition of interlocked molecular architectures.[42]

The key breakthrough was in 1989, where Sauvage and Dietrich-Bucheker synthesized a trefoil knot, based on the ubiquitous Cu^I/ phenanthroline system.[43] The original system involved linking of two phenanthroline units by a C$_4$ alkyl chain linker. This ligand successfully formed a double helical complex **23a** containing two Cu^I centres, along with a large proportion of undesired complex containing only one copper centre. The cyclisation of the double helical precursor formed a knotted complex **24a** in a low 3 % yield which was finally confirmed as the trefoil knot on analysis of the X-ray crystal structure.[44] The spacer group **X** (Scheme 1.10) between the two phenanthroline units proved crucial in the resulting yield of the trefoil knot. When the knot precursor contained a C$_6$ alkyl chain **23b** the resulting knot **24b** was

afforded in 8 % yield.[45] However, in later studies a 1,3-phenylene linker in the thread **23c** afforded the corresponding knot **24c** in 29 % yield.[46] In 1997, the combined use of the 1,3-phenylene spacer and ring closing alkene metathesis (with Grubbs' catalyst) gave an excellent 74 % yield of the requisite trefoil knot.[47,48]

23a X =(CH$_2$)$_4$
23b X =(CH$_2$)$_6$
23c X=1,3-phenylene

Cs$_2$CO$_3$, DMF, 60°C
ICH$_2$(CH$_2$OCH$_2$)$_5$CH$_2$I

24a X =(CH$_2$)$_4$ 3%
24b X =(CH$_2$)$_6$ 8%
24c X =1,3-phenylene 29%
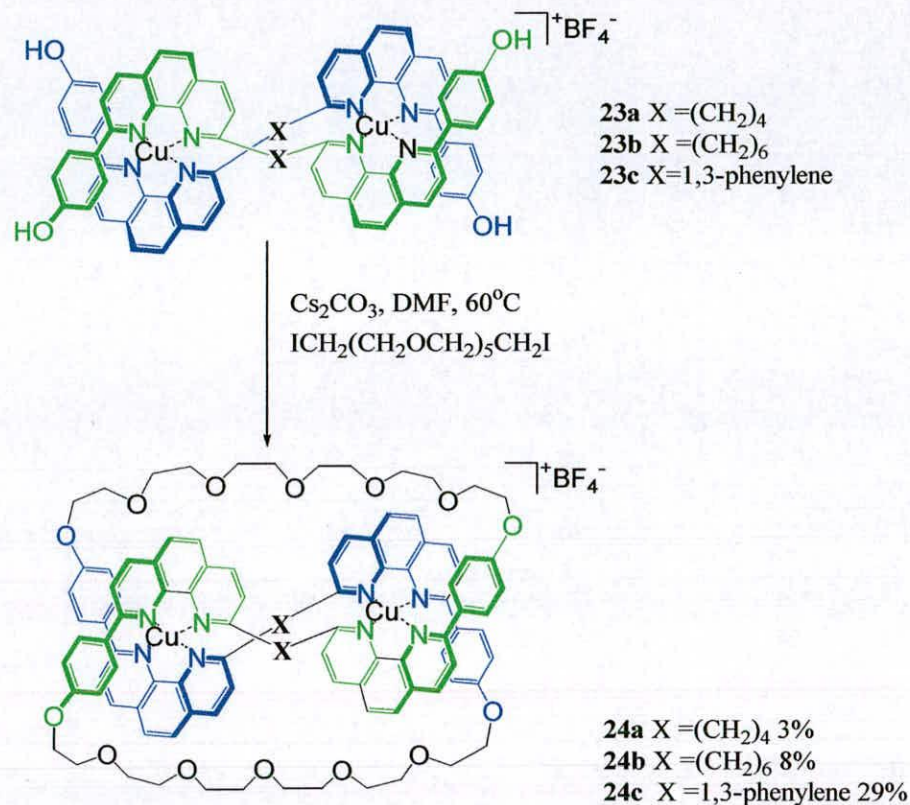
Scheme 1.10. The synthesis of trefoil knots assembled with a Cu^I template.

In 1994, Fujita and co-workers reported the synthesis of a [2]catenane containing kinetically labile palladium-pyridine coordination bonds (Scheme 1.11).[49] The formation of the [2]catenane was discovered in attempts to assemble coordination macrocycles. A mixture of ligand **25** and Pd(en)(NO$_3$)$_2$ in solution forms a rapid equilibrium between macrocycle **26a** and [2]catenane **27a** (Scheme 1.11). The driving force for the formation of the interlocked products derives from the efficient contact between the aromatic rings of the two macrocycles, most efficiently observed in aqueous solutions. The kinetically labile coordination bonds facilitate conversion of the two species *via* a proposed Möbius strip mechanism.[50]
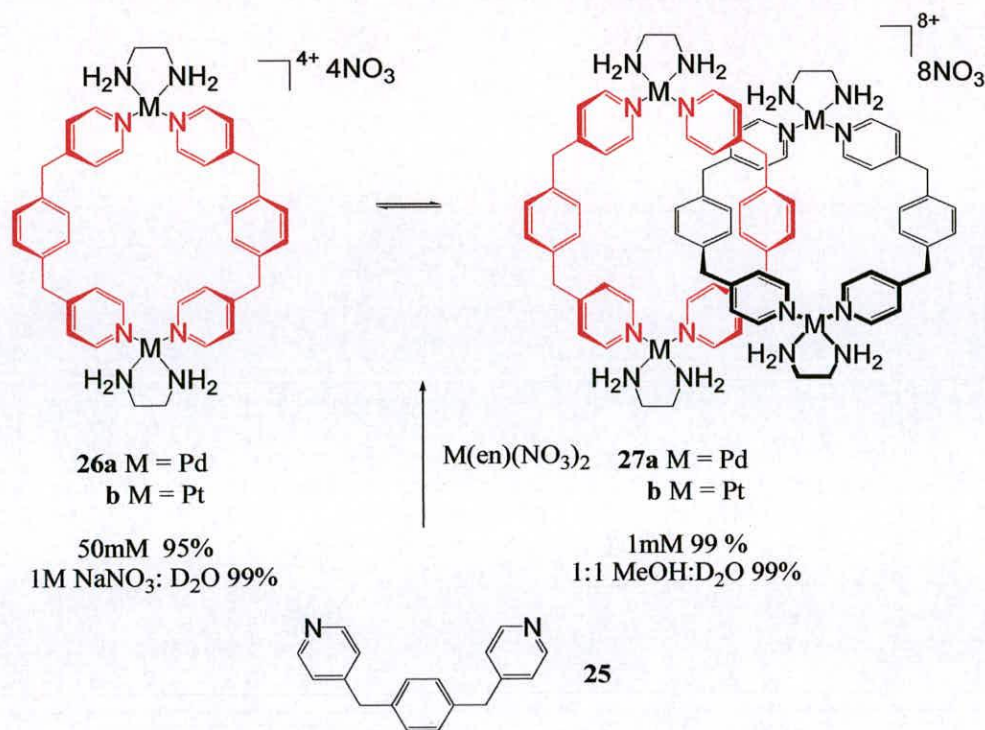
Scheme 1.11. The synthesis of "magic rings" containing palladium and platinum.

The product equilibrium between macrocycle **26a** and catenane **27a** can be perturbed by solvent polarity and concentration. For example, at high concentrations the catenane is the favoured product (99: 1), whereas at low concentrations the macrocycle is favoured. However, in polar solvents (D_2O: $NaNO_3$), even at low concentrations, the interlocked product is favoured as it minimises the hydrophobic interaction between the pyridine ligands and the solvent. In contrast, the ratio of **26a** decreases in a less polar medium (D_2O: CD_3OD).

Fujita has also reported the synthesis of a corresponding platinum analogue of the palladium system (Scheme 1.11).[51] The mixing of ligand **25** and $Pt(en)(NO_3)_2$ initially forms macrocycle **26b** and is not in equilibrium with other structures. This is because the coordination bonds between platinum-pyridine are much less labile than those of palladium. Upon addition of $NaNO_3$ and heating at 100 °C an equilibrium between [2]catenane **27b** and macrocycle **26b** arises strongly favouring the interlocked product. After cooling to room temperature and removing $NaNO_3$ the equilibrium favouring catenane is "locked". Due to the analogy between the locking

and unlocking of the equilibrium process Fujita called this platinum-based system a "molecular lock".

In 2000, Jeong and co-workers reported the self-assembly of a rotaxane *via* reversible coordinate bonds.[52] The ring component of the [2]rotaxane **28** is composed of macrocycle **29,** which is derived from reaction of acyclic pyridine containing component **30**, OsO$_4$ and 2,3-dimethylbutene (Scheme 1.12). This macrocycle is then mixed with the adipamide thread **31** which quantitatively forms the threaded [2]rotaxane **28** in solution.
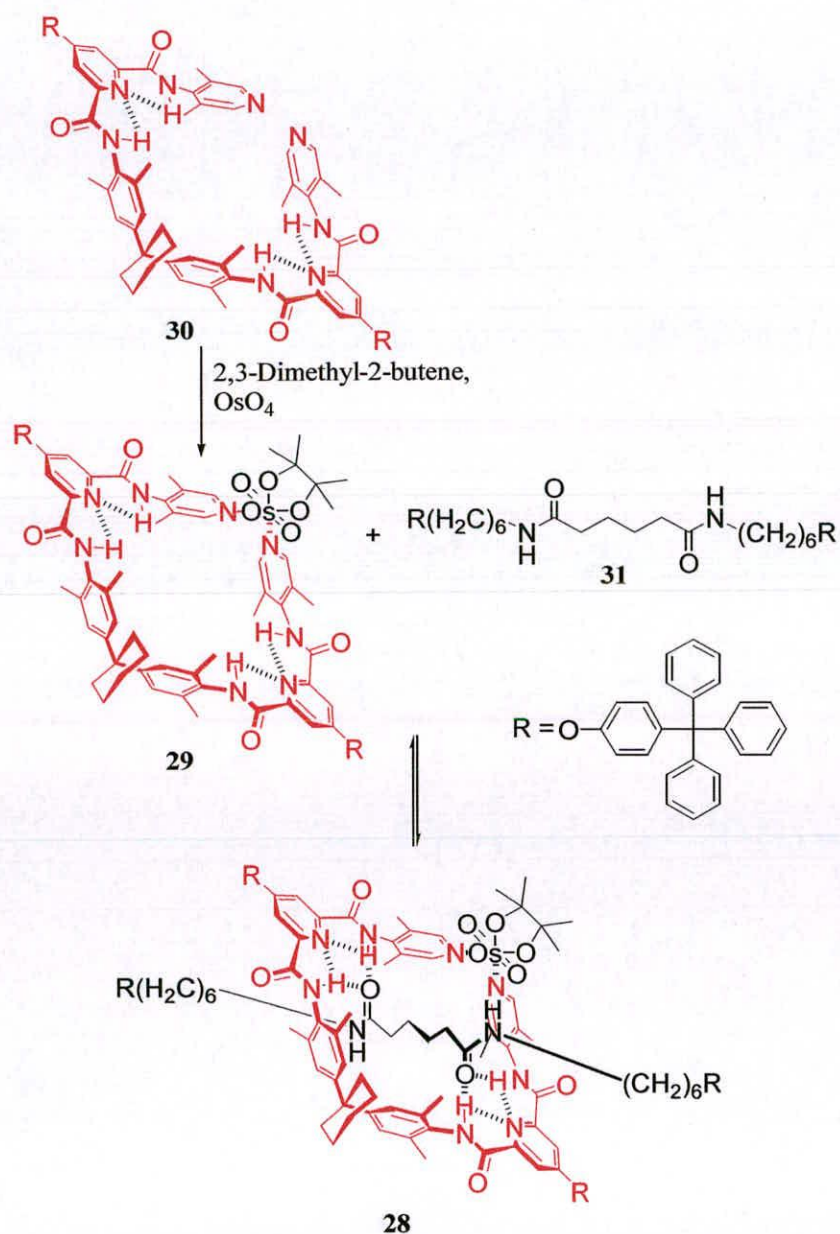
Scheme 1.12. The synthesis of a [2]rotaxane containing osmium in the macrocyclic component.

The rotaxane forms due to the macrocycle ring opening/ ring-closing at the osmium/ pyridine bonds, i.e. by reversible clipping. The driving force is provided by the amide hydrogen bonds between macrocycle and thread. However, the rotaxane **28** is not kinetically robust, an inherent limitation of all the products discussed in this section that contain metals within their macrocyclic framework. Jeong and co-workers have used the same methodology to afford corresponding [3]rotaxanes.[53] Catenanes have also been assembled with Au[I] centers in the macrocyclic framework. The approach exploits the coordination chemistry of Au[I] and was originally reported by Mingos and co-workers[54] and explored more recently by Puddephatt and co-workers.[55] The details of these systems will not be discussed any further here.

1.3.2 Hydrogen Bond-Assembled Interlocked Molecular Architectures

Hydrogen bonding is a unique noncovalent force by virtue of its key role in orchestrating the mechanisms of biological processes.[56] The key features of hydrogen bonding are its directionality, coupled with its ability to form arrays through cooperative effects. Taking inspiration and motivation from Nature, synthetic chemists have utilized these unique features of hydrogen bonding to access a range of well-defined supramolecular structures from small building blocks.[57] Interlocked molecular architectures can also be assembled *via* hydrogen bonding interaction between fragments containing donor and acceptor groups. This has been principally in the form of the amide function (which contains both donor and acceptor groups),[58] anionic centered acceptors[59] and ammonium ions/ crown ethers.[60]

1.3.2.1. Interlocked Molecular Architectures Molecular Assembled *via* Neutral Amide Hydrogen Bonding

The synthesis of neutral amide-based interlocked architectures began life in the early 1990's. The first synthesis of such a molecule was the serendipitous discovery of a [2]catenane by Hunter in 1992.[61] In earlier studies Hunter had designed and

synthesised macrocycle **32** (Figure 1.2) as a receptor for *p*-benzoquinone. This system was a proposed model for the study of fundamental processes in photosynthesis.[62]

32
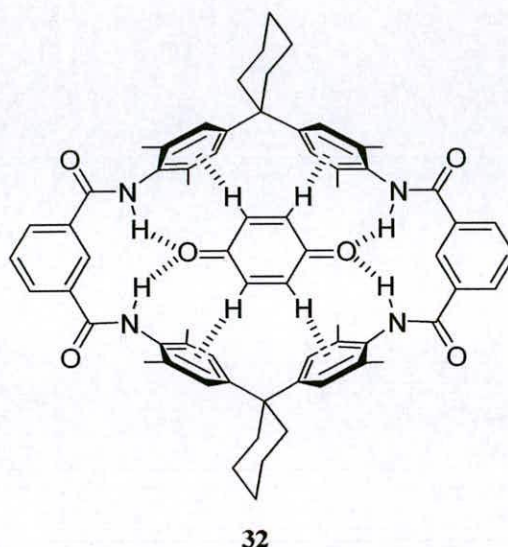
Figure 1.2. A tetra-amide containing macrocycle **32** designed as a host for *p*-benzoquinone

The macrocycle **32** was accessed *via* a direct [2+2] condensation of diamine **33** and isophthaloyl dichloride in a low 10 % yield (Scheme 1.12). In an attempt to obtain an improved yield of **32**, a two step approach was employed, whereby U-shape **34** was first prepared and subsequently reacted with isophthaloyl dichloride. The yield of macrocycle **32** was increased to 51 %, but two further products were also obtained. Unsurprisingly, tetrameric macrocycle **35** was afforded, but in addition a [2]catenane **36** was also obtained in an excellent 34 % yield. The nature of the interlocked structure was determined by elegant 2D and variable temperature ^{1}H NMR studies coupled with mass spectrometry analysis. Several years later an X-ray crystal structure determination of [2]catenane **36** displayed the hydrogen bonding interactions between the intertwined macrocycles responsible for its formation.[63]
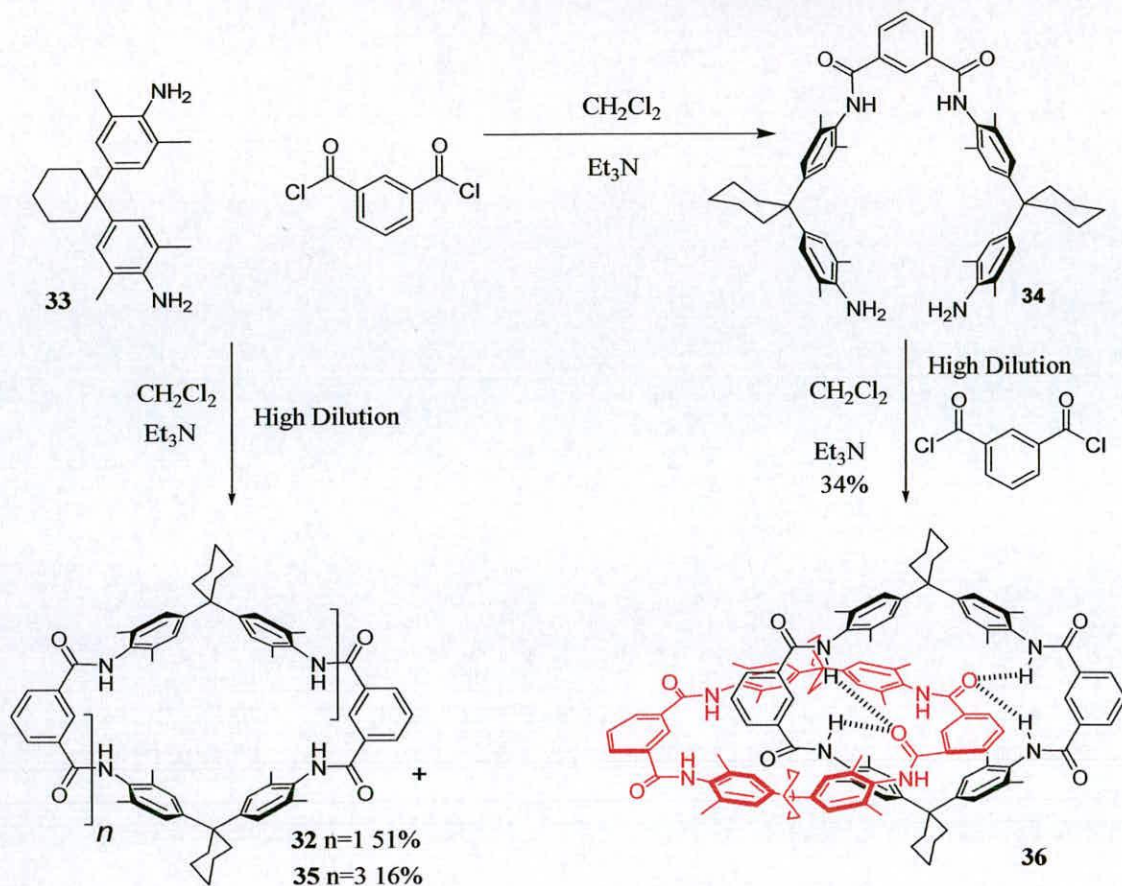
Scheme 1.13. The serendipitous synthesis of a [2]catenane according to Hunter.

The reaction of the corresponding pyridyl derivative furnished none of the simple dimer-dimer catenated product.[64] This is due to the favourable intramolecular hydrogen bonding interaction between the pyridine lone pair and the amide protons, which lock the amides into a NH *cis* conformation.
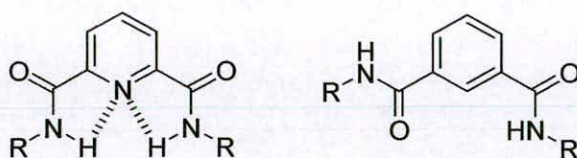
Figure 1.3. The conformational preferences of aromatic 1,3-diamides

Later in 1992, Vögtle and co-workers reported the synthesis of an analogous [2]catenane to that of Hunter's during attempts to make basket-shaped molecules.[65] Reaction of 5-methoxyisophthalic dichloride and diamine **33** in chlorobenzene at

50°C, under high dilution conditions gave [2]catenane **37** in 10 % yield (Scheme 1.14).
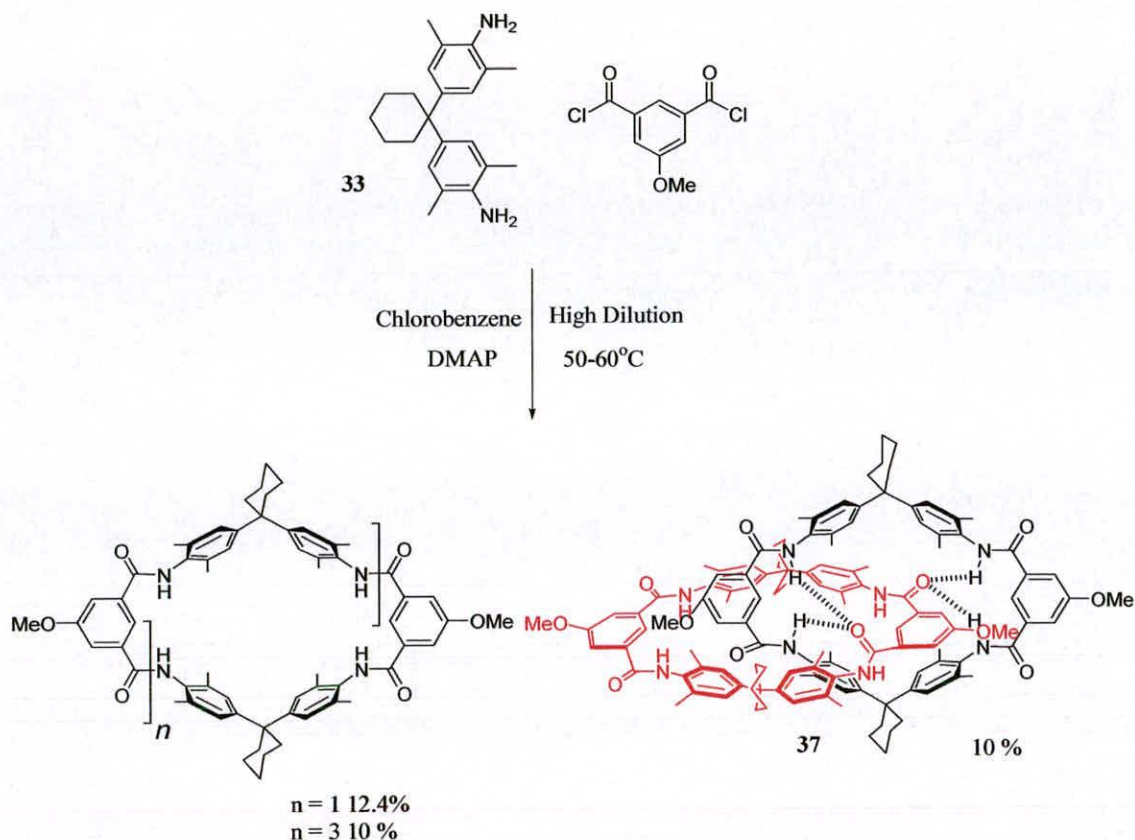
Scheme 1.14. Vögtle's synthesis of an amide based [2]catenane

Vögtle investigated the mechanism of catenane formation by making isomeric catenanes using the "U-shape" methodology of Hunter.[66] He proposed a mechanism whereby the isophthalic dichloride moiety 'nestles' in the cavity of the macrocycle and subsequently reacts with another amide U-shape whilst residing there. The more likely mechanism is the threading of a monoamide (formed upon initial reaction of U-shape with the acid chloride) with another macrocycle driven through hydrogen bonding. This was confirmed in later studies on analogous rotaxane-based systems.[67] In 1995, the X-ray crystal structure of a furan containing [2]catenane analogue showed a similar hydrogen bonding pattern to that of Hunter's.[68] In both the catenane systems of Hunter and Vögtle the bulky cyclohexyl groups prevent circumrotation between the two rings. Vögtle has extended the [2]catenane systems to synthesize analogues containing sulfonamide groups,[69] which induce chirality on

such systems, which display a pronounced Cotton effect in the aromatic region of the CD-spectrum.[70]

Vögtle extended the catenane synthesis furthermore in 1995 with the synthesis of amide-based rotaxanes **38a-h** in a 3-component *clipping* strategy (Scheme 1.15).[71] This *clipping* approach has been used to access a range of rotaxane architectures containing a plethora of central 'coordinating' units in combination with 4-trityl aniline as the bulky stopper group.[72]
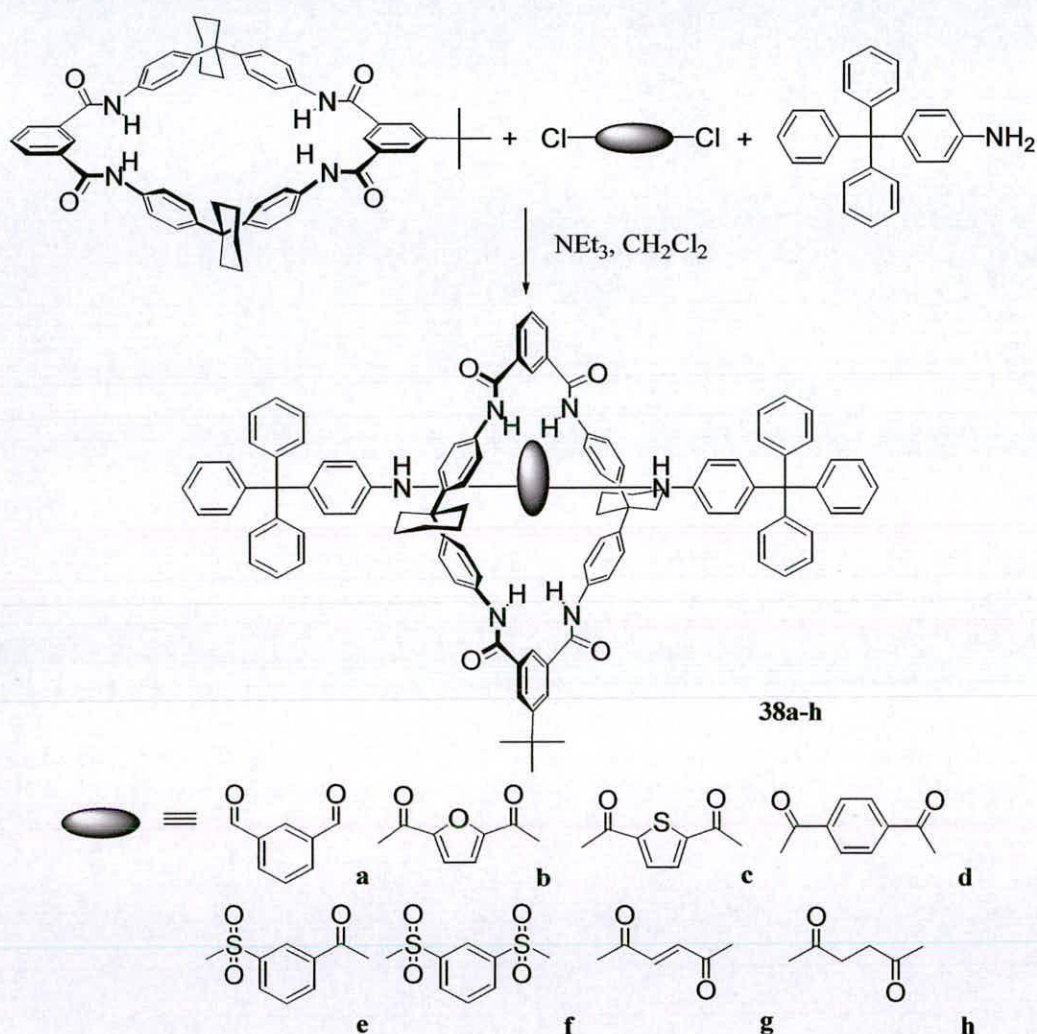
Scheme 1.15. Synthesis of amide-containing rotaxanes constructed *via* hydrogen bonding interactions

In 1995, Leigh and co-workers reported the serendipitous discovery of a benzylic amide [2]catenane **39** in attempts to develop a receptor for carbon dioxide (Scheme 1.16).[73] The reaction of isophthaloyl chloride and *p*-xylylene diamine affords [2]catenane in a 20 % yield as the only product. Again, as with the systems of

Hunter and Vögtle the assembly of the catenane is driven by complementary intramolecular hydrogen bonds between nascent macrocylic precursors, promoting cyclisation to form interlocked products. However, unlike the anilide systems of Hunter and Vögtle, the Leigh catenane system is remarkably tolerant to structural variation and despite its small size the two rings of the [2]catenane can circumrotate completely.[74]
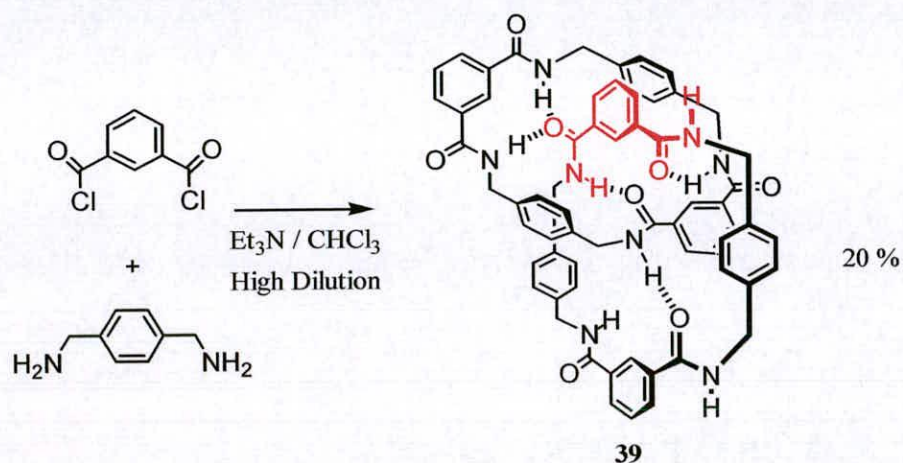
Scheme 1.16. The serendipitous synthesis of a benzylic amide catenane according to Leigh and co-workers.

In later studies Leigh and co-workers used the intercomponent hydrogen bonds that formed [2]catenane **39** to trap the benzylic amide macrocycle **40** on an isophthalamide linear thread **41**, in a five component assembly to afford [2]rotaxane **42** in 28 % yield (Scheme 1.17).[75] Disassembly of the resulting [2]rotaxane by removing the base-labile stoppers *via* tranesterification with sodium methoxide, afforded benzylic amide macrocycle **40** in a quantitative yield. The structure of [2]rotaxane **42** satisfies the hydrogen bonding requirements of the macrocycle internally and hence, displays high solubility in chloroform (100 g L^{-1}) as compared with the free macrocycle (1 mg L^{-1}).
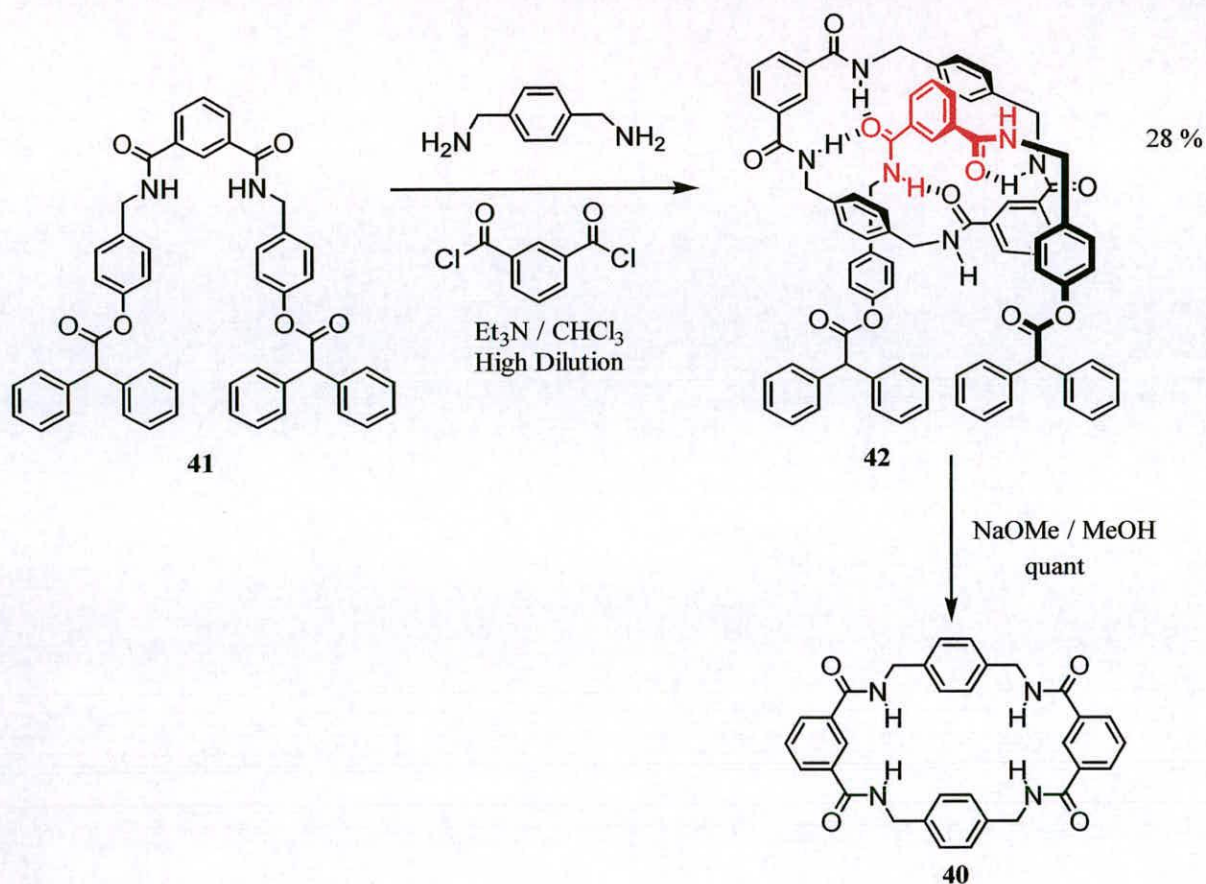
Scheme 1.17. The synthesis of an isophthalamide-based benzylic amide [2]rotaxane.

In 1997, Leigh and coworkers found that the simplest dipeptide, i.e., glycylglycine **43a** also 'traps out' the benzylic amide macrocycle to yield the corresponding [2]rotaxane **44a** in 62 % yield (Scheme 1.18).[76] Further studies showed that a range of dipeptide benzylic amide rotaxanes can be assembled, in good yields, as long as the *N*-terminal residue is glycine.[77]

The CD spectra of the resulting chiral dipeptide rotaxanes **44b-44e** show a strong response when compared to the corresponding thread whose CD spectra show no response. This difference can be unequivocally attributed to the interlocked nature of such systems, whereby the chiral centre of the dipeptide is transmitted through the macrocycle to the *C*-terminus diphenylmethine stopper. More intriguingly the CD response is variable on solvent environment such that in non-polar solvents, (e.g. CHCl$_3$) the response is strong and in polar solvents, (e.g. MeOH) the response is weak or non-existent. This variability is due to the relative "strengths" of the

intercomponent hydrogen bonds between thread and macrocycle in the respective solvents and hence the transmission of chirality is stronger when the hydrogen bonds are promoted between thread and macrocycle.

43a H
43b Me
43c CH$_2$CHMe$_2$
43d CH$_2$CH$_2$SMe
43e CH$_2$Ph

44a H 62%
44b Me 45%
44c CH$_2$CHMe$_2$ 37%
44d CH$_2$CH$_2$SMe 36%
44e CH$_2$Ph 32%
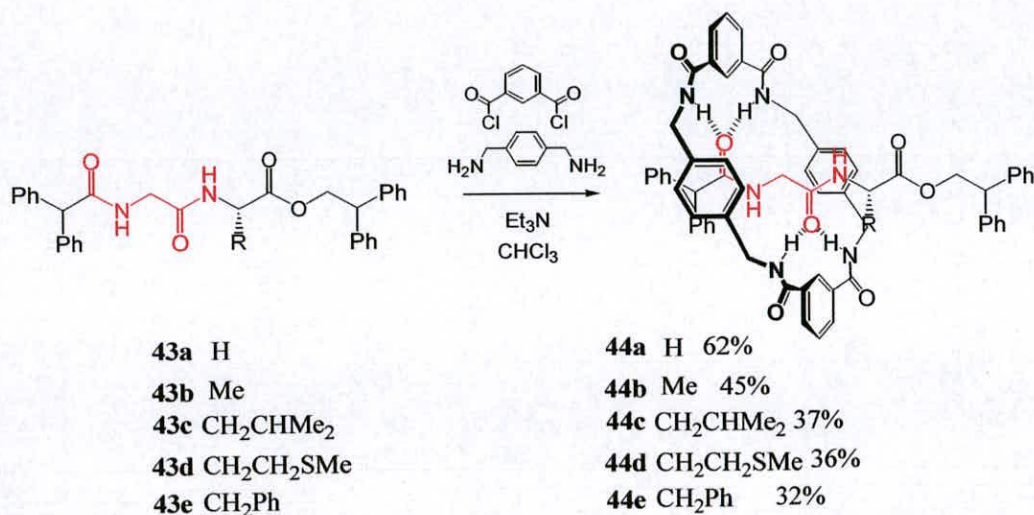
Scheme 1.18. The synthesis of a range of dipeptide-based benzylic amide [2]rotaxanes.

In 2001, Leigh and coworkers reported the synthesis of a fumaramide-based [2]rotaxane **46a** in a near quantitative 97 % yield (Scheme 1.19).[78] The excellent yield is due to the near-ideal spatial arrangement of the two amide carbonyls to template the benzylic amide macrocycle. The presence of the double bond also prevents the thread from forming intramolecular hydrogen bonds, which can be unfavorable for rotaxane formation. Finally the double bond infers rigidity on the thread and as a consequence the entropic cost due to complexation of the macrocycle to the thread is insignificant. The factors leading to such an excellent yield for the fumaramide thread are general. Hence, substitution of amides for poor hydrogen bond acceptors (i.e. esters) in the fumaric-based threads **45b-45c** still afford 35 % and 3 % of the corresponding [2]rotaxanes **46b-46c**.

45a X, Y = NH
45b X = NH, Y = O
45c X, Y = O

46a X, Y = NH   97%
46b X = NH, Y = O   35%
46c X, Y = O   3%
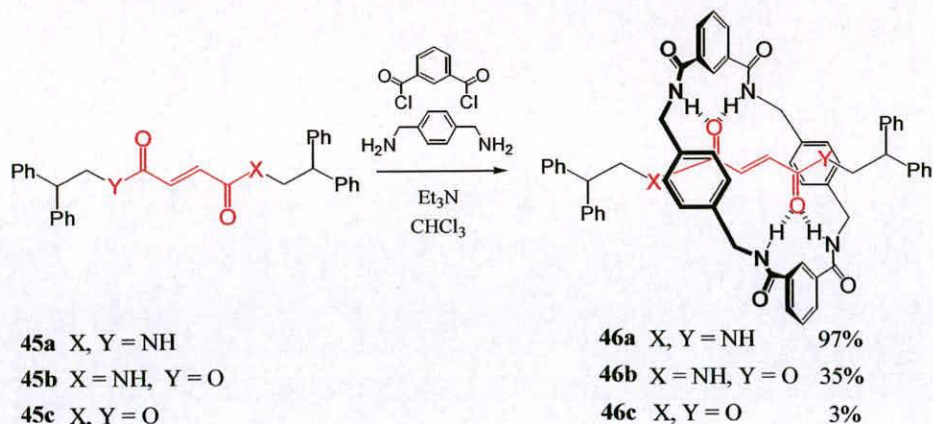
Scheme 1.19. The synthesis of fumaramide-based benzylic amide rotaxanes and ester containing analogues

Leigh and co-workers have also used complementary hydrogen bonding between amide functions to assemble catenanes and rotaxanes under thermodynamic control using ring closing alkene metathesis.[79]

1.3.2.2 Interlocked Molecular Architectures Assembled Through Hydrogen Bonding to Anions

Another way that hydrogen bonding can orchestrate the assembly of interlocked architectures is through the use of anions as templates. The first such example was in 1999 where Vögtle and co-workers used phenolate anions to complex to tetralactam macrocycle **47** and elaborate [2]rotaxanes by a *capping* procedure through nucleophilic substitution reactions (Scheme 1.20).[80] Thus, dibromide **49**, *p*-tritylphenol **48**, and macrocycle **47** were stirred at room temperature in the presence of potassium carbonate for 7 days to furnish the resulting [2]rotaxane **50** in 95 % yield.
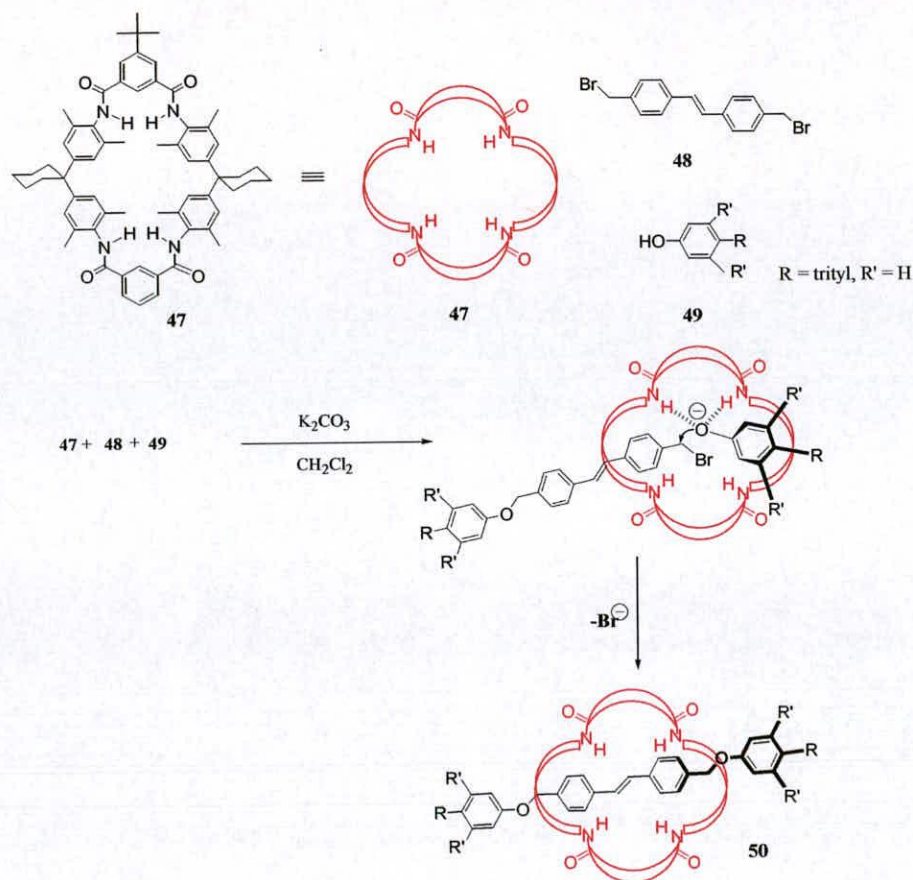
Scheme 1.20. The assembly of [2]rotaxanes through hydrogen bonding to a phenolate anion.

In later studies a number of other nucleophiles (thiols, tosylamides, thiophenols) also successfully gave [2]rotaxanes, but generally in lower yields (41-88 %) than the original system.[81] In 2002, Schalley and co-workers reported a detailed analysis of Vögtle's anionic template driven rotaxane synthesis.[82] The authors found that the macrocycle essentially acts as a 'protecting group' when complexed to the phenolate nucleophile and its subsequent reactivity depends on the steric demands of the bulky phenolate stopper.

Although ubiquitous in Nature and synthetic systems, anion templated assembly is under represented in the field of interlocked molecular architectures. This is often attributed to the relatively small ratio of charge to radius and sizable solvation energy as compared to cations.[83] However, Beer and co-workers have recently reported the anion-templated formation of pseudorotaxanes and rotaxanes using an acyclic chloride template.[84] The synthetic approach involves a cationic thread, designed to partially fill the coordination sphere of the strongly ion-paired chloride in a

noncompetitive solvent.   The empty coordination sphere was filled by an isophthalamide-based macrocycle of which simple derivatives are known chloride anion receptors.[85] The formation of pseudorotaxanes were successful, but usage of the *capping* methodology proved problematic in forming the requisite [2]rotaxane. The employment of clipping methodology successfully provided the interlocked [2]rotaxane architecture.   The dumbbell-shaped thread **51**, contained a methylated pyridinium salt which was complexed with isophthalamide U-Shape **52** appended with hydroquinone/ crown ether chain (Scheme 1.21).   The presence of terminal olefins in the chain allows macrocyclisation *via* ring closing metathesis using Grubbs' catalyst to afford [2]rotaxane **53a** in 47 % yield. The chloride anion is strongly bound in the cleft of the pyridinium ring by five hydrogen bonds from the thread and another two from the isophthalamide macrocycle. The use of bromide or hexafluorophosphate as the counter ion the thread provides none of the requisite products showing the complementary size of the chloride anion for the coordination cleft for rotaxane formation. A key difference between the anion assembled systems of Beer to those of Vögtle is that the template effect used to construct the molecule remains in the resulting interlocked architecture.   Hence, the hexafluorophosphate derivative **53b** can act as a selective receptor for anionic chloride.
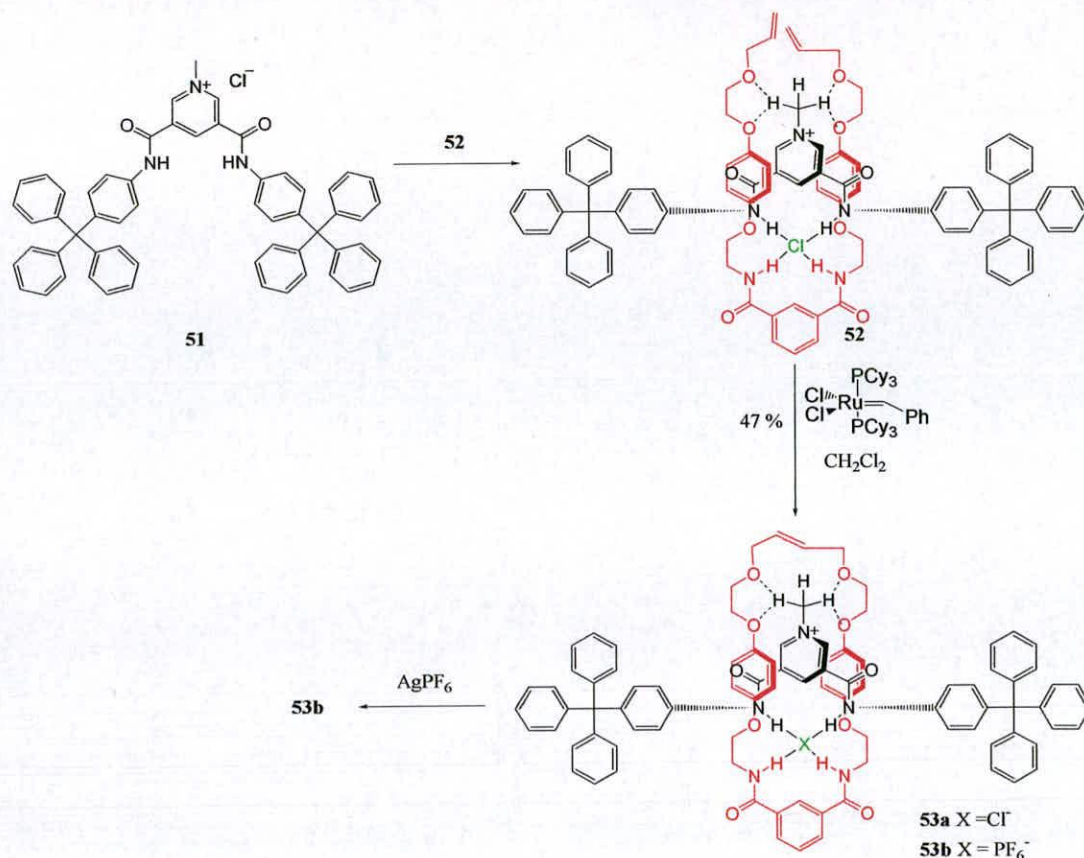
Scheme 1.21. The synthesis of [2]rotaxanes assembled *via* hydrogen bonding to a chloride anion.

1.3.2.3 Interlocked Molecular Architectures Containing Ammonium Ions and Crown Ethers

The association of substituted ammonium ions and macrocyclic polyethers is a venerable example of host-guest phenomena.[86] However, the discovery that appropriately-sized crown ethers can bind secondary ammonium ions in a *threaded*,[87] rather than a *face-to-face*[88] manner led to an opportunity to access a new family of interlocked molecules. The first interlocked architecture based on this hydrogen bonding motif was the synthesis of a [2]rotaxane by Busch and co-workers in 1995.[89] Busch and co-workers also reported the synthesis of a [3]rotaxane based on an analogous system (Scheme 1.22).[90] An aminothiol axle **54** is threaded through a crown ether macrocycle **55** and in the presence of iodine, oxidation of the thiols affords disulfide-containing [3]rotaxane **56** in a high yield of 84 %.
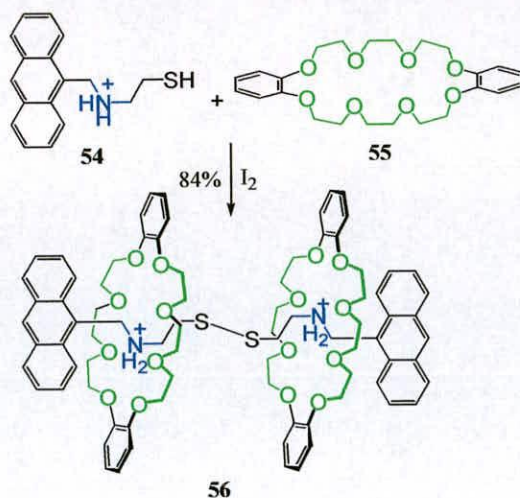
Scheme 1.22. The synthesis of a [3]rotaxane through molecular riveting

Stoddart and co-workers in contemporaneous studies synthesized [2] and [3]rotaxanes featuring threading of ammonium thread **57** (containing terminal azide functions) through dibenzo-24-crown-8.[91] The pseudorotaxane **58** was treated with dimethyl acetylene dicarboxylate under reflux to obtain [2]rotaxane **59** with triazole stoppers in a 31 % yield. The synthesis of an analogous thread containing two ammonium centers gave the corresponding [3]rotaxane in 10 % yield.
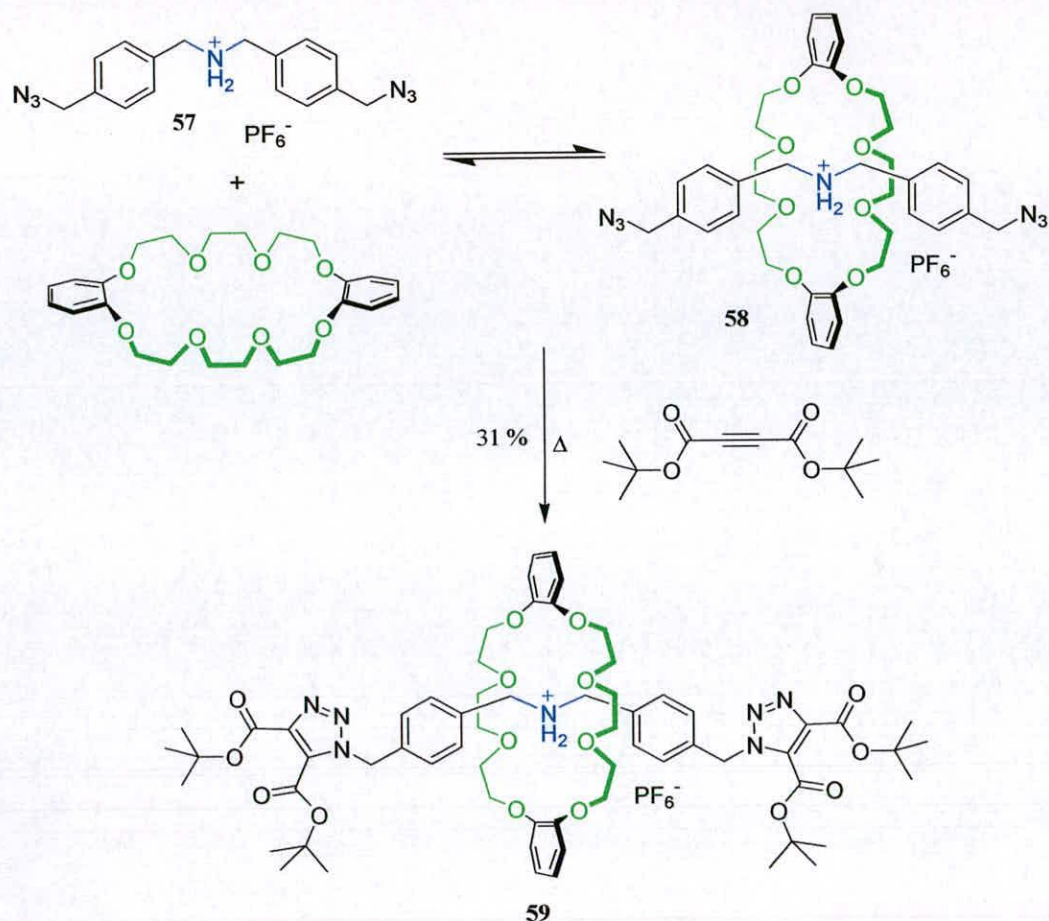
Scheme 1.23. Stoddart's synthesis of a [2]rotaxane with an ammonium ion/ crown ether motif.

The ammonium ion/ crown ether recognition motif has been used by Stoddart and co-workers to access rotaxanes under thermodynamic control.[92] The approach involves the use of reversible imine bonds to dynamically construct a [2]rotaxane from a threadlike component terminating with aldehyde functions. Hence, a 1:2:1 mixture of DB24C8, di-*tert*-butyl aniline, dialdehyde thread **60** in acetonitrile was allowed to equilibrate at room temperature (Scheme 1.24). After equilibrium had been reached the [2]rotaxane was found to be the major product **61** (47 %) by NMR spectroscopy along with the semi [2]rotaxane **62** (26 %) and other unthreaded species. The same equilibrium was attained when DB24C8 was added to a pre-equilibrated mixture of imine/ aldehyde components, hence demonstrating that thermodynamic control is operating. However, the imine-containing rotaxanes are kinetically unstable and cannot be isolated. The reduction of the imine bonds with PhSeH allows isolation of the amine stoppered rotaxane **63** in 17 % yield.
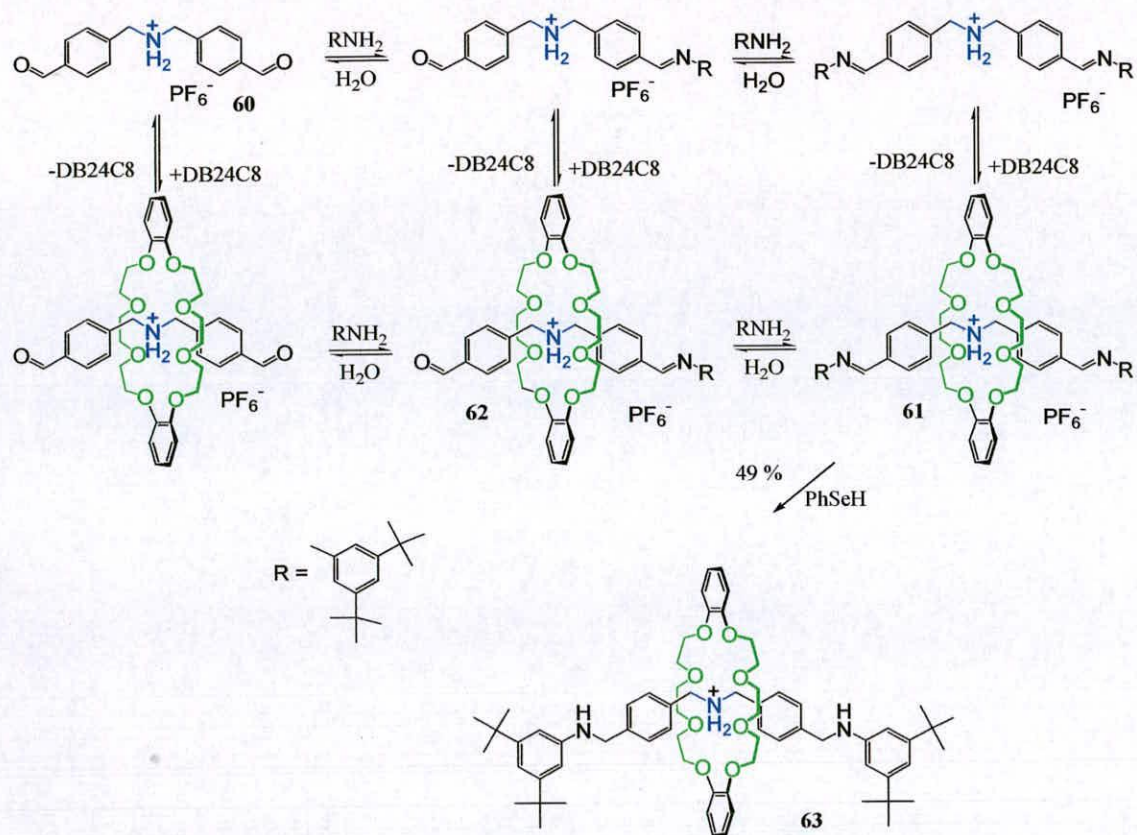
Scheme 1.24. The synthesis of [2]rotaxanes assembled under thermodynamic control.

Stoddart and co-workers have also described the synthesis of ammonium ion / crown ether rotaxanes assembled *via* reversible imine bond formation, but employing a *clipping* strategy.[93] In 1999, Stoddart and co-workers reported the synthesis of triphenylphosphonium-stoppered [2]rotaxanes in a *capping* procedure (Scheme 1.25).[94] Thus, reaction of dibenzylic bromide thread **64** with triphenylphosphine in the presence of DB24C8 gave the corresponding [2]rotaxane **65** in 55 % yield.

higher order rotaxanes   branched rotaxanes   molecular shuttles
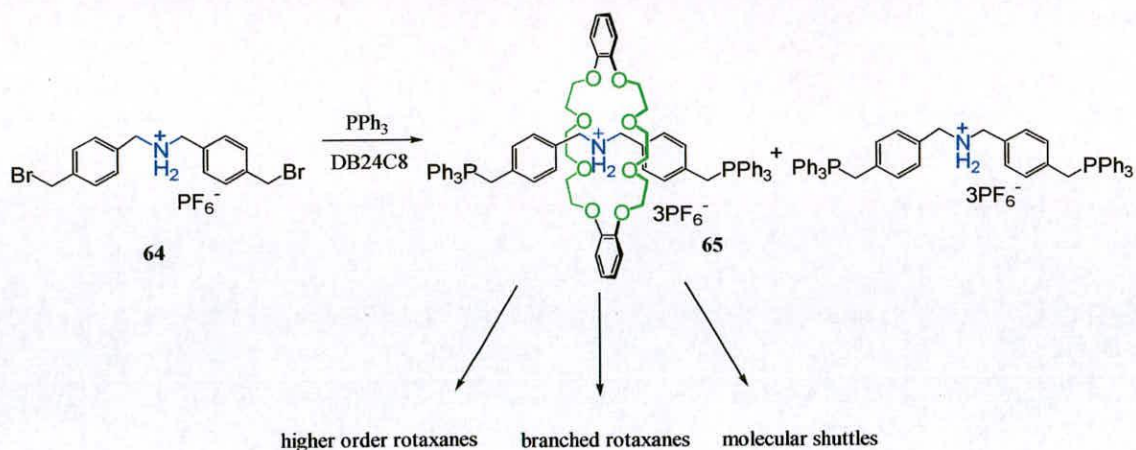
Scheme 1.25. The synthesis of triphenylphosponium stoppered [2]rotaxanes and their use in the construction of more complex molecular architectures.

The synthesis of phosphonium-based rotaxanes has allowed structural modifications of interlocked architectures to occur *via* Wittig olefination reactions. This is often referred to as "post assembly" modification and has been used to make a plethora of more complex interlocked architectures from simple rotaxane precursors.[95]

1.3.3. The Synthesis of Interlocked Molecular Architectures Based on π-Electron Acceptors and π-Electron Donors

The synthesis of this class of interlocked architecture began life in the design of synthetic receptors for the π-electron deficient herbicides diquat and paraquat by Stoddart and co-workers.[96] The macrocyclic polyether **66** was found to be one of the best receptors for paraquat and the paraquat derived cyclophane **67** is also an ideal host for 1,4-dimethoxybenzene (Scheme 1.26).[97] The determination of a number of X-ray crystal structures of inclusion complexes based on these motifs provided the inspiration for the synthesis of the first catenane of this series of interlocked architectures.[98]
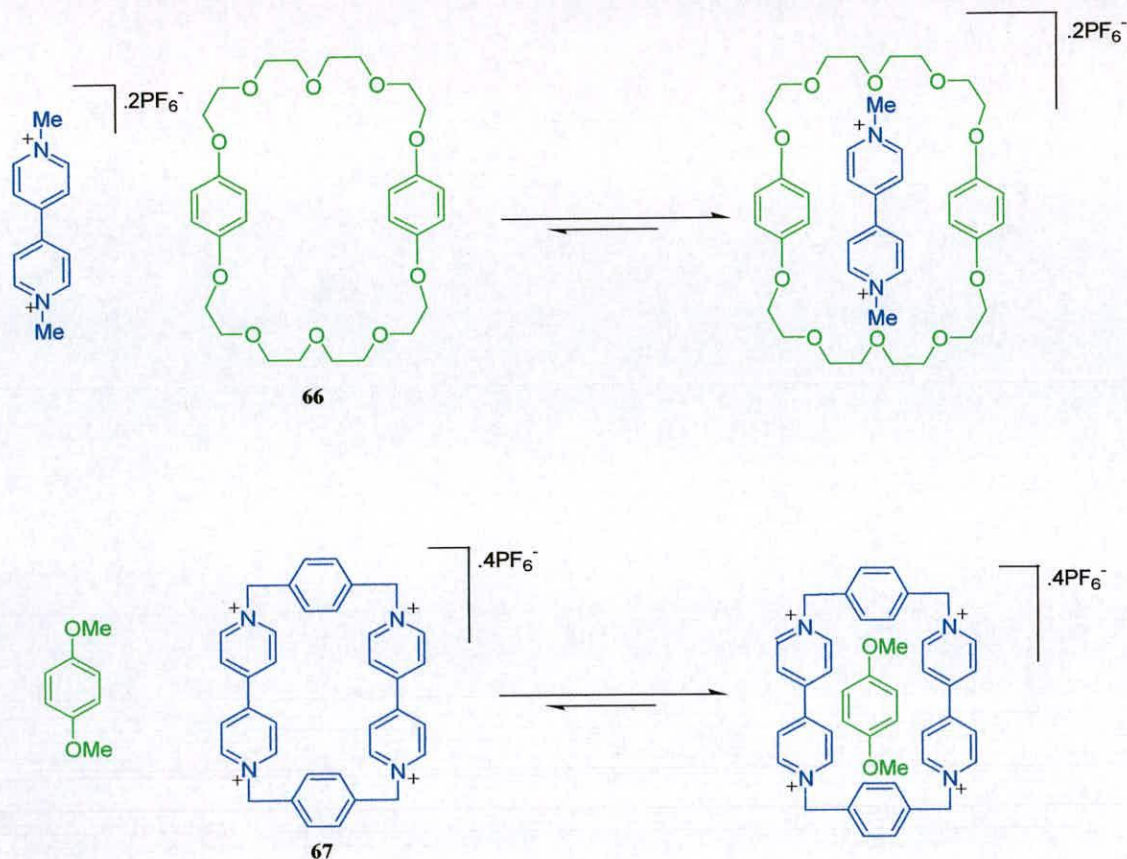
Scheme 1.26. Inclusion complexes utilizing aromatic π -π stacking interactions

The formation of paraquat derived cyclophane **67** in the presence of macrocyclic crown ether **66** afforded [2]catenane **68** in a 70 % yield (Scheme 1.27).[99] The resulting catenane is a strong red color indicating the presence of charge-transfer interactions. The primary driving force for the formation of the catenane was thought to be the complementary π-stacking between the respective components.[100] However, due to recent studies it is now accepted that hydrogen bonding interactions between the α-carbon hydrogens of the bipyridinium cations, and oxygen atoms in the polyether links of the crown ether are as important in their construction.[101]
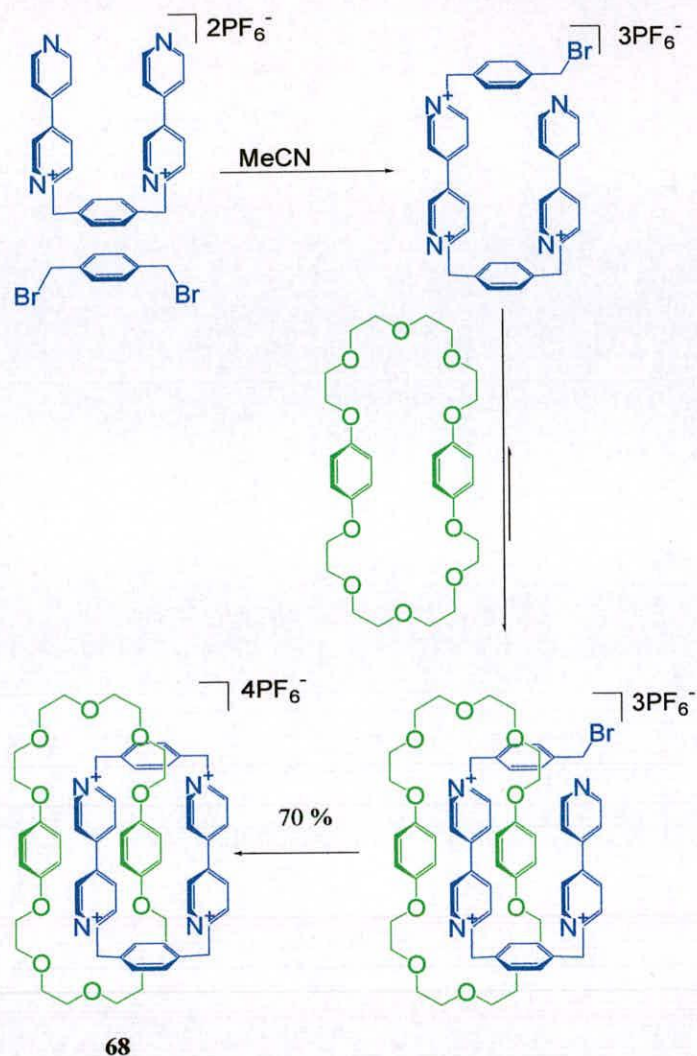
Scheme 1.27. The synthesis of a [2]catenane assembled through aromatic interactions

Stoddart and co-workers have made a range of catenane structures assembled *via* this recognition motif, culminating in the 'classic' first synthesis of olympiadane; a [5]catenane likened to the symbol of the International Olympic movement.[102] Stoddart and co-workers have also made a trefoil knot using this recognition motif.[103]

Figure 1.4. A representation of a crystal structure of olympiadane and its similarity to the symbol of the International Olympic movement

Stoddart and co-workers have also accessed rotaxanes using the paraquat/ crown ether recognition elements used to assemble catenanes. The linear element in the first syntheses of such rotaxanes was the polyether moiety, which was encircled by the bipyridinium-based macrocycle **67**.[104] The rotaxane **69** was prepared using both a *clipping* and *threading* methodologies respectively. The threading strategy involved adding a mixture of bipyridinium macrocycle **67** and hydroquinone polyether thread **70** to a solution of triisopropylsilyl triflate and 2,6-lutidine at room temperature to afford the [2]rotaxane **69**, in 22 % yield (Scheme 1.28). Alternatively, the dumbbell-shaped thread component **73** was treated with dibromide **71** and U-shape **72** to form [2]rotaxane **69** in a 14 % yield *via* a clipping strategy.
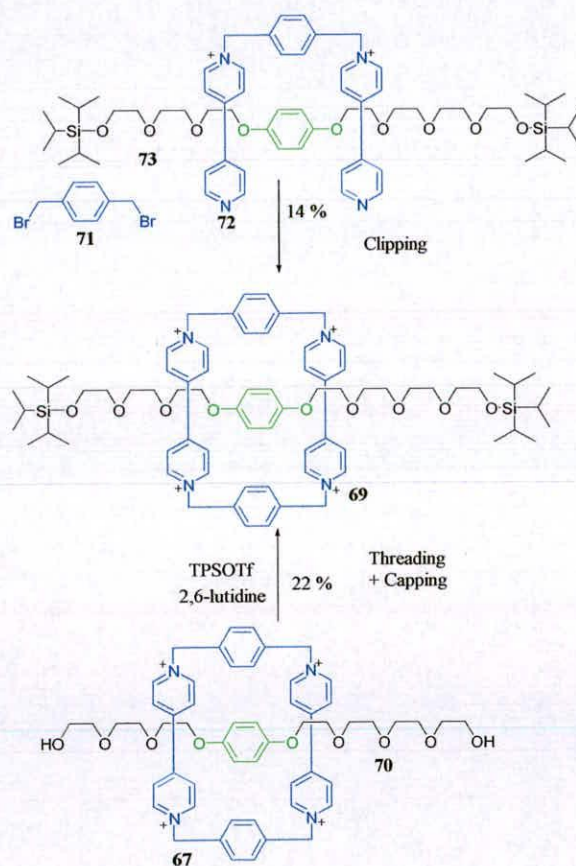
Scheme 1.28. A [2]rotaxane **69** prepared by clipping and threading: capping methodologies

In later studies Stoddart and co-workers exploited size-complementarity between the macrocyclic component and stoppers of the dumbbell-shaped component to obtain [2] and [3] rotaxanes respectively by a slippage methodology.[105] In this synthesis

the linear component contained bipyridinium unit **74** and was encircled by a crown ether macrocycle **66** (Scheme 1.29). As with any slippage synthesis the judicious choice of bulky stoppers is paramount in obtaining preparative yields of interlocked products. This is illustrated by replacement of a *tert*-butyl group **74a** in the dumbbell-shaped threads by the progressively smaller isopropyl **74b**, ethyl **74c**, methyl **74d**, and hydrogen groups **74e**. The reaction of these threads with four equivalents of crown ether macrocycle **66** gave higher yields with the less bulky derivatives, such that isopropyl derived thread gave none of the corresponding rotaxane **75b** and ethyl **75c**, methyl **75d** and hydrogen **75e** derivatives gave yields in a similar range (47-52%).

74a R=^{t}Bu
74b R=^{i}Pr
74c R=Et
74d R=Me
74e R=H

MeCN
60°C

75a R=^{t}Bu, 0 %
75b R=^{i}Pr, 0 %
75c R=Et 47 %
75d R=Me 50 %
75e R=H 52 %
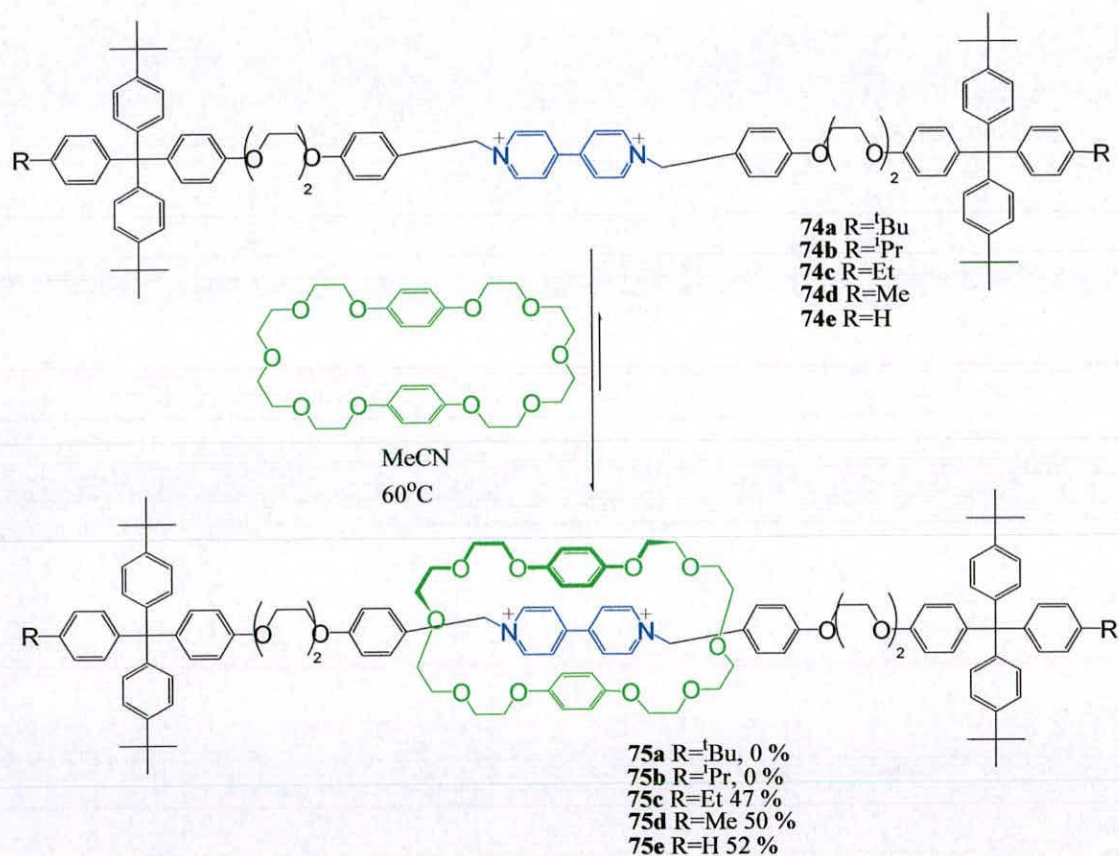
Scheme 1.29. The significance of stopper-size on preparative yields when employing the slipping approach

Tetrathiafulvalene (TTF) has also been used as the π-electron donor component in a number of catenane and rotaxane systems.[106]

Stoddart and co-workers have also constructed rotaxanes containing π-electron donor/ π-electron acceptor functions under thermodynamic control. Again as in

previous studies, the reversible nature of imine bond formation provided the key thermodynamic element to the system.[107]

In the late 1990's, Sanders and co-workers reported a series of catenanes based on π-π stacking interaction similar to those used to construct the interlocked systems detailed by Stoddart and co-workers.[108] However, whilst the crown ether derivative of the catenane remained constant, the complementary electron acceptor unit of the other macrocycle consisted of a neutral diimide moiety **76**. In the original system the diimide macrocycle was elaborated by coupling of appended terminal acetylenes using the Glaser reaction.[109] This was performed in the presence of preformed crown ether macrocycle **77** to obtain [2]catenane **78** in 52 % yield.
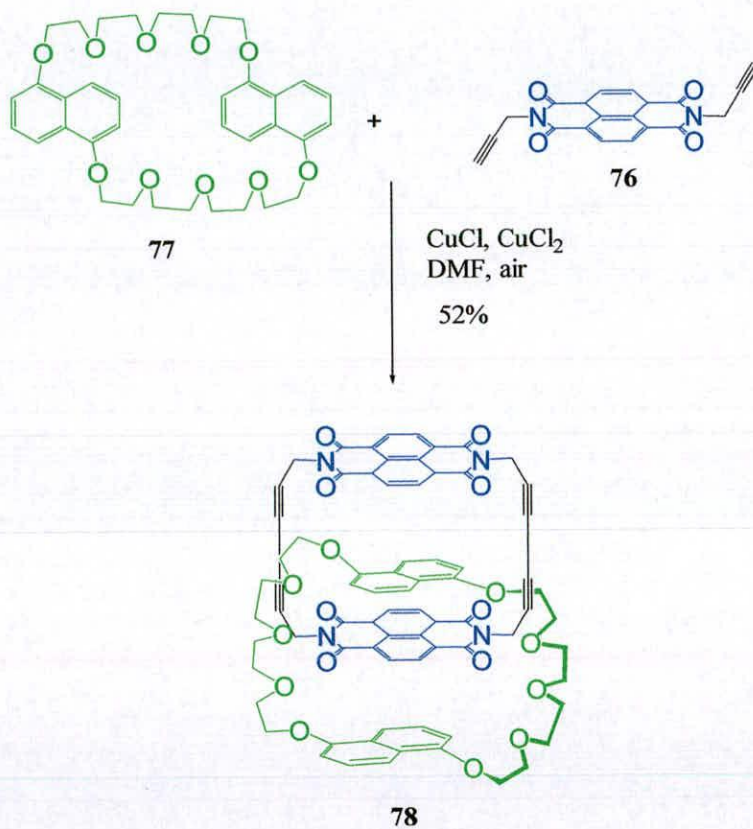
Scheme 1.30. The synthesis of a neutral catenane based on π-electron rich donors and π-electron poor acceptors.

In other studies Sanders and co-workers also observed the existence of C-H---O hydrogen bonds between the diimide methylene hydrogens and the central oxygen atoms of the crown polyether chain within their catenane systems (Figure 1.5).[110]
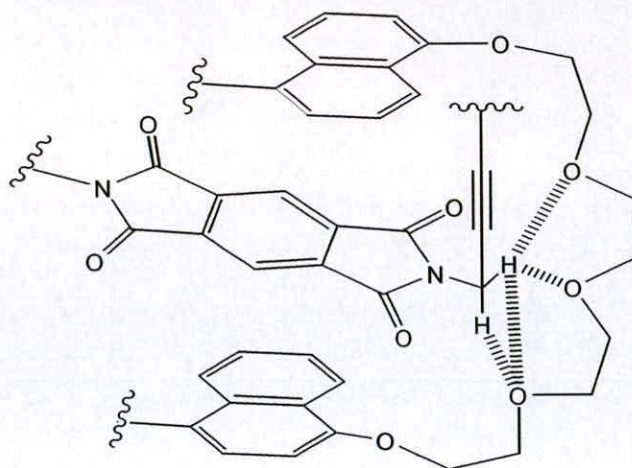
Figure 1.5. The role of C–H···O interactions in the assembly of catenanes containing diimide macrocycles

Sanders and co-workers have also formed similar systems under thermodynamic control using ring closing alkene metathesis.[111]

1.3.4 The Synthesis of Interlocked Molecular Architectures Based on Hydrophobic Effects

The synthesis of this category of interlocked molecules is not classed as a template directed process. However, that a plethora of macrocyclic hosts invoke the hydrophobic effect as the primary driving force for the assembly of a range of interlocked molecules is without question and, as such, this "motif" deserves its own section. The macrocycles involved in the elaboration of interlocked molecules exploiting the hydrophobic effect, include cyclodextrins,[112] cucubituril,[113] together with other cyclophanes.[114]

The first attempted synthesis of interlocked molecule was reported in 1958, by Lüttringhaus and co-workers.[115] They attempted to link dithiol compound **79** incorporating hydroquinone residue by oxidation in aqueous solution in the presence of β-cyclodextrin to prepare [2]catenane **80**. However, the synthesis failed, due probably to the insufficient length of the alkyl chains or their inappropriate conformation for mutual reactivity.
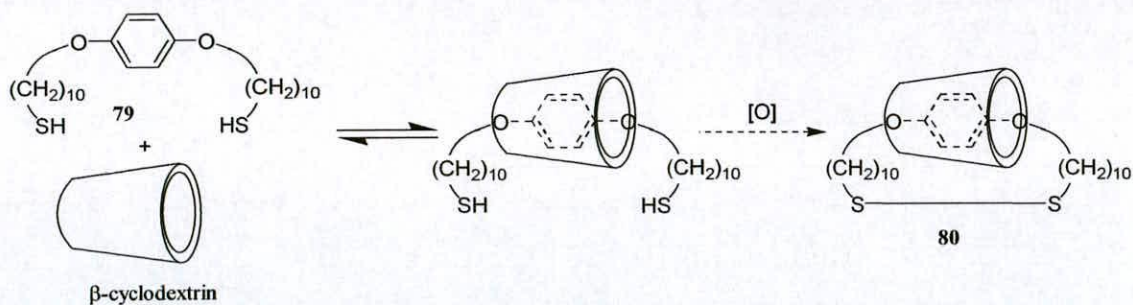
Scheme 1.31. The first attempted synthesis of a [2]catenane

In 1993, Stoddart and co-workers prepared the first catenane incorporating a cyclodextrin in a revisit of the original attempted catenane synthesis.[116] A mixture of polyether containing diamine **81** and methylated β-cyclodextrin was reacted under Schotten-Baumann conditions with terphthaloyl dichloride to yield a mixture of two [2]catenanes (one shown) and 2 isomeric [3]catenanes (not shown) with the [2]catenane **82** as the major product (3 %).
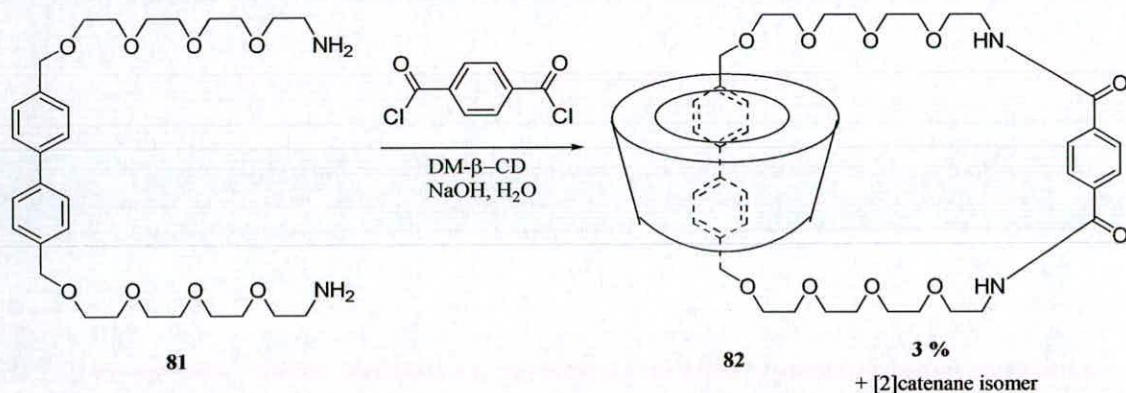
Scheme 1.32. The first synthesis of catenanes containing cyclodextrin as the macrocyclic component

In 1981, Ogino and co-workers provided the first interlocked molecule incorporating a cyclodextrin, namely a [2]rotaxane.[117] The strategy involved threading α– or β–cyclodextrin onto 1,12-diaminododecane in a solution of DMSO, followed by addition of *cis*-[CoCl$_2$(en)$_2$]Cl afforded yields of [2]rotaxane **83** of up to 24 %.[118] The same approach has been utilized in the synthesis of a number of rotaxane architectures incorporating cyclodextrins with coordinative bonds as stoppers.[119]
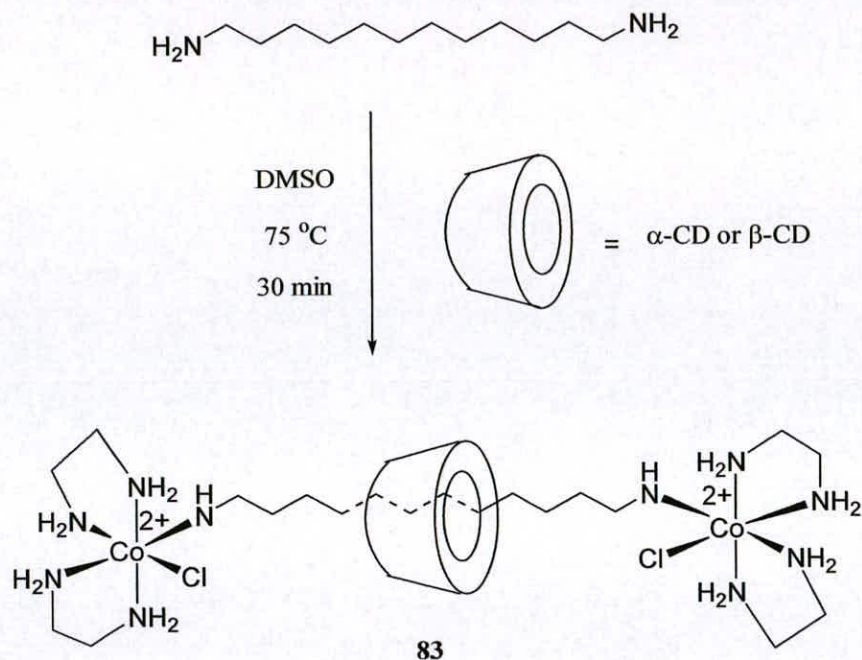
Scheme 1.33. Synthesis of a [2]rotaxane containing cyclodextrin as the macrocyclic component

Harada and co-workers[120] and others[121] have reported the synthesis of a series of polyrotaxanes containing cyclodextrins. One such polyrotaxane facilitated the synthesis of a fascinating tubular polymer structure reported in 1992.[122] A poly(ethyleneglycol) chain of 1450 MW was employed in tandem with α-cyclodextrin of which it forms complexes most efficiently. The resulting polyrotaxane **84** was cross-linked by reaction with epichlorohydrin in 10 % aqueous sodium hydroxide solution and then the stoppers were cleaved by treatment with 25 % sodium hydroxide to obtain the tubular polymer **85**. The tubular polymer molecular weight was determined to be about 17000 in an excellent 92 % yield.
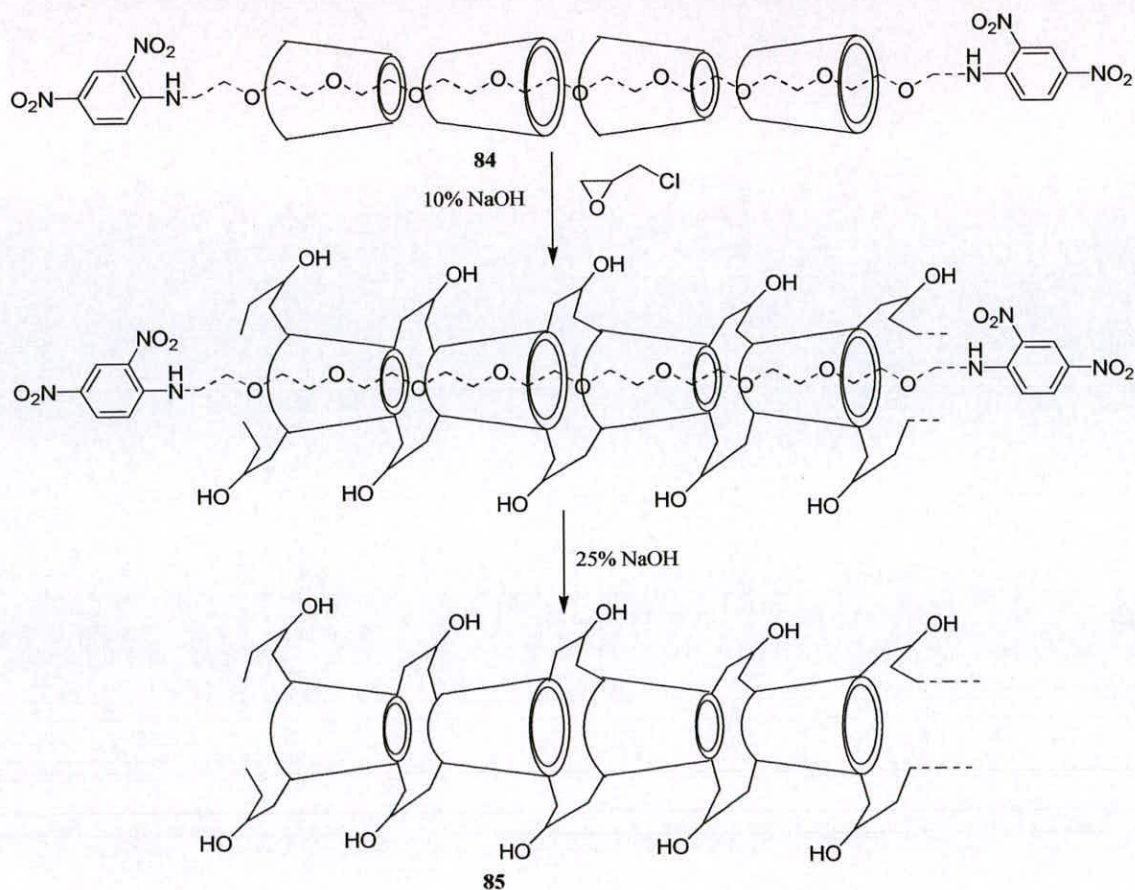
Scheme 1.34. The assembly of a tubular polymer facilitated by α-cyclodextrin-based polyrotaxane

In 1997, Anderson reported the synthesis of a range of water-soluble azo-dye rotaxanes using the hydrophobic effect to direct rotaxane formation.[123] The azobenzene diazonium salt **86** was added to an aqueous solution of β-napthol derivative **87** in the presence of α- or β-cyclodextrin or cyclophane **88** at 0 °C. In each case [2]rotaxanes were isolated, but the rotaxane **89** derived from cyclophane **88** gave the best yield of 46 %. The consequences of encapsulation were profound as all the rotaxanes derivatives proved to be more soluble (in most solvents) than the corresponding non-rotaxanated dyes. Anderson and co-workers have demonstrated that encapsulating dyes as rotaxanes can affect other desirable properties such as aggregation, bleaching and fluorescence efficiency.[124]
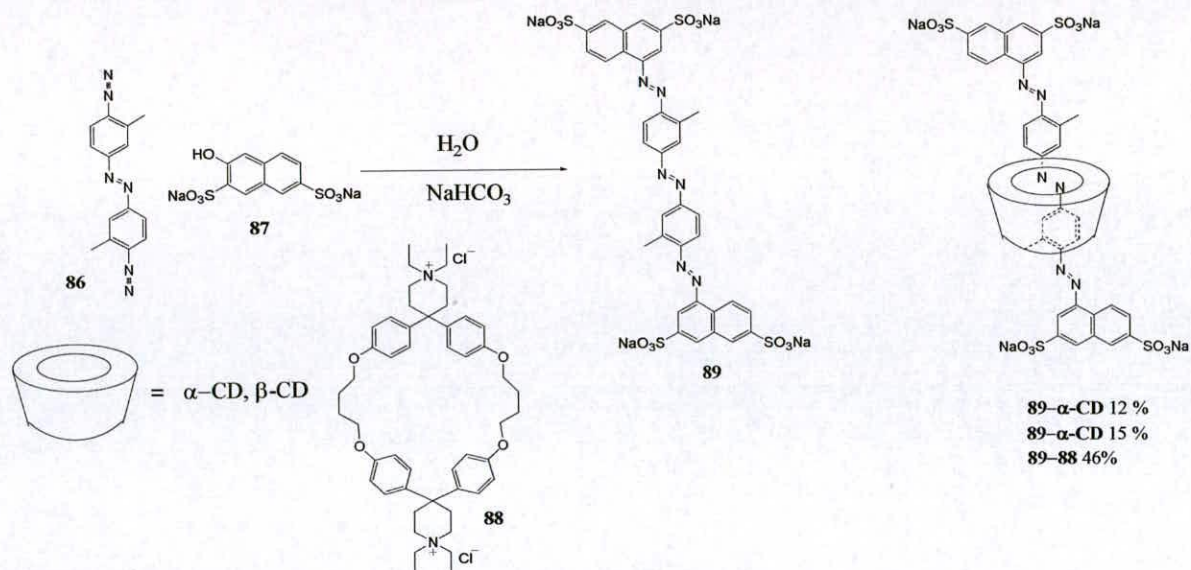
Scheme 1.35. The synthesis of azo-dye rotaxanes containing cyclodextrins

Anderson and co-workers have also employed cyclodextrin-based polyrotaxanes as insulated wires.[125] The polyrotaxanes were assembled by threading and capping through Suzuki reactions in the presence of suitable rod and cyclodextrin components in aqueous solution (Scheme 1.36).[126] The presence of the cyclodextrins in the backbone of the rotaxane leads to some desirable physical properties. The rotaxane reduces the tendency of the wires to aggregate, a necessary property in molecular electronics. The rotaxane **90** displays increased luminescence efficiency and blue-shifted emission. As the cyclodextrin protects the thread from external sources the stability is consequently greater and resistant to quenching from impurities. Finally, the greater water-solubility conferred by the presence of the cyclodextrins allows spin-coating without toxic solvents. Anderson has also reported the synthesis of molecular wires using the water soluble cyclophane **88**.[127]
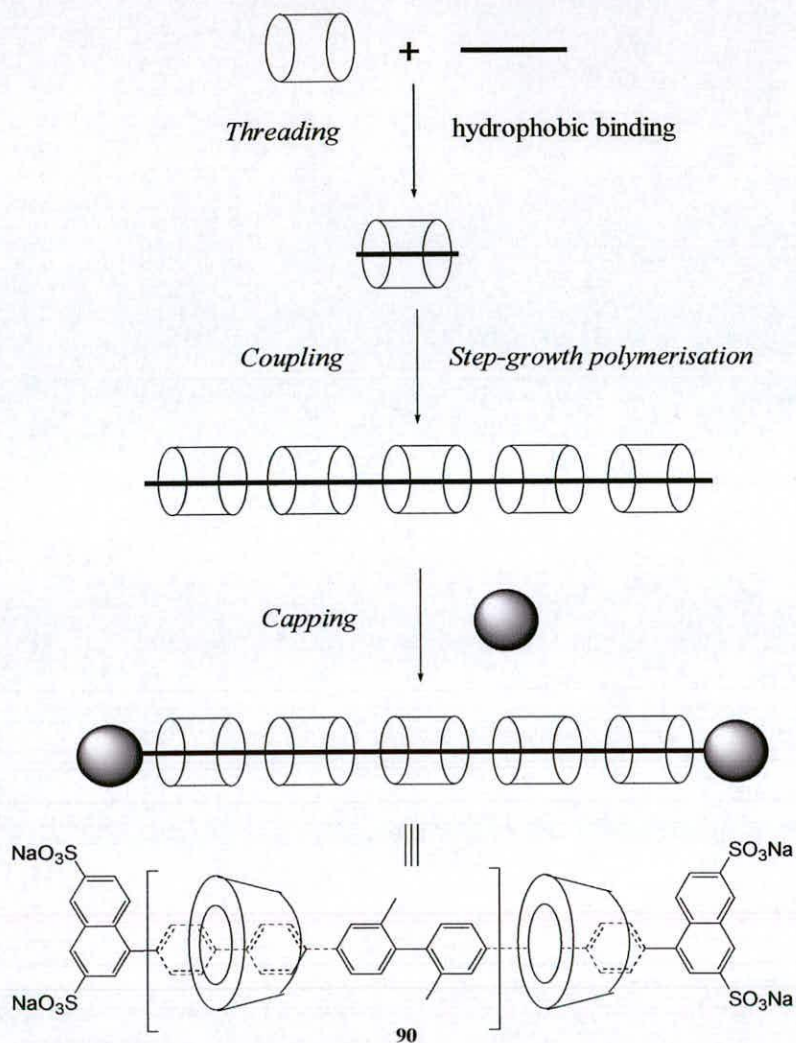
Scheme 1.36. The synthesis of cyclodextrin-containing molecular wires *via* Suzuki coupling in water.

1.4 Molecular-Level Machines

1.4.1 Introduction to Molecular-Level Machines

Macroscopic machines are in evidence in every sphere of our society and our reliance on them is obvious. Since the advent of silicon-based electronics the components of macroscopic machines have become ever smaller. However, today the limits of this miniaturization process are ever nearer, which entails a "novel" approach to this problem. This concept is called "bottom-up" approach and involves assembling molecular architectures to create in essence a molecular-level machine. This is of course not a new concept as the notion of molecular-level machines were first discussed by Nobel Laureate Richard P. Feynman in his address to the American Physical Society on December 29th 1959 at Caltech entitled *"There's Plenty of Room at the Bottom".*[128] Feynman's prophetic words indeed are seen as a seminal moment in what today is generally described as *Nanoscience* toward the goal of Nanotechnology. However, in reality only the first small steps have been taken along the road to the realization of molecular machines, through the "bottom-up" approach and only in the past few years have systematic studies been performed in the field.[129]

1.4.2 What is a Molecular-Level Machine?

A molecular level machine can be defined as an assembly of a discrete number of molecular components designed to perform mechanical-like movements (output) as a consequence of appropriate external stimulus (input). In analogy to macroscopic machines their molecular-scale counterparts are characterized by i) the kind of energy input supplied to make it work, ii) the type of movements performed by its components, iii) the manner in which its operation can be monitored and controlled, iv) the possibility to repeat the operation and establish a cyclic process, v) the timescale needed to complete a cycle of operation and vi) the function performed by the machine.

The energy supplied to the molecular machine can take several forms including, chemical, photochemical and electrochemical energy. The use of chemical energy in a molecular machine is clearly undesirable as the formation of waste products would compromise the workings of the machine in repeating cycles. Photochemical and electrochemical energy inputs in contrast can cause the occurrence of the necessary reactions without the formation of waste products. The repeating cycle characteristic of a molecular machine requires that any given chemical transformation must be reversible. Examples of such reactions are isomerisation of double bonds, acid-base reactions, redox processes and complexation-decomplexation equilibria, such as forming and breaking of hydrogen bonds.

The motions performed by the components of a molecular machine are somewhat dependent on whether the machine is molecular or supramolecular in nature, but whatever the movement performed, it must be of large amplitude. In classical molecules, the motions will involve the changes in their confirmation and/or configurations around covalent bonds. This change may be accompanied by the making and breaking of intramolecular noncovalent bonds which can create large amplitude motions in the superstructure, and hence, these changes constitute the movements in molecular-level machines. Interlocked molecular architectures offer a novel opportunity for large amplitude motions as opposed to classical molecules, as the intercomponents can move relative to one another, again due to making and breaking of noncovalent bonds. In terms of monitoring the operation of a machine, the movement of the components must trigger a readable change in the properties of the system. Photochemistry and electrochemistry are extremely useful in this scenario as both photons and electrons can, besides supplying the energy needed to make a machine work can also be useful to "read" the state of the system and thus, control and monitor the operation of the machine. Finally, the functions that can be performed as consequence of the submolecular motion of some of the machine components are, to large extent, still unpredictable and unexplored.

The most complicated molecular-level machines are obviously those found in Nature. Biological molecular machines are composed of assemblies of proteins and

their task is to convert energy from one form or location into another. Indeed in recent years the structure and mechanism of several biological molecular machines have been elucidated, further fueling the possibility of true synthetic molecular-level machines. Examples of such biological molecular motors include F_1-ATPase,[130] Myosin,[131] and RNA polymerase,[132] but they will not be discussed further here. Molecular level devices have also been devised containing covalently-connected rotating parts, which mimic the motions of macroscopic machines, for example, gears, [133] propellers,[134] and rotors.[135] Some of these systems can be said to be unidirectional in their rotary motion with respect to the covalent bond perturbed.[136] However, these systems will not be considered in detail and the reader is directed to the primary literature for further details.

1.4.3 Interlocked Molecules as Prototypes of Artificial Molecular Machines

The mechanical bond contained within interlocked molecules makes them excellent models for molecular-level machines. The mechanical bond, as discussed previously, allows the potential for relatively large amplitude motions. Perhaps the most versatile interlocked molecular architecture for studying large amplitude motions are rotaxanes. There are two distinct movements that the macrocycle can undergo with respect to its thread component. Pirouetting involves the macrocycle spinning around the thread component at a certain frequency, akin to a molecular gear, whereas translational movement occurs along the length of the thread. Rotaxanes as we have seen are assembled in the main by template-directed approaches. Thus, if two template units exist within a [2]rotaxane then translational motion can occur between the two units called "stations". Such a molecule is termed a molecular shuttle. The stations must present accessible free activation energy barriers between them and be located far enough apart so that the shuttling movement can be well distinguished from any other internal motion governed by conformational rearrangements. If the two stations are identical then the macrocycle can shuttle between them such that two "co-conformations"[137] are obtained,

however this performs no work and therefore does not fit into the description of a machine (Figure 1.6).
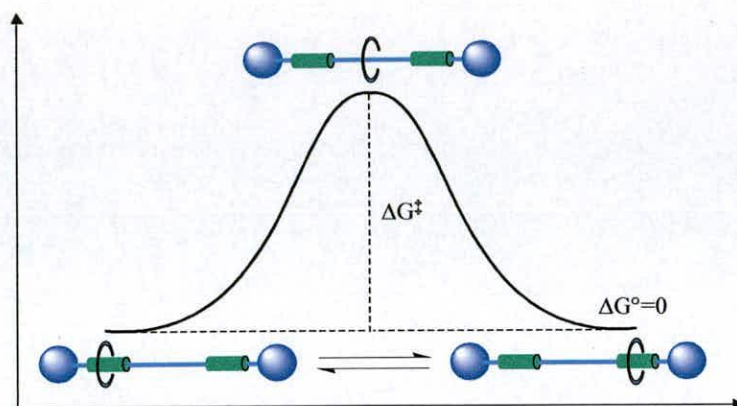
Figure 1.6. A cartoon representing the shuttling movement in a two degenerate stations-containing [2]rotaxane and the associate potential energy profile.

In order to perform work the stations must be different and hence the ΔG of the system is not zero. In a stimuli-responsive [2]rotaxane the macrocycle sits preferentially over the station that provides the best stabilization energy (*i.e.* state 1, station green). The application of an appropriate external stimulus applied, can then increase the binding affinity of the macrocycle for the initially less favored station (as in the cartoon of Figure 1.7) or destabilize the binding affinity of the macrocycle for the initially favored station. This ultimately results in the shuttling of the macrocycle over to the initially unfavored station (*i.e.* state 2, blue station) that now provides the best stabilization energy. Applying a second stimulus restores the original state and closes the cycle. All the stimuli-responsive molecular shuttles based on rotaxane architectures reported in literature work along these principles; the only difference lies in the nature of the stimuli applied.
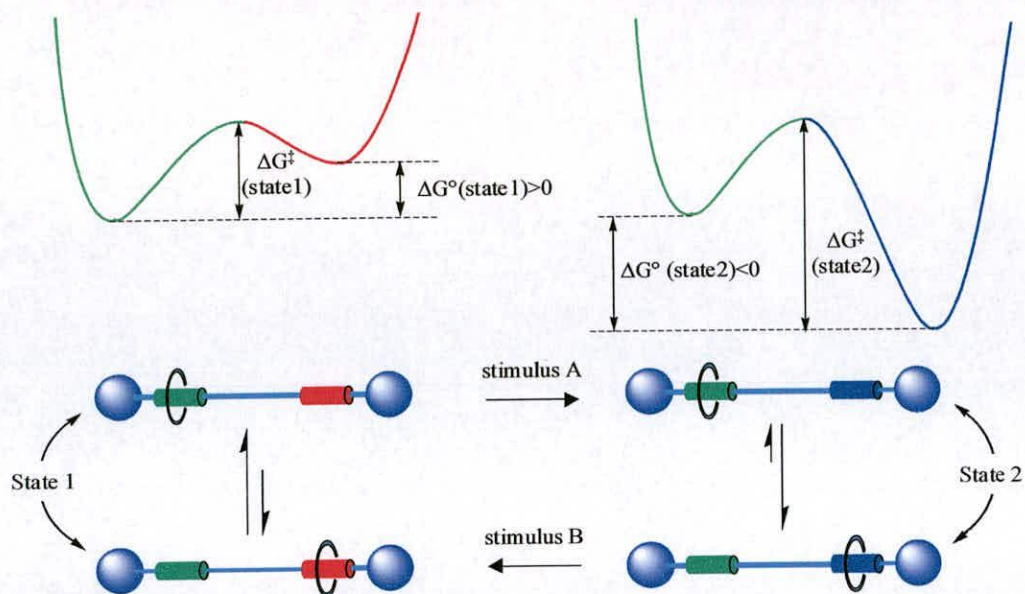
Figure 1.7. A cartoon representing a rotaxane as a molecular machine, showing the work cycle together with the associated potential energy curves for the two different states.

The same elements can exist within a catenane structure, where stations can exist within the ring structure of each of the macrocyclic components. As with their rotaxane counterparts the same movements can occur, i.e., pirouetting and translational motion with respect to one of the macrocyclic components, although technically these motions are both pirouetting if viewed from the perspective of the other ring. Another important goal is contained within the movement phenomena observed within catenated structures, that of the directionality of the translational motion. Hence, it is desirable to control the direction of any given movement within such systems. Nature provides an excellent example in which unidirectional motion is a key element in the function of a biological molecular motor in the guise of F_1-ATPase.[130]

Supramolecular complexes in the form of pseudorotaxanes[15] can also be considered as artificial molecular-level machines. However, while providing some good portents for the functioning and responses of corresponding interlocked molecules the lack of attendant mechanical bond allows dethreading and hence pseudorotaxanes are ultimately of less significance to this discussion.[138,139]

1.4.4 Molecular Machines Based on Interlocked Molecular Architectures Containing Transition Metal Ions

As we have seen previously, transition metals have been used effectively to construct interlocked molecular architectures in high yields. It would also seem, at first glance, that these molecules are also good candidates for molecular-level machines because transition metals have well studied redox properties which should enable the use of techniques, such as electrochemistry and photochemistry.[140]

Sauvage and co-workers provided an initial example of a switchable [2]catenate based on their stalwart Cu^I / phenanthroline system.[141] The switchable nature of the catenate was based on the preferred coordination number for two different redox states of copper. Hence, the construction of the catenate **91** itself is based on the preferred tetrahedral geometry of Cu^I oxidation state (CN = 4). Incorporation of a tridentate terpy ligand into the macrocyclic framework of one of the constituent rings of the [2]catenate provides the means for a 5-coordinate arrangement favored by the Cu^{II} oxidation state. Oxidation of the Cu^I catenate by chemical, electrochemical or photochemical[142] means, affords metastable Cu^I four coordinate system **92**. This transient species then undergoes rearrangement by circumrotation of one ring through another to afford the stable 5-coordinate Cu^{II} catenate **93**. The catenate **93** can be subsequently reduced back to the Cu^I oxidation state leading to the regenerate the starting complex. The kinetics of the circumrotation processes are contrasting in that formation of the Cu^{II} 5-coordinate system **93** is dependent on experimental conditions, whereas the regeneration of the original Cu^I 4-coordinate system is fast irrespective of the conditions employed. The formation of the Cu^{II} / 5-coordinate system **93** forms in minutes in anhydrous acetonitrile, but it requires hours or even days to go to completion in noncoordinating solvents or in the absence of coordinating anions. This indicates that the Cu^{II} species is stabilized by coordination to counterions or solvent molecules which lowers the energy barrier when relinquishing the phenanthroline unit from its coordination sphere in the initial step of the circumrotation process.
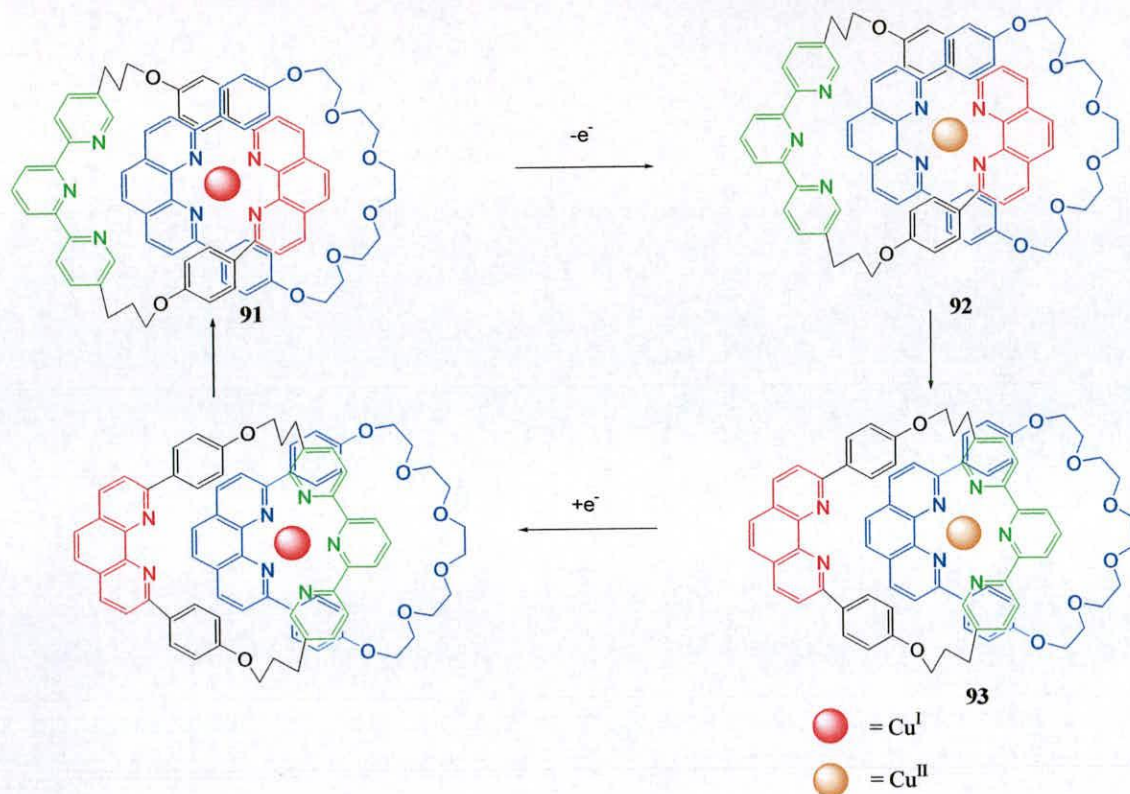
Scheme 1.37. An electrochemically-switchable copper-based catenate

Sauvage and co-workers, in subsequent studies has also reported the circumrotation of a symmetric [2]catenate incorporating two terpy and two phenanthroline ligands which can accommodate three distinct geometries within its central core.[143] Again chemical and electrochemical methods can be utilized to trigger the switching process.

Sauvage has also applied similar structural motifs in [2]rotaxanes to make molecular shuttles incorporating transition metals within their framework. The driving force again is based on the geometrical preferences of Cu^I and Cu^{II}-based complexes. The key requirement for such a system is the incorporation of two different coordinating units in the thread component of the rotaxane. The preparation of [2]rotaxane **94** incorporating tridentate terpy and bidentate phen units was reported in 1997 by Sauvage and co-workers.[144] The switching process is again triggered by oxidation of Cu^I to Cu^{II} by electrochemical means.[145] The conversion process from the copper (II) pentacordinate species **95** is relatively quick, but remains a slow process (hours), but is not affected by reaction conditions in contrast to the catenate systems. This is

a reflection of the "protection" afforded within catenated structure when compared to corresponding rotaxanes. The rate of conversion from the Cu^{II}-five coordinate to the Cu^{I}-four coordinate system is of a larger timeframe as compared to the corresponding catenate system, again because of structural considerations.
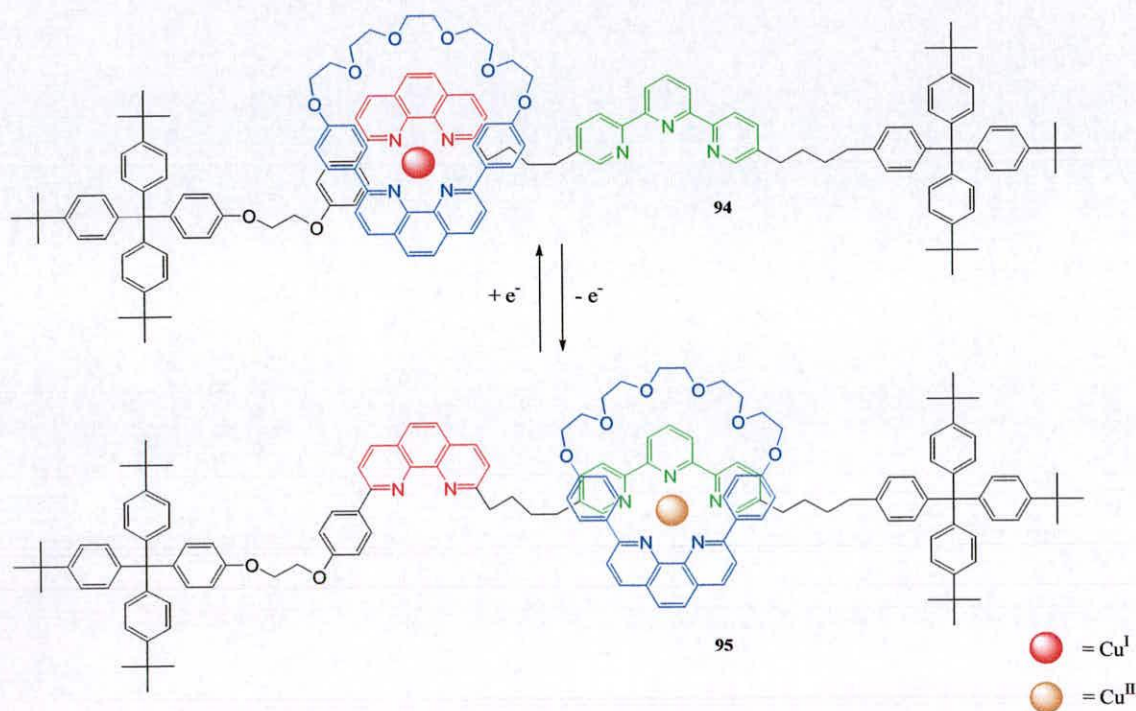
Scheme 1.38. An electrochemically-switchable copper-based [2]rotaxane

Sauvage and co-workers have also used electrochemical methods to induce pirouetting of the ring component in [2]rotaxane incorporating phen and terpy unit within the macrocyclic component.ion.[146]

In recent studies Sauvage and co-workers have also reported the synthesis of a so-called molecular muscle[147] which can adopt an extended and contracted conformation, which mimics the actin-myosin linear motor found in skeletal muscles.[130] The prerequisite for such a system is the formation of a doubly threaded topology shown in figure 1.8.

Extended Situation   Contracted Situation
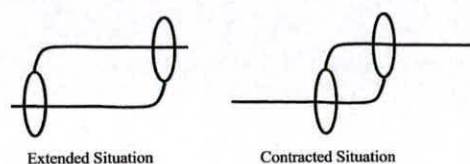
Figure 1.8. Doubly threaded topology-the precursor to a molecular muscle

The synthesis of such an assembly was reported in 2000 by Sauvage and co-workers.[148] The molecular muscle (a rotaxane-based dimer) was realized in 2001 and the movement is powered by the different coordination geometry adopted by the Cu^I and Zn^{II} cations. The molecule **96** was initially synthesized in its extended conformation with two Cu^I cations coordinating to two phenanthroline units each. Demetalation of **96** using KCN followed by treatment with Zn^{II} produces **97**, where contraction occurs in response to the new coordination requirements of the two Zn^{II} cations each coordinating a phenanthroline and a terpyridine unit. The original stretched conformation could be obtained again by subjecting **97** to $Cu(MeCN)_4 \cdot PF_6$. From CPK model estimations, the length of the compounds changes from 83 Å to 65 Å between extended and contracted situations, which is the same ratio as natural muscles (~27%).
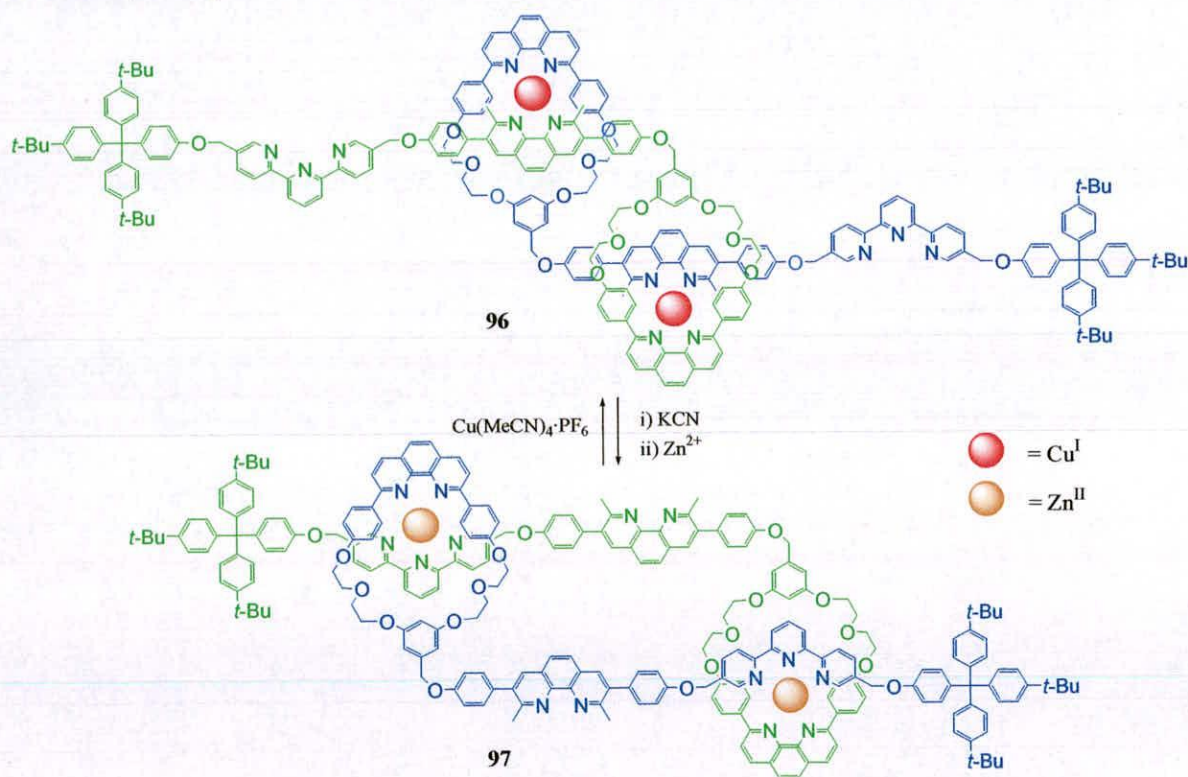
Scheme 1.39. The operation of a molecular muscle.

Sauvage and co-workers have reported a series of interlocked molecules involving controlled motion. However, despite the undoubted impressive nature of these molecules and the elegance of the associated photo- and electrochemical studies, the

general timescales on which the shuttling, pirouetting and circumrotating processes occur require a dramatic improvement if molecular-scale machines are to be feasible based on transition metal-based interlocked architectures.

In 2001, Jeong and co-workers reported the synthesis of molecular shuttle containing an osmate ester macrocycle.[52] However; the shuttle was kinetically unstable due to the reversible nature of the Os-N bonds. In 2003, Jeong and co-workers reported the synthesis of a corresponding system containing the less labile Re^I-bridged metallocycle, which is stable at room temperature.[149]

1.4.5 Molecular Machines Based on Interlocked Molecular Architectures Constructed *via* Hydrogen Bonding Interactions

In 1996, Leigh and co-workers reported the synthesis of a symmetrical [2]catenane **98** whose rings contain an isophthalic unit, together with a lipophilic alkyl chain moiety.[150] The amphiphilic catenane **98** displays solvent dependant translational isomerisation. Thus, in non-polar solvents, e.g. chloroform, the hydrogen bonds responsible for its formation are maintained **98a**, but in polar solvents, e.g. DMSO, the molecule undergoes a drastic rearrangement so that the alkyl chain fragments are buried in the centre of the molecule **98b**.

98a   **98b**
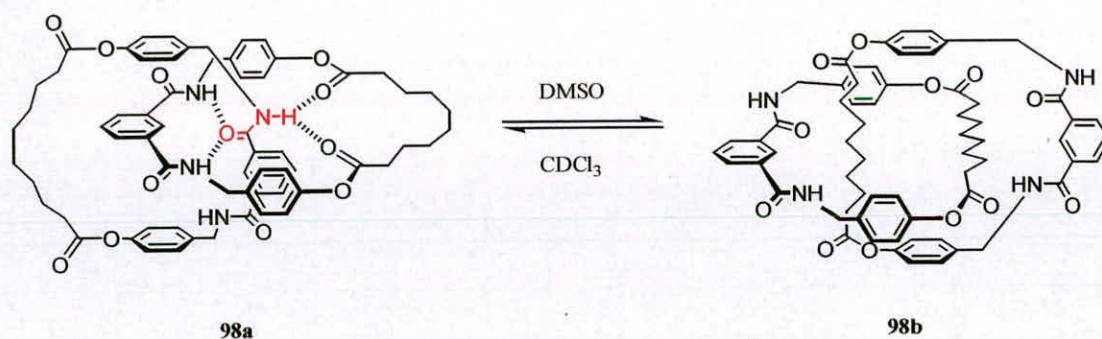
Scheme 1.40. Leigh's catenane chameleons

In 1997, Leigh and co-workers reported the same solvent-dependent translational isomerism in peptide-based [2]rotaxanes.[151] The molecular shuttles **99a-c** contain two identical glycylglycine stations separated by a variety of alkyl chain spacers. At room temperature in $CDCl_3$ the macrocycle shuttles between the two isoenergetic

stations spending half its time on each of the stations. The rate of shuttling depends on the distance between the two stations, with the macrocycle shuttling more rapidly the shorter the alkyl chain length. The shuttling movement occurs through the disruption of the hydrogen bonding interactions, which are the driving force for the formation of the rotaxane between the macrocyclic unit and the templating dipeptide station. The rate of shuttling can decreased by reducing the temperature or by the addition of a polar solvent such as methanol to compete with the intercomponent hydrogen bonds. Addition of a more polar solvent such as DMSO leads to the cessation of shuttling leading to the occupancy of the benzylic amide macrocycle on the alkyl chain.

CHCl$_3$ DMSO

99a, X=(CH$_2$)$_2$

99b, X=(CH$_2$)$_{10}$

99c, X=S
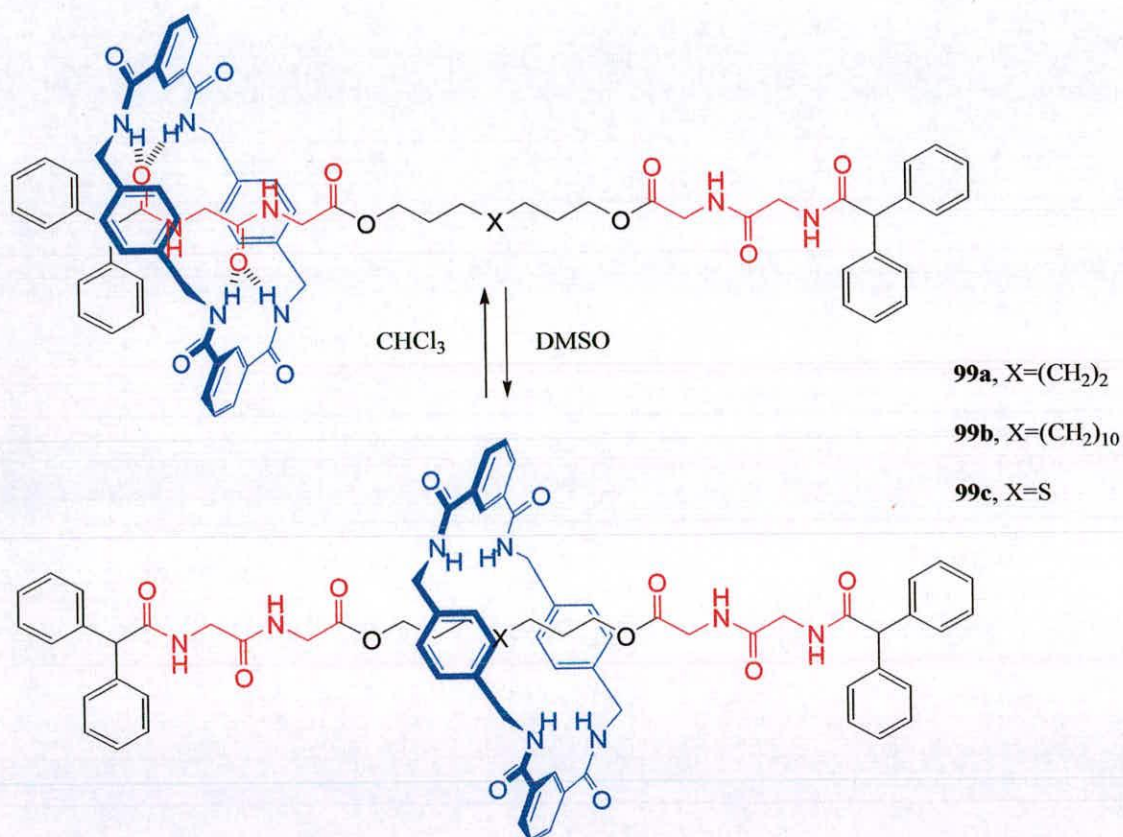
Scheme 1.41. Amphiphilic peptide-based molecular shuttles

Leigh and co-workers have utilized the photoactive fumaramide double bond to great effect in a number of benzylic amide-containing catenane and rotaxane based systems. The first example involves the treatment of a series of fumaramide-containing rotaxanes, e.g. *E*-**101** (Scheme 1.42) with light at 254nm causing isomerisation of the double bond (*E*→*Z*).[152] The rates of macrocyclic rotation of the

E- and *Z*-containing [2]rotaxanes were measured by ^{1}H NMR spectroscopy. The *Z*-derived rotaxane *Z*-**101** rotates faster by 6 orders of magnitude as compared to the corresponding *E*-isomer *E*-**101**. The rotaxane can be returned to its original state by thermal treatment of the *Z*-rotaxane at 120 °C for 4 days. This is clearly due to greater binding affinity of the benzylic amide macrocycle for the fumaramide template in contrast to the maleamide.
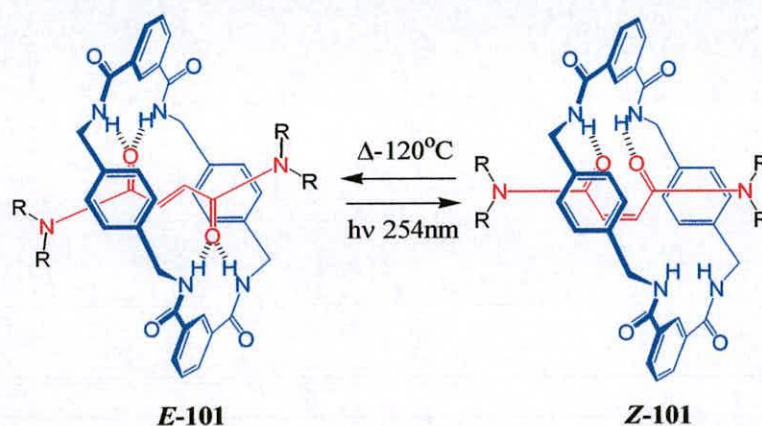
Scheme 1.42. The operation of a molecular accelerator

The fumaramide unit has also been incorporated into a molecular shuttle *E*-**102**, which is assembled through hydrogen bonding interactions.[153] The function of this molecular shuttle lies in the photochemical and thermal interconversion of fumaramide and maleamide groups. The incorporation of an amide-ester derived hydrogen-bond motif provides another binding site for the macrocycle. The irradiation of the fumaramide-based [2]rotaxane *E*-**102** resulted in isomerisation of the double bond with concomitant translocation of the macrocycle to the amide-ester station. The system can reset by thermal treatment at 120 °C for 4 days or reversible Michael addition. The system displays remarkable positional discrimination such that in both rotaxanes *E*-**102** and *Z*-**102** the station occupancy is approximately 95%.
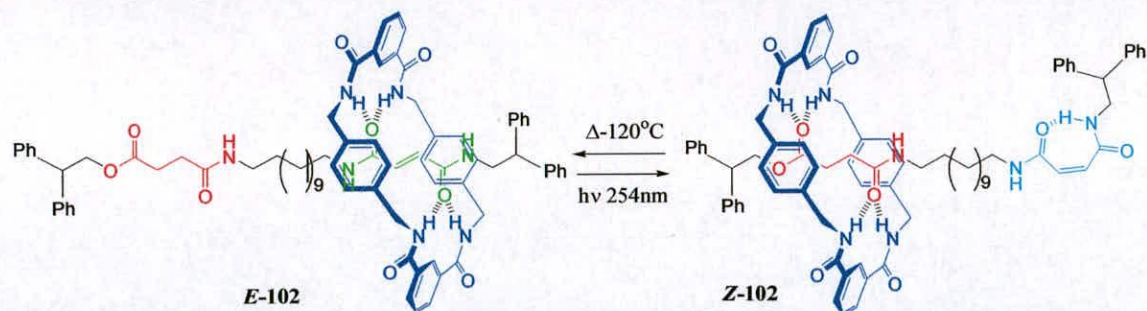
Scheme 1.43. Light and heat-switchable molecular shuttles with remarkable positional discrimination in the thread

Leigh and co-workers have also described the unidirectional motion in a 3-station [3]catenane containing two fumaramide-derived stations and an amide-ester derived station.[154] This represents the first example of an interlocked molecule displaying unidirectional rotation. It also demonstrates that chirality is not a prerequisite for unidirectional motion in interlocked molecular architectures as once thought.[155]

1.4.6 Molecular Machines Based on Interlocked Molecular Architectures Constructed by π-Electron rich Donors/ π-Electron Poor Acceptors

Stoddart has reported many examples of "controlled" motion in interlocked molecules using π-electron-deficient bipyridinium units and π-electron rich aromatic rich units. Indeed the first molecular shuttle was reported by Stoddart and co-workers in 1991.[156] The rotaxane 103^{4+} consists of a π-electron poor tetracationic cyclophane mechanically interlocked onto a linear thread containing two isoenergetic π-electron rich hydroquinone stations separated by a polyether spacer. Since the two stations are identical, the macrocyclic unit has no preference for either of the two sites and shuttles between them with a $k = 2360$ s^{-1} in $(CD_3)_2CO$ at 34 °C, as measured by ^1H NMR spectroscopy. The motion of the macrocycle is powered by the molecular tumbling of the medium which provides the energy required to overcome the free activation energy barrier between the two stations so that two "co-conformations" are obtained. This molecular shuttle does not perform any work because the $\Delta G°$ of the system is zero.
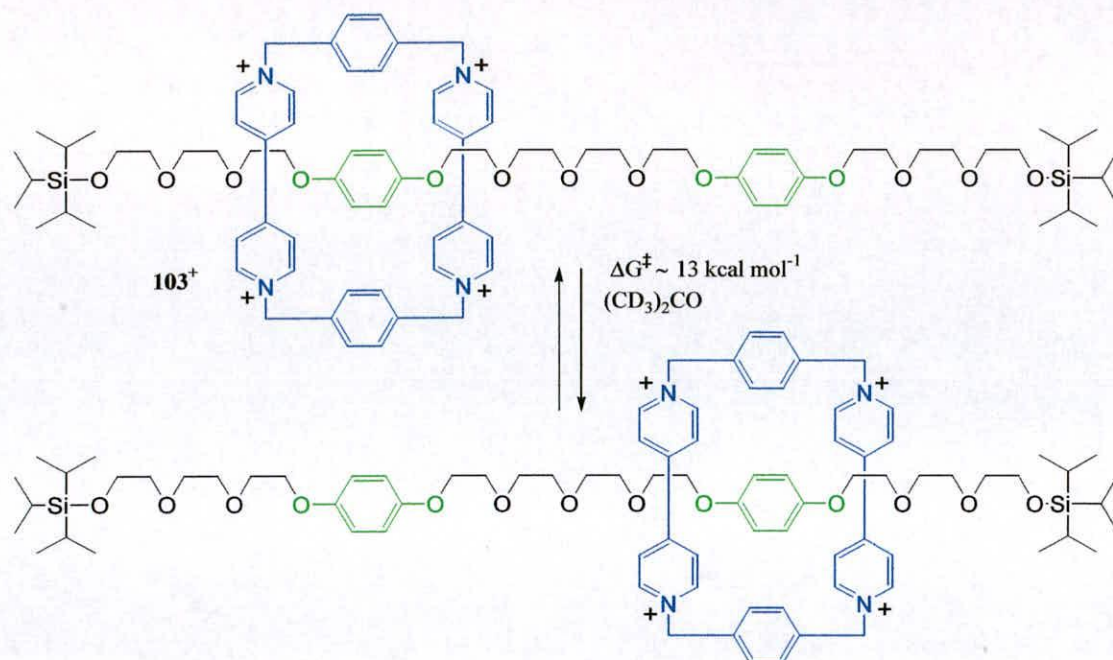
Scheme 1.44. The first molecular shuttle.

In order to have a stimuli-responsive [2]rotaxane the two binding sites on the thread must be different so that the $\Delta G°$ between the two stations is not zero. Stoddart and co-workers have described a number of molecular shuttles which were precursors to stimuli-responsive systems based on rotaxanes containing π-electron-deficient bipyridinium units and π-electron rich aromatic rich units.[157] In 1994, Stoddart and co-workers reported the first example of stimuli-responsive molecular shuttle.[158] This molecular shuttle consists of a π-electron poor tetracationic cyclophane macrocycle mechanically interlocked onto a thread containing two stations with different π-donor abilities, namely a benzidine and a biphenyl station. At –44 °C in CD_3CN the benzidine station has a greater π-electron donor ability than the biphenol station therefore the π-electron poor macrocyclic unit spends 84% of its time over it. An electrochemical stimulus oxidises the neutral benzidine unit to a monocationic radical (104^{4+}→105^{5+}·) and the resulting repulsion of charges induces the cyclophane unit to move to the biphenol station, which now provides the best stabilisation energy. Evidence of this molecular dynamic is obtained by analysing the cyclic voltammetric (CV) response of 104^{4+} and model compounds containing benzidine units. The shuttling process is reversible and cyclable therefore the original species 104^{4+} can be restored by reducing 105^{5+} restoring the original

equilibrium. The electrochemically-responsive tetracationic rotaxane **104**$^{4+}$ can also be switched by using a chemical stimulus. The macrocyclic cyclophane moves from the preferred benzidine station in **104**$^{4+}$ to the biphenol unit in **106**$^{6+}$ upon double protonation of the diamine unit. The shuttling movement can be reversed by deprotonation of the di-cationic amine upon addition of pyridine to **106**$^{6+}$ to afford the original species **104**$^{4+}$.
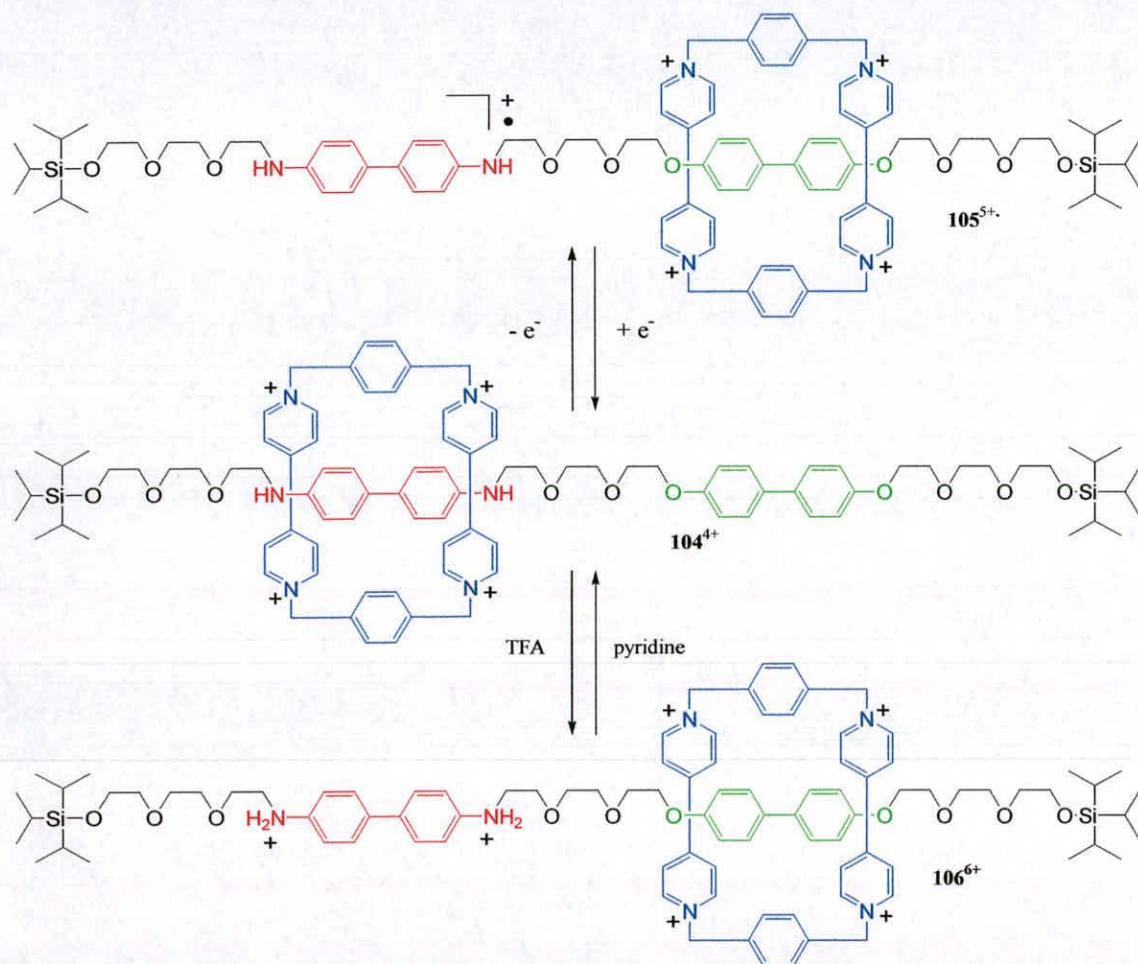
Scheme 1.45. Chemical and electrochemically driven molecular shuttle.

Stoddart and co-workers have also incorporated tetrathiafulvalene unit into the backbone of catenanes[159] and rotaxanes[160] to act as a redox active unit. In 1998, Stoddart reported the preparation of a [2]catenane **107** consisting of a π-electron poor tetracationic cyclophane macrocycle and a macrocycle incorporating a TTF unit and a π-electron rich 1,5-dioxynapthalene moiety.[161] The π-electron poor macrocycle encapsulates the TTF unit in the ground state of the system, but on

oxidation of the TTF unit by either chemical or electrochemical means causes translocation, such that the tetracationic cyclophane occupies the 1,5-dioxynapthalene moiety **108**. The oxidation/ reduction cycle can be repeated many times using both chemical and electrochemical methods.
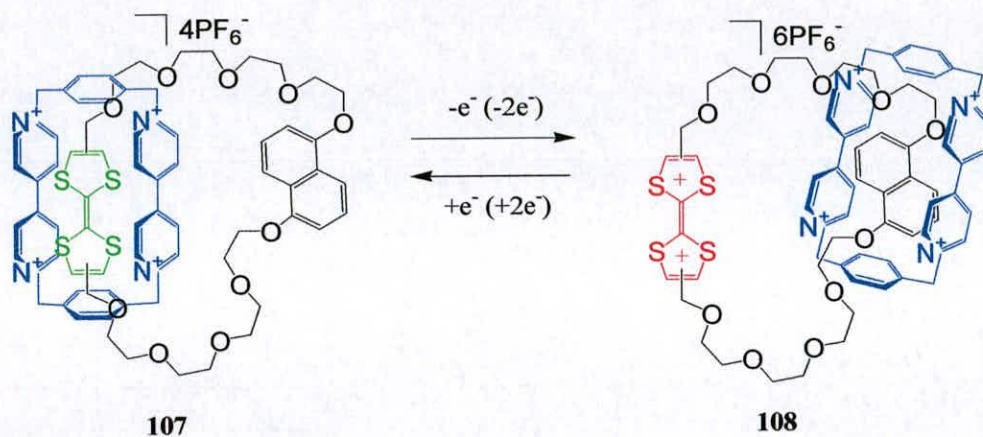
Scheme 1.46. Chemical and electrochemically-switchable [2]catenane incorporating a TTF unit.

The switchable [2]catenane **107** can form stable Langmuir films in the presence of dimyristoylphosphatidyl (DMPA) anions and monolayers were transferred onto a Au(111) substrate and studied by scanning tunnelling microscopy.[162] Differences were observed between the monolayer containing the two different translational isomer **107**, **108**, such that **107** conducted current above +0.3 V, whereas **108**, exhibited a linear I-V curve reminiscent of a metal. Stoddart and Heath reported the preparation of solid state version of the TTF-containing [2]catenane in 2000.[163] The switching device is fabricated from a single monolayer of [2]catenane anchored with DMPA counterions, and sandwiched between two electrodes. The device exhibits bistable current/ voltage characteristics and can be recycled many times under ambient temperature, with little loss of function. Stoddart and Heath have also exploited rotaxane architectures in electronic switching devices, but these systems lack the relative stability when compared to the corresponding catenanes.[164]

Stoddart has reported a series of molecular shuttles, whereby the thread component of the rotaxane incorporates both ammonium ion and bipyridinium binding sites (stations) for crown ether-based macrocycles. As one of the stations contains an ammonium ion, the most obvious stimuli to employ in switching the position of the

macrocycle is that of acid and base. Indeed Stoddart and co-workers reported the synthesis of an acid-base controllable molecular shuttle in 1997.[165] The synthesis of the [2]rotaxane **109**$^{3+}$ is achieved through a *threading/ capping* approach such that the macrocycle component occupies the ammonium ion moiety. Treatment of rotaxane **109**$^{3+}$with diisopropylethyl amine deprotonates the NH_2+ centre and the macrocycle moves to the bipyridinium station to form **110**$^{2+}$, as followed using ^1H NMR. The process can be reversed upon addition of TFA to **110**$^{2+}$, which reprotonates the NH_2 centre.
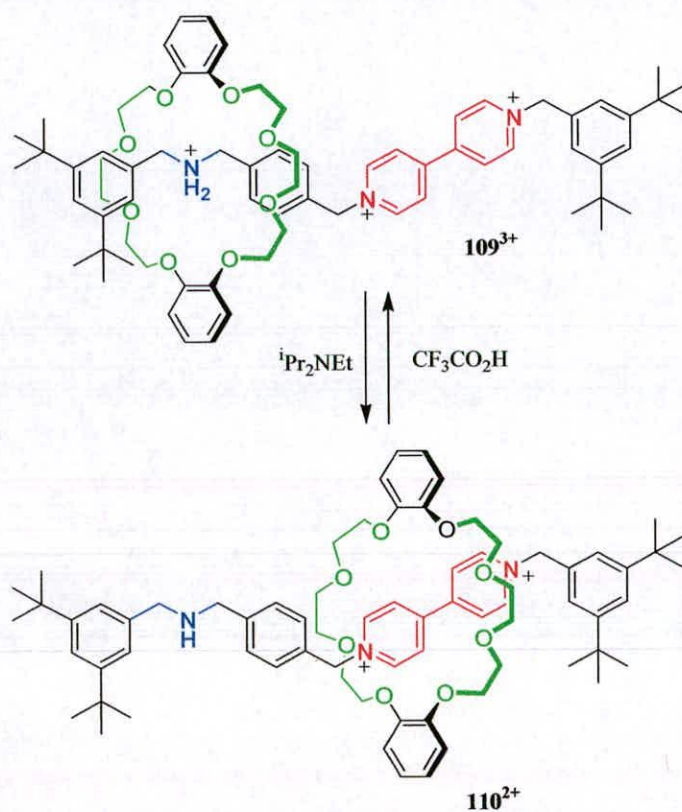
Scheme 1.47. Acid-base switchable molecular shuttle.

1.4.7 Molecular Machines Based on Interlocked Molecular Architectures Containing Cyclodextrins

The assembly of molecular shuttles containing cyclodextrins have also been reported.[166] In 1997, Nakashima and co-workers reported the synthesis of a light-driven molecular shuttle.[167] The molecular shuttle *E*-**111** contained a thread component incorporating a photoactive azobenzene unit encircled by an α-cyclodextrin macrocycle. The rotaxane *E*-**111** was prepared by threading of an azobenzene component through α-cyclodextrin. The cyclodextrin ring resides around the trans-azobenzene function. When the rotaxane *E*-**111** is exposed to light (360nm) the azobenzene unit isomerizes from *trans* to *cis* and the α-cyclodextrin translocates to reside on the ethylene glycol chains *Z*-**111**. The original rotaxane can be re-obtained by irradiation with light (430nm).
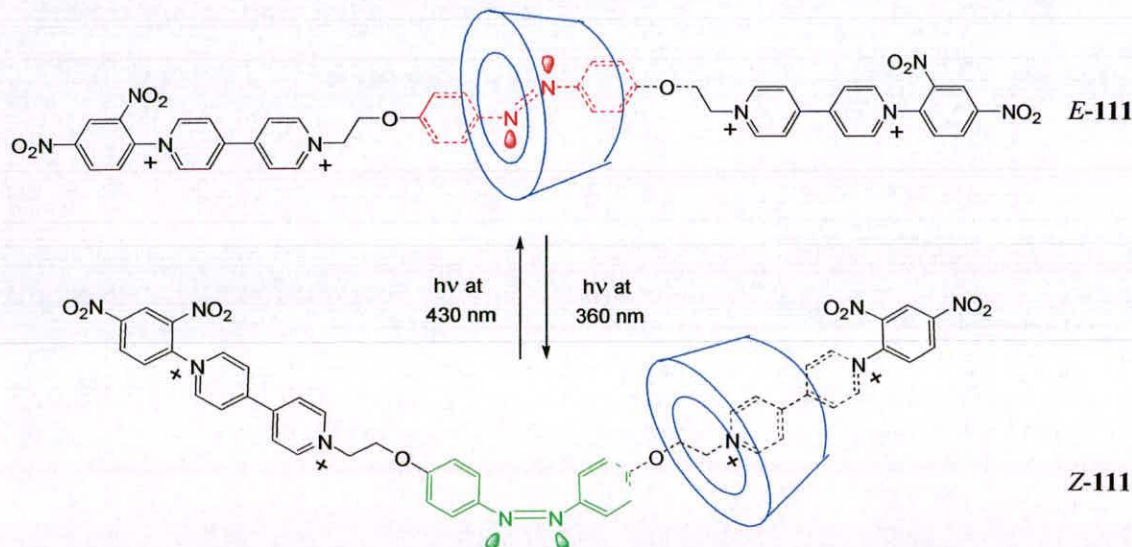
Scheme 1.48. Light-driven molecular shuttle based on a cyclodextrin-containing [2]rotaxane.

Recently an example of unidirectional shuttling in an α-cyclodextrin-containing [2]rotaxane has been reported by Anderson and co-workers (*E*-**112**, Scheme 1.49).[168] The translational movement of the macrocycle is based on the reversible *E/Z* photochemical isomerisation of a stilbene unit incorporated on the thread. Isomerisation at 340 nm of *E*-**112** to the *cis* isomer *Z*-**112** induces the macrocycle to move from the stilbene station in a unidirectional shuttling movement and brings the

major rim of the α-cyclodextrin close to one of the thread stoppers, as confirmed by NOE investigation. The co-conformer bearing the macrocycle over the other end of the thread is not observed. The $E{\rightarrow}Z$ isomerisation process can be reversed by irradiating Z-**112** at 265 nm to reform E-**112**.
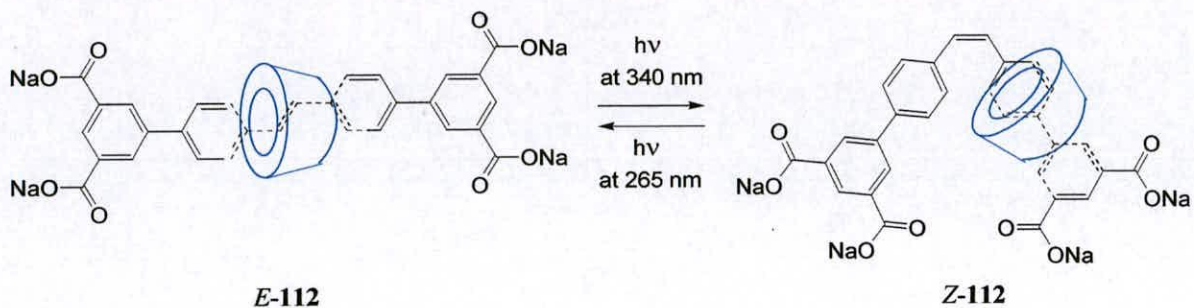
Scheme 1.49. Unidirectional motion in a cyclodextrin-containing [2]rotaxane.

Harada has also reported the synthesis of molecular shuttles, based on cyclodextrin derived rotaxanes that contain energetically favored and disfavored portions within the length of the thread component.[169]

Presently, the inherent limitations in stimuli-responsive molecular shuttles based on cyclodextrin derived rotaxanes are the positional discrimination in such systems, i.e. the binding strengths of stations (on the thread) for the macrocyclic components are non-existent or ill-defined at best. This is best illustrated in the above examples as the macrocycle tends to take the path of least resistance. More studies are required to clarify this situation.

1.5 Conclusions and Perspectives

As we have seen during this first chapter, interlocked molecular architectures have made the transition from mere laboratory curiosities to potentially useful molecules with possible applications in many spheres of applied science. This transition is due, in the main, to the exploitation of noncovalent interactions to pre-organize and assemble intermediates to access such constructs in high yields and also the associated novel properties conferred on such molecules, as a consequence of interlocking. The structural tolerance of many of these recognition motifs has been well explored and the synthesis of simple interlocked molecular architectures is no longer an obstacle. However, the incorporation of further levels of functionality and complexity within the framework of interlocked molecular architectures is a clear long-term objective if we are to be able to explore more applications and uses of such molecules. Another goal within the synthetic arena remains the controlled synthesis of more complex molecular architectures, such as Borromean rings and overhand knots to demonstrate the "state of the art".[170]

A few of the syntheses described in chapter 1 are those where the system is under thermodynamic control and in many of these examples the product distribution can be perturbed by altering the reaction conditions. At the present time many of the syntheses of interlocked molecules that are under thermodynamic control unfortunately afford kinetically unstable products. Hence, efforts should be centred on developing methodologies constructing interlocked molecules under thermodynamic control, but to afford products with the requisite kinetic stability. This goal has been aided and abetted in recent years by the development of so-called dynamic covalent chemistry (DCC).[171]

A clear target for many chemists in the field of interlocked molecular architectures is that of the generation of polymeric interlocked molecules such as polycatenanes and polyrotaxanes.[172] The tantalizing physical properties that could be bestowed on such mechanically interlocked polymers are exciting and include solubility, viscosity and intercomponent motion in the solid-state. However, whilst many

polymeric interlocked molecules[173] have been reported a clear improvement in the integrity of future systems remains a hurdle.

The most intriguing aspect of this future research is the possibility of using interlocked architectures as molecular-level devices. However, the research is currently at an embryonic stage and several issues remain if mechanically interlocked molecules are to advance to the next level of complexity towards true synthetic molecular machines. Many of the molecular shuttles detailed in Section 1.5 lack the positional discrimination or the shuttling timescales that would be needed in molecular machines. This fact needs to be addressed and could possibly be achieved through the using genuinely hybrid systems that combine advantages of both. A short term objective is to determine if the motion phenomena observed in interlocked molecules in solution state is transferred to the solid-state and with what efficiency. The efficient orderly assembly of molecular switches (based on interlocked molecules) onto surfaces such as gold and their subsequent fabrication into electrical junctions and circuits is also a necessary development. Clearly there are many obstacles to overcome if mechanically interlocked molecules are to realise their potential as molecular-level devices, but Feynman's vision appears to be in good hands.

Within the goals of designed research programmes, the potential for serendipitous discoveries and paradigms resulting from such phenomena are clearly a factor for the future prospects for the applications for interlocked molecular architectures. This can be observed within some of the examples contained within this introductory chapter. Clearly, however it is down to the creativity and imagination of the scientists involved in the field that will ultimately determine the fate of interlocked molecular architectures.

1.6 References

1   K. C. Nicolaou, E. J. Sorensen (Eds), *Classics in Total Synthesis*, VCH, Weinheim, **1996**.

2   G. L. Patrick (Ed), *An Introduction to Medicinal Chemistry*, Oxford University Press, New York, **2001**.

3   For reviews see: a) D. M. Walba, *Tetrahedron* **1985**, *41*, 3161-3212; b) G. A. Breault, C. A. Hunter, P. C. Mayers, *Tetrahedron* **1999**, *55*, 5265-5293.

4   For general review into the synthesis of interlocked molecular architectures see: a) D. B. Amabilino, J. F. Stoddart, *Chem. Rev.* **1995**, *95*, 2725-2828; b) J.-P. Sauvage, C. Dietrich-Buchecker (Eds.), *Molecular Catenanes Rotaxanes and Knots*: *A Journey Through the World of Molecular Topology*, Wiley-VCH, Weinheim, **1999**.

5   a) J.-M. Lehn, *Angew. Chem. Int. Ed. Engl.* **1990**, *29*, 1304-1319; b) J.-M. Lehn, *Supramolecular Chemisty: Concepts and Perspectives*, VCH, Weinheim, **1995**; c) Special issue on supramolecular chemistry see: *Proc. Natl. Acad. Sci. U. S. A.* **2002**, *99*, 4763-5206.

6   J-M. Lehn, *Angew. Chem. Int. Ed. Engl.* **1988**, *27*, 89-112.

7   D. J. Cram, *Angew. Chem. Int. Ed. Engl.* **1988**, *27*, 1009-1021.

8   C. J. Pedersen, *Angew. Chem. Int. Ed. Engl.* **1988**, *27*, 1021-1027.

9   a) *Comprehensive Supramolecular Chemistry*, **1996**, Pergamon, Oxford, UK; b) Special issue on molecular recognition see: *Chem. Rev.* **1997**, *97*, 1231-1734.

10   For reviews and discussions on self-assembly in natural and non-natural systems see: a) J. S. Lindsey *New J. Chem.* **1991**, *15*, 153-180; b) D. Philp, J. F. Stoddart, *Angew. Chem. Int. Ed. Engl.* **1996**, *35*, 1155-1196; c) G. M. Whitesides, J. P. Mathias, C. T. Seto, *Science* **1991**, *254*, 1312-1317; d) A. Klug, *Angew. Chem. Int. Ed. Engl.* **1983**, *22*, 565-582; e) D. S. Lawrence, T. Jiang, M. Levett, *Chem. Rev.* **1995**, *95*, 2229-2260.

11   For reviews of the use templates in synthesis see: a) S. Anderson, H. L. Anderson, J. K. M. Sanders, *Acc. Chem. Res.* **1993**, *26*, 469-475; b) R. Hoss, F. Vögtle, *Angew. Chem. Int. Ed. Engl.* **1994**, *33*, 375-384; c) F. Diederich, P. J. Stang (Eds), *Templated Organic Synthesis*, Wiley-VCH, Weinheim, 1999.

12   M. Venturi, A. Credi, V. Balzani (Eds), *Molecular Devices and Machines - A Journey into the Nanoworld*, Wiley-VCH, Weinheim, **2003**.

13   For a recent perspective on the novel properties of rotaxanes see: D. A. Leigh, A. Murphy, *Chem Ind.* **80**, 178-183.

14   For a recent discussion of the nomenclature of interlocked architectures see: O. Safarowsky, B. Windisch, A. Mohry, F. Vögtle, *J. Prakt. Chem.* **2000**, *342*, 437-444.

15   For a pictorial representation of more complex interlocked architectures see: T. J. Hubin, D. H. Busch, *Coord. Chem. Rev.* **2000**, *200*, 5-52.

16   P. R. Ashton, D. Philp, N. Spencer, J. F. Stoddart, *J. Chem. Soc. Chem. Commun.* **1991**, 1677-1679.

17   E. Wasserman, *J. Am. Chem. Soc.* **1960**, *82*, 4433-4434.

18   I. T. Harrison, S. Harrison, *J. Am. Chem. Soc.* **1967**, *89*, 5723-5724.

19   I. T. Harrison, *J. Chem. Soc. Chem. Commun.* **1972**, 231-232.

20   I. T. Harrison, *J. Chem. Soc. Perkin Trans. 1* **1974**, 301-304.

21   a) E. Wasserman, D. A. Ben-Efraim, R. Wolovsky, *J. Am. Chem. Soc.* **1968**, *90*, 3286-3287; b) R. Wolovsky, *J. Am. Chem. Soc.* **1970**, *92*, 2132-2133; c) D. A. Ben-Efraim, C. Batich, E. Wasserman, *J. Am. Chem. Soc.* **1970**, *92*, 2133-2135.

22   G. J. M. Gruter, O. S. Akkerman, F. Bickelhaupt, *Tetrahedron* **1996**, *52*, 2565-2572.

23   D. M. Walba, R. M. Richards, R. C. Haltiwanger, *J. Am. Chem. Soc.* **1982**, *104*, 3219-3221.

24   For an excellent review of Schill's early work see G. Schill (Ed), *Catenanes, Rotaxanes and Knots*; Academic Press, New York, 1971.

25   G. Schill, A. Lüttringhaus, *Angew. Chem. Int. Ed. Engl.* **1964**, *5*, 546-547.

26   N. V. Gerbeleu, V. B. Arion, J. Burgess (Eds), *Template Synthesis of Macrocyclic Compounds*, Wiley-WCH, Weinheim, **2003**.

27   N. F. Curtis, D. A. House, *Chem. Ind.* **1961**, *42*, 1708-1709.

28   M. C. Thompson, D. H. Busch, *J. Am. Chem. Soc.* **1964**, *86*, 3651-3656.

29   For an example see: T. J. McMurry, S. J. Rodgers, K. N. Raymond, *J. Am. Chem. Soc.* **1987**, *109*, 3451-3453.

30   H. L. Frisch, E. Wasserman, *J. Am. Chem. Soc.* **1961**, *83*,3789-3795.

31   C. O. Dietrich-Bucheker, J.-P. Sauvage, J.-P. Kintzinger, *Tetrahedron Lett.* **1983**, *24*, 5095-5098.

32   For reviews of Sauvage's early work see: a) C. O. Dietrich-Buchecker, J.-P. Sauvage, *Chem. Rev.* **1987**, *87*, 795-810; b) J.-P. Sauvage, *Acc. Chem. Res.* **1990**, *23*, 319-327.

33   C. O. Dietrich-Bucheker, J.-P. Sauvage, *Tetrahedron Lett.* **1983**, *24*, 5091-5094.

34   a) C. O. Dietrich-Bucheker, J.-P. Sauvage, J.-M. Kern, *J. Am. Chem. Soc.* **1984**, *106*, 3043-3045; b) C. O. Dietrich-Bucheker, J.-P. Sauvage, *Tetrahedron*, **1990**, *46*, 503-512.

35   a) A.-M. Albrecht-Gary, Z. Saad, C. O. Dietrich-Bucheker, J.-P. Sauvage, *J. Am. Chem. Soc.* **1985**, *107*, 3205-3209; b) A.-M. Albrecht-Gary, C. O. Dietrich-Bucheker, Z. Saad, J.-P. Sauvage, *J. Am. Chem. Soc.* **1988**, *110*, 1467-1472.

36   a) B. Mohr, M. Weck, J.-P. Sauvage, R. H. Grubbs, *Angew. Chem. Int. Ed. Engl.* **1997**, *36*, 1308-1310; b) M. Weck, B. Mohr, J.-P. Sauvage, R. H. Grubbs, *J. Org. Chem.* **1999**, *64*, 5463-5471.

37   R. H. Grubbs, S. J. Miller, G. C. Fu, *Acc. Chem. Res.* **1995**, *28*, 446-452.

38   D. A. Leigh, P. J. Lusby, S. J. Teat, A. J. Wilson, J. K. Y. Wong, *Angew. Chem. Int. Ed.* **2001**, *40*, 1538-1543.

39   A. L. Vance, N. W. Alcock, J. A. Heppert, D. H. Busch, *Inorg. Chem.* **1998**, *37*, 6912-6920.

40   C. Wu, P. R. Lecavalier, Y. X. Shen, H. W. Gibson, *Chem. Mat.* **1991**, *3*, 569-572.

41   M.-J. Blanco, M. C. Jiménez, J.-C. Chambron, V. Heitz, M. Linke, J.-P. Sauvage, *Chem. Soc. Rev.* **1999**, *28*, 293-305 and references cited therein.

42   a) E. Wasserman, *Sci. Am.* **1962**, *207*, 94-98; b) V. I. Sokolov, *Russ. Chem. Rev.* **1973**, *42*, 452-463.

43   C. O. Dietrich-Buchecker, J.-P. Sauvage, *Angew. Chem. Int. Ed. Engl.* **1989**, *28*, 189-192.

44   C. O. Dietrich-Buchecker, J. Guilhem, C. Pascard, J.-P. Sauvage, *Angew. Chem. Int. Ed. Engl.* **1990**, *29*, 1154-1156.

45   C. O. Dietrich-Bucheker, J.-F. Nierengarten, J.-P. Sauvage, N. Armaroli, V. Balzani, L. De Cola, *J. Am. Chem. Soc.* **1993**, *115*, 11237-11244.

46   C. O. Dietrich-Buchecker, J.-P. Sauvage, A. De Cian, J. Fischer, *J. Chem. Soc. Chem. Commun.* **1994**, 2231-2232.

47   C. Dietrich-Buchecker, G. Rapenne, J.-P. Sauvage, *Chem. Commun.* **1997**, 2053-2054.

48   C. Dietrich-Buchecker, G. Rapenne, J.-P. Sauvage, *Coord. Chem. Rev.* **1999**, *186*, 167-176.

49   M. Fujita, F. Ibukuro, H. Hagihara, K. Ogura, *Nature* **1994**, *367*, 720-723.

50   M. Fujita, F. Ibukuro, H. Seki, O. Kamo, M. Imanari, K. Ogura, *J. Am. Chem. Soc.* **1996**, *118*, 899-900.

51   M. Fujita, F. Ibukuro, K. Yamaguchi, K. Ogura, *J. Am. Chem. Soc.* **1995**, *117*, 4175-4176.

52   K.-S. Jeong, J. S. Choi, S.-Y. Chang, H.-Y. Chang, *Angew. Chem. Int. Ed.* **2000**, *39*, 1692-1695.

53   S.-Y. Chang, J. S. Choi, K.-S. Jeong, *Chem. Eur. J.* **2001**, *7*, 2687-2697.

54   D. P. Mingos, J. Yau, S. Menzer, D. J. Williams, *Angew. Chem. Int. Ed. Engl.* **1995**, *34*, 1894-1895.

55   a) C. P. McArdle, M. J. Irwin, M. C. Jennings, R. J. Puddephatt, *Angew. Chem. Int. Ed.* **1999**, *38*, 3376-3378; b) C. P. McArdle, M. J. Irwin, M. C. Jennings, J. J. Vittal, R. J. Puddephatt, *Chem. Eur. J.* **2002**, *8*, 723-734.

56   *Hydrogen Bonding in Biological Structures*; G. A. Jeffrey, W. Saenger, (Eds.), Springer-Verlag, Berlin, **1991**.

57   L. J. Prins, D. N. Reinhoudt, P. Timmerman, *Angew. Chem. Int. Ed.* **2001**, *40*, 2382-2426.

58   For reviews see: a) F. Vögtle, T. Dünnwald, T. Schmidt, *Acc. Chem. Res.* **1996**, *29*, 451-460; b) R. Jäger, F. Vögtle, *Angew. Chem. Int. Ed. Engl.* **1997**, *36*, 930-944.

59   For a recent review on anion-templated synthesis see: R. Vilar, *Angew. Chem. Int. Ed.* **2003**, *42*, 1460-1477.

60   For reviews see: a) P. T. Glink, C. Schiavo, J. F. Stoddart, D. J. Williams, *Chem. Commun.* **1996**, 1483-1490; b) S. J. Cantrill, A. R. Pease, J. F. Stoddart, *J. Chem. Soc. Dalton Trans.* **2000**, 3715-3734.

61   C. A. Hunter, *J. Am. Chem. Soc.* **1992**, *114*, 5303-5311.

62   C. A. Hunter, *J. Chem. Soc. Chem. Commun.* **1991**, 749-751.

63   H. Adams, F. J. Carver C. A. Hunter, *J. Chem. Soc. Chem. Commun.* **1995**, 809-810.

64   a) C. A Hunter, D. H. Purvis, *Angew. Chem. Int. Ed. Engl.* **1992**, *34*, 792-795; b) F. J. Carver, C. A. Hunter, R. J. Shannon, *J. Chem. Soc. Chem. Commun.* **1994**, 1277-1280.

65   F. Vögtle, S. Meier, R. Hoss, *Angew. Chem. Int. Ed. Engl.* **1992**, *31*, 1619-1622.

66   S. Ottens-Hildebrandt, S. Meier, W. Schmidt, F. Vögtle, *Angew. Chem. Int. Ed. Engl.* **1994**, *33*, 1767-1770.

67   C. Seel, A. H. Parham, O. Safarowsky, G. M. Hübner, F. Vögtle, *J. Org. Chem.* **1999**, *64*, 7236-7242.

68   S. Ottens-Hildebrandt, M. Nieger, K. Rissanen, J. Rouvinen, S. Meier, G. Harder, F. Vögtle, *J. Chem. Soc. Chem. Commun.* **1995**, 777-778.

69   S. Ottens-Hildebrandt, T. Schmidt, J. Harren, F. Vögtle, *Liebigs Ann.* **1995**, 1855-1860.

70   a) C. Yamamoto, Y. Okamoto, T. Schmidt, R. Jäger, F. Vögtle, *J. Am. Chem. Soc.* **1997**, *119*, 10547-10548; b) A. Mohry, F. Vögtle, M. Nieger, H. Hupfer, *Chirality* **2000**, *12*, 76-83.

71   F. Vögtle, M. Händel, S. Meier, S. Ottens-Hildebrandt, F. Ott, T. Schmidt, *Liebigs Ann.* **1995**, 739-743.

72   a) R. Jäger, S. Baumann, M. Fischer, O. Safarowsky, M. Nieger, F. Vögtle, *Liebigs Ann.* **1997**, 2269-2273; b) F. Vögtle, M. Händel, S. Ottens-Hildebrandt, W. Schmidt, *Synthesis* **1996**, 353-356; c) O. Braun, A. Hünten, F. Vögtle, *J. Prakt. Chem.* **1999**, *341*, 542-547; d) T. Dünnwald, A. H. Parham, F. Vögtle, Synthesis **1998**, 339-348.

73   A. G. Johnston, D. A. Leigh, R. J. Pritchard, M. D. Deegan, *Angew. Chem. Int. Ed. Engl.* **1995**, *34*, 1209-1212.

74   A. G. Johnston, D. A. Leigh, L. Nezhat, J. P. Smart, M. D. Deegan, *Angew. Chem. Int. Ed. Engl.* **1995**, *34*, 1212-1216.

75   a) A. G. Johnston, D. A. Leigh, A. Murphy, J. P. Smart, M. D. Deegan, *J. Am. Chem. Soc.* **1996**, *118*, 10662-10663. b) A. G. Johnston, D. A. Leigh, A. Murphy, J. P. Smart, *Bull. Soc. Chim. Belg.* **1996**, *105*, 721-727.

76   D. A. Leigh, A. Murphy, J. P. Smart, A. M. Z. Slawin, *Angew. Chem. Int. Ed. Engl.* **1997**, *36*, 728-732.

77   a) M. Asakawa, G. Brancato, M. Fanti, D. A. Leigh, T. Shimizu, A. M. Z. Slawin, J. K. Y. Wong, F. Zerbetto, S. W. Zhang, *J. Am. Chem. Soc.* **2002**, *124*, 2939-2950; b) G. Brancato, F. Coutrot, D. A. Leigh, A. Murphy, J. K. Y. Wong, F. Zerbetto, *Proc. Natl. Acad. Sci. U. S. A.* **2002**, *99*, 4967-4971.

78   F. G. Gatti, D. A. Leigh, S. A. Nepogodiev, A. M. Z. Slawin, S. J. Teat, J. K. Y. Wong, *J. Am. Chem. Soc.* **2001**, *123*, 5983-5989.

79   a) T. J. Kidd, D. A. Leigh, A. J. Wilson, *J. Am. Chem. Soc.* **1999**, *121*, 1599-1600; b) J. S. Hannam, T. J. Kidd, D. A. Leigh, A. J. Wilson, *Org. Lett.* **2003**, *5*, 1907-1910.

80   G. M. Hübner, J. Gläser, C. Seel, F. Vögtle, *Angew. Chem. Int. Ed.* **1999**, *38*, 383-386.

81   G. M. Hübner, C. Reuter, C. Seel, F. Vögtle, *Synthesis* **2000**, 103-108.

82   C. A. Schalley, G. Silva, C. F. Nising, P. Linnartz, *Helv. Chim. Acta* **2002**, *85*, 1578-1596.

83   a) A. Bianchi, K. James-Bowman, E. Garcia-España (Eds), *Supramolecular Chemistry of Anions*, Wiley-VCH, New York, 1997; b) P. D. Beer, P. A. Gale, *Angew. Chem. Int. Ed.* **2001**, *40*, 486-516; c) M. Berger, F. P. Schmidtchen, *Chem. Rev.* **1997**, *97*, 1609-1646.

84   a) J. A. Wisner, P. D. Beer, M. G. B. Drew, *Angew. Chem. Int. Edit.* **2001**, *40*, 3606-3609; b) J. A. Wisner, P. D. Beer, M. G. B. Drew, M. R. Sambrook, *J. Am. Chem. Soc.* **2002**, *124*, 12469-12476.

85   a) K. Kavallieratos, C. M. Bertao, R. H. Crabtree, *J. Org. Chem.* **1999**, *64*, 1675-1683; b) K. Kavallieratos, S. R. de Gala, D. J. Austin, R. H. Crabtree, *J. Am. Chem. Soc.* **1997**, *119*, 2325-2326.

86   a) C. J. Pedersen, *J. Am. Chem. Soc.* **1967**, *89*, 7017-7036; b) D. J. Cram, J. M. Cram, *Acc. Chem. Res.* **1978**, *11*, 8-14.

87   a) P. R. Ashton, P. J. Campbell, E. J. T. Chrystal, P. T. Glink, S. Menzer, D. Philp, N. Spencer, J. F. Stoddart, P. A. Tasker, D. J. Williams, *Angew. Chem. Int. Ed. Engl.* **1995**, *34*, 1865-1869; b) P. R. Ashton, E. J. T. Chrystal, P. T. Glink, S. Menzer, C. Schiavo, N. Spencer, J. F. Stoddart, P. A. Tasker, A. J. P. White, D. J. Williams, *Chem. Eur. J.* **1996**, *2*, 709-728.

88   J. C. Metcalfe, J. F. Stoddart, G. Jones, *J. Am. Chem. Soc.* **1977**, *99*, 8317-8319.

89   A. G. Kolchinski, D. H. Busch, N. W. Alcock, *J. Chem. Soc. Chem. Commun.* **1995**, 1289-1291.

90   A. G. Kolchinski, N. W. Alcock, R. A. Roesner, D. H. Busch, *Chem. Commun.* **1998**, 1437-1438.

91   P. R. Ashton, P. T. Glink, J. F. Stoddart, P. A. Tasker, A. J. P. White, D. J. Williams, *Chem. Eur. J.* **1996**, *2*, 729-736.

92   S. J. Cantrill, S. J. Rowan, J. F. Stoddart, *Org. Lett.* **1999**, *1*, 1363-1366.

93   P. T. Glink, A. I. Oliva, J. F. Stoddart, A. J. P. White, D. J. Williams, *Angew. Chem. Int. Ed.* **2001**, *40*, 1870-1875.

94   S. J. Rowan, S. J. Cantrill, J. F. Stoddart, *Org. Lett.* **1999**, *1*, 129-132.

95   S. H. Chiu, S. J. Rowan, S. J. Cantrill, J. F. Stoddart, A. J. P. White, D. L. Williams, *Chem. Eur. J.* **2002**, *8*, 5170-5183 and references cited therein.

96   L. A. Summers (Ed), *The Bipyridinium Herbicides*, Academic Press, London, **1980**.

97   a) B. Odell, M. V. Reddington, A. M. Z. Slawin, N. Spencer, J. F. Stoddart, D. J. Williams, *Angew. Chem. Int. Ed. Engl.* **1988**, *27*, 1547-1550; b) B. L. Allwood, H. Shahriarizavareh, J. F. Stoddart, D. J. Williams, *J. Chem. Soc. Chem. Commun.* **1987**, 1058-1061.

98   J. Y. Ortholand, A. M. Z. Slawin, N. Spencer, J. F. Stoddart, D. J. Williams, *Angew. Chem. Int. Ed. Engl.* **1989**, *28*, 1394-1395.

99   P. R. Ashton, T. T. Goodnow, A. E. Kaifer, M. V. Reddington, A. M. Z. Slawin, N. Spencer, J. F. Stoddart, C. Vicent, D. J. Williams, *Angew. Chem. Int. Ed. Engl.* **1989**, *28*, 1396-1399.

100   For reviews on aromatic interactions see a) C. A. Hunter, K. R. Lawson, J. Perkins, C. J. Urch, *J. Chem. Soc. Perkin Trans. 2* **2001**, 651-669; b) E. A. Meyer, R. K. Castellano, F. Diederich, *Angew. Chem. Int. Ed.* **2003**, *42*, 1210-1250.

101   K. N. Houk, S. Menzer, S. P. Newton, F. M. Raymo, J. F. Stoddart, D. J. Williams, *J. Am. Chem. Soc.* **1999**, *121*, 1479-1487.

102   D. A. Amabilino, P. R. Ashton, A. S. Reder, N. Spencer, J. F. Stoddart, *Angew. Chem. Int. Ed. Engl.* **1994**, *33*, 1286-1290.

103   P. R. Ashton, O. A. Matthews, S. Menzer, F. M. Raymo, N. Spencer, J. F. Stoddart, D. J. Williams, *Liebigs Ann.* **1997**, 2485-2494.

104   P. L. Anelli, P. R. Ashton, R. Ballardini, V. Balzani, M. Delgado, M. T. Gandolfi, T. T. Goodnow, A. E. Kaifer, D. Philp, M. Pietraszkiewicz, L. Prodi, M. V. Reddington, A. M. Z. Slawin, N. Spencer, J. F. Stoddart, C. Vicent, D. J. Williams, *J. Am. Chem. Soc.* **1992**, *114*, 193-218.

105   a) P. R. Ashton, M. Bělohradský, D. Philp, J. F. Stoddart, *J. Chem. Soc. Chem. Commun.* **1993**, 1269-1274; b) P. R. Ashton, M. Bělohradský, D. Philp, N. Spencer, J. F. Stoddart, *J. Chem. Soc. Chem. Commun.* **1993**, 1274-1277; c) M. Asakawa, P. R. Ashton, R. Ballardini, V. Balzani, M. Bělohradský, M. T. Gandolfi, O. Kocian, L. Prodi, F. M. Raymo, J. F. Stoddart, M. Venturi, *J. Am. Chem. Soc.* **1997**, *119*, 302-310.

106   For a recent review on tetrathiafulvalene derivatives in supramolecular chemistry see: M. B. Nielsen, C. Lombolt, J. Becher, *Chem. Soc. Rev.* **2000**, *29*, 153-164.

107   S. J. Rowan, J. F. Stoddart, *Org. Lett.* **1999**, *1*, 1913-1916.

108   For an excellent account of Sanders catenane syntheses see: L. Raehm, D. G. Hamilton, J. K. M. Sanders, *Synlett*, **2002**, 1743-1761.

109   a) D. G. Hamilton, J. K. M. Sanders, J. E. Davis, W. Clegg, S. J. Teat, *Chem. Commun.* **1997**, 897-898; b) D. G. Hamilton, J. E. Davis, L. Prodi, J. K. M. Sanders, *Chem. Eur. J.* **1998**, *4*, 608-620; c) D. G. Hamilton, L. Prodi, N. Feeder, J. K. M. Sanders, *J. Chem. Soc. Perkin Trans. 1* **1999**, 1057-1065.

110   J. G. Hansen, N. Feeder, D. G. Hamilton, M. J. Gunter, J. Becher, J. K. M. Sanders, *Org. Lett.* **2000**, *2*, 449-452.

111   D. G. Hamilton, N. Feeder, S. J. Teat, J. K. M. Sanders, *New. J. Chem.* **1998**, 1019-1021.

112   For a review of interlocked molecules containing cyclodextrins see: S. A. Nepogodiev, J. F. Stoddart, *Chem. Rev.* **1998**, *98*, 1959-1976.

113   For a review interlocked molecules containing cucurbituril see: K. Kim, *Chem. Soc. Rev.* **2002**, *31*, 96-107.

114   For a representative example see: S. Anderson, H. L. Anderson, *Angew. Chem. Int. Ed. Engl.* **1996**, *35*, 1956-1959.

115   A. Lüttringhaus, F, Cramer, H. Prinzbach, F. M. Henglein, *Liebigs Ann. Chem.* **1958**, *613*, 185-198.

116   a) D. Armspach, P. Ashton, C. P. Moore, N. Spencer, J. F. Stoddart, T. J. Wear, D. J. Williams, *Angew. Chem. Int. Ed. Engl.* **1993**, *32*, 854-858; b) D. Armspach, P. R. Ashton, R. Ballardini, V. Balzani, A. Godi, C. P. Moore, L. Prodi, N. Spencer, J. F. Stoddart, M. S. Tolley, T. J. Wear, D. J. Williams, *Chem. Eur. J.* **1995**, *1*, 33-55.

117   H. Ogino, *J. Am. Chem. Soc.* **1981**, *103*, 1303-1304.

118   H. Ogino, K. Ohata, *Inorg. Chem.* **1984**, *23*, 3312-3316.

119   a) J. S. Manka, D. S. Lawrence, *J. Am. Chem. Soc.* **1990**, *112*, 2440-2242; b) T. V. S. Rao, D. S. Lawrence, *J. Am. Chem. Soc.* **1990**, *112*, 3614-3615; c) R. Isnin, A. E. Kaifer, *J. Am. Chem. Soc.* **1991**, *113*, 8188-8190; d) R. S. Wylie, D. H. Macartney, *J. Am. Chem. Soc.* **1992**, *114*, 3136-3138.

120   a) A. Harada, J. Li, M. Kamachi, *Nature* **1992**, *356*, 325-327; b) A. Harada, J. Li, T. Nakamitsu, M. Kamachi, *J. Org. Chem.* **1993**, *58*, 7524-7528; c) A. Harada, J. Li, M. Kamachi, *J. Am. Chem. Soc.* **1994**, *116*, 3192-3196.

121   a) G. Wenz, B. Keller, *Angew. Chem. Int. Ed. Engl.* **1992**, *31*, 197-199; b) M. Born, H. Ritter, *Angew. Chem. Int. Ed. Engl.* **1995**, *34*, 309-311.

122   A. Harada, J. Li, M. Kamachi, *Nature* **1993**, *364*, 516-518.

123   S. Anderson, T. D. W. Claridge, H. L. Anderson, *Angew. Chem. Int. Ed. Engl.* **1997**, *36*, 1310-1313.

124   a) J. E. H. Buston, J. R. Young, H. L. Anderson, *Chem. Commun.* **2000**, 905-906; b) J. E. H. Buston, F. Marken, H. L. Anderson, *Chem. Commun.* **2001**,

1046-1047; c) M. R. Craig, M. G. Hutchings, T. D. W. Claridge, H. L. Anderson, *Angew. Chem. Int. Ed.* **2001**, *40*, 1071-1074.

125   P. N. Taylor, M. J. O'Connell, L. A. McNeill, M. J. Hall, R. T. Aplin, H. L. Anderson, *Angew. Chem. Int. Ed.* **2000**, *39*, 3456-3460.

126   F. Cacialli, J. S. Wilson, J. J. Michels, C. Daniel, C. Silva, R. H. Friend, N. Severin, P. Samori, J. P. Rabe, M. J. O'Connell, P. N. Taylor, H. L. Anderson, *Nature Mater.* **2002**, *1*, 160-164.

127   a) S. Anderson, R. T. Aplin, T. D. W. Claridge, T. Goodson, A. C. Maciel, G. Rumbles, J. F. Ryan, H. L. Anderson, *J. Chem. Soc. Perkin Trans. 1* **1998**, 2383-2397; b) P. N. Taylor, A. J. Hagan, H. L. Anderson, *Org. Biomol. Chem.* **2003**, *1*, 3851-3856.

128   R. P. Feynman, *Saturday Rev.* **1960**, *43*, 45-47.

129   For reviews on molecular machines see: a) V. Balzani, A. Credi, F. M. Raymo, J. F. Stoddart, *Angew. Chem. Int. Ed.* **2000**, *39*, 3349-3391; b) Special Issue on Molecular Machines: *Acc. Chem. Res.* **2001**, *34*, 409-522; c) J.-P. Sauvage Molecular Machines and Motors; Ed. Struct. Bonding (Berlin) **2001**, *99*.

130   a) P. D. Boyer, *Angew. Chem. Int. Ed.* **1998**, *37*, 2296-2307; b) J. E. Walker, *Angew. Chem. Int. Ed.* **1998**, *37*, 2308-2319; c) J. C. Skou, *Angew. Chem. Int. Ed.* **1998**, *37*, 2320-2328.

131   a) J. T. Finer, R. M. Simmons, J. A. Spudich, *Nature*, **1994**, *368*, 113-115; b) R. D. Vall, R. A. Milligan, *Science* **1999**, *288*, 88-95.

132   M. D. Wang, M. J. Schnitzer, H. Yin, R. Landick, J. Gelles, S. M. Block, *Science* **1998**, *282*, 902-907.

133   For a review see: K. Mislow, *Acc. Chem. Res.* **1976**, *9*, 26-33 and references cited therein.

134   For a review see: K. Mislow, *Acc. Chem. Res.* **1988**, *21*, 175-182 and references cited therein.

135   a) B. L. Feringa, W. F. Jager, B. Delange, E. W. Meijer, *J. Am. Chem. Soc.* **1991**, *113*, 5468-5470; b) T. R. Kelly, M. C. Bowyer, K. V. Bhaskar, D. Bebbington, A. Garcia, F. R. Lang, M. H. Kim, M. P. Jette, *J. Am. Chem. Soc.* **1994**, *116*, 3657-3658; c) T. R. Kelly, I. Tellitu, J. P. Sestelo, *Angew.*

Chem. Int. Ed. Engl. **1997**, *36*, 1866-1868; d) N. Harada, A. Saito, N. Koumura, H. Uda, B. deLange, W. F. Jager, H. Wynberg, B. L. Feringa, *J. Am. Chem. Soc.* **1997**, *119*, 7241-7248; e) N. Harada, A. Saito, N. Koumura, D. C. Roe, W. F. Jager, R. W. J. Zijlstra, B. deLange, B. L. Feringa, *J. Am. Chem. Soc.* **1997**, *119*, 7249-7255; f) N. Harada, N. Koumura, B. L. Feringa, *J. Am. Chem. Soc.* **1997**, *119*, 7256-7264.

136   a) T. R. Kelly, H. De Silva, R. A. Silva, *Nature* **1999**, *401*, 150-152; b) T. R. Kelly, R. A. Silva, H. De Silva, S. Jasmin, Y. J. Zhao, *J. Am. Chem. Soc.* **2000**, *122*, 6935-6949; c) N. Koumura, R. W. J. Zijlstra, R. A. van Delden, N. Harada, B. L. Feringa, *Nature* **1999**, *401*, 152-155; d) N. Koumura, E. M. Geertsema, A. Meetsma, B. L. Feringa, *J. Am. Chem. Soc.* **2000**, *122*, 12005-12006.

137   M. C. T. Fyfe, P. T. Glink, S. Menzer, J. F. Stoddart, A. J. P. White, D. J. Williams, *Angew. Chem. Int. Ed. Engl.* **1997**, *36*, 2068-2070.

138   For examples of pseudorotaxanes as molecular-level machines see: a) R. Ballardini, V. Balzani, M. T. Gandolfi, L. Prodi, M. Venturi, D. Philp, H. G. Ricketts, J. F. Stoddart, *Angew. Chem. Int. Ed. Engl.* **1993**, *32*, 1301-1303; b) J.-P. Collin, P. Gaviña, J.-P. Sauvage, *Chem. Commun.* **1996**, 2005-2006; c) P. R. Ashton, R. Ballardini, V. Balzani, M. Gómez-López, S. E. Lawrence, M.-V. Martínez-Díaz, M. Montalti, A. Piersanti, L. Prodi, J. F. Stoddart, D. J. Williams, *J. Am. Chem. Soc.* **1997**, *119*, 10641-10651; d) P. R. Ashton, R. Ballardini, V. Balzani, S. E. Boyd, A. Credi, M. T. Gandolfi, M. Gómez-López, S. Iqbal, D. Philp, J. A. Preece, L. Prodi, H. G. Ricketts, J. F. Stoddart, M. S. Tolley, M. Venturi, A. J. P. White, D. J. Williams, *Chem. Eur. J.* **1997**, *3*, 152-170; e) P. R. Ashton, R. Ballardini, V. Balzani, M. C. T. Fyfe, M. T. Gandolfi, M.-V. Martínez-Díaz, M. Morosini, C. Schiavo, K. Shibata, J. F. Stoddart, A. J. P. White, D. J. Williams, *Chem. Eur. J.* **1998**, *4*, 2332-2341; f) P. R. Ashton, R. Ballardini, V. Balzani, E. C. Constable, A. Credi, O. Kocian, S. J. Langford, J. A. Preece, L. Prodi, E. R. Schofield, N. Spencer, J. F. Stoddart, S. Wenger, *Chem. Eur. J.* **1998**, *4*, 2413-2422; g) P. R. Ashton, V. Balzani, O. Kocian, L. Prodi, N. Spencer, J. F. Stoddart, *J. Am. Chem. Soc.* **1998**, *120*, 11190-11191; h) P. R. Ashton, R. Ballardini, V.

Balzani, A. Credi, K. R. Dress, E. Ishow, C. J. Kleverlaan, O. Kocian, J. A. Preece, N. Spencer, J. F. Stoddart, M. Venturi, S. Wenger, *Chem. Eur. J.* **2000**, *6*, 3558-3574; i) V. Balzani, A. Credi, M. Venturi, *Proc. Natl. Acad. Sci. U. S. A.* **2002**, *99*, 4814-4817.

139 For a paper detailing the realationship between the behavior of pseudorotaxanes and their corresponding interlocked rotaxanes see: M. Asakawa, C. L. Brown, S. Menzer, F. M. Raymo, J. F. Stoddart, D. J. Williams, *J. Am. Chem. Soc.* **1997**, *119*, 2614-2627.

140 For reviews of molecular-level machine based on interlocked molecules containing transition metals see: a) J.-P. Sauvage, *Acc. Chem. Res.* **1998**, *31*, 611-619; b) J.-P. Collin, C. Dietrich-Buchecker, P. Gaviña, M. C. Jiménez-Molero, J.-P. Sauvage, *Acc. Chem. Res.* **2001**, *34*, 477-487; c) L. Raehm, J.-P. Sauvage, in *Molecular Machines and Motors, Vol. 99*, **2001**, pp. 55-78.

141 A. Livoreil, C. Dietrich-Buchecker, J.-P. Sauvage, *J. Am. Chem. Soc.* **1994**, *116*, 9399-9400.

142 A. Livoreil, J.-P. Sauvage, N. Armaroli, V. Balzani, L. Flamigni, B. Ventura, *J. Am. Chem. Soc.* **1997**, *119*, 12114-12124.

143 D. J. Cárdenas, A. Livoreil, J.-P. Sauvage, *J. Am. Chem. Soc.* **1996**, *118*, 11980-11981.

144 P. Gaviña, J.-P. Sauvage, *Tetrahedron Lett.* **1997**, *38*, 3521-3524.

145 N. Armaroli, V. Balzani, J.-P. Collin, P. Gaviña, J.-P. Sauvage, B. Ventura, *J. Am. Chem. Soc.* **1999**, *121*, 4397-4408.

146 L. Raehm, J.-M. Kern, J.-P. Sauvage, *Chem. Eur. J.* **1999**, *5*, 3310-3317.

147 a) M. C. Jiménez, C. Dietrich-Buchecker, J.-P. Sauvage, *Angew. Chem. Int. Ed.* **2000**, *39*, 3284-3287; b) M. C. Jiménez-Molero, C. Dietrich-Buchecker, J.-P. Sauvage, *Chem. Eur. J.* **2002**, *8*, 1456-1466.

148 M. C. Jiménez, C. Dietrich-Buchecker, J.-P. Sauvage, A. De Cian, *Angew. Chem. Int. Ed.* **2000**, *39*, 1295-1298.

149 S.-Y. Chang, K.-S. Jeong, *J. Org. Chem.* **2003**, *68*, 4014-4019.

150 D. A. Leigh, K. Moody, J. P. Smart, K. J. Watson, A. M. Z. Slawin, *Angew. Chem. Int. Ed. Engl.* **1996**, *35*, 306-310.

151   A. S. Lane, D. A. Leigh, A. Murphy, *J. Am. Chem. Soc.* **1997**, *119*, 11092-11093.

152   F. G. Gatti, S. Lent, J. K. Y. Wong, G. Bottari, A. Altieri, M. A. F. Morales, S. J. Teat, C. Frochot, D. A. Leigh, A. M. Brouwer, F. Zerbetto, *Proc. Natl. Acad. Sci. U. S. A.* **2003**, *100*, 10-14.

153   A. Altieri, G. Bottari, F. Dehez, D. A. Leigh, J. K. Y. Wong, F. Zerbetto, *Angew. Chem. Int. Ed.* **2003**, *42*, 2296-2300.

154   D. A. Leigh, J. K. Y. Wong, F. Dehez, F. Zerbetto, *Nature* **2003**, *424*, 174-179.

155   C. A. Schalley, K. Beizai, F. Vögtle, *Acc. Chem. Res.* **2001**, *34*, 465-476.

156   P. L. Anelli, N. Spencer, J. F. Stoddart, *J. Am. Chem. Soc.* **1991**, *113*, 5131-5133.

157   a) P. R. Ashton, R. A. Bissell, N. Spencer, J. F. Stoddart, M. S. Tolley, *Synlett* **1992**, 914-918; b) P. R. Ashton, R. A. Bissell, R. Górski, D. Philp, N. Spencer, J. F. Stoddart, M. S. Tolley, *Synlett* **1992**, 919-922; c) P. R. Ashton, R. A. Bissell, N. Spencer, J. F. Stoddart, M. S. Tolley, *Synlett* **1992**, 923-926; d) P. L. Anelli, M. Asakawa, P. R. Ashton, R. A. Bissell, G. Clavier, R. Górski, A. E. Kaifer, S. J. Langford, G. Mattersteig, S. Menzer, D. Philp, A. M. Z. Slawin, N. Spencer, J. F. Stoddart, M. S. Tolley, D. J. Williams, *Chem. Eur. J.* **1997**, *3*, 1113-1135.

158   R. A. Bissell, E. Córdova, A. E. Kaifer, J. F. Stoddart, *Nature* **1994**, *369*, 133-137.

159   M. Asakawa, P. R. Ashton, V. Balzani, S. E. Boyd, A. Credi, G. Mattersteig, S. Menzer, M. Montalti, F. M. Raymo, C. Ruffilli, J. F. Stoddart, M. Venturi, D. J. Williams, *Eur. J. Org. Chem.* **1999**, 985-994.

160   a) J. O. Jeppesen, J. Perkins, J. Becher, J. F. Stoddart, *Org. Lett.* **2000**, *2*, 3547-3550; b) J. O. Jeppesen, J. Perkins, J. Becher, J. F. Stoddart, *Angew. Chem. Int. Ed.* **2001**, *40*, 1216-1221.

161   a) M. Asakawa, P. R. Ashton, V. Balzani, A. Credi, C. Hamers, G. Mattersteig, M. Montalti, A. N. Shipway, N. Spencer, J. F. Stoddart, M. S. Tolley, M. Venturi, A. J. P. White, D. J. Williams, *Angew. Chem. Int. Edit.* **1998**, *37*, 333-337; b) V. Balzani, A. Credi, G. Mattersteig, O. A. Matthews,

F. M. Raymo, J. F. Stoddart, M. Venturi, A. J. P. White, D. J. Williams, *J. Org. Chem.* **2000**, *65*, 1924-1936.

162   M. Asakawa, M. Higuchi, G. Mattersteig, T. Nakamura, A. R. Pease, F. M. Raymo, T. Shimizu, J. F. Stoddart, *Adv. Mater.* **2000**, *12*, 1099-1102.

163   C. P. Collier, G. Mattersteig, E. W. Wong, Y. Luo, K. Beverly, J. Sampaio, F. M. Raymo, J. F. Stoddart, J. R. Heath, *Science* **2000**, *289*, 1172-1175.

164   a) C. P. Collier, E. W. Wong, M. Bělohradský, F. M. Raymo, J. F. Stoddart, P. J. Kuekes, R. S. Williams, J. R. Heath, *Science* **1999**, *285*, 391-394; b) E. W. Wong, C. P. Collier, M. Bělohradský, F. M. Raymo, J. F. Stoddart, J. R. Heath, *J. Am. Chem. Soc.* **2000**, *122*, 5831-5840; c) C. P. Collier, J. O. Jeppesen, Y. Luo, J. Perkins, E. W. Wong, J. R. Heath, J. F. Stoddart, *J. Am. Chem. Soc.* **2001**, *123*, 12632-12641.

165   a) M.-V. Martínez-Díaz, N. Spencer, J. F. Stoddart, *Angew. Chem. Int. Ed. Engl.* **1997**, *36*, 1904-1907; b) P. R. Ashton, R. Ballardini, V. Balzani, I. Baxter, A. Credi, M. C. T. Fyfe, M. T. Gandolfi, M. Gómez-López, M.-V. Martínez-Díaz, A. Piersanti, N. Spencer, J. F. Stoddart, M. Venturi, A. J. P. White, D. J. Williams, *J. Am. Chem. Soc.* **1998**, *120*, 11932-11942.

166   For a review see: A. Harada, *Acc. Chem. Res.* **2001**, *34*, 456-464.

167   H. Murakami, A. Kawabuchi, K. Kotoo, M. Kunitake, N. Nakashima, *J. Am. Chem. Soc.* **1997**, *119*, 7605-7606.

168   C. A. Stanier, S. J. Alderman, T. D. W. Claridge, H. L. Anderson, *Angew. Chem. Int. Ed.* **2002**, *41*, 1769-1772.

169   Y. Kawaguchi, A. Harada, *Org. Lett.* **2000**, *2*, 1353-1356.

170   For synthetic studies towards Borromean rings see: a) C. Mao, W. Sun, N. C. Seeman, *Nature* **1997**, *386*, 137-138; b) H. Wu, S. Brittain, J. Anderson, B. Grzybowski, S. Whitesides, G. M. Whitesides, *J. Am. Chem. Soc.* **2000**, *122*, 12691-12699; c) J. C. Loren, M. Yoshizawa, R. F. Haldimann, A. Linden, J. S. Siegel, *Angew. Chem. Int. Ed.* **2003**, *115*, 5880-5883.

171   For a review see: S. J. Rowan, S. J. Cantrill, G. R. L. Cousins, J. K. M. Sanders, J. F. Stoddart, *Angew. Chem. Int. Ed.* **2002**, *41*, 898-952.

172   For reviews on polymeric interlocked architectures: a) F. M. Raymo, J. F. Stoddart, *Chem. Rev.* **1999**, *99*, 1643-1663; b) A. Harada, *Acta. Polym.* **1998**, *49*, 3-17.

173   a) Y. Geerts, D. Muscat, K. Müllen, *Macromol. Chem. Phys.* **1995**, *196*, 5425-3435; b) J. L. Weidmann, J.-M. Kern, J.-P. Sauvage, Y. Geerts, D. Muscat, K. Müllen, *Chem. Commun.* **1996**, 1243-1244; c) S. Menzer, A. J. P. White, D. J. Williams, M. Bělohradský, C. Hamers, F. M. Raymo, A. N. Shipway, J. F. Stoddart, *Macromolecules*, **1998**, *31*, 295-307; d) D. Muscat, W. Köhler, H. J. Räder, K. Martin, S. Mullins, B. Müller, K. Müllen, Y. Geerts, *Macromolecules*, **1998**, *32*, 1737-1745.

CHAPTER TWO

Flexible Hydrogen Bonding Templates

"The difference between fiction and reality? Fiction has to make sense."

Tom Clancy

2.0 Introduction

Hydrogen bonding is a unique noncovalent force by virtue of its key role in orchestrating the mechanisms of biological processes.[1] The key features of hydrogen bonding are its directional nature coupled with the ability to form arrays through cooperative effects. Taking inspiration and motivation from Nature, synthetic chemists have utilized these unique features of hydrogen bonding to access a range of well-defined supramolecular structures from small building blocks.[2] However, despite the recent advances in noncovalent syntheses many of the products obtained from such processes are kinetically unstable. Hydrogen bonding interactions have also been successfully exploited to prepare a range of mechanically interlocked molecules[3] including catenanes,[4-6] rotaxanes[7-10] and knots.[11,12] As molecular compounds, these constructs offer the potential for novel properties and functions, coupled with the kinetic stability found in traditional covalent structures.[13] Rotaxanes are perhaps the most versatile architectures in the arena of mechanically interlocked molecules and hydrogen bonding offers a particularly powerful method of preorganizing precursors to direct their formation.[7a,14]

2.1 Previous Studies on the Formation of Benzylic Amide Macrocycle-Containing [2]Rotaxanes

We have previously reported the synthesis of benzylic amide macrocycle-containing rotaxanes *via* a five component clipping strategy directed by complementary hydrogen bonds promoting interlocking, between a thread component and a forming macrocycle in nonpolar solvents.[7a,14] The use of isophthalamide,[7a] peptide[14a-c] and fumaramide-based threads[14d] (Scheme 2.1) has led to the synthesis of a range of rotaxanes and molecular shuttles[15] in good to excellent (28-97 %) yields. In all of the previous examples we have reported, the thread components contain two suitably spaced hydrogen bond-accepting carbonyls, which can assume a *transoid* arrangement to efficiently bind to the forming macrocycle, thus, promoting interlocking. This is best illustrated by the example of the fumaramide thread **1** which affords corresponding benzylic amide rotaxane **4** in a near quantitative 97 %

ield.[14d] The reason the reaction is so efficient is that the double bond holds the hydrogen bonding groups of the thread in a close-to-perfect arrangement for macrocycle to cyclize around it. Not only does the double bond provide rigidity but it also holds the two carbonyls of the thread at the correct distance and orientation to allow the forming macrocycle to adopt a low energy chair-like conformation around it. Indeed, the preorganization of the thread template is so effective that when the amides were substituted for weak hydrogen bond acceptors, such as esters, (**2, 3**) rotaxanes are still formed (**5, 6**).
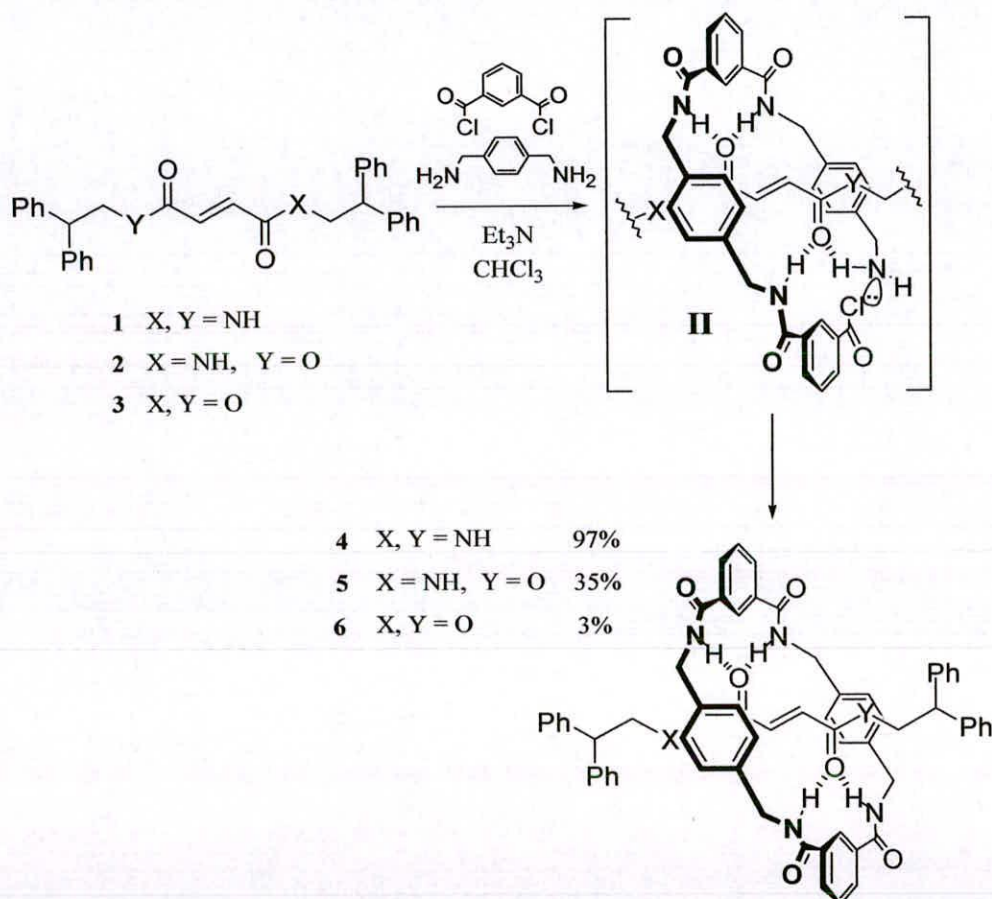
Scheme 2.1. Rotaxane-formation *via* preorganised, rigid fumaryl-based hydrogen bond templates.

Here we explore the scope and structural tolerance for the formation of benzylic amide macrocycle-containing rotaxanes by reducing the number of acceptor and donor sites present for in the thread component to obtain a range of new structural motifs available for mechanical interlocking. In tandem, we explore the directing effects of the hydrogen bonding between the forming macrocycle and thread and the

efficacy of the assembly process when competing factors (flexibility, intracomponent hydrogen bonding and non-optimal hydrogen bonding arrangements) are introduced. Together these studies afford us a greater understanding of the specific interactions that are required prior to interlocking and allow us to postulate a more accurate mechanistic rationale for the formation of benzylic amide-containing macrocycle rotaxanes.

2.2 Results and Discussion

2.2.1 Rotaxane Formation Using Threads Containing One Binding Site

From our previous studies we can consider two reasonable mechanistic intermediates (Figure 2.1) that will promote interlocking when using the isophthalic-based macrocycle. Analysis of intermediate **A** where the macrocyclic precursor is bound through 1,3 bifurcated amide hydrogen bonding to the amide carbonyl of the template and through a single hydrogen bond from the carbonyl of the linear precursor provided grounds for optimism. Clearly in the absence of a second carbonyl group in the thread only a very weak hydrogen bond from the amine of the macrocyclic precursor is lost and is almost certainly not the key interaction promoting interlocking.

X = O and Y = NH,
or
X = H$_2$ and Y = CH$_2$
Z = H or Me
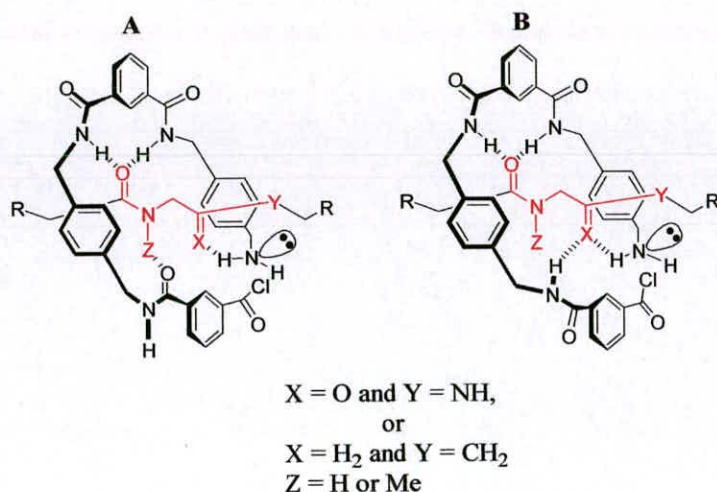
Figure 2.1. Possible mechanistic intermediates *via* which hydrogen bond-assembled rotaxanes containing one- and two-site templates may form using isophthalic-based macrocycles.

Encouraged, it was decided to probe further the limitations of this *clipping* strategy. Hence, single-site threads **7-13** (Scheme 2.2) were prepared[16] and each subjected to standard rotaxane formation, i.e. the simultaneous addition of eight equivalents of *p*-xylylene diamine and isophthaloyl dichloride (CHCl₃, Et₃N, 4 h, high dilution) to a solution of each thread.
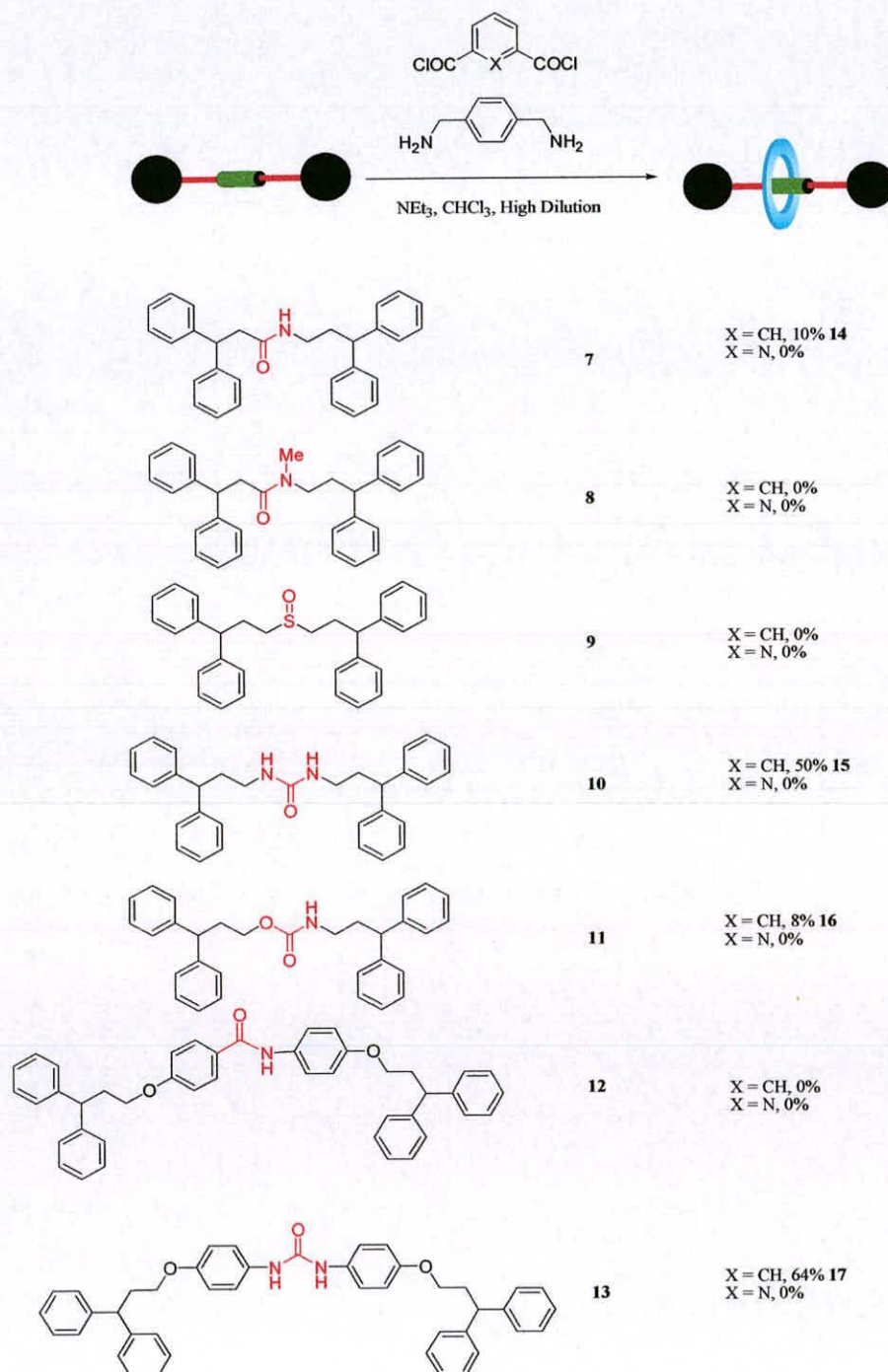
Scheme 2.2 The hydrogen bond-directed assembly of rotaxanes **14-17** from threads **7-13**.

The monoamide thread **7** (the simplest single site thread) gave the corresponding rotaxane **14** in a low, but satisfactory 10% yield. ^{1}H NMR spectra in CDCl$_3$ of rotaxane **14** display some of the typical features of hydrogen bond-assembled rotaxanes (Figure 2.2). The ABX system for the benzylic protons H$_E$ results from the prochiral nature of the macrocycle. Thread protons H$_{a-f}$ are all shielded by the macrocyclic sheath and thus move upfield relative to the component thread, except the amide NH$_c$ which moves downfield indicating that the shielding effect is offset by hydrogen-bonding to the macrocycle.
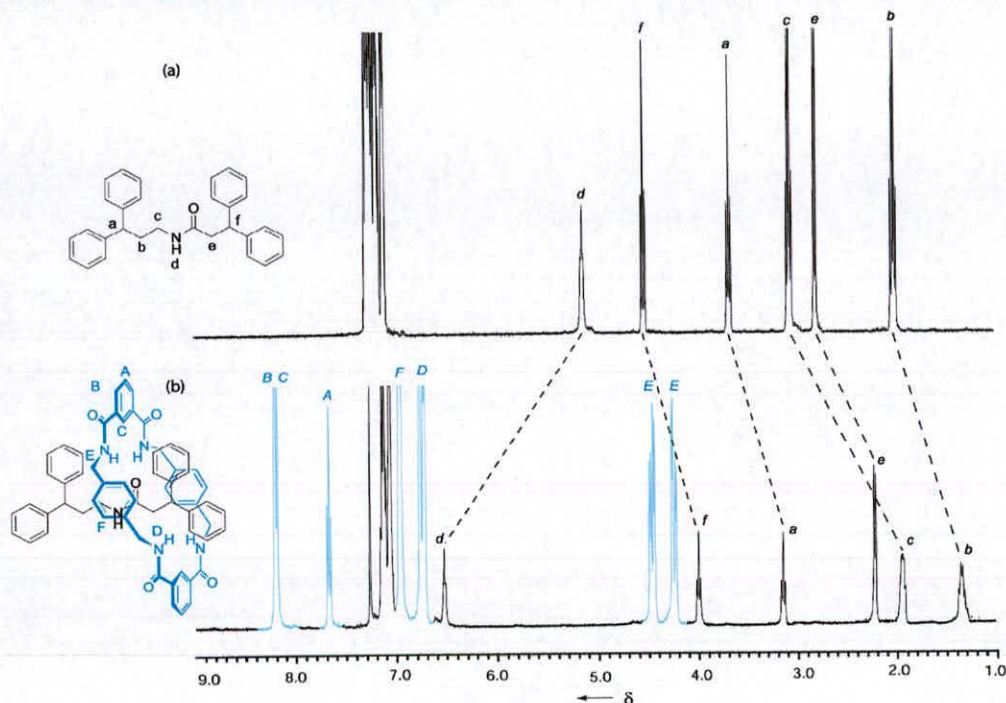
Figure 2.2. ^{1}H NMR spectra (400 MHz, CDCl$_3$) of (a) monoamide thread **7** and (b) monoamide rotaxane **14**.

Single crystals suitable for investigation by X-ray crystallography were obtained from the slow evaporation of water into a solution of the rotaxane **14** in dimethylsulfoxide. The results confirm the interlocked architecture and support the possibility of an even simpler mechanistic intermediate than **A** (Figure 2.1) involving only one hydrogen bond from the carbonyl of the thread to an isophthalamide cleft and another hydrogen bond from the NH of the thread to the other cleft (Figure 2.3).
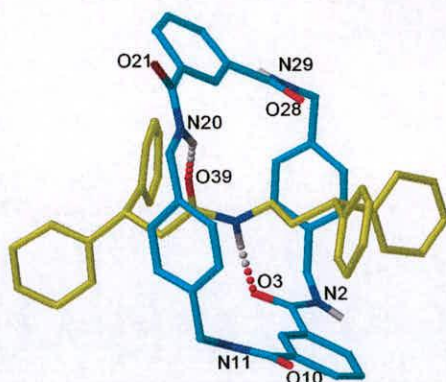
Figure 2.3. X-Ray crystal structure of the monoamide [2]rotaxane **14**. Intramolecular hydrogen bond distances and angles: N20H–O39 1.39 Å, 144.9°; N40H–O3 1.71 Å, 175.5°.

In contrast to monoamide thread **7**, the urea thread **10** afforded the corresponding rotaxane **15** in a remarkable 50 % yield. This may not be surprising as ureas are much more efficient hydrogen bonding acceptors than amides.[17] The high isolated yield could also be enhanced due to the excellent solubility of urea-containing rotaxane **15** as compared with monoamide rotaxane **14**. Rotaxane **15** yielded single crystals suitable for investigation from the slow evaporation of water into a solution of the rotaxane in dimethylsulfoxide. The results confirm the interlocked architecture and once again support the possibility of mechanistic intermediate **A** involving a bifurcated hydrogen-bond from the urea carbonyl to an isophthalamide cleft and another hydrogen-bond from a urea NH to the other (albeit via a water molecule!) (Figure 2.4). It is also interesting to note that this structure shows the macrocycle can adopt boat type conformations in addition to chair type conformations that have been observed in all previously reported structures of this type.
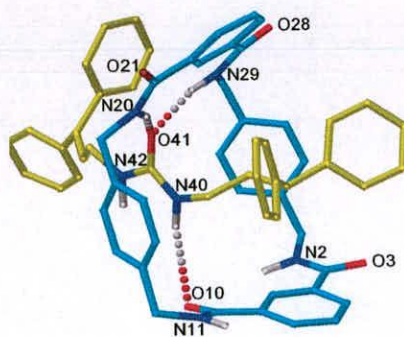
Figure 2.4. X-Ray crystal structure of the urea rotaxane **15**. Intramolecular hydrogen bond distances and angles: N20H-O41 1.96 Å, 164.2°, N29H-O41 2.08 Å, 163.8°, N40H-O10 3.15 Å, 113.3°.

In addition to the monoamide **7** and urea **10** threads analogous aryl-containing threads **12** and **13** were also prepared. The treatment of these two threads to standard rotaxane forming conditions afforded none of the monoamide rotaxane, but 64 % of the corresponding urea rotaxane **17**. The contrast in these results indicates that despite the structural tolerance of the reaction, there is a fine line between success and total failure. The ^{1}H NMR spectra of **17** in CDCl$_3$ (Figure 2.5) shows the macrocycle shielding the aromatic protons of the thread (H$_d$ and H$_e$) and causing the urea protons (NH$_f$) to move downfield, suggesting the macrocycle is hydrogen bonding to the template.
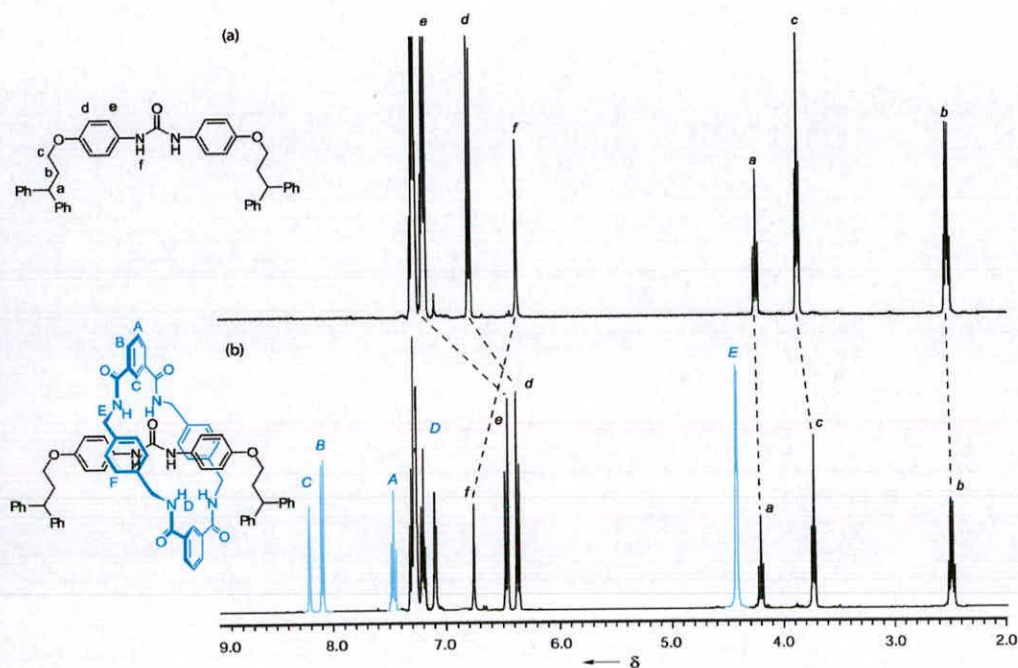
Figure 2.5. ^{1}H NMR spectra (400 MHz, CDCl$_3$) of (a) urea thread **13** and (b) urea rotaxane **17**.

The solid-state structure of rotaxane **17** (Figure 2.6) confirms this fact as the macrocycle is bound to the thread through 1,3 bifurcated amide hydrogen bonding to the amide carbonyl of the template and through a single hydrogen bond from the carbonyl of the linear precursor, in an identical manner to the "proposed" mechanistic intermediate **A** (Figure 2.1).
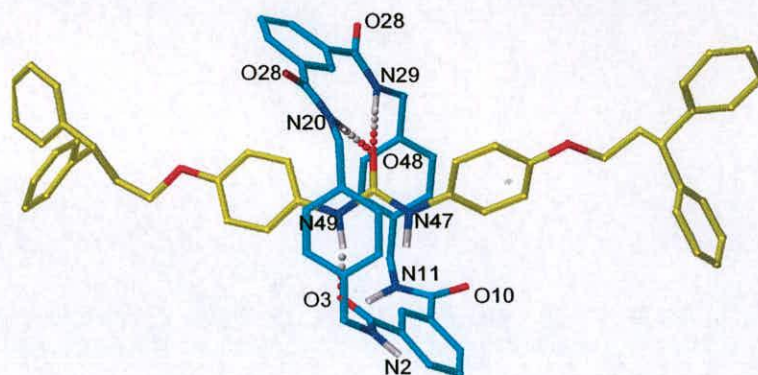
Figure 2.6. X-Ray crystal structure of the urea rotaxane **17**. Intramolecular hydrogen bond distances and angles: O3-HN49 1.77 Å 164.1° NH29-O48 2.04 Å 175.8° NH20-O48 2.03 Å 174.6°.

The corresponding carbamate thread **11** was also subjected to the standard rotaxane reaction conditions, but proved to be unstable in this media. However 8 % of the corresponding rotaxane **16** was afforded and single crystals suitable for X-ray crystallography were obtained which show a standard bifurcated hydrogen bond from two NH's of the macrocycle to the carbamate carbonyl of the thread (Figure 2.7). In addition, there is evidence of a hydrogen bond of 2.95 Å from a NH of the macrocycle to the sp^3 oxygen of the carbamate thread. Whist being long, this is clearly a directional interaction and has precedent in benzylic amide rotaxanes (see Figure 3.4-Chapter 3).
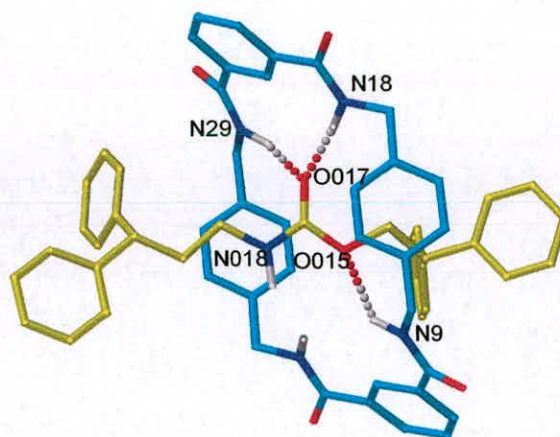
Figure 2.7. X-Ray crystal structure of the carbamate rotaxane **16**. Intramolecular hydrogen bond distances and angles: N18H-O017 2.17 Å 168.6° N29H-O017 2.08 Å 167.0° N9H-O015 2.95 Å145.9°

Given the support that the successful assembly, crystallographic and spectroscopic data lend to the proposal that intermediates such as **A** can lead to interlocked products, the results can be rationalized from first principles. Consideration of the remaining mechanistic pathway shown in Figure 2.1 aids this process. For macrocyclisation to be promoted by the template then hydrogen bonding above and below the horizontal plane of the thread must occur. Therefore if only a single site template is employed then hydrogen bonding must use both the donor and acceptor of that site explaining the failure of threads **8** and **9** (possessing only a tertiary amide or sulfoxide acceptor) to yield rotaxane.

The second issue concerns the conformational flexibility of the linear precursor prior to macrocyclisation. 1,3-isophthaloyl diamides preferentially adopt syn-anti conformations in the absence of suitable guests whereas 1,3-pyridine diamides prefer syn-syn conformations owing to the favorable NH-pyridine interaction and unfavorable carbonyl-pyridine interaction.[18] In the case of rotaxane assembly, this is limiting as certain macrocyclisation promoting interactions between the immediate precursor to macrocyclisation and thread will be eliminated due to conformational "locking" (Figure 2.8). The same holds true where fewer sites are available within the thread as fewer orientations between thread and precursor that promote ring closure from the same number of conformers are available. This results in lower yields and sometimes no detectable yield of rotaxane at all as the assembly is under kinetic control. Thus, treatment of the threads **7-13** with 2,6-pyridinedicarbonyl dichloride and *p*-xylylene diamine yielded none of the desired [2]rotaxane in each case.

X = O and Y = NH,
or
X = H₂ and Y = CH₂
Z = H or Me
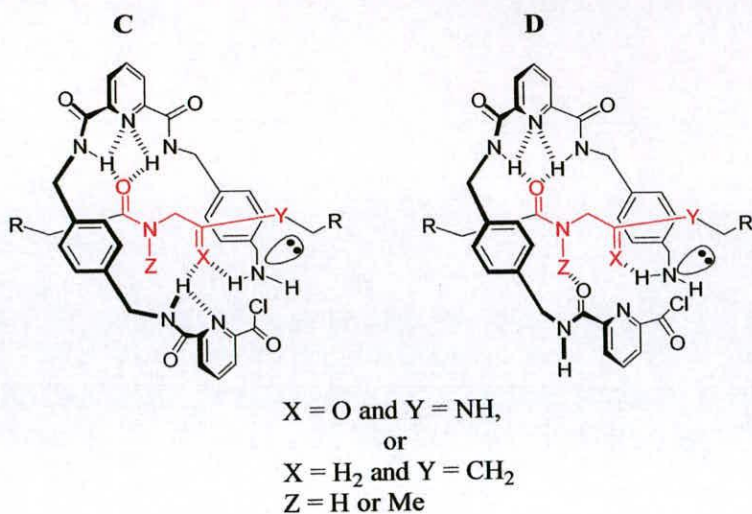
Figure 2.8. Possible mechanistic intermediates *via* which hydrogen bond-assembled rotaxanes containing one- and two-site templates may form using 2,6-pyridyl-based macrocycles.

2.2.2 Spacing out the Binding Sites

The features of the fumaramide template maximize the number and strength of hydrogen bonds between the thread and the forming macrocycle. We decided to test the directing power of hydrogen bonding in rotaxane synthesis by: (i) eliminating the rigidity provided by the double bond in the thread (simultaneously both increasing the number of possible C–C bond rotamers in the thread and introducing the possibility of intracomponent hydrogen bonding which would have to be broken in order to make the hydrogen bond sites of the thread available as a template); (ii) varying the number of carbon atoms (lengthening the distance) between the hydrogen bonding sites of the thread and; (iii) removal of hydrogen bond donor groups in the threads (in point (ii)) by methylation of the amide functions to reduce intramolecular assistance to rotaxane formation.

The introduction of flexibility not only leads to an increased number of possible conformations of the thread present in solution but also gives rise to the possibility of intramolecular hydrogen bonding, promoted by the nonpolar solvent environment (e.g. CHCl₃), forming cyclic structures (Figure 2.9). A study by Gellman[19] using variable temperature (VT) NMR and IR spectroscopy confirmed the presence of such cyclic structures in alkyl diamides and showed the shift in the equilibrium between

the linear conformations of systems containing two amides separated by methylene groups with their cyclic intramolecularly bonded structures as the number of methylene groups between the hydrogen bonding sites increases. The presence of significant quantities of internally hydrogen bonded cyclic structures would be unfavorable for rotaxane formation since the hydrogen bond requirements of the template would be internally satisfied and the hydrogen bond donors and acceptor groups would be poorly predisposed for rotaxane formation.
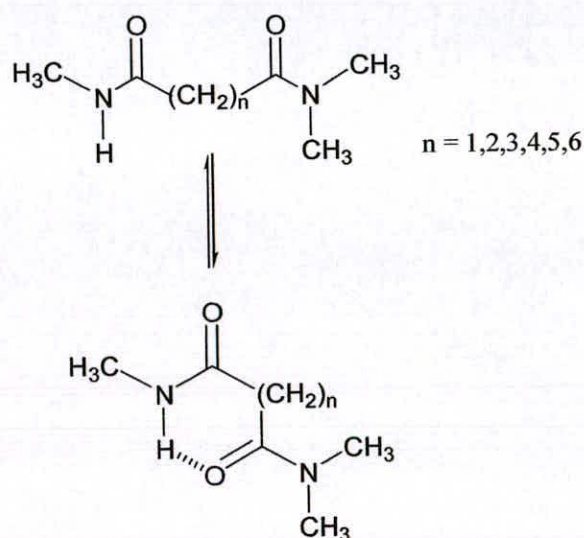
Figure 2.9. Internal hydrogen bonding of flexible diamide threads in nonpolar solvent such as $CHCl_3$

A series of diamide threads **18–28** were prepared (Scheme 2.3), each in one step from the corresponding commercially available *bis*-acid chloride and 2,2-diphenylethylamine (CH_2Cl_2, Et_3N, 16 h, 76–90 % yields). Standard rotaxane formation was performed on each thread, yielding the desired [2]rotaxanes **29–39** remarkably in *every* case! (Scheme 2.3).

18 n = 1	**21** n = 4	**24** n = 7				
19 n = 2	**22** n = 5	**25** n = 8	**27** n = 12			
20 n = 3	**23** n = 6	**26** n = 10	**28** n = 14			

29	n = 1	8 %
30	n = 2	52 %
31	n = 3	3 %
32	n = 4	8 %
33	n = 5	14 %
34	n = 6	17 %
35	n = 7	15 %
36	n = 8	18 %
37	n = 10	12 %
38	n = 12	10 %
39	n = 14	10 %
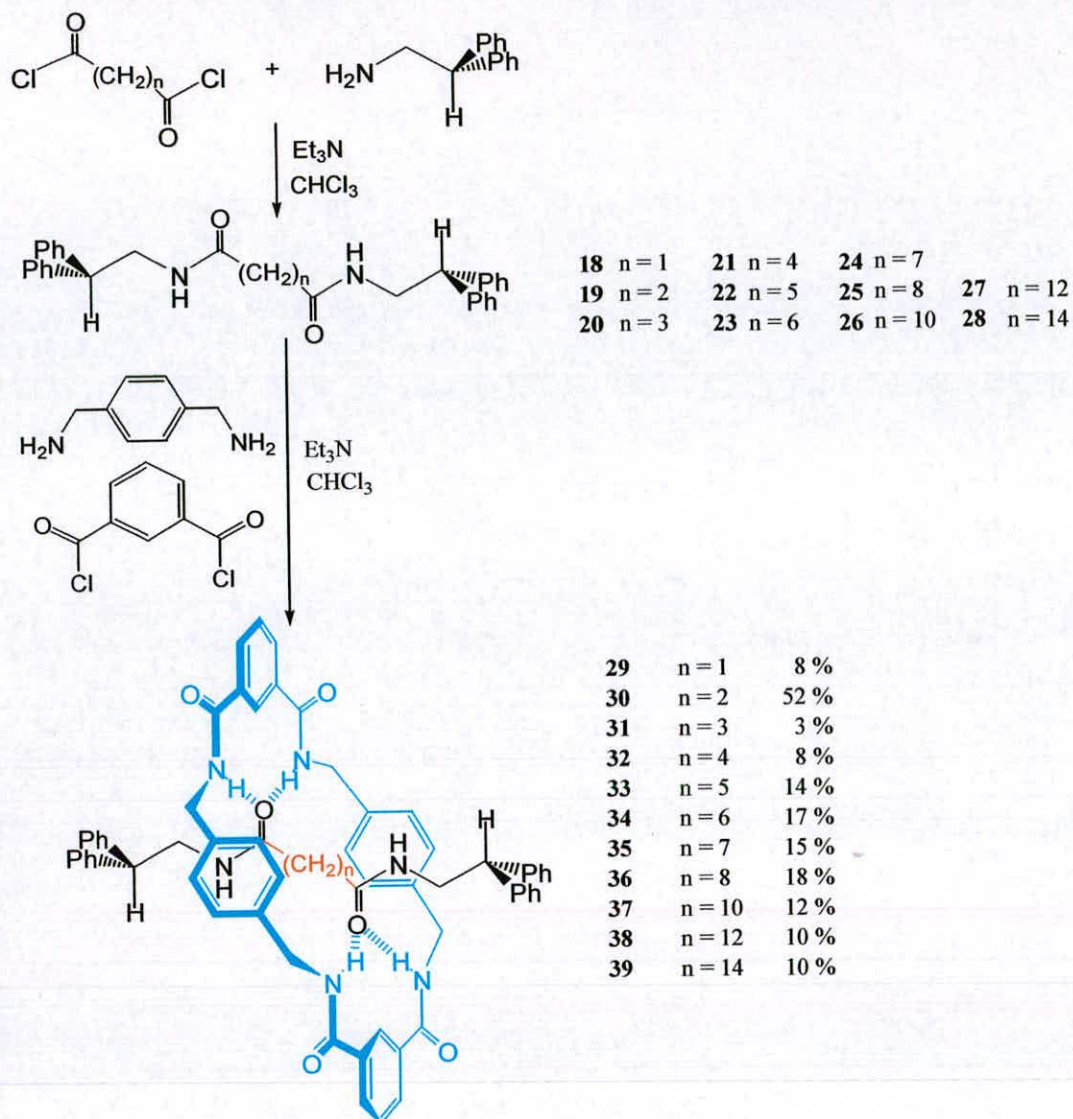
Scheme 2.3. Synthesis of diamide threads, **18–28** and rotaxanes, **29–39** containing up to fourteen methylene groups between the two templating sites.

Single crystals were obtained by either slow infusion of diethyl ether or MeOH into a close-to-saturated solution of each rotaxane in chloroform (**33–39**, tetrachloroethane for **36**) or slow infusion of water vapour into a solution of the rotaxane in acetone (**29**), DMF (**30**), or ethanol (**31**) and analyzed by X-ray crystallography using either synchrotron or Mo$_{K\alpha}$ radiation sources. Comparing the yields of the various rotaxanes with the X-ray crystal structures and the ^{1}H NMR spectra in CDCl$_3$

provides some interesting insights into the directing influence of hydrogen bonding in these systems.

Comparison of the yield and solid-state structure of the succinamide rotaxane **30** (Figure 2.10a) with that of the fumaramide rotaxane **4** (Figure 2.10b) shows that eliminating the preorganizing effect of the double bond results in a decrease in yield of almost half (52 %, *c.f.* **4** (97 %)-Scheme 2.1) and reduces the number of intramolecular hydrogen bonds between the macrocycle and the thread in the solid state from four to two.
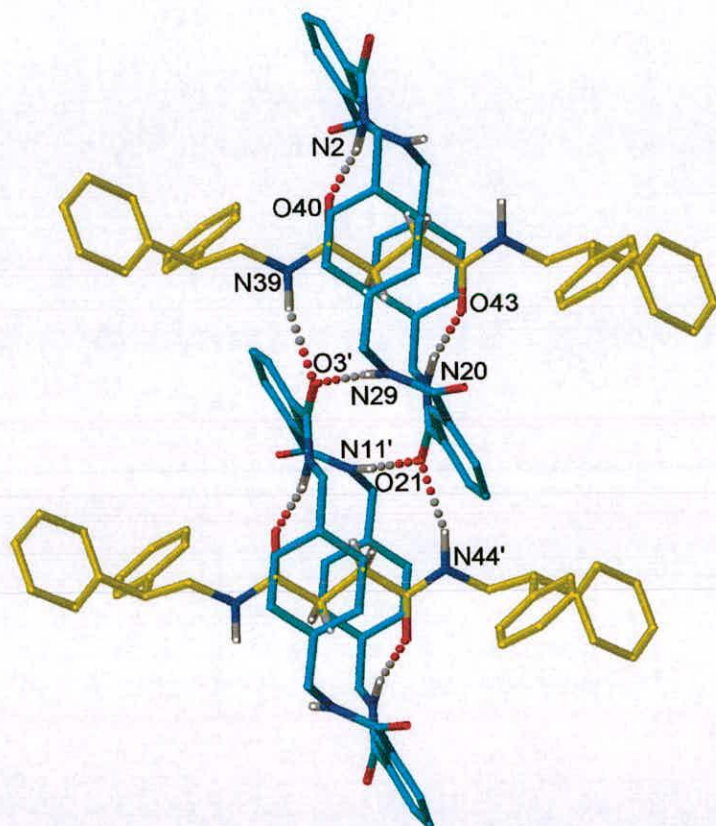
Figure 2.10a. X-ray crystal structure of succinamide [2]rotaxane, **30**. Intramolecular hydrogen bond distances and angles: O40–HN2/O43–HN20 1.88 Å, 165.3°. Intermolecular hydrogen bond distances:+N39H–O3'/O21–HN44' 2.21 Å, 161.8°; N29H–O3'/O21–HN11' 2.00 Å, 162.1°.
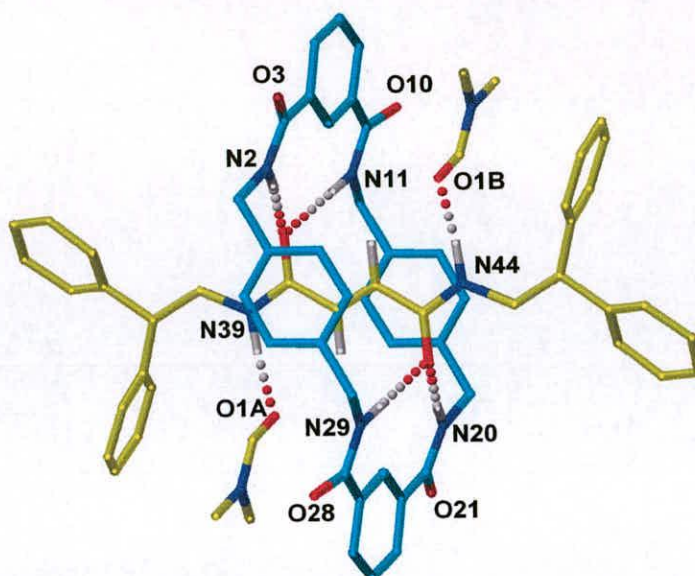
Figure 2.10b. X-ray crystal structure of fumaramide [2]rotaxane, **4**. X-ray crystal structure of the fumaramide [2]rotaxane **4**. Intramolecular hydrogen bond distances are the following: O40-HN2, O43-HN20 1.98 Å, 164.5°; O40-HN11-O43-HN29 2.06 Å, 162.6°.

Whilst there is a compensating increase in the number of intermolecular hydrogen bonds in the solid-state structure of **30**, a virtually identical packing architecture could be – but is not – formed by the fumaramide rotaxane and so this can be interpreted as a consequence of weaker hydrogen bonding interactions between the components in the succinamide rotaxane, **30**. It is interesting to note that a similar succinamide rotaxane prepared by the Vögtle group gave only 0.5 % of rotaxane,[20] although the "threading" method of rotaxane formation used involves only three-components in the assembly reaction compared to the five-component clipping method described here.

Remarkably, reducing or increasing what we assume is the near-optimum length spacer of two carbon atoms by one to give malonamide **29** and glutaramide **31** diamides still results in [2]rotaxane formation. The yields are consequentially low, 8 and 3 % respectively. In the standard staggered conformation of C_1 and C_3 alkyl chains the carbonyl groups would be on the same side of the thread and therefore not predisposed to template rotaxane formation; whereas in the cyclic form the hydrogen bond sites are tied up through intramolecular hydrogen bonding.

It appears that the macrocycle is able to bind to the internally hydrogen bonded cyclic structure of the malonamide thread (Figure 2.11a). This results in a highly unusual triply hydrogen bonded (all three intramolecular H-bonds) carbonyl group (O40). The glutaramide thread takes a different solution and the C_3 chain pays the thermodynamic cost of adopting a conformation with a gauche C–C bonding interaction in the backbone in order to position the amide carbonyl groups on opposite sides of the thread so that they can both hydrogen bond to the macrocycle (Figure 2.11b).
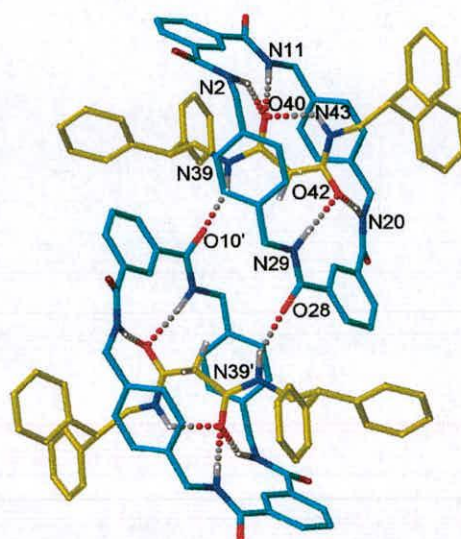
Figure 2.11a. X-ray crystal structure of malonamide [2]rotaxane, **29**. Intramolecular hydrogen bond distances and angles: O40–HHN2 2.49 Å, 153.1°; O40–HN11 1.89 Å, 168.3°; O40–HN43 2.05 Å, 126.3°; O42–HN20 2.32 Å, 173.7°; O42–HN29 1.95 Å, 173.2°. Intermolecular hydrogen bond distances and angles: N39H–O10'/O28–HN39' 1.94 Å, 148.7°.
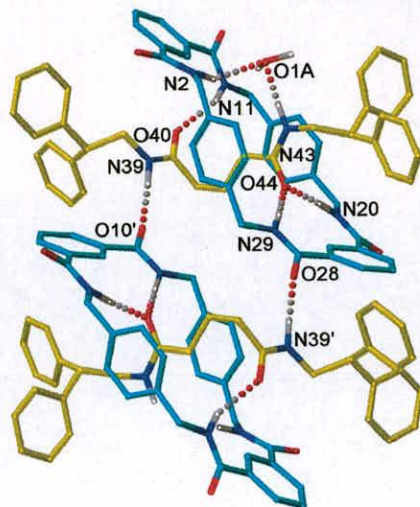
Figure 2.11b. X-ray crystal structure of glutaramide [2]rotaxane, **31**. Intramolecular hydrogen bond distances and angles: O40–HN11 2.01 Å, 138.7°; O44–HN20 2.02 Å, 175.0°; O44–HN29 1.91 Å, 177.3°. Intermolecular hydrogen bond distances and angles: N2H–O1A 2.22 Å, 141.2°; N43H–O1A 1.83 Å, 164.0°; N39H–O10'/O28–HN39' 1.85 Å, 162.8°.

Adding a further methylene group to produce a C_4 adipamide thread **32** predisposes the carbonyl groups to be on opposite sides of the thread, as in the fumaramide and succinamide templates, but almost doubles the distance between the hydrogen bonding sites in a staggered chain conformation (3.87 → 6.37 Å).

The solid-state structure of the rotaxane **32** (Figure 2.12) shows that the macrocycle is able to overcome this problem without recourse to a sterically unfavorable thread geometry by adopting a stretched half-chair conformation. The yield of rotaxane is still low (8%). Gellman's study[19] of alkyl diamides (although they studied hydrogen bonding in tertiary amides not secondary) suggests that adipamide has a greater enthalpic driving force to form intramolecularly hydrogen bonded (in this case, nine-membered) rings than most other alkyl diamides, the larger ring size giving rise to more linear intramolecular hydrogen bonds.
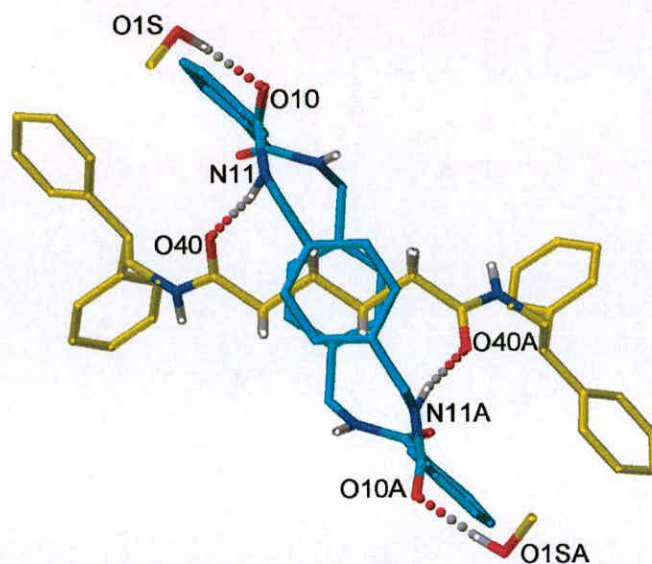
Figure 2.12a. X-Ray crystal structure of adipamide [2]rotaxane, **32**, crystals grown from CHCl₃/MeOH. Intramolecular hydrogen bond distances and angles: O40–HN11/O40A–HN11A 2.00 Å, 168.8°. Intermolecular hydrogen bond distances and angles: O10–HO1S/O10–HO1SA 1.98 Å, 176.7°.
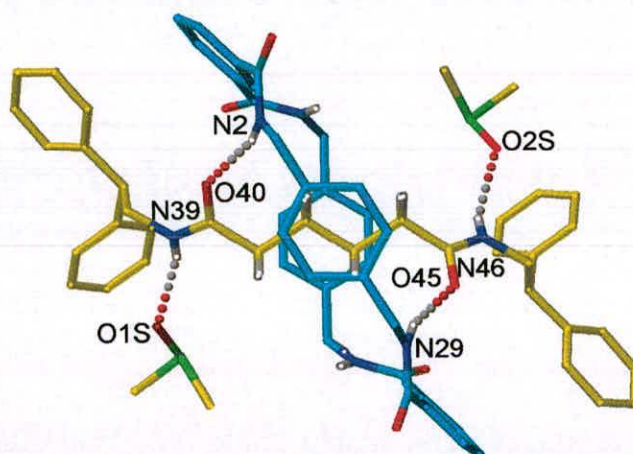
Figure 2.12b. X-Ray crystal structure of adipamide [2]rotaxane, **32**, crystals grown from DMSO. Intramolecular hydrogen bond distances and angles: O40–HN2 2.22 Å, 163.0°; O45–HN29 2.18 Å, 160.7°. Intermolecular hydrogen bond distances and angles: N39H–O1S 2.20 Å, 155.2°; N46H–O2S 2.23 Å, 153.2°.

It is interesting to note that the solid-state structure of the adipamide rotaxane is virtually identical whether the crystals were grown from a solution of nonpolar $CHCl_3$ (Figure 2.12a) with infusion of MeOH or from a polar medium, DMSO, with infusion of H_2O (Figure 2.12b). The only significant difference in the structures is that solvent molecules bind to the amide NH groups of the thread in the $DMSO/H_2O$ system and to the amide carbonyl groups of the macrocycle with the $CHCl_3/MeOH$ system. The conformations and co-conformation of the thread and macrocycle are essentially unaffected by the incorporated solvent molecules, or the nature of the environment that the crystals were grown from, and the position of the macrocycle is best suited to maximize its hydrogen bonding interactions with the adipamide thread. Normally, benzylic amide macrocycle-based rotaxanes and catenanes are extremely sensitive to the polarity of the environment; solvents like DMSO disrupt the intercomponent amide–amide hydrogen bonds and polarophobic effects drive lipophilic groups inside the macrocycle to escape a polar solvent shell.[21] The effect has been used to translocate the macrocycle along the thread in amphiphilic peptide molecular shuttles.

However, in the adipamide [2]rotaxane **32** the lack of influence of the nature of the solvent of crystallization on the solid-state structure is translated through to the solution structure of the rotaxane in nonpolar and polar media as illustrated by the respective ^1H NMR spectra in $CDCl_3$ and d_6-DMSO (Figure 2.13). The position of macrocycle in each case can be determined by the upfield shift of the thread protons due to the shielding effects of the xylylene rings of the macrocycle. In $CDCl_3$ both sets of methylene protons in the template region of the thread, H_d and H_e, are shielded upfield by 1.14 and 0.97 ppm respectively (Figure 2.13a and 2.13b). The relative chemical shifts of these protons in the thread and rotaxane in d_6-DMSO show almost identical shifts, 1.04 and 0.96 ppm respectively (Figure 2.13c and 2.13d). Thus it can be seen that the adipamide binding site is perfectly balanced. Hydrogen bonds to the amide groups of the thread hold it in place in a nonpolar solvent, and the polarophobic nature of the adipyl alkyl chain holds it in the same place in a highly polar solvent!
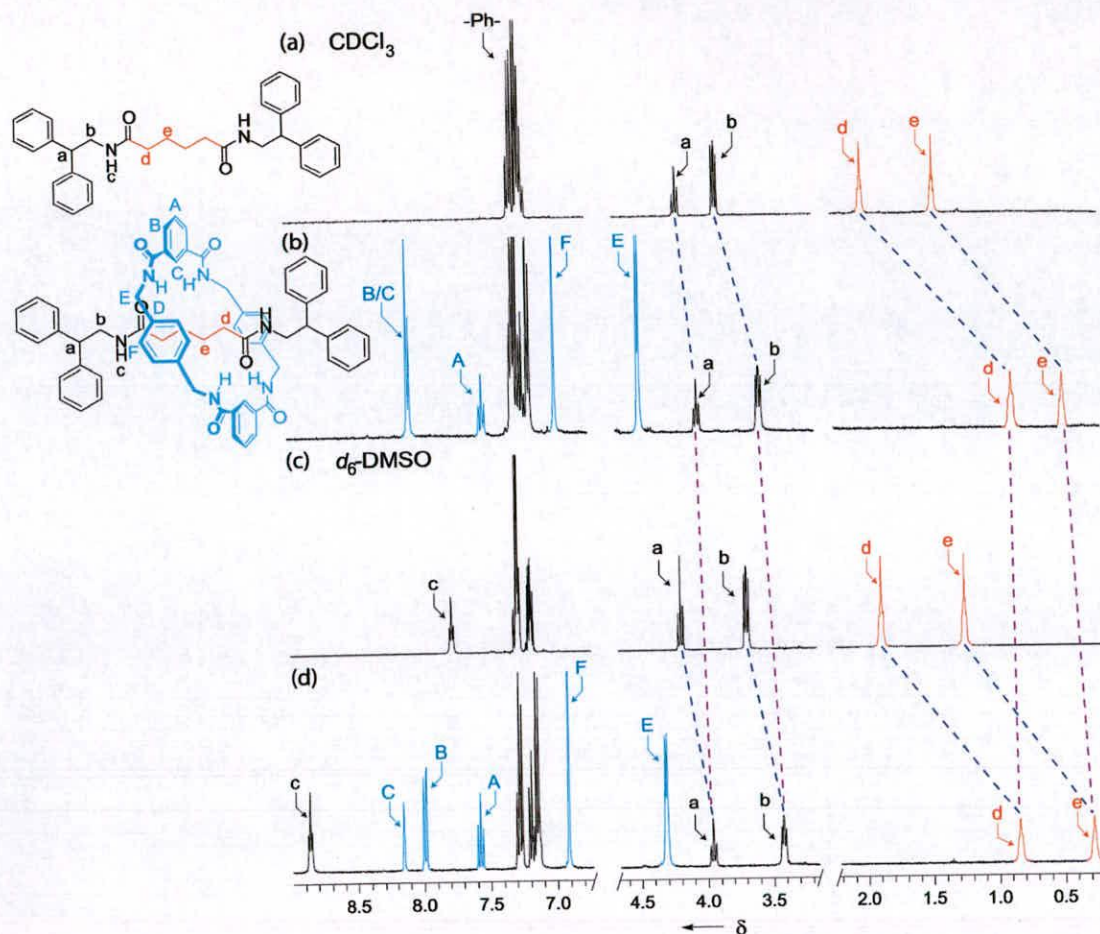
Figure 2.13. ^{1}H NMR spectra (400 MHz, 300 K) of the adipamide thread and [2]rotaxane: (a) **21** CDCl$_3$, (b) **32** CDCl$_3$, (c) **21** d_6-DMSO and (d) **32** d_6-DMSO.

When the number of methylene groups in the template site of the thread increases to n=5, 6 and 7, the crystal structures (Figure 2.14a, 2.14b and 2.14c) of the rotaxanes **33–35** are very different to the solid-state structure of the shorter threads.

(a)
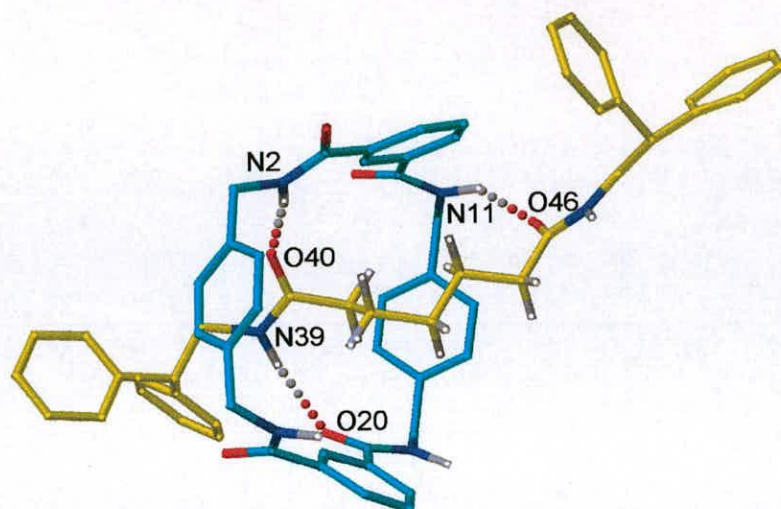
(b)
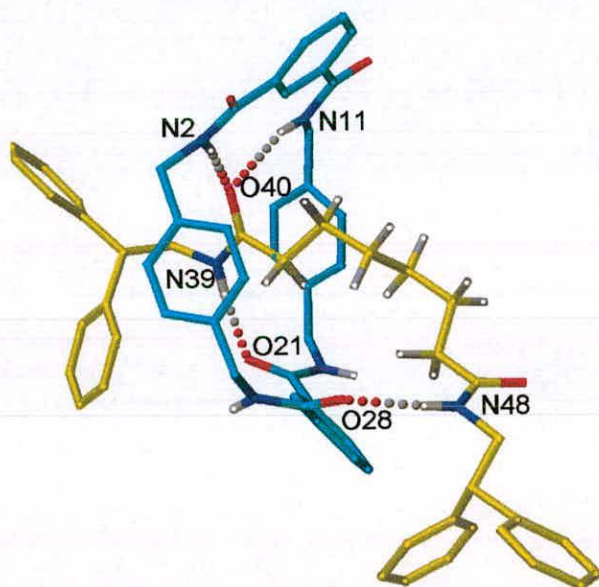
Figure 2.14a and Figure 2.14b. *X*-Ray crystal structure of (a) pimelamide [2]rotaxane, **33**. Intramolecular hydrogen bond distances and angles: N39H–O20   2.21 Å, 158.8°; O40–HN2   1.85 Å, 153.4°; O46–HN11   1.97 Å, 144.3°; (b) suberamide [2]rotaxane, **34**. Intramolecular hydrogen bond distances and angles: N39H–O21 2.01 Å, 167.9°;   O40–HN2 2.14 Å, 168.1°; O40–HN11 2.42 Å, 164.2°; N48H–O28 2.12 Å, 169.0°.
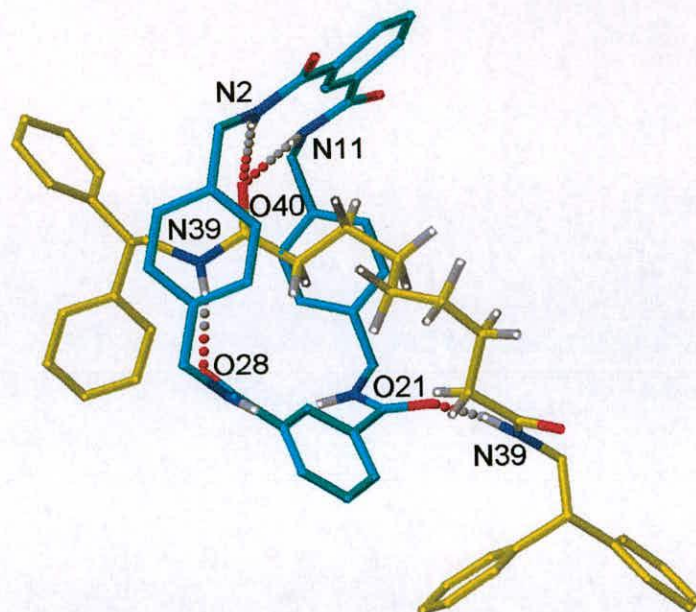
Figure 2.14c. *X*-Ray crystal structure of azelamide [2]rotaxane, **35**. Intramolecular hydrogen bond distances and angles: N39H–O28 2.12 Å, 168.5°; O40, HN2 2.42 Å, 162.7°; O40–HN11 2.16 Å, 164.6°; N39H–O21 1.96 Å, 159.5°.

In all three cases, the macrocycle adopts a boat-like conformation, encapsulating one of the two amide groups of the thread, and hydrogen bonds to the second amide binding site by folding of the thread backbone. As the thread increases in length, the folding necessarily becomes more and more pronounced. The ^{1}H NMR spectra (Figure 2.15) show that the corresponding CDCl$_3$ solution structure in all three cases – and in contrast to the adipamide rotaxane – is very different to the snapshot picture captured in the solid-state structure.

The X-ray crystal structures of **33–35** show that the macrocycle essentially sits over one amide group in the solid state. The comparison of the shifts of protons in the threads and rotaxanes show that this is not the case in CDCl$_3$.
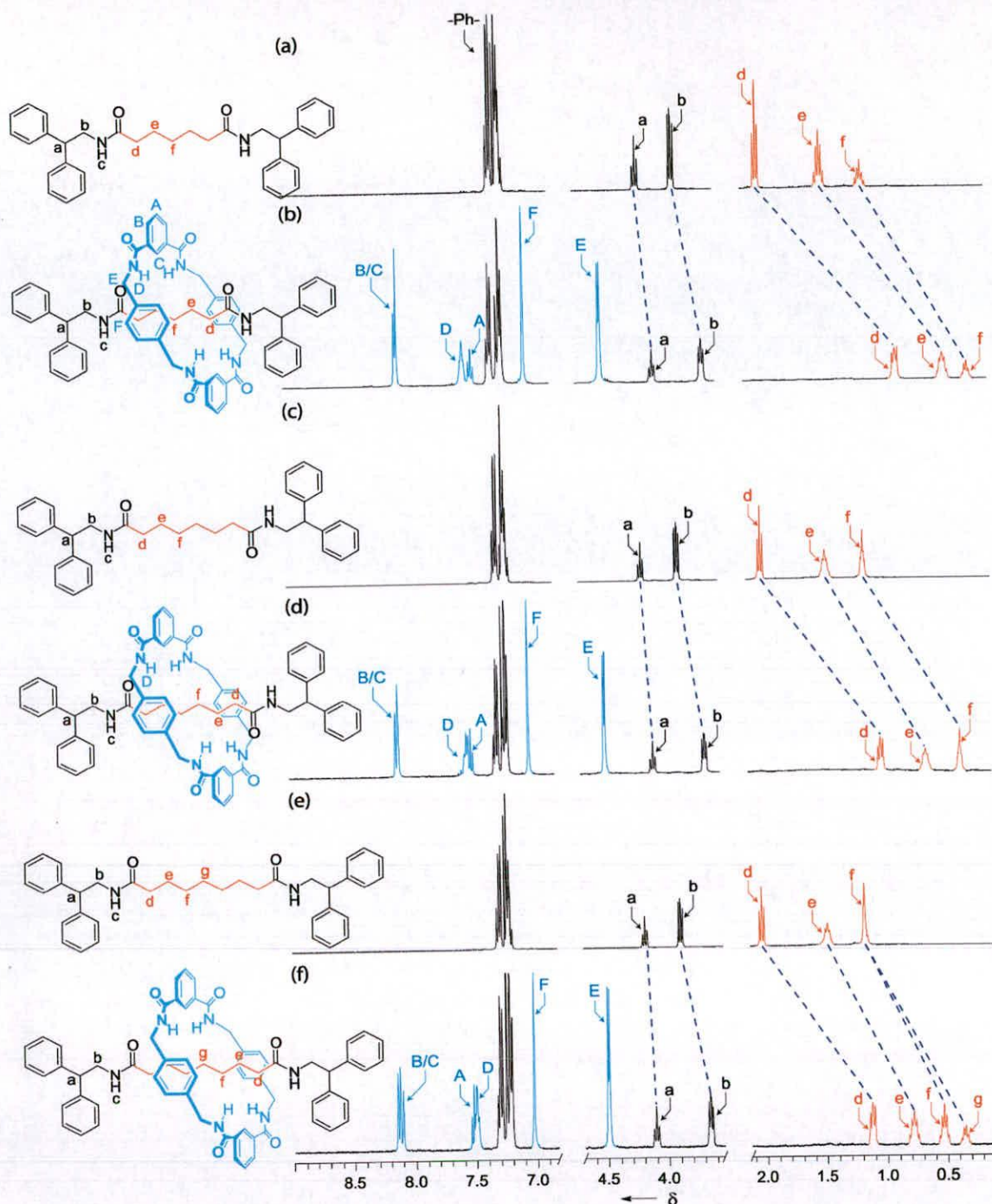
Figure 2.15. ^{1}H NMR spectra (400 MHz, 300 K) in CDCl$_3$ of (a) pimelamide thread, **22**, (b) pimelamide [2]rotaxane, **33**, (c) suberamide thread, **23**, (d) suberamide [2]rotaxane **34**, (e) azelamide thread, **24** and (f) azelamide [2]rotaxane **35**.

In fact, in each rotaxane the shielding of each methylene group is virtually the same as any other indicating that in CDCl$_3$ solution the macrocycle is reasonably evenly distributed all along the diamide thread. This could result from a nonspecific binding

mode of the macrocycle to the thread or, more likely, indicates that the type of co-conformations seen in the X-ray structures are in equilibrium with another major co-conformation where the macrocycle sits in the centre of the thread and bridges the two thread amide groups.

The yield of [2]rotaxane formation for template spacers n= 5, 6 and 7 are similar at 14, 17 and 15% respectively.

The hydrogen bond directed-assembly of benzylic amide rotaxanes is so efficient and effective that [2]rotaxane was still obtained on increasing the number of methylene groups between the two amides from n= 8 to n= 14. With the longer spacer, the solid-state structure of the rotaxanes, **36–39**, is very different to those seen previously (Figure 2.16).
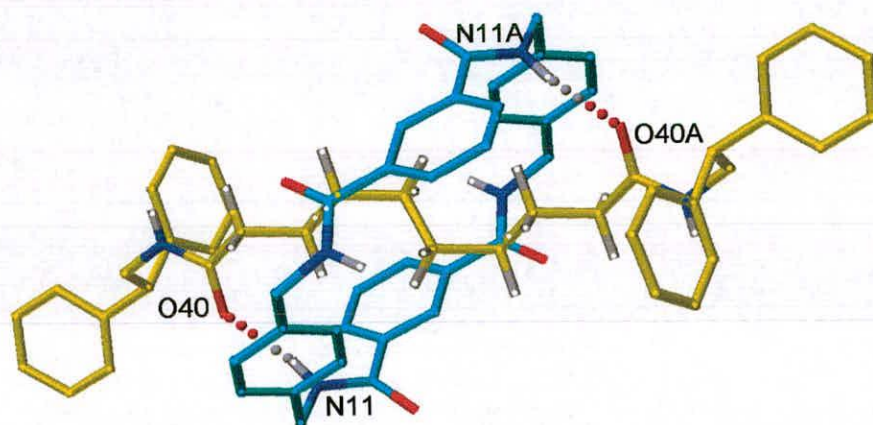
Figure 2.16a. X-Ray crystal structure of sebacamide [2]rotaxane, **36**, intramolecular hydrogen bond distances and angles: O40–HN11/O40A–N11A 2.05 Å, 168.2°

(b)
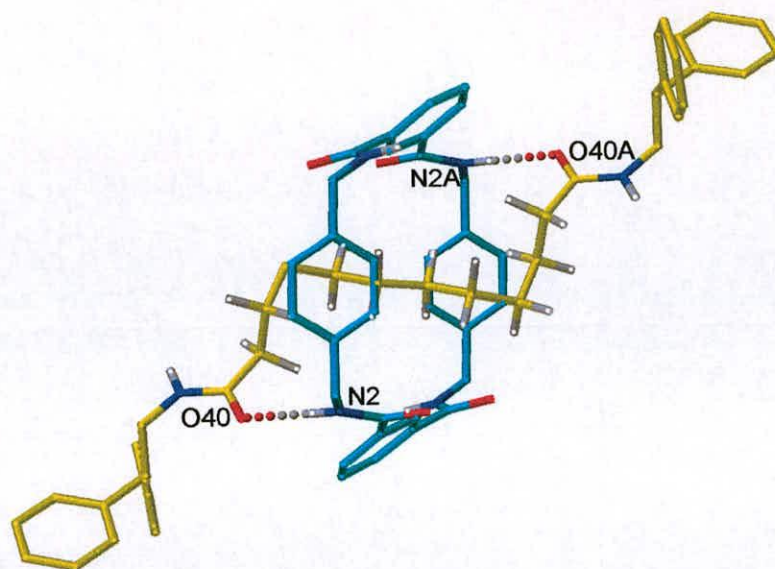
(c)
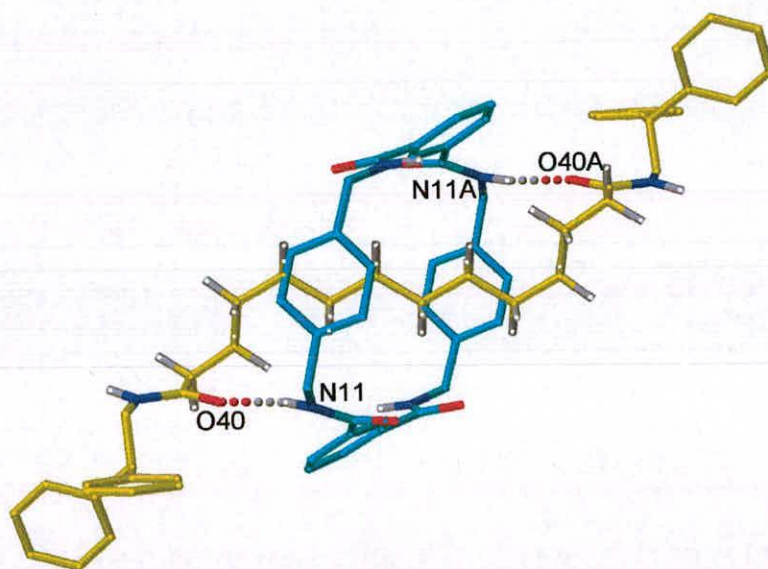
Figure 2.16b and Figure 2.16c. X-Ray crystal structure of (b) 1,10-decanediamide [2]rotaxane, **37**, intramolecular hydrogen bond distances and angles: O40–HN2/O40A–HN2A 2.00 Å, 172.3°, (c) 1,12-dodecanediamide [2]rotaxane, **38**, intramolecular hydrogen bond distances and angles:O40–HN11/O40A–HN11A 1.92 Å, 156.4°.
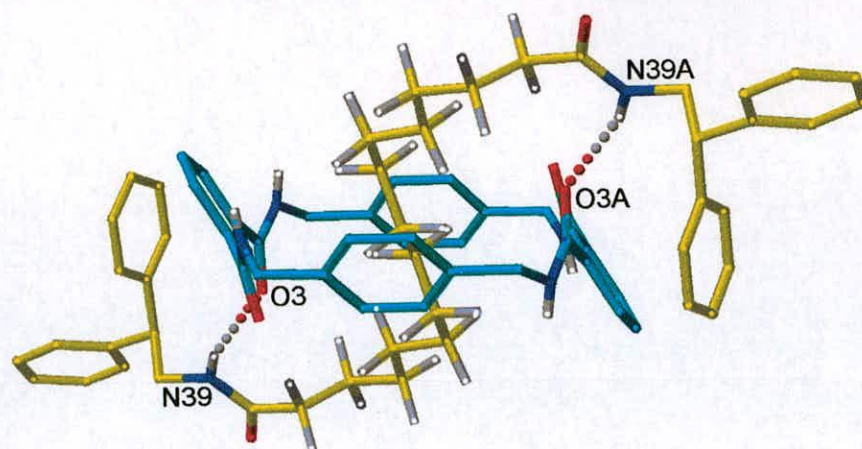
Figure 16d. *X*-Ray crystal structure of 1,14-tetradecanediamide [2]rotaxane, **39**, intramolecular hydrogen bond distances and angles: O3–HN39/O3A–HN39A 2.24 Å, 151.7°.

With ≥8 methylene groups in the spacer, the size of the ring that would be required for the thread to fold back to hydrogen bond to the macrocycle if it were encapsulating a single amide residue is so large that that co-conformation is no longer seen in the solid state. Instead, the macrocycle maximizes its intramolecular hydrogen bonding interactions by residing at the center of the thread which assumes an "S"-shape conformation. As the number of methylene groups increases from 8 to 14, the curvature of the "S" becomes more pronounced. In all four rotaxanes, the macrocycle is able to adopt a low energy chair-like conformation. In contrast to the crystal structures, the ^{1}H NMR spectra of **36–39** and their respective threads (Figure 2.17) follow the same trends as those of rotaxanes and threads n=5–7, namely a similar degree of shielding for all the methylene groups between the amide groups of the thread.
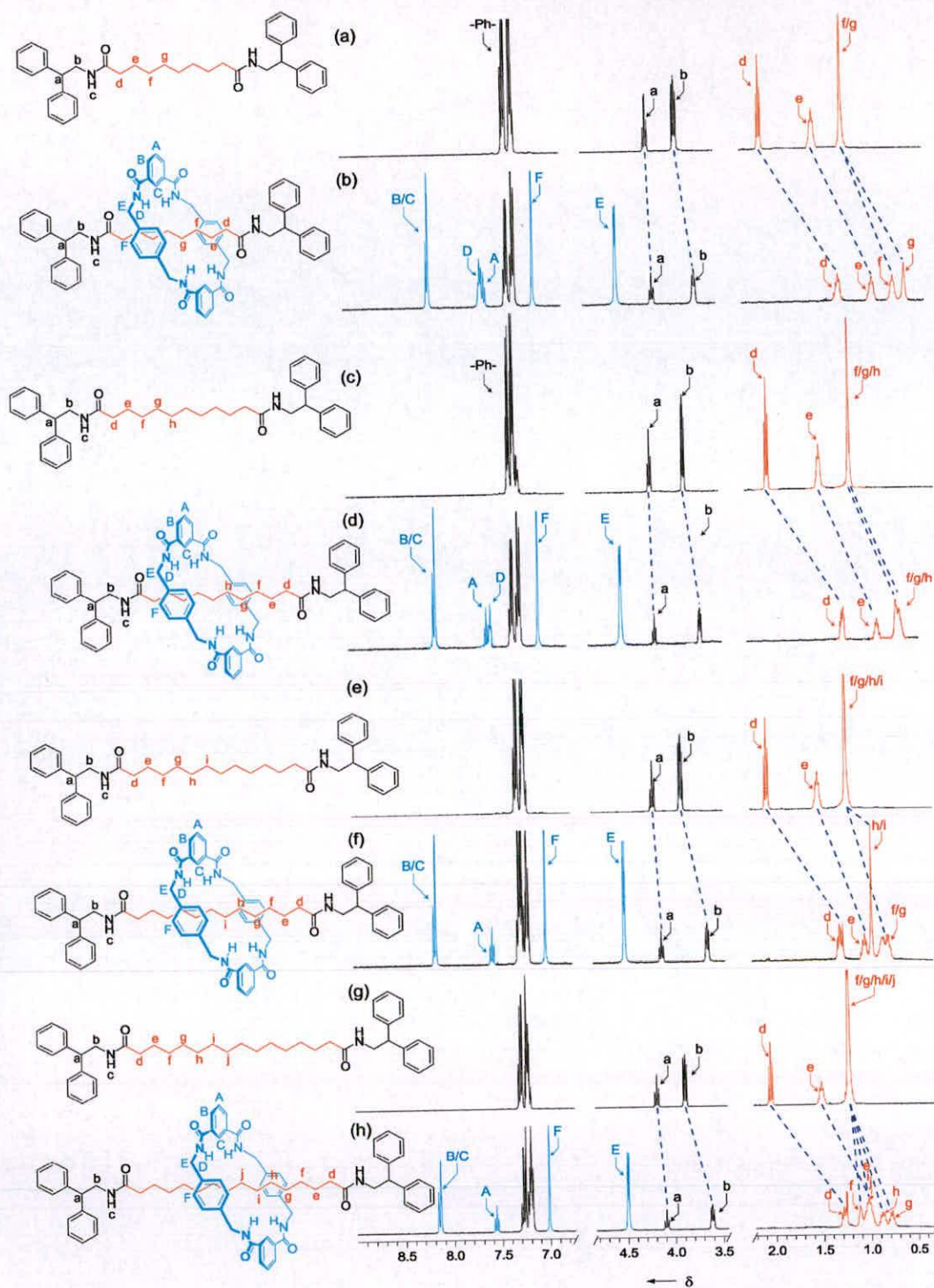
Figure 2.17. ^{1}H NMR spectra (400 MHz, 300 K) in CDCl$_3$ of (a) sebacamide thread, **25**; (b) sebacamide [2]rotaxane, **36**; (c) 1,10-decandiamide thread, **26**; (d) 1,10-decandiamide thread, **26**; [2]rotaxane, **37**; (e) 1,12-dodecanediamide thread, **27**; (f) 1,12-dodecanediamide thread [2]rotaxane **38**; (g) 1,14-tetradecanediamide thread, **28**; (h) 1,14-tetradecanediamide [2]rotaxane **39**.

What are the solution structures of rotaxanes **33-39** in CDCl₃? Although their crystal structures fall into two very different classes, the ¹H NMR spectra follow very similar trends. It seems likely that both amide-encapsulated (type **I**) and alkyl chain-encapsulated (type **II**) co-conformations exist in solution for all these rotaxanes and what differs with the increasing length of the alkyl chain is their relative stabilities and thus populations (Figure 2.18). When the chain is short (C_5–C_7), co-conformer **I** dominates (as there are two amides per chain there are two such co-conformers, **I$_a$** and **I$_b$**); when the chain is long (C_8–C_{14}) co-conformer **II** becomes relatively more stable (Figure 2.18a). In 'shuttling' from **I$_a$** and **I$_b$**, a low energy route is likely to be co-conformer **II**. Although the solution behavior of amphiphilic peptide-based molecular shuttles is different to these single amide shuttles in that the macrocycle is clearly located around the peptide stations in CDCl₃, it may be that the low energy route for shuttling in those rotaxanes involves a structure that bridges both peptide units (**IV**, Figure 2.18b).

(a)

Two types of translational isomers present in CDCl₃ solution

(b)

Only one type of translational isomer present in solution
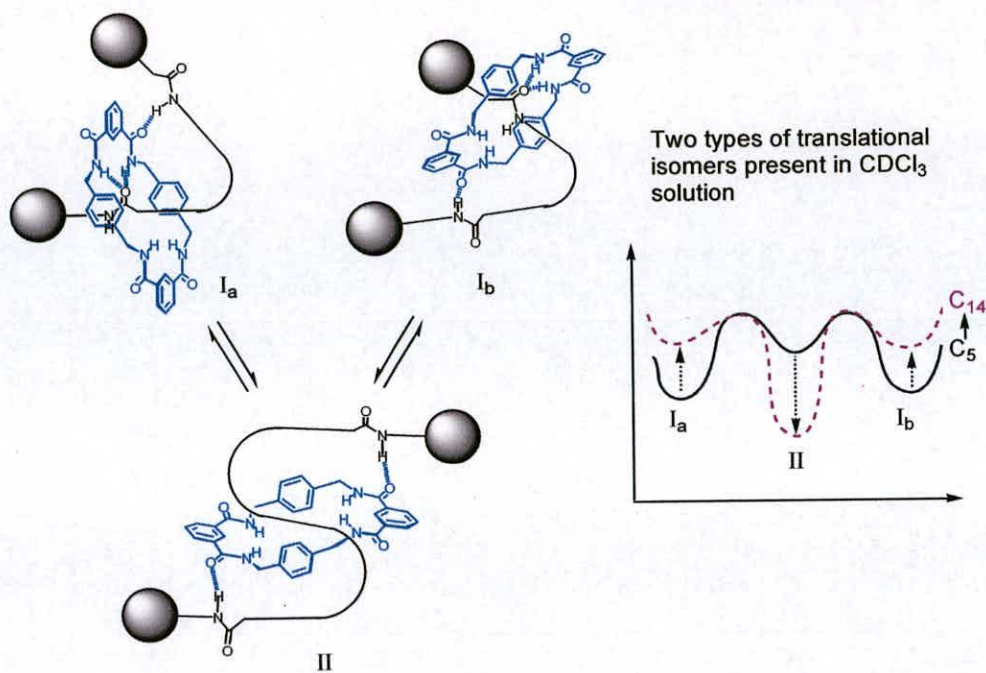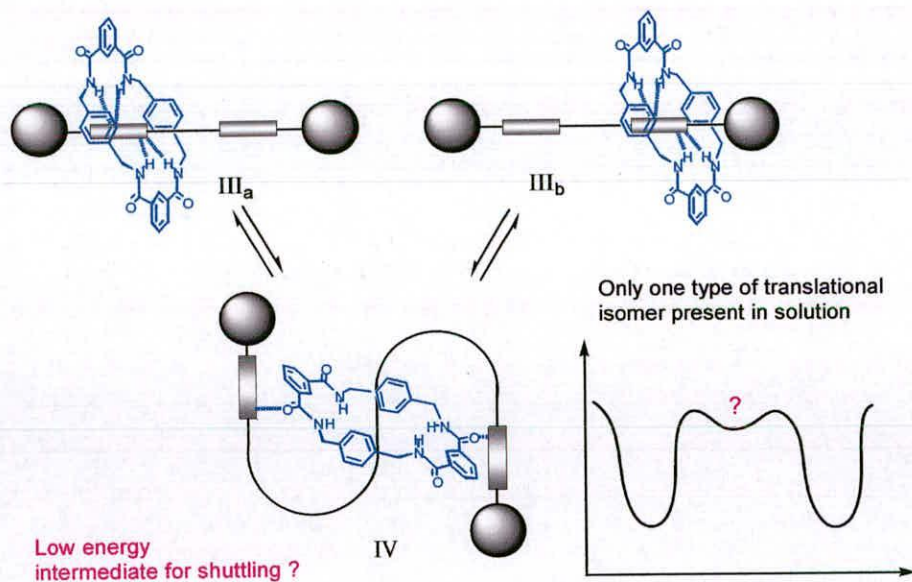
Figure 2.18. Co-conformations existing in solution of (a) amphiphilic amide-based rotaxanes, **29–39**; (b) amphiphilic peptide-based molecular shuttles, **40**.

To reassert this fact, the shuttling behaviour of a [2]rotaxane **40**, (containing two diamide stations-Figure 2.19), analogous to single amide [2]rotaxane **38** was studied.
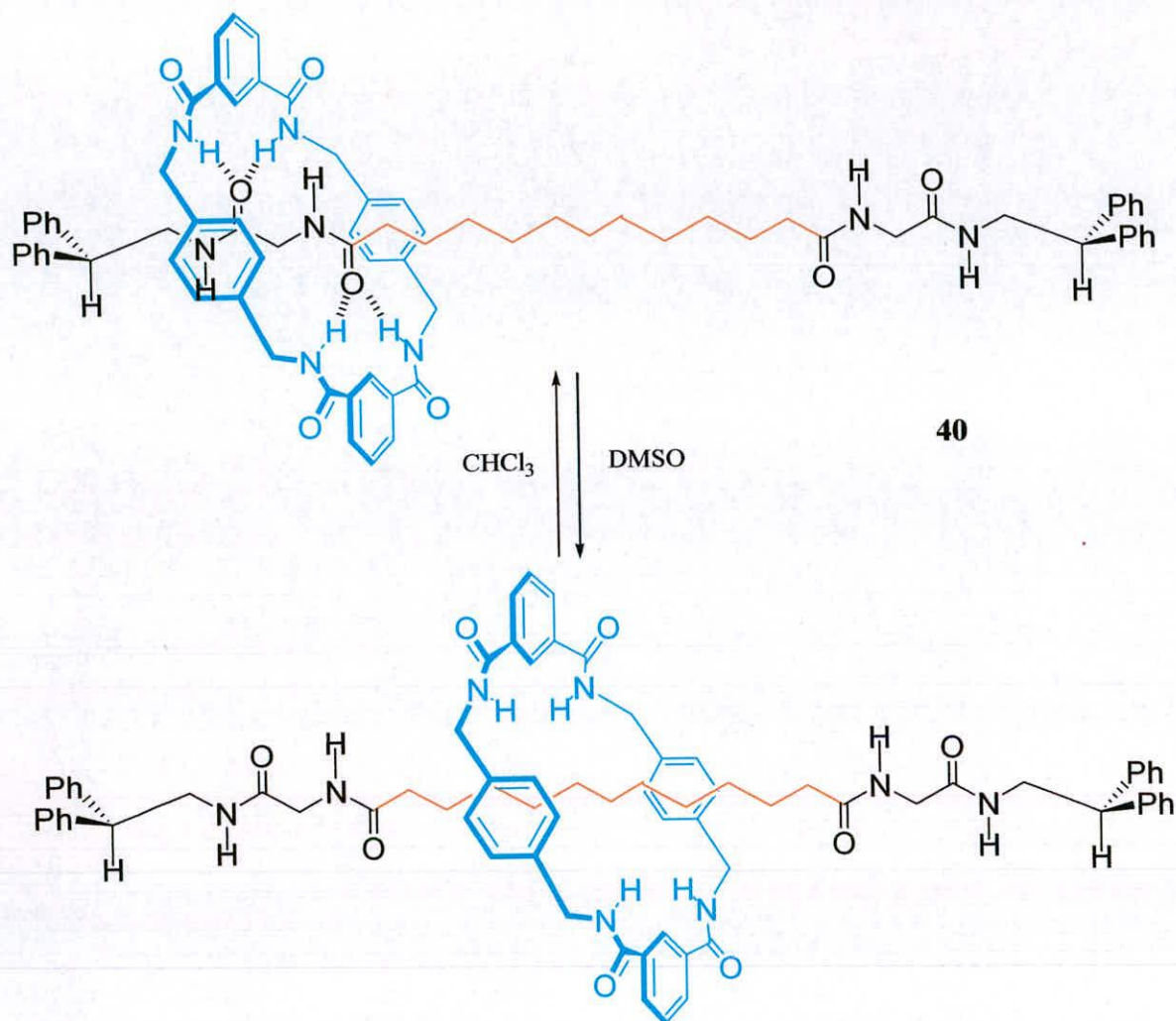
Figure 2.19. Operation of a solvent-dependent molecular shuttle **40** containing two diamides analogous to rotaxane **38**

Analysis of ^{1}H NMR spectra of **40** in CDCl$_3$ shows that the macrcocycle is shuttling between the two degenerate stations, but no significant shielding of the alkyl chain protons is observed. However, in d_6-DMSO the macrocycle clearly resides on the alkyl chain portion of the thread due to strong shielding of the associated protons.
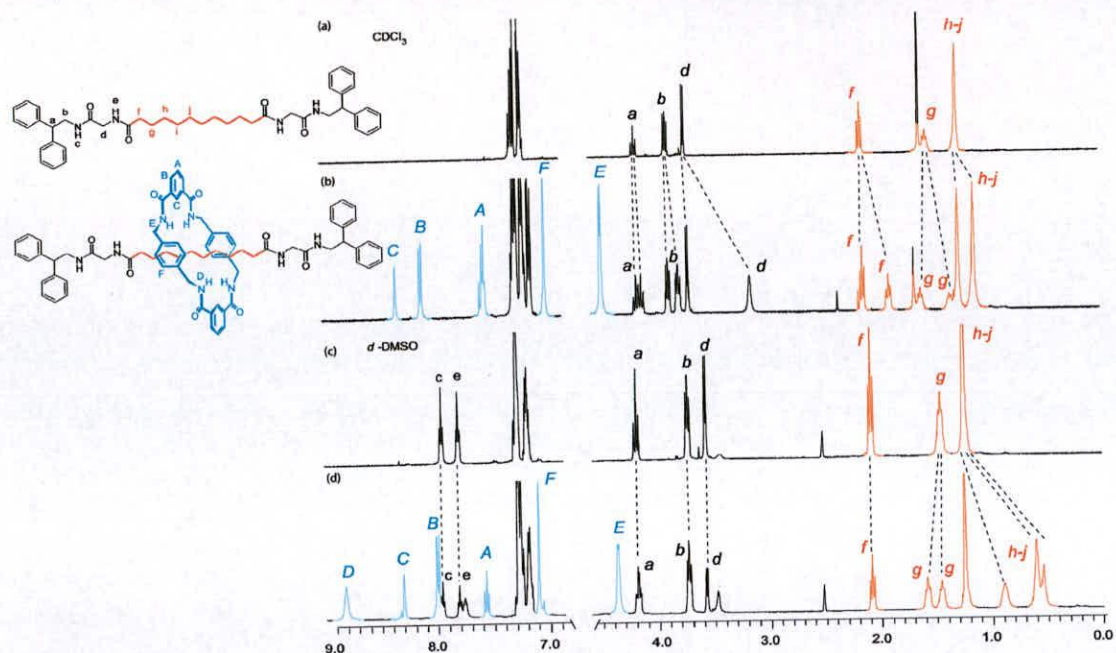
Figure 2.20. ^{1}H NMR spectra (400 MHz): (a) *thread*-**40** CDCl$_3$, (b) **40** CDCl$_3$, (c) *thread*-**40** d_6-DMSO and (d) **40** d_6-DMSO.

The number of relatively low energy conformations of the C$_{14}$ spacer template is considerable, with greater than 4 million (3^{14}) C–C rotamers theoretically available. Nevertheless, the yield of the [2]rotaxane is comparable to most of the others in this series. Are all these thread conformations really templates for rotaxane formation? Of course, they do not have to be. If uncatalyzed cyclization of the precursor to macrocycle is very slow but template-induced cyclization about the thread to give rotaxane is very fast then only a small fraction of threads have to be able to adopt a suitable conformation for significant amounts of rotaxane to be formed. However, if the template encompasses the whole length of the alkyl chain in each case, then a decrease in yield of rotaxane formation with increasing chain length would be expected. Since this is not observed in this series, this implies that – in the longer rotaxanes – the macrocycle cyclizes essentially around a single amide group and the part that the second amide plays in the cyclization process is relatively unimportant.

2.2.3 Removing the Donor Groups on the Spaced-out Threads

To test the above hypothesis the hydrogen bond donor groups in a selected number of the diamide threads were removed by methylation of the secondary amide functions. In doing this we hope to prove that in threads in which the spacer is longer, e.g., C_{14} the contribution to rotaxane formation whereby a second amide on the thread assists this process will be very small. Therefore, if the C_{14} thread **28** (Scheme 2.3) is indeed complexing the macrocycle *via* a single amide group and the donor sites have been removed, the thread would behave like thread **8** and [2]rotaxane should not be observed. Hence a series of tertiary diamide threads **42-49** were prepared (Scheme 2.4), in an analogous manner to diamide threads **18-28**, but using *N*-methyl-2,2-diphenylethylamine **41** as the stopper amine. The threads **42-49** were again subjected to standard rotaxane forming conditions (Scheme 2.4).

The molecular structures shown for the threads:

42 n = 2	**44** n = 4	**46** n = 8	**48** n = 12
43 n = 3	**45** n = 6	**47** n = 10	**49** n = 14

50	n = 2	26 %
51	n = 3	0.3 %
52	n = 4	0.2 %
53	n = 6	1.2 %
54	n = 8	0.8 %
55	n = 10	0.6 %
	n = 12	0 %
	n = 14	0 %
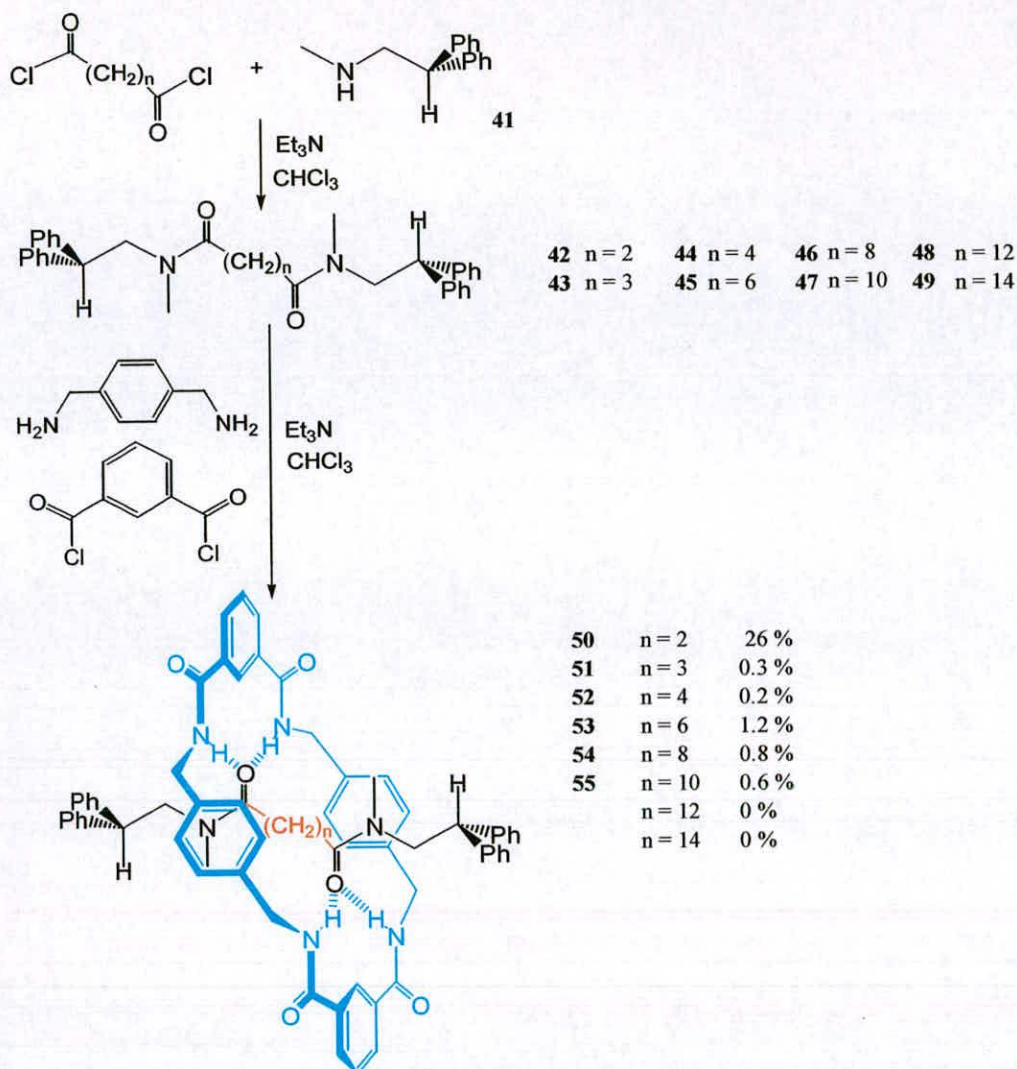
Scheme 2.4. Synthesis of tertiary diamide threads, **42–49** and rotaxanes, **50–55**.

The succinic derived rotaxane **50** (n=2) was isolated in an excellent 26 % yield. This is obviously the largest isolated yield of a [2]rotaxane in the dimethylated series, due primarily to the ideal spatial arrangement of the amide carbonyl groups of the succinic thread **42** to bind the benzylic amide macrocycle. However due the removal hydrogen bond-donors in the thread (i.e. by methylation of the secondary amide functions) the thread can no longer bind the macrocycle in a manner such as intermediate **A** (Figure 2.1), but only in a manner such as intermediate **B**. Hence, the number of intermediates that can promote interlocking are reduced leading to a reduction in the observed yield. In addition, the introduction of tertiary amide functions also introduces rotamer populations, some of which will be

conformationally unsuitable or too sterically encumbered, for rotaxane formation. The isolated yield of succinic rotaxane **50** is remarkably high when compared to the corresponding dimethylated fumaramide derivative of rotaxane **4**, which is obtained in 33 % yield.[22] The reasons for this difference are not immediately clear, but may be a reflection of deleterious effects operating in the fumaric derivative and not the succinic thread, rather than *vice versa*. The X-ray crystal structure of rotaxane **50** shows a pair of bifurcated hydrogen bonds to the succinamide-carbonyl, again a reflection of the interactions occurring during the formation of the rotaxane.
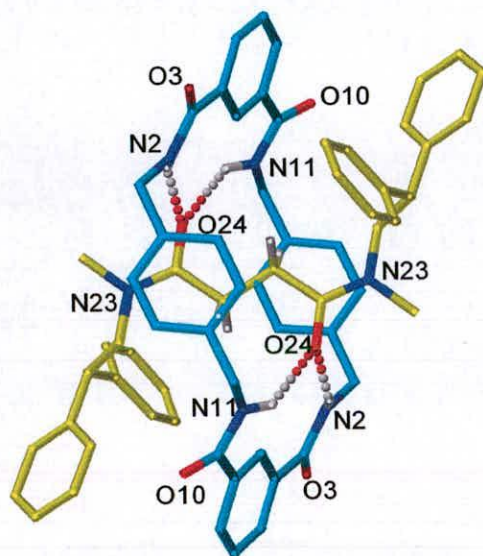
Figure 2.21. X-Ray crystal structure of [2]rotaxane **50**, intramolecular hydrogen bond distances and angles: N2H-O24 2.11 Å 144.3° N11H-O24 2.53Å 145.5°.

The treatment of threads **43-47** to standard rotaxane formation conditions, gave trace, but isolable amounts of the corresponding [2]rotaxanes **51-55**, but threads **48** and **49** gave none of the desired [2]rotaxane. This suggests that when the hydrogen bond donating ability of the thread is removed, then deviation from the optimal intercarbonyl distance needed to bind the macrocycle leads to a dramatic reduction in yield eventually leading to no isolable rotaxane. These observations indicate that the two amide groups are participating in the interlocking process, however it would appear that at longer chain lengths this is further reduced to an extent where no rotaxane is isolated.[23]

2.3 Conclusion

The hydrogen bond-directed assembly of benzylic amide macrocycle-containing rotaxanes is clearly a remarkable process. Indeed, the process can tolerate thread molecules containing only a single binding site within its structure, occasionally affording corresponding [2]rotaxanes in good yields. This now suggests potential routes to a range of functional thread molecules that could directly form benzylic amide macrocycle-containing rotaxanes, e.g. urea dyes. Perhaps, more remarkably the 5-component clipping reaction can tolerate flexibility and intramolecular hydrogen bonds within the studied thread elements and it is *still* possible to form rotaxanes, albeit in moderate to poor yields, even with a far from optimized template. However, removal of the complementary donor element of binding sites has profound effects on the resulting yield of rotaxane and as such clearly plays an essential role in the interlocking process, even when intercomponent interactions to these groups are not observed in the solid-state structure of the resulting products. Notwithstanding, the general process of benzylic amide rotaxane formation is indeed a prime example of the unique way in which hydrogen bonding can orchestrate many components to elaborate products of high complexity, even in the presence of competing factors.

2.4 References

1   G. A. Jeffrey, W. Saenger, (Eds.), *Hydrogen Bonding in Biological Structures,* Springer-Verlag, Berlin, **1991**.

2   L. J. Prins, D. N. Reinhoudt, P. Timmerman, *Angew. Chem. Int. Ed.* **2001**, *40,* 2382-2426.

3   For reviews of mechanically interlocked architectures see: a) D. B. Amabilino, J. F. Stoddart, *Chem. Rev.* **1995**, *95,* 2725-2828; b) J.-P. Sauvage, C. Dietrich-Buchecker (Eds.), *Molecular Catenanes Rotaxanes and Knots*: *A Journey Through the World of Molecular Topology,* Wiley-VCH, Weinheim, **1999**; c) G. A. Breault, C. A. Hunter, P. C. Mayers, *Tetrahedron* **1999**, *55,* 5265-5293.

4   For examples of catenanes assembled using intercomponent amide hydrogen bonds see: a) C. A. Hunter, *J. Am. Chem. Soc.* **1992**, *114,* 5303-5311; b) F. Vögtle, S. Meier, R. Hoss, *Angew. Chem. Int. Ed. Engl.* **1992**, *31,* 1619-1622; c) A. G. Johnston, D. A. Leigh, R. J. Pritchard, M. D. Deegan, *Angew. Chem. Int. Ed. Engl.* **1995**, *34,* 1209-1212.

5   For examples of catenanes assembled through crown ether/ ammonium ion NH^{+}---O hydrogen bonds see: a) S. H. Chiu, A. M. Elizarov, P. T. Glink, J. F. Stoddart, *Org. Lett.* **2002**, *4,* 3561-3564; b) H. Iwamoto, K. Itoh, H. Nagamiya, Y. Fukazawa, *Tetrahedron Lett.* **2003**, *44,* 5773-5776.

6   Although thought to assemble primarily through π-π interactions the presence of CH---O hydrogen bonds between electron deficient components and crown ether functions are equally important in the assembly of a class of interlocked molecules. For examples of catenanes assembled in this way see: a) P. R. Ashton, T. T. Goodnow, A. E. Kaifer, M. V. Reddington, A. M. Z. Slawin, N. Spencer, J. F. Stoddart, C. Vicent, D. J. Williams, *Angew. Chem. Int. Ed. Engl.* **1989**, *28,* 1396-1399; b) D. G. Hamilton, J. K. M. Sanders, J. E. Davies, W. Clegg, S. J. Teat, *Chem. Commun.* **1997**, 897-898.

7   For representative examples of rotaxanes assembled using intercomponent neutral amide hydrogen bonds see: a) A. G. Johnston, D. A. Leigh, A. Murphy, J. P. Smart, M. D. Deegan, *J. Am. Chem. Soc.* **1996**, *118,* 10662-10663; b) R.

Jäger, F. Vögtle, *Angew. Chem. Int. Ed. Engl.* **1997**, *36*, 930-944 and references cited therein.

8   For examples of rotaxanes assembled using anions as hydrogen bond templates see: a) G. M. Hübner, J. Glaser, C. Seel, F. Vögtle, *Angew. Chem. Int. Ed.* **1999**, *38*, 383-386; b) J. A. Wisner, P. D. Beer, M. G. B. Drew, M. R. Sambrook, *J. Am. Chem. Soc.* **2002**, *124*, 12469-12476; c) P. Ghosh, O. Mermagen, C. A. Schalley, *Chem. Commun.* **2002**, 2628-2629.

9   For representative examples of rotaxanes assembled using crown ether/ ammonium ion NH$^+$---O hydrogen bonds see: a) P. R. Ashton, P. T. Glink, J. F. Stoddart, P. A. Tasker, A. J. P. White, D. J. Williams, *Chem. Eur. J.* **1996**, *2*, 729-736; b) P. T. Glink, A. I. Oliva, J. F. Stoddart, A. J. P. White, D. J. Williams, *Angew. Chem. Int. Edit.* **2001**, *40*, 1870-1875.

10   For representative examples of rotaxanes assembled through CH---O hydrogen bonds between π-electron donors and π-electron acceptors see see: a) P. L. Anelli, P. R. Ashton, R. Ballardini, V. Balzani, M. Delgado, M. T. Gandolfi, T. T. Goodnow, A. E. Kaifer, D. Philp, M. Pietraszkiewicz, L. Prodi, M. V. Reddington, A. M. Z. Slawin, N. Spencer, J. F. Stoddart, C. Vicent, D. J. Williams, *J. Am. Chem. Soc.* **1992**, *114*, 193-218; b) D. B. Amabilino, P. R. Ashton, M. Bělohradský, F. M. Raymo, J. F. Stoddart, *J. Chem. Soc. Chem. Commun.* **1995**, 747-750.

11   For an example of a knot assembled using intercomponent amide hydrogen bonds see: O. Safarowsky, M. Nieger, R. Fröhlich, F. Vögtle, *Angew. Chem. Int. Ed.* **2000**, *39*, 1616-1619.

12   For an example of a knot assembled through CH---O hydrogen bonds between π-electron donors and π-electron acceptors see: P. R. Ashton, O. A. Matthews, S. Menzer, F. M. Raymo, N. Spencer, J. F. Stoddart, D. J. Williams, *Liebigs Ann.* **1997**, 2485-2494.

13   D. A. Leigh, A. Murphy, *Chem. Ind.* **1999**, 178-184.

14   a) D. A. Leigh, A. Murphy, J. P. Smart, A. M. Z. Slawin, *Angew. Chem. Int. Ed. Engl.* **1997**, *36*, 728-732; b) W. Clegg, C. Gimenez-Saiz, D. A. Leigh, A. Murphy, A. M. Z. Slawin, S. J. Teat, *J. Am. Chem. Soc.* **1999**, *121*, 4124-4129; c) M. Asakawa, G. Brancato, M. Fanti, D. A. Leigh, T. Shimizu, A. M. Z.

Slawin, J. K. Y. Wong, F. Zerbetto, S. W. Zhang, *J. Am. Chem. Soc.* **2002**, *124*, 2939-2950; d) F. G. Gatti, D. A. Leigh, S. A. Nepogodiev, A. M. Z. Slawin, S. J. Teat, J. K. Y. Wong, *J. Am. Chem. Soc.* **2001**, *123*, 5983-5989.

15   a) A. S. Lane, D. A. Leigh, A. Murphy, *J. Am. Chem. Soc.* **1997**, *119*, 11092-11093; b) A. M. Brouwer, C. Frochot, F. G. Gatti, D. A. Leigh, L. Mottier, F. Paolucci, S. Roffia, G. W. H. Wurpel, *Science* **2001**, *291*, 2124-2128; c) G. W. H. Wurpel, A. M. Brouwer, I. H. M. van Stokkum, A. Farran, D. A. Leigh, *J. Am. Chem. Soc.* **2001**, *123*, 11327-11328; d) A. Altieri, G. Bottari, F. Dehez, D. A. Leigh, J. K. Y. Wong, F. Zerbetto, *Angew. Chem. Int. Ed.* **2003**, *42*, 2296-2300; e) T. Da Ros, D. M. Guldi, A. F. Morales, D. A. Leigh, M. Prato, R. Turco, *Org. Lett.* **2003**, *5*, 689-691; f) J. S. Hannam, T. J. Kidd, D. A. Leigh, A. J. Wilson, *Org. Lett.* **2003**, *5*, 1907-1910; g) A. Alteri, F. G. Gatti, E. R. Kay, D. A. Leigh, D. Martel, F. Paolucci, A. M. Z. Slawin, J. K. Y. Wong, *J. Am. Chem. Soc.* **2003**, *125*, 8644-8654.

16   The details of the synthesis of threads **7-13** and their precursors can be found in the experimental section 2.5.

17   E. M. Arnett, E. J. Mitchell, T. S. S. R. Murty, *J. Am. Chem. Soc.* **1974**, *96*, 3875-3891.

18   a) P. A. Brooksby, C. A. Hunter, A. J. McQuillan, D. H. Purvis, A. E. Rowan, R. J. Shannon, R. Walsh, *Angew. Chem. Int. Ed. Engl.* **1994**, *33*, 2489-2491; b) F. J. Carver, C. A. Hunter, R. J. Shannon, *J. Chem. Soc. Chem. Commun.* **1994**, 1277-1280; c) C. A. Hunter, D. H. Purvis, *Angew. Chem. Int. Ed. Engl.* **1992**, *31*, 792-795.

19   a) S. H. Gellman, P. D. Gregory, G.-B. Liang, B. R. Adams, *J. Am. Chem. Soc.* **1991**, *113*, 1164-1173; b) G.-B. Liang, J. M. Desper, S. H. Gellman, *J. Am. Chem. Soc.* **1993**, *115*, 925-938.

20   R. Jäger, S. Baumann, M. Fischer, O. Safarowsky, M. Nieger, F. Vögtle, *Liebigs Ann.* **1997**, 2269-2273.

21   D. A. Leigh, K. Moody, J. P. Smart, K. J. Watson, A. M. Z. Slawin, *Angew. Chem. Int. Ed. Engl.* **1996**, *35*, 306-310.

22   F. G. Gatti, S. Lent, J. K. Y. Wong, G. Bottari, A. Altieri, M. A. F. Morales, S. J. Teat, C. Frochot, D. A. Leigh, A. M. Brouwer, F. Zerbetto, *Proc. Natl. Acad. Sci. U. S. A.* **2003**, *100*, 10-14.

23   Clearly when such small yields are obtained the potential margin of error between the isolated yield and the "real figure" is vastly increased, hence comparisons are less accurate. In addition, the failure to isolate rotaxane in the case of C_{12} and C_{14} spacers may be a reflection of the low yield and as a consequence the rotaxanes may have been present, but were simply not isolated. Having said this, rotaxane formation was attempted on the threads at least three times and despite observation in the mass spectrum in some instances, the requisite rotaxanes were never actually isolated. We therefore surmise that, this is in essence a reflection of the formation of the products, not solely a function of the difficulty of isolation.

2.5 Experimental

2.5.1 Synthesis of Single-Site Rotaxanes 14-17, Threads 7-13 and precursors S1-S7.
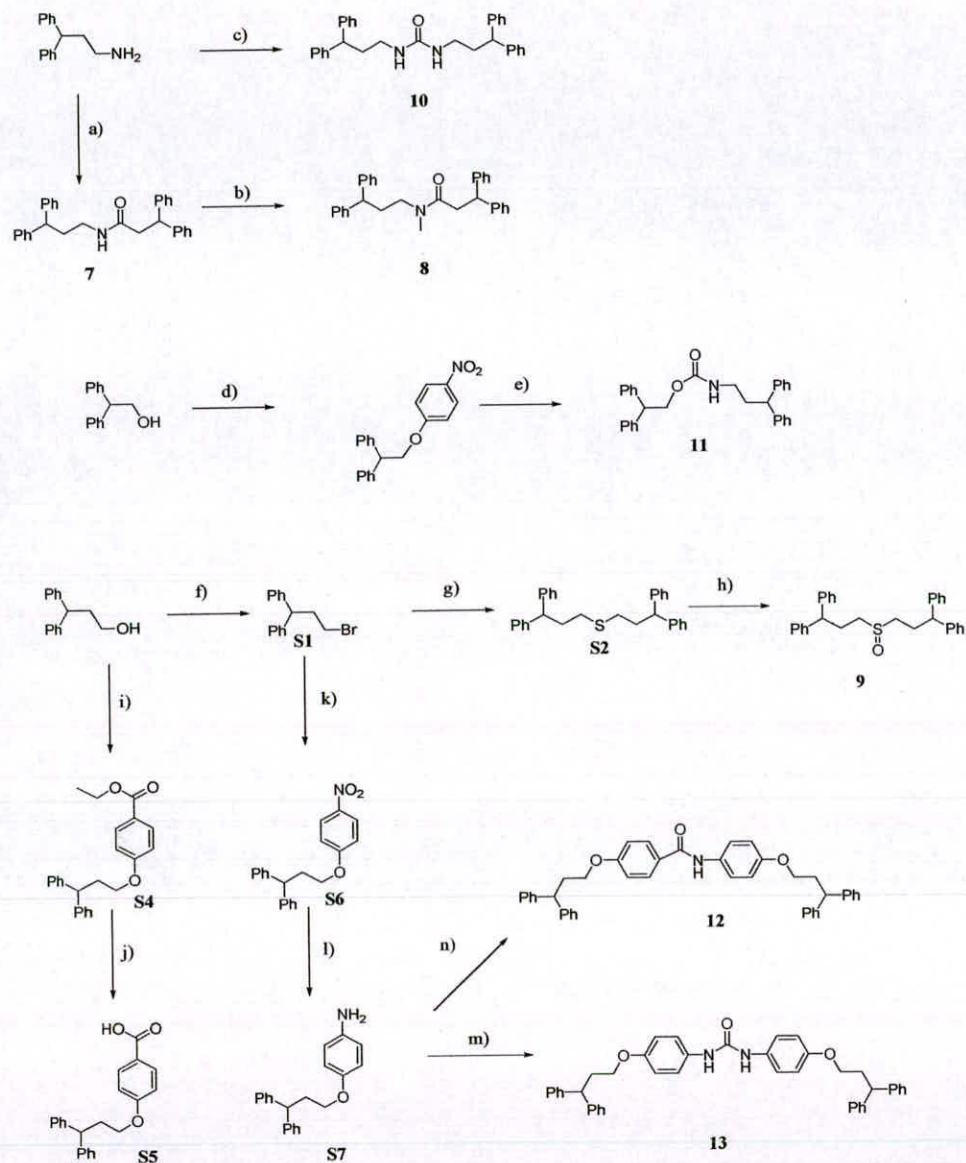
Scheme 2.5. The synthesis of threads **7-13** and precursors **S1–S7.** a) 2,2-diphenylpropanoic acid, EDCI, HOBt, Et$_3$N, CH$_2$Cl$_2$, 71 %; b) MeI, NaH, THF, 95 %; c) carbonyldiimidazole, THF, 95 %; d) 4-nitrophenyl chloroformate, 4-DMAP, CH$_2$Cl$_2$, 80 %; e) 3,3-diphenylpropylamine, 4-DMAP, CH$_2$Cl$_2$ 30 %; f) CBr$_4$, PPh$_3$, THF, 76 %; g) Na$_2$S, EtOH, 24 %; h) *m*-CPBA, CH$_2$Cl$_2$, 66 %; i) 3,3-diphenylpropanol, PPh$_3$, DEAD, THF, 82 %; j) NaOH, EtOH, H$_2$O, Δ, 97 %; k) **S1**, 4-nitrophenol, K$_2$CO$_3$, NaI, 2-butanone, Δ, 87 %; l) hydrazine hydrate, 5 % Pd/C, EtOH, 96 %; m) EDCI, HOBt, Et$_3$N, CH$_2$Cl$_2$, 51 %; n) carbonyldiimidazole, THF, 76 %. For the synthesis of corresponding [2]rotaxanes **14-17** see Scheme 2.2

N-(3,3-diphenylpropyl)-3,3-diphenylpropanamide (7)
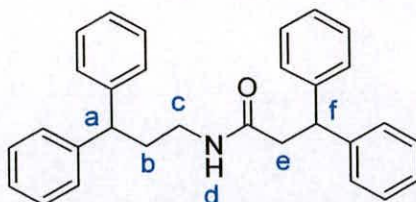
HOBt (3.29 g, 24.3 mmol) was added in one portion to a stirred solution of 3,3-diphenylpropionic acid (5.00 g, 22.1 mmol) and triethylamine (2.97 g, 24.3 mmol) in dichloromethane (100 mL) at 0°C. The reaction mixture was stirred at 0 °C for 10 min, then EDCI (4.66 g, 24.3 mmol) was then added portionwise over 5 min to the reaction mixture. The reaction mixture was stirred for a further 20 min, then 3,3-diphenylpropylamine (5.14 g, 24.3 mmol) was added portionwise over 5 min. The reaction mixture was stirred at 0°C for 1 h, then allowed to warm to room temperature and stirred for a further 18 h. The reaction mixture was washed with 1 M aqueous hydrochloric acid (2 x 30 mL), saturated aqueous sodium hydrogen carbonate (2 x 30 mL), saturated aqueous sodium chloride (2 x 20 mL), dried (MgSO$_4$) and concentrated under reduced pressure to leave a colorless solid, which was recrystallized from toluene to give **7** as a colorless solid. Yield 3.06 g (71 %); m.p. 117-118 °C; ^{1}H NMR (400 MHz, CDCl$_3$): δ = 7.30-7.11 (m, 20H, ArH-stopper), 5.13 (br t, 1H, J = 5.5 Hz, NH$_d$), 4.53 (t, 1H, J = 7.5 Hz, CH$_f$), 3.68 (t, 1H, J = 7.0 Hz, CH$_a$), 3.07 (dt, 2H, J = 7.0 Hz, J = 5.5 Hz, CH$_c$), 2.80 (d, 2H, J = 7.5 Hz, CH$_e$), 2.02 (q, 2H, J = 7.0 Hz, CH$_b$); ^{13}C NMR (100 MHz, CDCl$_3$): δ = 171.3 (s, NHCO), 144.5 (s, ArC-ipso-stopper), 144.1 (q, ArC-ipso-stopper), 129.0 (d, ArC-stopper), 128.9 (d, ArC-stopper), 128.2 (d, ArC-stopper), 128.1 (d, ArC-stopper), 127.0 (d, ArC-stopper), 126.8 (d, ArC-stopper), 49.0 (d, CH$_a$), 47.9 (d, CH$_f$), 43.9 (t, CH$_c$), 38.6 (t, CH$_b$), 35.3 (t, CH$_e$); LRMS (FAB+ mNBA matrix) *m/z* (rel. int.): 420 (85.3 %) [(M+H)$^+$]; Anal. calcd for C$_{30}$H$_{29}$NO (419.56): C 85.9, H 6.9, N 3.3. found: C, 85.7, H 7.1; N 3.5.

N-(3,3-diphenylpropyl)-N-methyl-3,3-diphenylpropanamide (8)
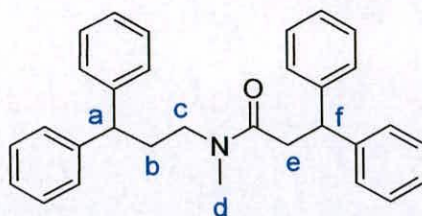
Sodium hydride (60% dispersion in oil, 830 mg, 20.8 mmol) was added portionwise over 10 min to a stirred solution of **7** (1.00 g, 2.40 mmol) in THF (20 mL) under an atmosphere of nitrogen at 0 °C. After 10 min methyl iodide (1.30 mL, 20.8 mmol) was added in one portion at 0 °C and then the reaction mixture was heated at 40 °C for 2 h. 1 M aqueous ammonia solution (20 mL) was then added and the reaction mixture stirred until effervescence ceased. The reaction mixture was concentrated under reduced pressure and the residue was partitioned between water (50 mL) and ethyl acetate (50 mL). The layers were separated and the organic layer was washed with 1 M aqueous hydrochloric acid (2 x 20 mL), saturated aqueous sodium hydrogen carbonate (2 x 20 mL), dried (MgSO$_4$) and concentrated under reduced pressure. The residue was purified by column chromatography on silica gel using hexane: ethyl acetate (3: 1) as eluent to give **8** as a yellow oil. Yield 1.00 g (95 %); ^{1}H NMR (400 MHz, C$_2$D$_2$Cl$_4$): ratio E:Z = 1:1, δ = 7.33-7.04 (m, Ar$\underline{H}$-stopper), 4.62 (t, J = 7.0 Hz, C$\underline{H}_a$), 4.53 (t, J = 7.0 Hz, C$\underline{H}_a$), 3.79 (t, J = 7.0 Hz C$\underline{H}_f$), 3.77 (t, J = 7.0 Hz C$\underline{H}_f$), 3.19 (t, J = 7.0 Hz, C$\underline{H}_c$), 3.04 (t, J = 7.0 Hz, C$\underline{H}_c$), 2.94 (d, J = 7.0 Hz, C$\underline{H}_e$), 2.80 (s, C$\underline{H}_d$), 2.78 (s, C$\underline{H}_d$), 2.66 (d, J = 7.0 Hz, C$\underline{H}_e$), 2.15 (m, J = 7.0 Hz, C$\underline{H}_b$); ^{13}C NMR (100 MHz, C$_2$D$_2$Cl$_4$): δ = 171.8 (CH$_d$N$\underline{C}$O), 171.8 (CH$_d$N$\underline{C}$O), 145.5 (s, Ar$\underline{C}$-ipso), 144.9 (s, Ar$\underline{C}$-ipso), 130.0 (d, Ar$\underline{C}$-stopper), 129.7 (d, Ar$\underline{C}$-stopper), 129.7 (d, Ar$\underline{C}$-stopper), 129.6 (d, Ar$\underline{C}$-stopper), 129.0 (d, Ar$\underline{C}$-stopper), 128.9 (d, Ar$\underline{C}$-stopper), 128.8 (d, Ar$\underline{C}$-stopper), 128.7 (d, Ar$\underline{C}$-stopper), 127.9 (d, Ar$\underline{C}$-stopper), 127.5 (d, Ar$\underline{C}$-stopper), 127.5 (d, Ar$\underline{C}$-stopper), 127.5 (d, Ar$\underline{C}$-stopper), 50.3 (d, $\underline{C}$H$_a$), 49.6 (d, $\underline{C}$H$_a$), 49.3 (t, $\underline{C}$H$_c$), 48.3 (t, $\underline{C}$H$_c$), 48.1 (d, $\underline{C}$H$_f$), 48.0 (d, $\underline{C}$H$_f$), 40.4 (t, $\underline{C}$H$_e$), 39.6 (t, $\underline{C}$H$_e$), 36.8 (q, $\underline{C}$H$_d$), 35.2 (t, $\underline{C}$H$_b$), 34.6 (q, $\underline{C}$H$_d$), 33.9 (t, $\underline{C}$H$_b$); LRMS (FAB+ mNBA matrix) m/z (rel. int.): 434 (87.2 %) [M+H$^+$].

3,3-Diphenyl-1-bromopropane (S1)
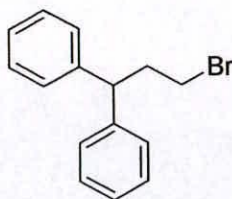
This compound was prepared as described in G. S. Hamilton, Y.-Q. Wu, D. C. Limburg, D. E. Wilkinson, M. J. Vaal, J.-H. Li, C. Thomas, W. Huang, H. Sauer, D. T. Ross, R. Soni, Y. Chen, H. Guo, P. Howorth, H. Valentine, S. Liang, D. Spicer, M. Fuller, J. P.Steiner, *J. Med. Chem.* **2002**, *45*, 3549-3557 and showed identical spectroscopic data to that reported therein.

Bis-(3,3-diphenylpropyl)thioether (S2)
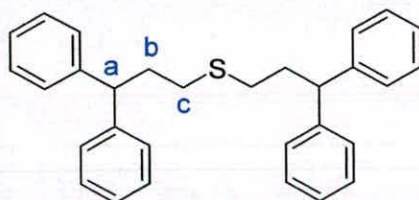
Sodium sulphide hydrate (350 mg, 3.63 mmol) was added to a stirred solution of **S1** (2.00 g, 7.26 mmol) in ethanol (25 mL) at room temperature. The reaction mixture was stirred at room temperature for 16 h. The reaction mixture was then concentrated, dissolved in dichloromethane (50 mL) and washed with saturated aqueous sodium hydrogen carbonate (25 mL), dried (MgSO$_4$) and concentrated under reduced pressure. The residue was purified by column chromatography on silica using hexane: toluene (5: 1) as eluent to give **S2** as a clear oil. Yield 0.40 g (24 %); ^{1}H NMR (400 MHz, CDCl$_3$): δ = 7.22 (m, 20H, ArC$\underline{H}$-stopper), 4.07 (t, 2H, J = 7.6 Hz, C$\underline{H}_a$), 2.41 (t, 4H, J = 7.6 Hz, C$\underline{H}_c$), 2.26 (q, 4H, J = 7.6 Hz, C$\underline{H}_b$); ^{13}C NMR (100MHz, CDCl$_3$) δ = 144.6 (s, Ar$\underline{C}$-ipso-stopper), 128.9 (d, Ar$\underline{C}$-stopper), 128.3 (d, Ar$\underline{C}$-stopper), 126.7 (d, Ar$\underline{C}$-stopper), 50.3 (d, $\underline{C}$H$_a$), 35.7 (t, $\underline{C}$H$_c$), 30.5 (t, $\underline{C}$H$_b$); LRMS (FAB+ mNBA matrix) m/z (rel. int.): 423 (74.3 %) [(M+H)$^+$].

Bis-(3,3-diphenylpropyl)sulphoxide (9)
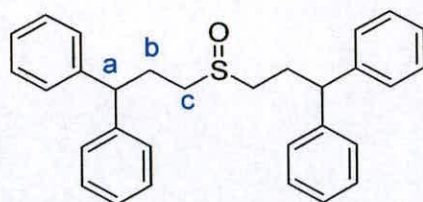
50-55 % *m*-CPBA (1.20 g, 6.80 mmol) was added in one portion to a stirred solution of **S2** (1.40 g, 3.40 mmol) in dichloromethane (200 mL) at room temperature. After 25 min the solution was washed with sodium metabisulphate (50 mL), saturated aqueous sodium hydrogen carbonate (50 mL), dried (MgSO$_4$ and concentrated under reduced pressure. The residue was purified by passage through a short pad of silica gel using dichloromethane as eluent to give **9** as a clear oil. Yield 0.980 g (66 %); ^{1}H NMR (400 MHz, CDCl$_3$) δ = 7.20 (m, 20H, Ar$\underline{H}$-stopper), 3.97 (t, 2H, *J* = 7.0 Hz, C$\underline{H}_a$), 2.47 (m, 8H, C$\underline{H}_b$, C$\underline{H}_c$); ^{13}C NMR (100 MHz, CDCl$_3$) δ = 143.6 (Ar$\underline{C}$-ipso-stopper), 129.1 (d, Ar$\underline{C}$-stopper), 128.2 (d, Ar$\underline{C}$-stopper), 127.1 (d, Ar$\underline{C}$-stopper), 51.1 (t, $\underline{C}$H$_c$), 50.7 (d, $\underline{C}$H$_a$), 28.8 (t, $\underline{C}$H$_b$); LRMS (FAB+ mNBA matrix) *m/z* (rel. int.): 439 (94.3 %) [(M+H)$^+$].

N,N'-*bis*(3,3-diphenylpropyl)urea (10)
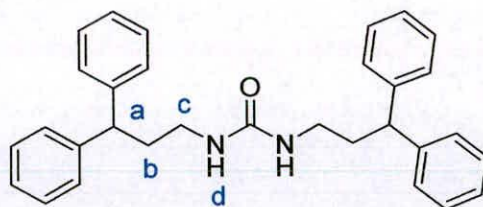
Carbonyldiimidazole (5.50 g, 33.9 mmol) was added to a stirred solution of 3,3-diphenylpropylamine (13.0 g, 61.7 mmol) in THF (200 mL) at 0 °C. The reaction mixture was stirred at room temperature for 16 h. The solvent was removed under reduced pressure and the residue was dissolved in dichloromethane (50 mL) and washed with 1 M aqueous hydrochloric acid (2 x 30 mL), saturated aqueous sodium hydrogen carbonate (2 x 30 mL), dried (MgSO$_4$) and concentrated under reduced

pressure to give **S6** as a colorless solid. Yield 14.4 g (95 %); m.p. 128-131°C; ^{1}H NMR (400 MHz, CDCl$_3$): δ = 7.34-7.14 (m, 20H, Ar$\underline{H}$-stopper), 5.91 (bt, 2H, *J* = 5.5 Hz, N$\underline{H}_d$), 3.97 (t, 2H, *J* = 7.0 Hz, C$\underline{H}_a$), 2.88 (dt, 4H, *J* = 5.5 Hz, *J* = 7.0 Hz, C$\underline{H}_b$), 2.13 (q, 4H, *J* = 7.0 Hz, C$\underline{H}_b$); ^{13}C NMR (100 MHz, CDCl$_3$): δ = 158.4 (s, NH$\underline{C}$ONH), 145.2 (s, Ar$\underline{C}$-ipso-stopper), 128.8 (d, Ar$\underline{C}$-stopper), 127.8 (d, Ar$\underline{C}$-stopper), 126.4 (d, Ar$\underline{C}$-stopper), 48.3 (d, $\underline{C}$H$_a$), 38.4 (t, $\underline{C}$H$_c$), 35.9 (t, $\underline{C}$H$_b$); LRMS (FAB+, *m*BNA matrix): *m/z* = 449 [M+H$^+$]; Anal. calcd for C$_{31}$H$_{32}$N$_2$O (448.60): C 83.0; H 7.1; N 6.25. found: C 83.23; H 7.09; N 6.48.

2,2-Diphenylethyl-4'-nitrophenyl carbonate (S3)
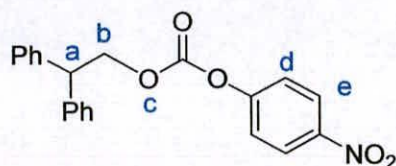
2,2-Diphenylethanol (2.00 g, 10.1 mmol) was added in one portion to a stirred solution of 4-nitrophenyl chloroformate (2.03 g, 10.1 mmol) and catalytic 4-DMAP in dichloromethane (80 mL) at 0 °C. The reaction mixture was stirred at room temperature for 6 h. The reaction mixture was then washed with water (2 x 30 mL), dried (MgSO$_4$) and concentrated under reduced pressure to give **S3** as a colorless solid. Yield 2.93 g, (80 %); m.p. 106-108 °C; ^{1}H NMR (400 MHz, CDCl$_3$): δ = 8.18 (d, 2H, *J* = 9.0 Hz, ArC$\underline{H}_e$), 7.33-7.19 (m, 10H, Ar$\underline{H}$), 4.81 (d, 2H, *J* = 8.0 Hz, C$\underline{H}_b$), 4.65 (t, 1H, *J* = 8.0 Hz, C$\underline{H}_a$).

(3,3-Diphenylpropyl)-carbamic acid 2,2-diphenylethyl ester (11)
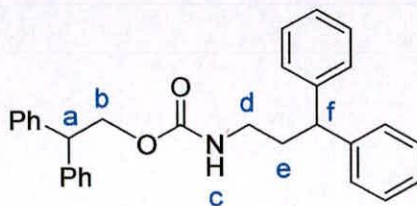
3,3-Diphenylpropylamine (1.16 g, 5.51 mmol) was added in one portion to a stirred solution of **S3** (2.00 g, 5.51 mmol) and catalytic 4-DMAP in dichloromethane (30 mL) at 0 °C. The reaction mixture was stirred at room temperature for 3 h. The reaction mixture was then washed with water (2 x 20 mL), dried (MgSO$_4$) and

concentrated under reduced pressure to give **S4** as a colorless solid. Yield 0.719 g, (30 %); ^{1}H NMR (400 MHz, CDCl$_3$): δ = 7.37-7.15 (m, 20H, Ar$\underline{H}$), 5.72 (br s, 1H, N$\underline{H}_c$) 4.72 (d, 2H, J = 7.2 Hz, C$\underline{H}_b$), 4.65 (t, 1H, J = 7.2 Hz, C$\underline{H}_a$), 4.02 (t, 1H, J = 7.0 Hz, C$\underline{H}_f$), 2.96 (m, 2H, C$\underline{H}_d$), 2.13 (m, 2H, C$\underline{H}_e$); ^{13}C NMR (100 MHz, CDCl$_3$): δ = 159.2 (s, Ar$\underline{C}$-ipso), 151.5 (s, O$\underline{C}$O), 145.2 (s, Ar$\underline{C}$-ipso), 143.0 (s, Ar$\underline{C}$-ispo), 129.1 (d, Ar$\underline{C}$-stopper), 128.4 (d, Ar$\underline{C}$-stopper), 126.2 (d, Ar$\underline{C}$-stopper), 69.2 (t, $\underline{C}$H$_b$), 50.1 (d, $\underline{C}$H$_a$), 48.3 (d, $\underline{C}$H$_f$), 41.6 (t, $\underline{C}$H$_d$), 35.9 (t, $\underline{C}$H$_e$).

4-(3,3-diphenylpropyloxy)-benzoic acid ethyl ester (S4)
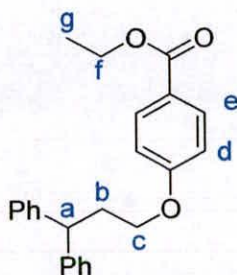
DEAD (1.85 mL, 9.42mmol) was added dropwise over 20 min to a stirred solution of ethyl 4-hydroxybenzoate (1.42 g, 8.56 mmol), 3,3-diphenylpropanol (2.00 g, 9.42 mmol), triphenylphosphine (2.47 g, 9.42 mmol) in THF (95 mL) at 0 °C under an atmosphere of nitrogen. The reaction mixture was allowed to warm to room temperature over 2 h and stirred at room temperature for 16 h. The reaction mixture was concentrated under reduced pressure and the residue was triturated with hexane. The resulting precipitate was filtered and the residue was purified by column chromatography on silica gel using hexane: ethyl acetate (4: 1) as eluent to give a colorless oil which was triturated with Et$_2$O to give **S4** as a colorless solid. Yield 2.53 g (82 %); m.p. 208-211 °C; ^{1}H NMR (400 MHz, CDCl$_3$): δ = 7.96 (d, 2H, J = 8.5 Hz, Ar$\underline{H}_e$), 7.31-7.17 (m, 10H, Ar$\underline{H}$-stopper), 6.83 (d, 2H, J = 8.5 Hz, Ar$\underline{H}_d$), 4.33 (q, 2H, J = 7.0 Hz, C$\underline{H}_f$), 4.24 (t, 1H, J = 7.8 Hz, C$\underline{H}_a$), 3.93 (t, 2H, J = 6.3 Hz, C$\underline{H}_c$), 2.57-2.52 (m, 2H, C$\underline{H}_b$), 1.37 (t, 3H, J = 7.3 Hz, C$\underline{H}_g$); ^{13}C NMR (100 MHz, CDCl$_3$) δ = 165.9 (s, $\underline{C}$O$_2$Et), 162.6 (s, Ar$\underline{C}$-ipso), 144.0 (s, Ar$\underline{C}$-ipso-stopper), 131.4 (d, $\underline{C}$H$_e$), 128.2 (d, Ar$\underline{C}$-stopper), 127.8 (d, Ar$\underline{C}$-stopper), 126.6 (Ar$\underline{C}$-stopper), 123.3

(s, Ar$\underline{C}$-ipso), 114.5 (d, $\underline{C}H_d$), 66.0 (t, $\underline{C}H_c$), 60.5 (t, $\underline{C}H_f$), 47.1 (d, $\underline{C}H_a$), 34.7 (t, $\underline{C}H_b$), 14.3 (q, $\underline{C}H_g$); LRMS (FAB+ mNBA matrix) *m/z* (rel. int.): 361 (85.3 %) [(M+H)⁺], HRMS (FAB+) calcd for $C_{24}H_{25}O_3$ [(M+H)⁺] 361.1787. Found 361.1781.

4-(3,3-diphenylpropyloxy)-benzoic acid (S5)
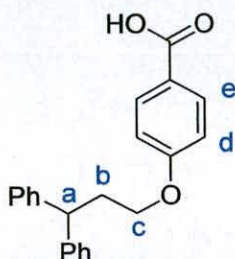
Sodium hydroxide (41.7 mL of a 1 M aqueous solution, 41.7 mmol) was added to a stirred solution of **S4** (5.00 g, 13.9 mmol) in ethanol (150 mL) at room temperature. The reaction mixture was heated at reflux for 3 h. The reaction mixture was cooled and solution was acidified to pH 1 by the dropwise addition of 1 M aqueous hydrochloric acid. The resulting precipitate was filtered to give **S5** as a colorless solid. Yield 4.47 g (97 %); m.p. 212-213 °C; ¹H NMR (100 MHz, d_6-DMSO): δ = 12.62 (br s, 1H, CO$_2$$\underline{H}$), 7.87 (d, 2H, *J* = 8.5 Hz, Ar$\underline{H}_e$), 7.37-7.17 (m, 10H, Ar$\underline{H}$-stopper), 6.95 (d, 2H, *J* = 8.5 Hz, Ar$\underline{H}_d$), 4.22 (t, 1H, *J* = 8.0 Hz, C$\underline{H}_a$), 3.93 (t, 2H, *J* = 6.5 Hz, C$\underline{H}_c$), 2.56-2.50 (m, 2H, C$\underline{H}_b$); ¹³C NMR (100 MHz, CDCl$_3$) δ = 167.3 (s, $\underline{C}O_2H$), 162.4 (s, Ar$\underline{C}$-ipso), 144.0 (s, Ar$\underline{C}$-ipso-stopper), 131.0 (d, Ar$\underline{C}H_e$), 128.8 (d, Ar$\underline{C}$-stopper), 127.9 (d, Ar$\underline{C}$-stopper), 126.6 (d, Ar$\underline{C}$-stopper), 123.3 (s, Ar$\underline{C}$-ipso), 114.5 (d, Ar$\underline{C}H_d$), 66.3 (t, $\underline{C}H_c$), 47.1 (d, $\underline{C}H_a$), 34.2 (t, $\underline{C}H_b$); LRMS (FAB+ mNBA matrix) *m/z* (rel. int.): 333 (14.0 %) [(M+H)⁺], HRMS (FAB+) calcd for $C_{22}H_{21}O_3$ [(M+H)⁺] 333.1491. Found 333.1491.

1-(3,3-diphenylpropyloxy)-4-nitrobenzene (S6)

4-Nitrophenol (2.00 g, 14.4 mmol), **S1** (4.38 g, 15.8 mmol), anhydrous potassium carbonate (19.9 g, 144 mmol) and sodium iodide (one crystal) in 2-butanone (120 mL) were heated under reflux for 12 h. The reaction mixture was filtered and concentrated under reduced pressure. The residue was dissolved in chloroform (200 mL) and washed with saturated aqueous sodium hydrogen carbonate (2 x 20 mL), dried (MgSO$_4$) and concentrated under reduced pressure. The residue was recrystallized from ethyl acetate to give **S6** as a light yellow solid. Yield 4.17 g (87 %); mp 106-108 °C; ^{1}H NMR (400 MHz, CDCl$_3$): δ = 8.16 (d, 2H, *J* = 9.3 Hz, ArCH$_e$), 7.32-7.19 (m, 10H, ArH-stopper), 6.87 (d, 2H, *J* = 9.3 Hz, ArH$_d$), 4.23 (t, 1H, *J* = 7.8 Hz, CH$_a$), 3.98 (t, 2H, *J* = 6.4 Hz, CH$_c$), 2.60-2.55 (m, 2H, CH$_b$); ^{13}C NMR (100 MHz, CDCl$_3$): δ = 163.9 (s, ArC-ipso), 143.8 (s, ArC-ipso), 141.8 (s, ArC-ipso), 127.8 (d, ArC-stopper), 126.5 (d, ArCH$_e$), 125.8 (d, ArC-stopper), 114.4 (d, ArCH$_d$), 66.8 (t, CH$_c$), 47.1 (d, CH$_a$), 34.6 (t, CH$_b$); LRMS (FAB+ mNBA matrix) *m/z* (rel. int.): 334 (74.1 %) [(M+H)$^+$], HRMS (FAB+) calcd for C$_{21}$H$_{20}$NO$_3$ [(M+H)$^+$] 334.1443. Found 334.1442.

4-(3,3-Diphenylpropyloxy)-aniline (S7)

Hydrazine hydrate (1.15 mL, 18.9 mmol) was added dropwise over 1 min to a stirred solution of **S6** (2.10 g, 6.31 mmol) and 10 % palladium on carbon (210 mg, 10 % w/w) in ethanol (100 mL) at room temperature. The reaction mixture was then heated at reflux for 1 h. The reaction mixture was then cooled and filtered through a pad of Celite® and the filtrate was concentrated under reduced pressure. The residue was dissolved in ethyl acetate (100 mL) and washed with water (2 x 50 mL), dried (MgSO$_4$) and concentrated under reduced pressure. The residue was recrystallized from ethyl acetate to give **S7** as a colorless solid. Yield 1.85 g (96 %); mp 100-102 °C; ^{1}H NMR (400 MHz, CDCl$_3$): δ = 7.31-7.17 (m, 10H, Ar$\underline{H}$-stopper), 6.68 (d, 2H, J = 8.6 Hz, Ar$\underline{H}_d$), 6.61 (d, 2H, J = 8.6 Hz, Ar$\underline{H}_e$), 4.23 (t, 1H, J = 7.8 Hz, C$\underline{H}_a$), 3.82 (t, 2H, J = 6.6 Hz, C$\underline{H}_c$), 3.43 (br s, 2H, N$\underline{H}_f$) 2.52-2.47 (m, 2H, C$\underline{H}_b$); ^{13}C NMR (100 MHz, CDCl$_3$): δ = 152.0 (s, Ar$\underline{C}$-ipso), 144.3 (s, Ar$\underline{C}$-ipso-stopper), 139.3 (s, Ar$\underline{C}$-ipso), 128.4 (d, Ar$\underline{C}$-stopper), 127.9 (d, Ar$\underline{C}$-stopper), 126.2 (d, Ar$\underline{C}$-stopper), 116.2 (d, Ar$\underline{C}H_e$), 115.7 (d, Ar$\underline{C}H_d$), 66.5 (t, $\underline{C}H_c$) 47.2 (d, $\underline{C}H_a$), 35.0 (t, $\underline{C}H_b$); LRMS (FAB+ mNBA matrix) m/z (rel. int.): 304 (87.1 %) [(M+H)$^+$], HRMS (FAB+) calcd for C$_{21}$H$_{21}$NO [(M+H)$^+$] 303.1623. Found 303.1626.

4-(3,3-Diphenylpropyloxy)-*N*-(4-(3,3-diphenylpropyloxy) phenyl benzamide (12)

HOBt (0.673 g, 4.97 mmol), was added in one portion to a stirred solution of **S5** (1.10 g, 3.31 mmol) and triethylamine (1.38 mL, 9.90 mmol) in dichloromethane (40 mL) at 0 °C. After 10 min EDCI (0.952 g, 4.97 mmol) was added in one portion, with stirring at 0 °C. After a further 20 min **S7** (1.00 g, 3.31 mmol) was added in one portion with stirring at 0°C. The reaction mixture was stirred at room temperature for 20 h. The reaction mixture was washed with 1 M aqueous hydrochloric acid (2 x 30 mL), saturated aqueous hydrogen carbonate and saturated aqueous sodium chloride solution, dried (MgSO$_4$) and concentrated under reduced pressure. The resulting residue was recrystallized from chloroform: hexane to give **12** as a colorless solid. Yield 1.04 g (51 %); m.p. 212-214 °C; ^{1}H NMR (400 MHz, CDCl$_3$): δ = 7.78 (d, 2H, *J* = 8.8 Hz, ArH$_e$), 7.59 (s, 1H, NH$_f$), 7.47 (d, 2H, *J* = 9.0 Hz, CH$_g$), 7.32-7.19 (m, 20 H, ArH-stopper), 6.89 (d, 2H, *J* = 8.8 Hz, CH$_d$), 6.83 (d, 2H, *J* = 9.0 Hz, CH$_h$), 4.26 (t, 2H, *J* = 8.0 Hz, CH$_a$ & CH$_k$), 3.96 (t, 2H, *J* = 6.3 Hz, CH$_c$), 3.90 (t, 2H, *J* = 6.3 Hz, CH$_i$), 2.59-2.51 (m, 4H, CH$_b$ & CH$_j$); ^{13}C NMR (100 MHz, CDCl$_3$) δ = 165.1 (s, NHCO), 155.8 (s, ArC-ipso), 144.2 (s, ArC-ipso), 144.0 (s, ArC-ipso-stopper), 128.7 (d, ArC-stopper), 128.6 (d, ArC-stopper), 128.5 (d, ArC-stopper), 127.9 (d, ArC-stopper), 127,8 (d, ArC-stopper), 127.1 (d, ArC-stopper), 126.4 (d, ArC$_e$), 126.3 (d, ArC$_g$), 114.9 (d, ArC$_d$), 114.5 (d, ArC$_h$), 66.2 (t, CH$_i$), 66.1 (t, CH$_c$), 49.1 (d, CH$_k$), 47.2 (d, CH$_a$), 34.9 (t, CH$_b$), 34.8 (t, CH$_j$); LRMS (FAB+ mNBA matrix) *m/z* (rel. int.): 618 (19.0 %) [(M+H)$^+$], HRMS (FAB+) calcd for C$_{43}$H$_{41}$N$_2$O$_3$ [(M+H)$^+$] 618.3008. Found 618.3009.

N-N'-Bis-(3,3-diphenylpropanoxy) phenyl urea (13)

Carbonyldiimidazole (0.320 g, 1.98 mmol) was added to a stirred solution of **S7** (1.00 g, 3.30 mmol) in anhydrous THF (50 mL) at 0 °C. The reaction mixture was stirred at room temperature for 16 h. The solvent was removed under reduced pressure and the residue was dissolved in dichloromethane (50 mL) and washed with 1 M aqueous hydrochloric acid (2 x 30 mL), saturated aqueous sodium hydrogen carbonate (2 x 30 mL), dried (MgSO$_4$) and concentrated under reduced pressure to give **13** as a colorless solid. Yield: 1.58 g (76%); m.p. 208-211 °C; ^{1}H NMR (400 MHz, CDCl$_3$): δ = 7.29-7.18 (m, 24H, ArH-stopper & ArH$_e$), 6.80 (d, 4H, J = 8.5 Hz, ArH$_d$), 6.22 (s, 2H, NHCONH), 4.24 (t, 2H, J = 8.3 Hz, CH$_a$), 3.87 (t, 4H, J = 6.2 Hz, CH$_c$), 2.55-2.50 (m, 4H, CH$_b$); ^{13}C NMR (100 MHz, d_6-DMSO): δ = 153.9 (s, NHCONH), 153.3 (s, ArC-ipso), 133.6 (s, ArC-ipso), 128.8 (d, ArC-stopper), 128.0 (d, ArC-stopper), 126.5 (d, ArC-stopper), 120.1 (d, ArC$_d$), 114.9 (d, ArC$_e$), 66.1 (t, CH$_c$), 47.1 (d, CH$_a$), 34.4 (t, CH$_b$); LRMS (FAB+ mNBA matrix) m/z (rel. int.): 633 (91.5 %) [(M+H)$^+$], HRMS (FAB+) calcd for C$_{43}$H$_{41}$N$_2$O$_3$ [(M+H)$^+$] 633.3117. Found 633.3117.

General method for the preparation of benzylic amide macrocycle [2]rotaxanes, 14–17. The threads, (1.00 mmol, 1 equiv.) and triethylamine (2.79 mL, 20.0 mmol, 20 equiv.) were dissolved in chloroform (100 mL) (stabilised with amylenes) and stirred vigorously whilst solutions of *p*-xylylene diamine (1.09 g, 8.0 mmol, 8 equiv.) in chloroform (45 mL) and isophthaloyl dichloride (1.63 g, 8.0 mmol, 8.0 equiv.) in chloroform (45 mL) were simultaneously added over a period of 4 hours using motor-driven syringe pumps. The resulting suspension was filtered and concentrated under reduced pressure to leave unconsumed thread and [2]rotaxane in solution. This mixture was subjected to column chromatography on silica gel using dichloromethane: methanol as eluent to yield, in order of elution, the unconsumed thread and [2]rotaxane.

([2](1,7,14,20-Tetraaza-2,6,15,19-tetraoxo-3,5,9,12,16,18,22,25 tetrabenzocyclohexacosane)-*N*-(3,3-diphenylpropyl)-3,3-diphenylpropanamide (14)

Selected data for ([2](1,7,14,20-Tetraaza-2,6,15,19-tetraoxo-3,5,9,12,16,18,22,25 tetrabenzocyclohexacosane)-*N*-(3,3-diphenylpropyl)-3,3-diphenylpropanamide (14). Yield: 0.086 g (9 %); m.p. 299-300 °C; ^{1}H NMR (400 MHz, d_6-DMSO): δ = 8.66 (t, 4H, J = 5.5 Hz, NH$_D$), 8.36 (s, 2H, ArH$_A$), 8.15 (d, 4H, J = 7.5 Hz, ArH$_B$), 7.71 (t, 2H, J = 8.0 Hz, ArH$_C$), 7.23-7.13 (m, 6H, ArH-stopper), 7.02 (m, 10H, ArCH), 6.61 (s, 8H, ArH$_F$), 6.59-6.51 (m, 5H, ArH-stopper, NH$_d$), 4.37 (dd, 4H, J = 5.0 Hz, J = 13.9 Hz, CH$_E$), 4.11 (t, 1H, J = 7.5 Hz, CH$_a$), 4.08 (dd, 4H, J = 5.0 Hz, J = 13.9 Hz, CH$_E$), 3.10 (t, 1H, J = 7.5 Hz, CH$_f$), 2.17 (d, 2H, J = 7.5 Hz, CH$_e$), 1.46

(m, 2H, CH_c), 0.96 (bm, 2H, CH_b); ^{13}C NMR (100 MHz, d_6-DMSO): δ = 170.8 (s, NHCO), 165.6 (s, NH$_D$$C$O), 145.2 (s, Ar$C$-ipso-stopper), 144.4 (s, ArC-ipso-stopper), 137.6 (s, ArC-ipso-xylylene), 134.7 (s, ArC-ipso-isophthaloyl), 130.6 (d, ArC_B), 129.2 (d, ArC_F), 128.6 (d, ArC_A), 128.6 (d, ArC-stopper), 128.5 (d, ArC-stopper), 128.4 (d, ArC-stopper), 127.8 (d, ArC-stopper), 127.3 (d, ArC-stopper), 126.3 (d, ArC-stopper), 126.1 (d, ArC_C), 48.9 (d, CH_a), 46.1 (t, CH_f), 43.1 (t, CH_E), 39.4 (from HMQC underneath d_6-DMSO, CH_c), 37.7 (t, CH_b), 33.8 (t, CH_e); LRMS (FAB+ mNBA matrix) m/z (rel. int.): 952 (19.0 %) $[(M+H)^+]$, Anal. calcd for $C_{62}H_{57}N_5O_5$ (952.15): C 78.2; H 6.0; N 7.4; found: C 78.0; H 6.0; N 7.4.
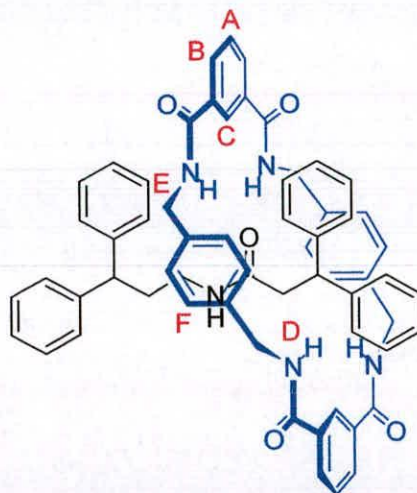
X-ray crystallographic structure determination, crystals of rotaxane grown in dimethylsulfoxide, 14 $C_{66}H_{70}N_6O_8S$, M = 1095.33, crystal size 0.10 × 0.06 × 0.02 mm, monoclinic P2(1)/c, a = 25.979(2), b = 11.7341(10), c = 19.473(2) Å, β = 106.529(2)°, V = 5690.9(9)Å^3, Z = 4, ρ_{calcd} = 1.278 Mg m^{-3}; MoK/α synchotron radiation (graphite monochromator, λ = 0.68840 Å), μ = 0.120 mm^{-1}, T = 150(2)K. 39607 data (15730 unique, R_{int} = 0.0877, 1.86<θ<29.44°), were collected on a Siemens SMART CCD diffractometer using narrow frames (0.3° in ω), and were corrected semi-empirically for absorption and incident beam decay. The structure was solved by direct methods and refined by full-matrix least-squares on F^2 values of all data (G.M.Sheldrick, SHELXTL manual, Siemens Analytical X-ray Instruments, Madison WI, USA, 1993, version 5.0) to give wR = $\{\Sigma[w(F_o^2-F_c^2)^2]/\Sigma[w(F_o^2)^2]\}^{1/2}$ = 0.2364, conventional R = 0.0941 for F values of 15680 reflections with F_o^2>2$\sigma(F_o^2)$, S = 1.013 for 735 parameters. Residual electron density extremes were 0.658 and -0.432 Å^{-3}. Hydrogens were added in calculated positions and constrained to a Riding model.

([2](1,7,14,20-Tetraaza-2,6,15,19-tetraoxo-3,5,9,12,16,18,22,25

tetrabenzocyclohexacosane)- *N,N'-bis-***(3,3-diphenylpropyl)urea rotaxane (16)**

Selected Data for ([2](1,7,14,20-Tetraaza-2,6,15,19-tetraoxo-3,5,9,12,16,18,22,25 tetrabenzocyclohexacosane)- *N,N'-bis-***(3,3-diphenylpropyl)urea rotaxane, 16.**
Yield: 0.58 g (50 %); m.p. 137-139 °C; ^{1}H NMR (400 MHz, CDCl$_3$): δ = 8.31 (s, 2H, ArH$_C$), 8.23 (dd, 4H, J = 7.5 Hz, ArH$_B$), 7.69 (t, 2H, J = 7.5 Hz, ArH$_A$), 7.23-7.14 (m, 24H, ArH-stopper & NH$_D$), 6.89 (s, 8H, ArH$_F$), 4.43 (d, 8H, J = 5.5 Hz, CH$_E$), 4.31 (t, 2H, J = 5.0 Hz, NHCONH), 3.48 (t, 2H, J = 7.5 Hz, CH$_a$), 2.35 (dt, 4H, J = 7.5 Hz, J = 5.0 Hz, CH$_c$), 1.55 (q, 4H, J = 7.5 Hz, CH$_b$), ^{13}C NMR (100 MHz, CDCl$_3$): δ = 166.5 (s, NH$_D$CO), 159.5 (s, NHCONH), 144.3 (s, ArC-ipso-stopper), 137.6 (s, ArC-ipso-xylylene), 134.3 (s, ArC-ipso-isophthaloyl), 131.4 (d, ArC$_B$), 129.8 (d, ArC$_F$), 128.9 (d, ArC$_A$), 128.8 (d, ArC-stopper), 127.1 (d, ArC-stopper), 126.9 (d, ArC-stopper), 125.3 (d, ArC$_C$), 49.1 (d, CH$_a$), 44.6 (t, CH$_E$), 39.4 (CH$_c$), 36.2 (t, CH$_b$); LRMS (FAB+ mNBA matrix) m/z (rel. int.): 981 (12.0 %) [(M+H)$^{+}$]; Anal. calcd for C$_{63}$H$_{60}$N$_6$O$_5$ (981.19): C 77.14; H 6.12; N 8.57; found: C 77.39; H 5.98; N 8.42.

X-ray crystallographic structure determination, crystals of rotaxane grown in dimethylsulfoxide, 16. C$_{66}$H$_{70}$N$_6$O$_8$S, M = 1095.33, crystal size 0.10 × 0.06 × 0.02 mm, monoclinic P2(1)/c, a = 25.979(2), b = 11.7341(10), c =

19.473(2) Å, $\beta = 106.529(2)°$, $V = 5690.9(9)$Å^3, $Z = 4$, $\rho_{calcd} = 1.278$ Mg m^{-3}; MoK/α synchotron radiation (graphite monochromator, $\lambda = 0.68840$ Å), $\mu = 0.120$ mm^{-1}, $T = 150(2)$K. 39607 data (15730 unique, $R_{int} = 0.0877$, $1.86 < \theta < 29.44°$), were collected on a Siemens SMART CCD diffractometer using narrow frames (0.3° in ω), and were corrected semi-empirically for absorption and incident beam decay. The structure was solved by direct methods and refined by full-matrix least-squares on F^2 values of all data (G.M.Sheldrick, SHELXTL manual, Siemens Analytical X-ray Instruments, Madison WI, USA, 1993, version 5.0) to give $wR = \{\Sigma[w(F_o^2 - F_c^2)^2]/\Sigma[w(F_o^2)^2]\}^{1/2} = 0.2364$, conventional $R = 0.0941$ for F values of 15680 reflections with $F_o^2 > 2\sigma(F_o^2)$, $S = 1.013$ for 735 parameters. Residual electron density extremes were 0.658 and -0.432 Å^{-3}. Hydrogens were added in calculated positions and constrained to a Riding model.

([2](1,7,14,20-Tetraaza-2,6,15,19-tetraoxo-3,5,9,12,16,18,22,25 tetrabenzocyclohexacosane) 3,3-Diphenylpropyl)-carbamic acid 2,2-diphenylethyl ester (17)

([2](1,7,14,20-Tetraaza-2,6,15,19-tetraoxo-3,5,9,12,16,18,22,25 tetrabenzocyclohexacosane carbamate rotaxane, 17 Yield: 0.58 g (8 %); ^{1}H NMR (400 MHz, CDCl$_3$): δ = 8.23 (s, 2H, ArC$_C$), 8.12 (dd, 4H, J = 7.5 Hz, J = 1.5 Hz, ArH$_B$), 7.46 (t, 2H, J = 7.5 Hz, ArH$_A$), 7.37-7.15 (m, 20H, ArH-stopper), 7.07 (s, 8H, ArH$_F$), 6.02 (d, 4H, J = 7.0 Hz, CH$_c$), 4.62 (d, 2H, J = 7.2 Hz, CH$_b$), 4.47 (d, 8H, J = 5.5 Hz, CH$_E$), 4.32 (t, 1H, J = 7.2 Hz, CH$_a$), 3.97 (t, 1H, J = 7.0 Hz, CH$_f$), 3.72 (t, 2H, J = 6.5 Hz, CH$_c$), 2.76 (m, 2H, CH$_d$), 2.51-2.46 (m, 4H, CH$_b$), 2.11 (m, 2H, CH$_e$); ^{13}C NMR (100 MHz, CDCl$_3$): δ = 166.8 (s, NH$_D$CO), 159.2 (s, ArC-ipso), 151.8 (s, OCO), 144.2 (s, ArC-ipso-stopper), 137.2 (s, ArC-ipso-xylylene), 133.9 (s, ArC-ipso-isophthaloyl), 130.9 (d, ArC$_B$), 129.3 (d, ArC-stopper), 128.0 (d, ArC-stopper), 126.4 (d, ArC-stopper), 125.2 (d, ArC$_C$), 119.8 (d, CH$_d$), 114.5 (d, CH$_e$), 69.2 (t, CH$_b$), 48.3 (d, CH$_f$), 47.2 (d, CH$_a$), 44.6 (t, CH$_E$) 35.9 (t, CH$_e$);

X-ray crystallographic structure determination, crystals of rotaxane grown in dimethylsulfoxide, 17. $C_{62}H_{61}N_5O_8$, $M = 1004.16$, colourless block, crystal size $0.46 \times 0.27 \times 0.27$ mm, triclinic, P_{-1}, $a = 10.8448(10)$, $b = 11.0664(10)$, $c = 25.451(2)$ Å, $\alpha = 92.305(2)$ $\beta = 101.260(2)$ $\gamma = 116.905(2)°$, $V = 2642.4(4)$ Å^3, $Z = 2$, $\rho_{calcd} = 1.262$ mg m^{-3}; Mo$_{K\alpha}$ radiation (graphite monochromator, $\lambda = 0.71073$ Å), $\mu = 0.084$ mm^{-1}, $T = 220(2)$ K. 10904 data (6806 unique, $R_{int} = 0.0792$, $2.09 < \theta < 22.50°$), were collected on a Siemens SMART CCD diffractometer using narrow frames ($0.3°$ in ω), and were corrected semiempirically for absorption and incident beam decay. The structure was solved by direct methods and refined by full-matrix least-squares on F^2 values of all data (G. M. Sheldrick, SHELXTL manual, Siemens Analytical X-ray Instruments, Madison WI, USA, 1994, version 5) to give $wR = \{\Sigma[w(F_o^2 F_c^2)^2]/\Sigma[w(F_o^2)^2]\}^{1/2} = 0.2744$, conventional $R = 0.1123$ for F values of 6806 reflections with $F_o^2 > 2\sigma F_o^2$), $S = 1.167$ for 708 parameters. Residual electron density extremes were 0.277 and -0.308 eÅ^{-3}. Amide hydrogen atoms were refined isotropically with the remainder constrained; anisotropic displacement parameters were used for all non-hydrogen atoms.
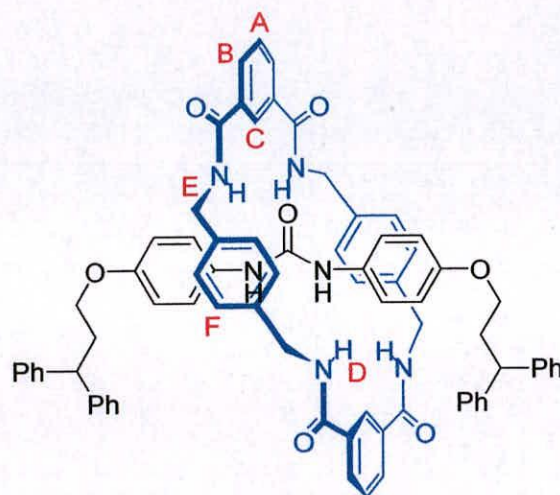
([2](1,7,14,20-Tetraaza-2,6,15,19-tetraoxo-3,5,9,12,16,18,22,25 tetrabenzocyclohexacosane *N-N'-bis-***(3,3-diphenylpropanoxy) phenyl urea rotaxane, (18)**

([2](1,7,14,20-Tetraaza-2,6,15,19-tetraoxo-3,5,9,12,16,18,22,25 tetrabenzocyclohexacosane *N-N'-bis-***(3,3-diphenylpropanoxy) phenyl urea rotaxane, 18** Yield: 0.58 g (64 %); m.p. 137-139 °C; ^{1}H NMR (400 MHz, CDCl$_3$): δ = 8.21 (s, 2H, ArH$_C$), 8.10 (dd, 4H, J = 7.5 Hz, J = 1.5 Hz, ArH$_B$), 7.47 (t, 2H, J = 7.5 Hz, ArH$_A$), 7.32-7.18 (m, 20H, ArH-stopper), 7.05 (s, 8H, ArH$_F$), 6.75 (s, 2H, NHCONH), 6.46 (d, 4H, J = 7.0 Hz, CH$_d$), 6.36 (d, 4H, J = 7.0 Hz, CH$_e$), 4.42 (d, 8H, J = 5.5 Hz, CH$_E$), 4.20 (t, 2H, J = 7.8 Hz, CH$_a$), 3.72 (t, 2H, J = 6.5 Hz, CH$_c$), 2.51-2.46 (m, 4H, CH$_b$); ^{13}C NMR (100 MHz, CDCl$_3$): δ = 166.8 (s, NH$_D$CO), 154.5 (s, NHCONH), 144.2 (s, ArC-ipso-stopper), 137.2 (s, ArC-ipso-xylylene), 133.9 (s, ArC-ipso-isophthaloyl), 130.9 (d, ArC$_B$), 130.7 (s, ArC-ipso-thread), 129.3 (d, ArC-stopper), 128.0 (d, ArC-stopper), 126.4 (d, ArC-stopper), 125.2 (d, ArC$_C$), 119.8 (d, ArC$_d$), 114.5 (d, ArH$_e$), 66.1 (t, CH$_c$), 47.2 (d, CH$_a$), 44.6 (t, CH$_E$) 34.8 (t, CH$_b$); LRMS (FAB+ mNBA matrix) m/z (rel. int.): 1165 (22.3 %); Anal. calcd for C$_{75}$H$_{68}$N$_6$O$_7$ (1165.38): C, 77.30; H, 5.88; N, 7.21; found: C, 77.19; H, 5.82; N, 7.51.

X-ray crystallographic structure determination, crystals of rotaxane grown in CHCl$_3$/Et$_2$O, 18. C$_{75}$H$_{68}$N$_6$O$_7$, M = 1095.33, crystal size 0.10 × 0.06 × 0.02 mm,

monoclinic P2(1)/c, $a = 25.979(2)$, $b = 11.7341(10)$, $c = 19.473(2)$ Å, $\beta = 106.529(2)°$, $V = 5690.9(9)$Å^3, $Z = 4$, $\rho_{calcd} = 1.278$ Mg m^{-3}; MoK/α synchotron radiation (graphite monochromator, $\lambda = 0.68840$ Å), $\mu = 0.120$ mm^{-1}, $T = 150(2)$K. 39607 data (15730 unique, $R_{int} = 0.0877$, $1.86 < \theta < 29.44°$), were collected on a Siemens SMART CCD diffractometer using narrow frames ($0.3°$ in ω), and were corrected semi-empirically for absorption and incident beam decay. The structure was solved by direct methods and refined by full-matrix least-squares on F^2 values of all data (G.M.Sheldrick, SHELXTL manual, Siemens Analytical X-ray Instruments, Madison WI, USA, 1993, version 5.0) to give $wR = \{\Sigma[w(F_o^2 - F_c^2)^2]/\Sigma[w(F_o^2)^2]\}^{1/2} = 0.2364$, conventional $R = 0.0941$ for F values of 15680 reflections with $F_o^2 > 2\sigma(F_o^2)$, $S = 1.013$ for 735 parameters. Residual electron density extremes were 0.658 and -0.432 Å^{-3}. Hydrogens were added in calculated positions and constrained to a Riding model.

2.5.2 Synthesis of Rotaxanes 29-40 and 50-55, Threads 18-28 and 42-49, S10 and precursors S8-S9.
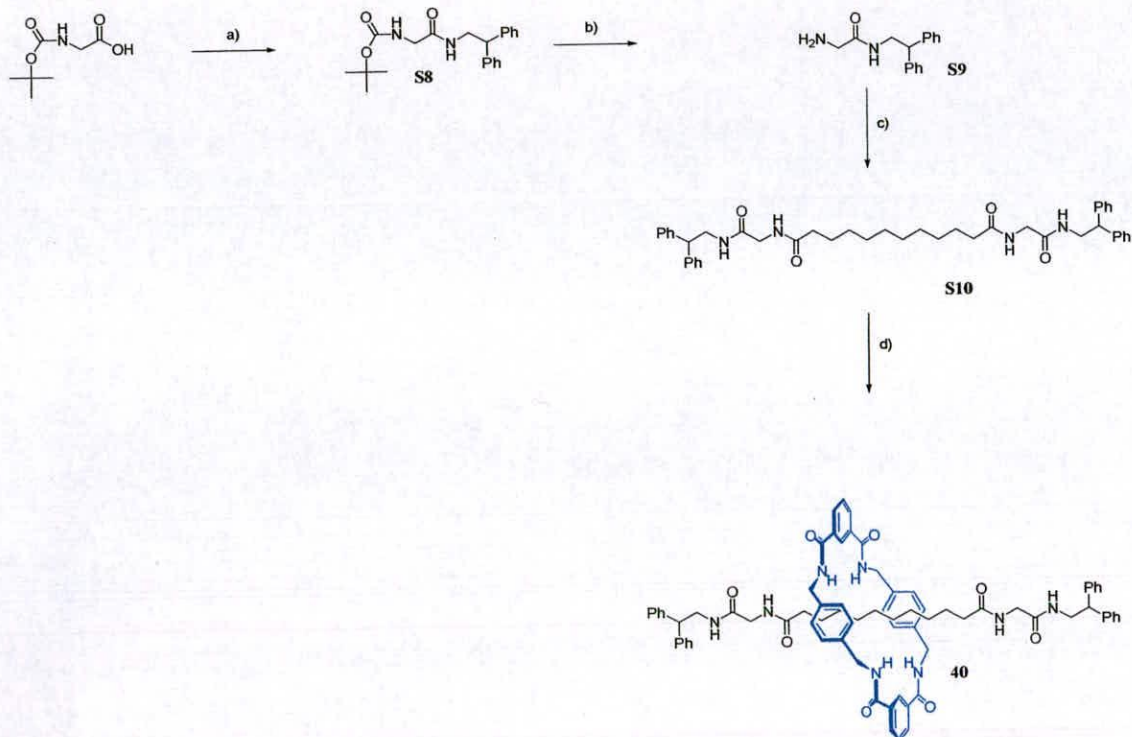
Scheme 2.6 The synthesis of rotaxane **40**, thread **S10** and precursors **S8** and **S9**. a) 2,2-diphenylethylamine, EDCI, HOBt, Et$_3$N, CH$_2$Cl$_2$, 71 %; b) AcCl, MeOH, 95 %; c) dodecanoyl dichloride, Et$_3$N, CH$_2$Cl$_2$, 74 %; d) p-xylylenediamine, isophthaloyl dichloride, Et$_3$N, CHCl$_3$, 41 %. For the synthesis of threads **18-28**, and rotaxanes **29-39** see Scheme 2.3. For the synthesis of threads **42-49** and rotaxanes **50-55** see Scheme 2.4.

General method for the preparation of diacid chloride. The diacid chloride derivatives for the preparation of threads **18–26 and 42-47** were purchased from Aldrich and used without further purification. For **27-28** and **48-49**, the diacid chloride derivatives were prepared from the corresponding diacid purchased from Aldrich using the following general method: To a stirred solution of diacid (3.5 mmol, 1 equiv.) in 20 mL of dichloromethane was added thionyl chloride (2.0 mL, 28 mmol, 8 equiv.), one drop of DMF (cat.) and stirred at 65 °C for 2 h. Distillation of thionyl chloride and dichloromethane yielded the acid chloride as a yellow oil which was used immediately.

2,2-Diphenylethyl-*N*-methyl amine (41)
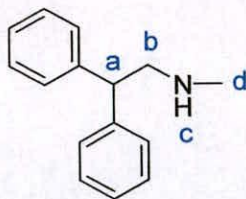
N-Methylamine (38.3 mL, 76.5 mmol, 2 M solution in methanol) was added dropwise over 5 min to a stirred solution of diphenylacetaldehyde (5.00 g, 25.5 mmol), 4Å molecular sieves (3.00 g) in methanol (20 mL) at room temperature. The reaction mixture was stirred at room temperature for 1 h. Subsequently sodium borohydride (2.90 g, 76.5 mmol) was carefully added portionwise over 20 min at 0 °C. The reaction mixture was stirred at room temperature for 3 h then 1 M aqueous hydrochloric acid was added and the volatile solvents removed under reduced pressure. The aqueous layer was then extracted with ethyl acetate (2 x 50 mL) and basified to pH 8 by the dropwise addition of aqueous sodium hydroxide solution (1 M) at 0 °C. The aqueous layer was then extracted with ethyl acetate (3 x 100 mL), dried (MgSO$_4$) and concentrated under reduced pressure to give **41** as a clear oil. Yield 4.71 g, (91 %); ^{1}H NMR (400 MHz, CDCl$_3$): δ = 7.40-7.20 (m, 10H, Ar$\underline{H}$), 4.22 (t, 1H, J = 7.5 Hz C$\underline{H}_a$), 3.21 (d, 2H, J = 8.1 Hz, C$\underline{H}_b$), 2.44 (s, 3H, C$\underline{H}_d$); ^{13}C NMR (100 MHz, CDCl$_3$): δ = 143.1 (s, Ar$\underline{C}$-ipso), 128.9 (d, Ar$\underline{C}$), 128.2 (d, Ar$\underline{C}$), 126.8 (d, Ar$\underline{C}$), 56.8 (t, $\underline{C}$H$_b$), 51.2 (d, $\underline{C}$H$_a$), 36.5 (q, $\underline{C}$H$_d$);

General method for the preparation of alkyl diamide threads and alkyl dimethylamide threads, 18-28, 42-49. To a solution of 2,2-diphenylethyl amine (2.1 mmol, 2.1 equiv.) or **41** (2.1 mmol, 2.1 equiv.) and triethylamine (2.5 mmol, 2.5 equiv.) in dichloromethane (10 mL) was added the relevant diacid chloride (1 mmol, 1 equiv.) in dichloromethane (5 mL) over 10 min at 0 °C. The reaction mixture was allowed to warm to room temperature and stirred for 16 h. The resulting mixture was washed with 1 M aqueous hydrochloric acid (2 x 10 mL), saturated aqueous sodium hydrogen carbonate (2 x 10 mL), saturated aqueous sodium chloride (10 mL), dried (MgSO$_4$) and concentrated under reduced pressure to give the desired thread as colorless solids or colorless oils.

General method for the preparation of benzylic amide macrocycle [2]rotaxanes, 29–40, 50-55. The threads **18-28, S10, 42-49** The threads, (1.00 mmol, 1 equiv.) and triethylamine (2.79 mL, 20.0 mmol, 20 equiv.) were dissolved in chloroform (100 mL) (stabilised with amylenes) and stirred vigorously whilst solutions of *p*-xylylene diamine (1.09 g, 8.0 mmol, 8.0 equiv.) in chloroform (45 mL) and isophthaloyl dichloride (1.63 g, 8.0 mmol, 8.0 equiv.) in chloroform (45 mL) were simultaneously added over a period of 4 hours using motor-driven syringe pumps. The resulting suspension was filtered and concentrated under reduced pressure to leave unconsumed thread and [2]rotaxane in solution. This mixture was subjected to column chromatography on silica gel using dichloromethane: methanol as eluent to yield, in order of elution, the unconsumed thread and [2]rotaxane.

N,N'-bis-**(2,2-Diphenylethyl)malonamide, (18)**
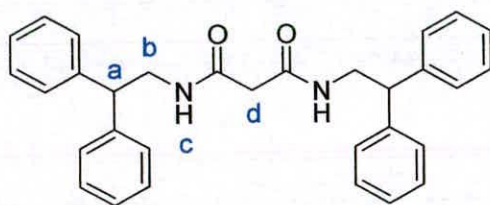
Selected data for *N,N'-bis*-(2,2-diphenylethyl)malonamide, 18: Yield 7.23 g (76 %); m.p. 174–175 °C; ^{1}H NMR (400 MHz, d_6-DMSO): δ = 7.99 (t, 2H, J = 5.6 Hz, NH$_d$), 7.34–7.17 (m, 20H, ArH-stopper), 4.14 (t, 2H, J = 7.7 Hz, CH$_a$), 3.69 (dd, 4H, J = 7.7 Hz, J = 5.6 Hz, CH$_b$), 2.90 (s, 2H, CH$_d$); ^{13}C NMR (100 MHz, d_6-DMSO): δ = 167.3 (s, NHCO), 142.0 (s, ArC-ipso-stopper), 129.1 (d, ArC-stopper), 128.4 (d, ArC-stopper), 127.3 (d, ArC-stopper), 50.8 (d, CH$_a$), 44.3 (t, CH$_b$), 43.1 (t, CH$_d$); LRMS (FAB+ mNBA matrix) *m/z* (rel. int.): 463 [(M+H)$^{+}$] (89 %); Anal. calcd for C$_{31}$H$_{30}$N$_2$O$_2$ (462.58): C 80.49, H 6.54, N 6.06, found: C 80.60, H 6.50, N 5.88.

N,N'-bis-(2,2-Diphenylethyl)succinamide, (19)
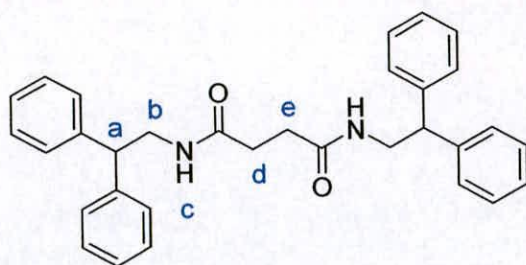
Selected data for *N,N'-bis*-(2,2-diphenylethyl)succinamide, 19: Yield 4.00 g (62 %); m.p. 280 °C; ^{1}H NMR (400 MHz, CDCl$_3$): δ = 7.32-7.17 (m, 20H, Ar$\underline{H}$-stopper), 5.52 (t, 2H, J = 5.8 Hz, N$\underline{H}_c$), 4.14 (t, 2H, J = 8.0 Hz, C$\underline{H}_a$), 3.82 (dd, 4H, J = 8.0 Hz, J = 5.8 Hz, C$\underline{H}_b$), 2.27 (s, 4H, C$\underline{H}_d$ & C$\underline{H}_e$); ^{13}C NMR (100 MHz, CDCl$_3$): δ = 172.5 (s, NH$\underline{C}$O), 142.3 (s, Ar$\underline{C}$-ipso-stopper), 129.1 (d, Ar$\underline{C}$-stopper), 128.4 (d, Ar$\underline{C}$-stopper), 127.2 (d, Ar$\underline{C}$-stopper), 51.0 (d, $\underline{C}$H$_a$), 44.3 (t, $\underline{C}$H$_b$), 31.9 (t, $\underline{C}$H$_d$ & $\underline{C}$H$_e$); LRMS (FAB+ mNBA matrix) m/z (rel. int.): 477 (89 %)[(M+H)$^+$]; Anal. calcd for C$_{32}$H$_{32}$N$_2$O$_2$ (476.61): C 80.64, H 6.77, N 5.88, found: C 80.51, H 6.76, N 5.67.

N,N'-bis-(2,2-Diphenylethyl)glutaramide, (20)
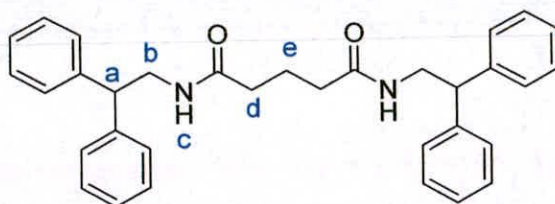
Selected data for *N,N'-bis*-(2,2-diphenylethyl)glutaramide, 20: Yield 7.50 g (76 %); m.p. 190-192 °C; ^{1}H NMR (400 MHz, CDCl$_3$): δ = 7.34-7.22 (m, 20H, Ar$\underline{H}$-stopper), 5.33 (br t, 2H, N$\underline{H}_c$), 4.22 (t, 2H, J = 7.7 Hz, C$\underline{H}_a$), 3.82 (dd, 4H, J = 7.7 Hz, J = 5.6 Hz, C$\underline{H}_b$), 1.91 (t, 4H, J = 7.7 Hz, C$\underline{H}_d$), 1.82 (t, 2H, J = 7.7 Hz, C$\underline{H}_e$); ^{13}C NMR (100 MHz, CDCl$_3$): δ = 172.7 (s, NH$\underline{C}$O), 142.3 (d, Ar$\underline{C}$-ipso-stopper), 129.2 (d, Ar$\underline{C}$-stopper), 128.5 (d, Ar$\underline{C}$-stopper), 127.3 (d, Ar$\underline{C}$-stopper), 51.0 (d, $\underline{C}$H$_a$), 44.1 (t, $\underline{C}$H$_b$), 35.2 (t, $\underline{C}$H$_d$), 22.1 (t, $\underline{C}$H$_e$); LRMS (FAB+ mNBA matrix) m/z

(rel. int.): 492 (94%) [(M+H)$^+$]; Anal. calcd for $C_{33}H_{34}N_2O_2$ (490.64): C 80.78, H 6.98, N 5.71, found: C 80.70, H 6.69, N 5.78.

N,N'-bis-(2,2-Diphenylethyl)adipamide, (21)
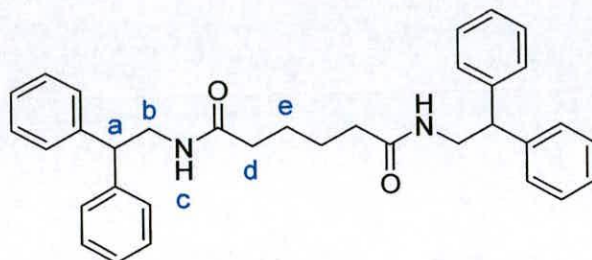
Selected data for *N,N'-bis*-(2,2-diphenylethyl)adipamide, 21: Yield 2.18 g (79 %); m.p. 183 °C; ^{1}H NMR (400 MHz, CDCl$_3$): δ = 7.31-7.19 (m, 20H, Ar$\underline{H}$-stopper), 5.48 (br t, 2H, N$\underline{H}_c$), 4.18 (t, 2H, *J* = 7.8 Hz, C$\underline{H}_a$), 3.88 (dd, 4H, *J* = 7.8 Hz, *J* = 5.8 Hz, C$\underline{H}_b$), 2.09-2.01 (m, 4H, C$\underline{H}_d$), 1.45-1.40 (m, 4H, C$\underline{H}_e$); ^{13}C NMR (100 MHz, CDCl$_3$): δ = 172.6 (s, NH$\underline{C}$O), 141.9 (s, Ar$\underline{C}$-ipso-stopper), 128.7 (d, Ar$\underline{C}$-stopper), 128.1 (d, Ar$\underline{C}$-stopper), 126.8 (d, Ar$\underline{C}$-stopper), 50.6 (d, $\underline{C}$H$_a$), 43.7 (t, $\underline{C}$H$_b$), 36.1 (t, $\underline{C}$H$_d$), 24.7 (t, $\underline{C}$H$_e$); HRMS (FAB+ THIOG matrix): calcd for $C_{34}H_{37}N_2O_2$ [(M+H)$^+$] 505.2870. Found 505.2855.

N,N'-bis-(2,2-Diphenylethyl)pimelamide, (22)
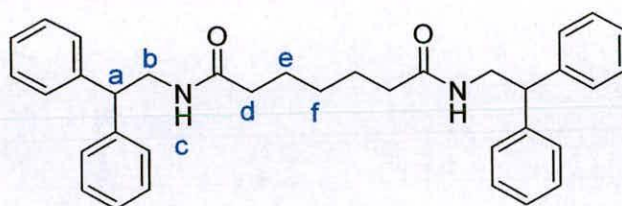
Selected data for *N,N'-bis*-(2,2-diphenylethyl)pimelamide, 22: Yield 2.26 g (86 %); m.p. 138 °C; ^{1}H NMR (400 MHz, CDCl$_3$): δ = 7.32-7.19 (m, 20H, Ar$\underline{H}$-stopper), 5.35 (br t, 2H, N$\underline{H}_c$), 4.18 (t, 2H, *J* = 8.1 Hz, C$\underline{H}_a$), 3.88 (dd, 4H, *J* = 8.1 Hz, *J* = 5.8 Hz, C$\underline{H}_b$), 2.00 (t, 4H, *J* = 7.3 Hz, C$\underline{H}_d$), 1.47 (q, 4H, *J* = 7.3 Hz, C$\underline{H}_e$), 1.13-1.10 (m, 2H, C$\underline{H}_f$); ^{13}C NMR (100 MHz, CDCl$_3$): δ = 172.8 (s, NH$\underline{C}$O), 141.9 (s, Ar$\underline{C}$-ipso-

stopper), 128.7 (d, Ar$\underline{C}$-stopper), 128.1 (d, Ar$\underline{C}$-stopper), 126.8 (d, Ar$\underline{C}$-stopper), 50.6 (d, $\underline{C}H_a$), 43.7 (t, $\underline{C}H_b$), 36.3 (t, $\underline{C}H_d$), 28.4 (t, $\underline{C}H_e$), 25.1 (t, $\underline{C}H_f$); HRMS (FAB+ THIOG matrix): calcd for $C_{35}H_{38}N_2O_2$ [(M+H)$^+$] 519.3022. Found 519.3012.

N,N'-bis-(2,2-Diphenylethyl)suberamide, (23)
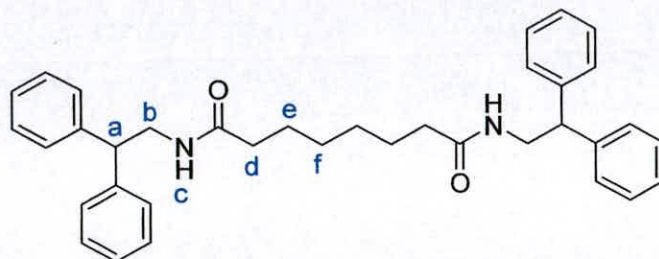
Selected data for *N,N'-bis*-(2,2-diphenylethyl)suberamide, 23: Yield 2.20 g (87 %); m.p. 137 °C; ^{1}H NMR (400 MHz, CDCl$_3$): δ = 7.32–7.19 (m, 20H, Ar$\underline{H}$-stopper), 5.40 (br t, 2H, J = 5.8 Hz, N$\underline{H}_c$), 4.18 (t, 2H, J = 8.1 Hz, $\underline{C}H_a$), 3.88 (dd, 4H, J = 8.1 Hz, J = 5.8 Hz, $\underline{C}H_b$), 2.01 (t, 4H, J = 7.3 Hz, $\underline{C}H_d$), 1.47-1.40 (m, 4H, $\underline{C}H_e$), 1.15-1.10 (m, 4H, $\underline{C}H_f$); ^{13}C NMR (100 MHz, CDCl$_3$): δ = 173.0 (s, NH$\underline{C}$O), 141.9 (s, Ar$\underline{C}$-ipso-stopper), 128.7 (d, Ar$\underline{C}$-stopper), 128.1 (d, Ar$\underline{C}$-stopper), 126.8 (d, Ar$\underline{C}$-stopper), 50.6 (d, $\underline{C}H_a$), 43.7 (t, $\underline{C}H_b$), 36.5 (t, $\underline{C}H_d$), 28.6 (t, $\underline{C}H_e$), 25.3 (t, $\underline{C}H_f$); HRMS (FAB+ THIOG matrix): calcd for $C_{36}H_{41}N_2O_2$ [(M+H)$^+$] 533.3159. Found 533.3168.

N,N'-bis-(2,2-diphenylethyl)azelamide, (24)
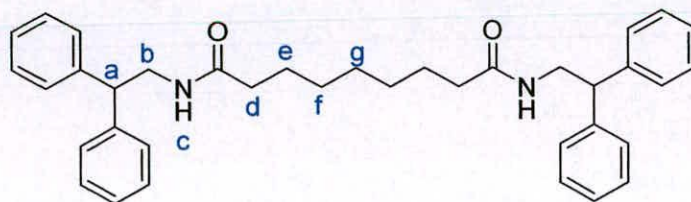
Selected data for *N,N'-bis*-(2,2-diphenylethyl)azelamide, 24: Yield 2.14 g (88 %); m.p. 144 °C; ^{1}H NMR (400 MHz, CDCl$_3$): δ = 7.32–7.19 (m, 20H, Ar$\underline{H}$-stopper), 5.35 (br t, 2H, N$\underline{H}_c$), 4.18 (t, 2H, J = 8.1 Hz, $\underline{C}H_a$), 3.89 (dd, 4H, J = 8.1 Hz, J = 5.8

Hz, C$\underline{H}_b$), 2.03 (t, 4H, *J* = 7.6 Hz, C$\underline{H}_d$), 1.48-1.38 (m, 4H, C$\underline{H}_e$), 1.17-1.12 (m, 6H, C$\underline{H}_f$ & C$\underline{H}_g$); ^{13}C NMR (100 MHz, CDCl$_3$): δ = 173.1 (s, NH$\underline{C}$O), 141.9 (s, Ar$\underline{C}$-ipso-stopper), 128.7 (d, Ar$\underline{C}$-stopper), 128.1, (d, Ar$\underline{C}$-stopper), 126.8 (d, Ar$\underline{C}$-stopper), 50.6 (d, $\underline{C}$H$_a$), 43.7 (t, $\underline{C}$H$_b$), 36.6 (t, $\underline{C}$H$_d$), 28.9 (t, $\underline{C}$H$_e$), 28.8 (t, $\underline{C}$H$_f$), 25.5 (t, $\underline{C}$H$_g$); HRMS (FAB+ THIOG matrix): calcd for C$_{37}$H$_{43}$N$_2$O$_2$ [(M+H)$^+$] 547.3341. Found 547.3325.

N,N'-bis-(2,2-diphenylethyl)sebacamide, (25)
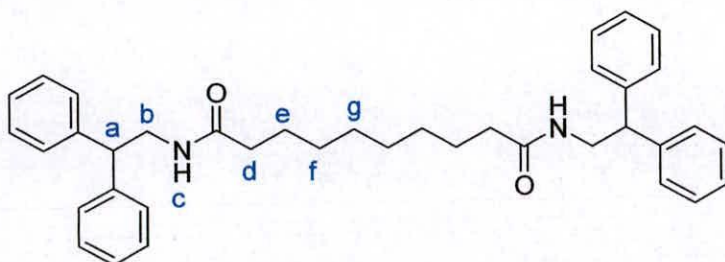
Selected data for *N,N'-bis*-(2,2-diphenylethyl)sebacamide, 25: Yield 1.92 g (82 %); m.p. 138 °C; ^{1}H NMR (400 MHz, C$_2$D$_2$Cl$_4$): δ = 7.33-7.21 (m, 20H, Ar$\underline{H}$-stopper), 5.37 (br t, 2H, N$\underline{H}_c$), 4.15 (t, 2H, *J* = 7.8 Hz, C$\underline{H}_a$), 3.85 (dd, 4H, *J* = 5.8 Hz, *J* = 7.8 Hz, C$\underline{H}_b$), 2.01 (t, 4H, *J* = 7.6 Hz, C$\underline{H}_d$), 1.46-1.32 (m, 4H, C$\underline{H}_e$), 1.15 (br s, 8H, C$\underline{H}_f$ & C$\underline{H}_g$); ^{13}C NMR (100 MHz, CDCl$_3$): δ = 173.1 (s, NH$\underline{C}$O), 141.9 (s, Ar$\underline{C}$-ipso-stopper), 128.7 (d, Ar$\underline{C}$-stopper), 128.1, (d, Ar$\underline{C}$-stopper), 126.8 (d, Ar$\underline{C}$-stopper), 50.6 (d, $\underline{C}$H$_a$), 43.7 (t, $\underline{C}$H$_b$), 36.7 (t, $\underline{C}$H$_d$), 29.2 (t, $\underline{C}$H$_e$), 29.0 (t, $\underline{C}$H$_f$), 25.6 (t, $\underline{C}$H$_g$); HRMS (FAB+ THIOG matrix): calcd for C$_{38}$H$_{45}$N$_2$O$_2$ [(M+H)$^+$] 561.3474. Found 561.3481.

N,N'-bis-(2,2-diphenylethyl)decanamide, (26)
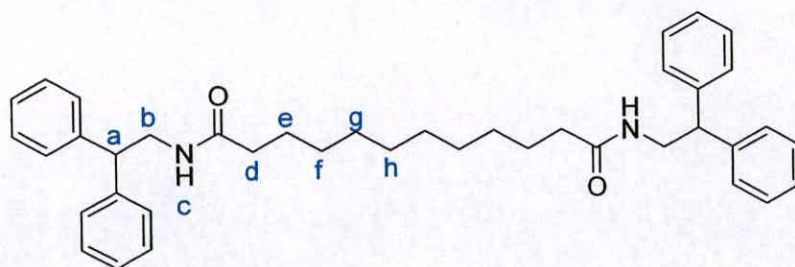
Selected data for *N,N'-bis*-(2,2-diphenylethyl)decanamide, 26: Yield 1.87 g (85 %); m.p. 137 °C; ^{1}H NMR (400 MHz, CDCl$_3$): δ = 7.32–7.19 (m, 10H, Ar$\underline{H}$-stopper), 5.37 (br t, 2H, N$\underline{H}_c$), 4.18 (t, 2H, J = 7.8 Hz, C$\underline{H}_a$), 3.88 (dd, 2H, J = 7.8 Hz, J = 5.8 Hz, C$\underline{H}_b$), 2.04 (t, 4H, J = 7.6 Hz, C$\underline{H}_d$), 1.50-1.41 (m, 4H, C$\underline{H}_e$), 1.20 (br s, 8H, C$\underline{H}_f$, C$\underline{H}_g$ & C$\underline{H}_h$); ^{13}C NMR (100 MHz, CDCl$_3$): δ = 173.1 (s, NH$\underline{C}$O), 141.9 (s, Ar$\underline{C}$-ipso-stopper), 128.7 (d, Ar$\underline{C}$-stopper), 128.1 (d, Ar$\underline{C}$-stopper), 126.8 (d, Ar$\underline{C}$-stopper), 50.6 (d, $\underline{C}$H$_a$), 43.7 (t, $\underline{C}$H$_b$), 36.8 (t, $\underline{C}$H$_d$), 29.3 (t, $\underline{C}$H$_e$), 29.2 (t, $\underline{C}$H$_f$), 29.1 (t, $\underline{C}$H$_g$), 25.6 (t, $\underline{C}$H$_h$); HRMS (FAB+ mNBA matrix): calcd for C$_{40}$H$_{49}$N$_2$O$_2$ [(M+H)$^+$] 589.3794. Found 589.3780.

N,N'-bis(2,2-diphenylethyl)dodecanamide, (27)
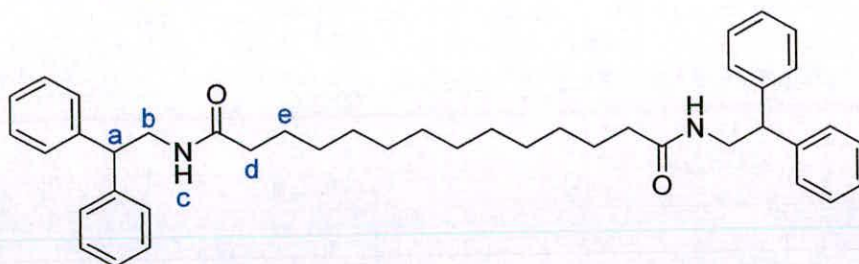
Selected data for *N,N'-bis*-(2,2-diphenylethyl)dodecanamide, 27: Yield 1.88 g (90 %); m.p. 137 °C; ^{1}H NMR (400 MHz, CDCl$_3$): δ = 7.32-7.19 (m, 20H, Ar$\underline{H}$-stopper), 5.37 (br t, 2H, J = 5.8 Hz, N$\underline{H}_c$), 4.18 (t, 2H, J = 7.8 Hz, C$\underline{H}_a$), 3.88 (dd, 4H, J = 7.8 Hz, J = 5.8 Hz, C$\underline{H}_b$), 2.04 (t, 4H, J = 7.6 Hz, C$\underline{H}_d$), 1.50-1.36 (m, 4H, C$\underline{H}_e$), 1.30-1.21 (m, 16H, -C$\underline{H}_2$-alkyl); ^{13}C NMR (100 MHz, CDCl$_3$): δ = 173.1 (s, NH$\underline{C}$O), 141.9 (s, Ar$\underline{C}$-ipso-stopper), 128.7 (d, Ar$\underline{C}$-stopper), 128.1 (d, Ar$\underline{C}$-stopper), 126.8

(d, ArC-stopper), 50.6 (d, CHa), 43.7 (t, CHb), 36.8 (t, CHd), 29.5 (t, -CH2-), 29.4 (t, -CH2-), 29.3 (t, -CH2-), 29.2 (t, -CH2-), 25.7 (t, -CH2-); HRMS (FAB+ THIOG matrix): calcd for $C_{42}H_{53}N_2O_2$ [(M+H)$^+$] 617.4111. Found 617.4107.

N,N'-*bis*-(2,2-diphenylethyl)tetradecanamide, (28)
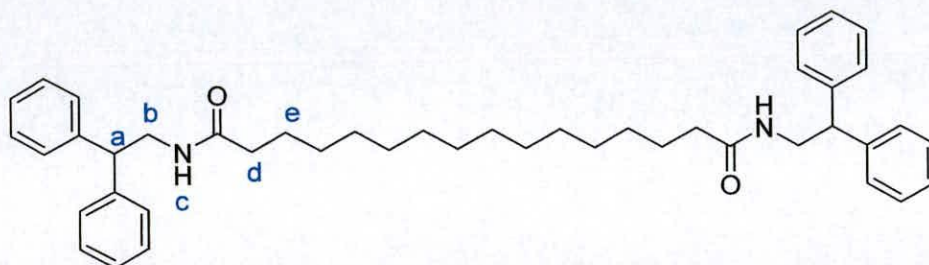
Selected data for N,N'-*bis*-(2,2-diphenylethyl)tetradecanamide, 28: Yield 1.64 g (82 %); m.p. 140 °C; ^{1}H NMR (400 MHz, CDCl$_3$): δ = 7.32-7.19 (m, 20H, ArH-stopper), 5.35 (br t, 2H, NHc), 4.18 (t, 2H, J = 7.8 Hz, CHa), 3.88 (dd, 4H, J = 7.8 Hz, J = 5.8 Hz, CHb), 2.04 (t, 4H, J = 7.8 Hz, CHd), 1.51-1.36 (m, 4H, CHe), 1.22-1.10 (m, 20H, -CH2-alkyl); ^{13}C NMR (100 MHz, CDCl$_3$): δ = 173.1 (s, NHCO), 141.9 (s, ArC-ipso-stopper), 128.7 (d, ArC-stopper), 128.1 (d, ArC-stopper), 126.8 (d, ArC-stopper), 50.6 (d, CHa), 43.7 (t, CHb), 36.8 (t, CHd), 29.6 (t, -CH2-), 29.6 (t, -CH2-), 29.4 (t, -CH2-), 29.3 (t, -CH2-), 29.2 (t, -CH2-), 25.7 (t, -CH2-); HRMS (FAB+, THIOG matrix): calcd for $C_{44}H_{57}N_2O_2$ [(M+H)$^+$] 645.4425. Found 645.4420.

X-ray crystallographic structure determination of thread, 28: $C_{44}H_{56}N_2O_2$, M = 644.91, crystal size 0.10 × 0.08 × 0.08 mm, triclinic, P-1, a = 5.1811(2), b = 8.9518(4), c = 19.9950(8) Å, α = 78.2590(10), β = 89.1620(10), γ = 82.8780(10)°, V = 900.91(6) Å^3, Z = 1, ρ_{calcd} = 1.189 Mg m^{-3}; synchrotron radiation (CCLRC Daresbury Laboratory Station 9.8, silicon monochromator, λ = 0.68950 Å), μ = 0.072 mm^{-1}, T = 150(2) K. 9199 data (4877 unique, R_{int} = 0.0249, 2.34 < θ < 30.36°), were collected on a Siemens SMART CCD diffractometer using narrow frames (0.3° in ω), and were corrected semiempirically for absorption and incident beam decay (transmission 1.00–0.74). The structure was solved by direct methods

and refined by full-matrix least-squares on F^2 values of all data (G. M. Sheldrick, SHELXTL manual, Siemens Analytical X-ray Instruments, Madison WI, USA, 1994, version 5) to give $wR = \{\Sigma[w(F_o^2-F_c^2)^2]/\Sigma[w(F_o^2)^2]\}^{1/2} = 0.1490$, conventional $R = 0.0588$ for F values of 4877 reflections with $F_o^2 > 2\sigma(F_o^2)$, $S = 1.027$ for 221 parameters. Residual electron density extremes were 0.347 and –0.259 eÅ^{-3}. Amide hydrogen atoms were refined isotropically with the remainder constrained; anisotropic displacement parameters were used for all non-hydrogen atoms.

([2](1,7,14,20-Tetraaza-2,6,15,19-tetraoxo-3,5,9,12,16,18,22,25 tetrabenzocyclohexacosane)-*(N,N'-bis*-(2,2-diphenyl-ethyl)-malonamide)-rotaxane, (29)
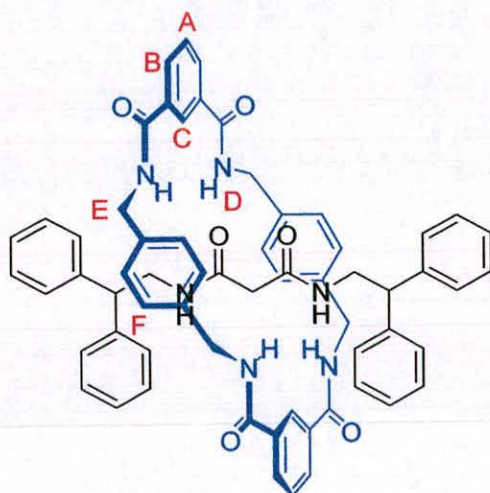
Selected data for ([2](1,7,14,20-Tetraaza-2,6,15,19-tetraoxo-3,5,9,12,16,18,22,25 tetrabenzocyclohexacosane)-*(N,N'-bis*-(2,2-diphenyl-ethyl)-malonamide)-rotaxane, 29: Yield 0.08 g (8 %); m.p. 266–267 °C; ^{1}H NMR (400 MHz, d_6-DMSO): $\delta = 8.59$ (t, 4H, $J = 4.8$ Hz, N$\underline{H}_D$), 8.18 (br s, 2H, Ar$\underline{H}_C$), 8.08 (d, 4H, $J = 7.8$ Hz, Ar$\underline{H}_B$), 7.68 (t, 2H, $J = 7.8$ Hz, Ar$\underline{H}_A$), 7.63 (t, 2H, $J = 5.3$ Hz, N$\underline{H}_d$), 7.25-7.05 (m, 20H, Ar$\underline{H}$-stopper), 6.87 (s, 8H, Ar$\underline{H}_F$), 4.29 (d, 8H, $J = 4.8$ Hz, C$\underline{H}_E$), 3.80 (t, 2H, $J = 7.8$ Hz, C$\underline{H}_a$), 3.39 (dd, 4H, $J = 7.8$ Hz, $J = 5.3$ Hz, C$\underline{H}_b$), 1.48 (s, 2H, C$\underline{H}_d$); ^{13}C NMR (100 MHz, CDCl$_3$): $\delta = 167.6$ (s, NH$\underline{C}$O), 166.4 (s, NH$_D\underline{C}$O), 143.2 (s, Ar$\underline{C}$-ipso-stopper), 137.2 (Ar$\underline{C}$-ipso-xylylene), 134.7 (Ar$\underline{C}$-ipso-isophthaloyl),

---

130.6 (d, Ar$\underline{C}_B$), 129.0 (d, Ar$\underline{C}_F$), 128.9 (d, Ar$\underline{C}_A$), 128.7 (d, Ar$\underline{C}$-stopper), 127.9 (d, Ar$\underline{C}$-stopper), 126.7 (d, Ar$\underline{C}$-stopper), 126.5 (d, Ar$\underline{C}_C$), 50.1 (d, $\underline{C}H_a$), 44.1 (t, $\underline{C}H_b$), 43.4 (t, $\underline{C}H_E$), 40.0 (t, $\underline{C}H_d$); LRMS (FAB+ mNBA matrix) *m/z* (rel. int.): 995 (71.2 %) [(M+H)$^+$]; Anal. calcd for $C_{63}H_{58}N_6O_6$ (995.17): C 76.03, H 5.87, N 8.45, found C 75.75, H 5.88, N 8.11.

X-ray crystallographic structure determination, crystals of rotaxane grown in acetone/H$_2$O, 29: $C_{64.50}H_{64}N_6O_{7.50}$, M = 1043.22, crystal size 0.15 × 0.15 × 0.15 mm, triclinic, P-1, a = 11.0013(4), b = 14.6086(5), c = 18.5866(6) Å, α = 92.8550(10), β = 95.2040(10), γ = 101.1940(10)°, V = 911.3(2) Å^3, Z = 2, ρ_{calcd} = 1.190 Mg m^{-3}; Mo$_{K\alpha}$ radiation (graphite monochromator, λ = 0.71073 Å), μ = 0.079 mm^{-1}, T = 293(2) K. 16933 data (11048 unique, R_{int} = 0.1247, 1.42 < θ < 26.41°), were collected on a Siemens SMART CCD diffractometer using narrow frames (0.3° in ω), and were corrected semiempirically for absorption and incident beam decay (transmission 1.00–0.09). The structure was solved by direct methods and refined by full-matrix least-squares on F^2 values of all data (G. M. Sheldrick, SHELXTL manual, Siemens Analytical X-ray Instruments, Madison WI, USA, 1994, version 5) to give wR = {$\Sigma[w(F_o^2-F_c^2)^2]/\Sigma[w(F_o^2)^2]$}$^{1/2}$ = 0.3019, conventional R = 0.0939 for F values of 11048 reflections with $F_o^2 > 2\sigma(F_o^2)$, S = 1.278 for 344 parameters. Residual electron density extremes were 0.751 and –0.261 eÅ^{-3}. Amide hydrogen atoms were refined isotropically and subject to a distance constraint N–H = 0.98 Å, with the remainder atoms constrained; anisotropic displacement parameters were used for all non-hydrogen atoms.

([2](1,7,14,20-Tetraaza-2,6,15,19-tetraoxo-3,5,9,12,16,18,22,25 tetrabenzocyclohexacosane)-*(N,N'-bis*-(2,2-diphenyl-ethyl)-succinamide)-rotaxane, (30)
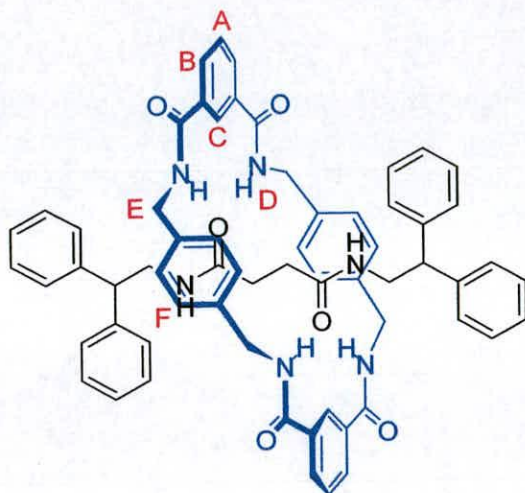
Selected data for ([2](1,7,14,20-Tetraaza-2,6,15,19-tetraoxo-3,5,9,12,16,18,22,25 tetrabenzocyclohexacosane)-*(N,N'-bis*-(2,2-diphenyl-ethyl)-succinamide)-rotaxane, 30: Yield 0.50 g (52 %); m.p. 330 °C, (decomp); ^{1}H NMR (400 MHz, $C_2D_2Cl_4$): δ = 8.33 (br s, 2H, Ar$\underline{H}_C$), 8.14 (dd, 4H, J = 7.8, J = 1.3 Hz, Ar$\underline{H}_B$), 7.59 (t, 2H, J = 7.8 Hz, Ar$\underline{H}_A$), 7.35 (br t, 4H, J = 5.3 Hz, N$\underline{H}_D$), 7.24–7.10 (m, 20H, ArC$\underline{H}$-stopper), 6.71 (s, 8H, Ar$\underline{H}_F$), 5.53 (br t, 2H, N$\underline{H}_c$), 4.31 (d, 8H, J = 5.0 Hz, C$\underline{H}_E$), 3.93 (t, 2H, J = 7.8 Hz, C$\underline{H}_a$), 3.59-3.50 (m, 4H, C$\underline{H}_b$), 0.74 (br s, 4H, C$\underline{H}_d$); ^{13}C NMR (100 MHz, d_6-DMSO): δ = 172.8 (s, NH$\underline{C}$O), 166.5 (s, NH$_D\underline{C}$O), 141.4 (s, Ar$\underline{C}$-ipso-stopper), 137.6 (s, Ar$\underline{C}$-ipso-xylylene), 134.0 (s, Ar$\underline{C}$-ipso-isophthaloyl), 130.8 (d, Ar$\underline{C}_B$), 129.3 (d, Ar$\underline{C}_F$), 129.0 (d, Ar$\underline{C}_A$), 128.9 (d, Ar$\underline{C}$-stopper), 127.8 (d, Ar$\underline{C}$-stopper), 127.2 (d, Ar$\underline{C}$-stopper), 125.4 (d, Ar$\underline{C}_C$), 49.4 (d, $\underline{C}H_a$), 44.3 (t, $\underline{C}H_b$), 43.7 (t, $\underline{C}H_E$) 28.4 (t, $\underline{C}H_d$); LRMS (FAB+ mNBA matrix) *m/z* (rel. int.): 1010 (32.1 %) [(M+H)$^+$]; Anal. calcd for $C_{64}H_{60}N_6O_6$ (1009.20): C 76.17, H 5.99, N 8.33, found C 76.42, H 5.96, N 8.29.

X-ray crystallographic structure determinations, crystals of rotaxane grown in DMF/H$_2$O, 30: $C_{76}H_{88}N_{10}O_{10}$, M = 1301.56, crystal size 0.24 × 0.06 × 0.06 mm, triclinic, *P*-1, a = 9.8887(5), b = 13.1481(6), c = 15.3131(7) Å, $α$ = 108.0300(10), $β$

$= 106.0530(10)$, $\gamma = 101.9480(10)°$, $V = 1723.58(14)$ Å^3, $Z = 1$, $\rho_{calcd} = 1.254$ Mg m^{-3}; Mo$_{K\alpha}$ radiation (graphite monochromator, $\lambda = 0.71073$ Å), $\mu = 0.084$ mm^{-1}, $T = 293(2)$ K. 8463 data (4770 unique, $R_{int} = 0.0628$, $1.50 < \theta < 23.31°$), were collected on a Siemens SMART CCD diffractometer using narrow frames (0.3° in ω), and were corrected semiempirically for absorption and incident beam decay (transmission 1.00–0.70). The structure was solved by direct methods and refined by full-matrix least-squares on F^2 values of all data (G. M. Sheldrick, SHELXTL manual, Siemens Analytical X-ray Instruments, Madison WI, USA, 1994, version 5) to give $wR = \{\Sigma[w(F_o^2-F_c^2)^2]/\Sigma[w(F_o^2)^2]\}^{1/2} = 0.1902$, conventional $R = 0.0866$ for F values of 4770 reflections with $F_o^2 > 2\sigma(F_o^2)$, $S = 1.103$ for 446 parameters. Residual electron density extremes were 0.356 and -0.250 eÅ^{-3}. Amide hydrogen atoms were refined isotropically and subject to a distance constraint N–H = 0.98 Å, with the remainder atoms constrained; anisotropic displacement parameters were used for all non-hydrogen atoms.

([2](1,7,14,20-Tetraaza-2,6,15,19-tetraoxo-3,5,9,12,16,18,22,25 tetrabenzocyclohexacosane)-(N,N'-bis-(2,2-diphenylethyl)glutaramide)-rotaxane, (31)

Selected data for ([2](1,7,14,20-Tetraaza-2,6,15,19-tetraoxo-3,5,9,12,16,18,22,25 tetrabenzocyclohexacosane)-(*N,N'-bis*-(2,2-diphenylethyl)glutaramide)- rotaxane, 31: Yield 6.3 mg (3 %); ^{1}H NMR (400 MHz, CDCl$_3$): δ = 8.17–8.15 (m, 6H, ArC$\underline{\text{H}}_\text{C}$ & ArC$\underline{\text{H}}_\text{B}$), 7.60 (t, 2H, J = 8.2 Hz, Ar$\underline{\text{H}}_\text{A}$), 7.41 (t, 4H, J = 5.5 Hz, N$\underline{\text{H}}_\text{D}$), 7.30-7.10 (m, 20H, Ar$\underline{\text{H}}$-stopper), 7.02 (s, 8H, Ar$\underline{\text{H}}_\text{F}$), 5.50 (t, 2H, J = 5.3 Hz, N$\underline{\text{H}}_\text{c}$), 4.53 (d, 8H, J = 5.5 Hz, C$\underline{\text{H}}_\text{E}$), 3.99 (t, 2H, J = 7.9 Hz, C$\underline{\text{H}}_\text{a}$), 3.52 (dd, J = 7.9 Hz, J = 5.4 Hz, C$\underline{\text{H}}_\text{b}$), 1.56 (t, 4H, J = 7.4 Hz, C$\underline{\text{H}}_\text{d}$), 0.65-0.56 (m, 4H, C$\underline{\text{H}}_\text{e}$); ^{13}C NMR (100 MHz, CDCl$_3$): δ = 173.6 (s, NH$\underline{\text{C}}$O), 166.9 (s, NH$_\text{D}\underline{\text{C}}$O), 141.9 (s, Ar$\underline{\text{C}}$-ipso-stopper), 138.2 (s, Ar$\underline{\text{C}}$-ipso-xylylene), 134.8 (s, Ar$\underline{\text{C}}$-ipso-isophthaloyl), 131.6 (d, Ar$\underline{\text{C}}_\text{B}$), 129.6 (d, Ar$\underline{\text{C}}_\text{F}$), 129.3 (d, Ar$\underline{\text{C}}_\text{A}$), 129.1(d, Ar$\underline{\text{C}}$-stopper), 128.4 (d, Ar$\underline{\text{C}}$-stopper), 127.5 (d, Ar$\underline{\text{C}}$-stopper), 125.9 (d, Ar$\underline{\text{C}}_\text{C}$), 50.5 (d, $\underline{\text{C}}$H$_\text{a}$), 44.5 (t, $\underline{\text{C}}$H$_\text{b}$), 44.4 (t, $\underline{\text{C}}$H$_\text{E}$), 30.1 (t, $\underline{\text{C}}$H$_\text{d}$), 18.7 (t, $\underline{\text{C}}$H$_\text{e}$); LRMS (FAB+ mNBA matrix) m/z (rel. int.): 1024 [(M+H)$^+$]; Anal. calcd for C$_{65}$H$_{62}$N$_6$O$_6$ (1023.20): C 76.30, H 6.11, N 8.21, found C 76.32, H 6.17, N 8.29.

X-ray crystallographic structure determinations, crystals of rotaxane grown in EtOH/H$_2$O, 31: C$_{67}$H$_{69}$N$_6$O$_8$, M = 1086.28, crystal size 0.20 × 0.18 × 0.15 mm, triclinic, *P*-1, a = 10.2229(2), b = 17.437, c = 18.3469(3) Å, α = 62.9370(10), β = 89.6630(10), γ = 86.55°, V = 2906.25(7) Å^3, Z = 2, ρ_{calcd} = 1.241 Mg m^{-3}; Mo$_{\text{K}\alpha}$ radiation (graphite monochromator, λ = 0.71073 Å), μ = 0.082 mm^{-1}, T = 180(2) K. 18358 data (13260 unique, R_{int} = 0.0290, 2.00 < θ < 29.11°), were collected on a Siemens SMART CCD diffractometer using narrow frames (0.3° in ω), and were corrected semiempirically for absorption and incident beam decay. The structure was solved by direct methods and refined by full-matrix least-squares on F^2 values of all data (G. M. Sheldrick, SHELXTL manual, Siemens Analytical X-ray Instruments, Madison WI, USA, 1994, version 5) to give wR = $\{\Sigma[w(F_o^2 - F_c^2)^2]/\Sigma[w(F_o^2)^2]\}^{1/2}$ = 0.1877, conventional R = 0.0683 for F values of 13260 reflections with $F_o^2 > 2\sigma(F_o^2)$, S = 1.018 for 750 parameters. Residual electron density extremes were 0.536 and –0.450 eÅ^{-3}. Amide hydrogen atoms were refined isotropically with the remainder constrained; anisotropic displacement parameters were used for all non-hydrogen atoms.

([2](1,7,14,20-Tetraaza-2,6,15,19-tetraoxo-3,5,9,12,16,18,22,25 tetrabenzocyclohexacosane)-(*N,N'-bis*(2,2-diphenylethyl)adipamide)-rotaxane, (32)

Selected data for ([2](1,7,14,20-Tetraaza-2,6,15,19-tetraoxo-3,5,9,12,16,18,22,25 tetrabenzocyclohexacosane)-(*N,N'-bis*(2,2-diphenylethyl)adipamide)-rotaxane,

32: Yield 164 mg (8 %); m.p. 264 °C; ^{1}H NMR (400 MHz, CDCl$_3$): δ = 8.09 (br s, 4H, Ar$\underline{H}_B$), 8.07 (br s, 2H, Ar$\underline{H}_C$), 7.53 (t, 2H, J = 7.8 Hz, Ar$\underline{H}_A$), 7.31-7.16 (m, 24H, N$\underline{H}_D$ & Ar$\underline{H}$-stopper), 6.98 (s, 8H, Ar$\underline{H}_F$), 5.76 (br t, 2H, N$\underline{H}$CO), 4.48 (d, 8H, J = 5.6 Hz, C$\underline{H}_E$), 4.04 (t, 2H, J = 7.8 Hz, C$\underline{H}_a$), 3.57 (dd, 4H, J = 7.8 Hz, J = 5.6 Hz, C$\underline{H}_b$), 0.87-0.74 (m, 4H, C$\underline{H}_d$), 0.48-0.37 (m, 4H, C$\underline{H}_e$); ^{13}C NMR (100 MHz, CDCl$_3$): δ = 173.5 (s, NH$\underline{C}$O), 166.5 (s, NH$_D\underline{C}$O), 142.0 (s, Ar$\underline{C}$-ipso-thread), 137.8 (s, Ar$\underline{C}$-ipso-xylylene), 134.1 (s, Ar$\underline{C}$-ipso-isophthaloyl), 131.2 (d, Ar$\underline{C}_B$), 129.3 (d, Ar$\underline{C}_F$), 128.8 (d, Ar$\underline{C}_A$), 128.7 (d, Ar$\underline{C}$-stopper), 128.0 (d, Ar$\underline{C}$-stopper), 127.0 (d, Ar$\underline{C}$-stopper), 124.6 (d, Ar$\underline{C}_C$), 50.2 (d, $\underline{C}$H$_a$), 44.2 (t, $\underline{C}$H$_b$), 43.9 (t, $\underline{C}$H$_E$), 34.8 (t, $\underline{C}$H$_d$), 23.8 (t, $\underline{C}$H$_e$);. HRMS (FAB+ THIOG matrix): calcd for C$_{66}$H$_{65}$N$_6$O$_6$ 1037.4940 [M+H]$^+$. Found 1037.4966.

X-ray crystallographic structure determinations: Crystals of rotaxane grown in CHCl$_3$/MeOH, 32: C$_{68}$H$_{72}$N$_6$O$_6$, M = 1101.32, crystal size 0.10 × 0.06 × 0.05 mm, monoclinic, *C2/c*, a = 30.939(6), b = 11.3129(18), c = 18.568(3) Å, $β$ =

$118.147(17)°$, $V = 5730.5(17)$ Å^3, $Z = 4$, $\rho_{calcd} = 1.277$ Mg m^{-3}; synchrotron radiation (CCLRC Daresbury Laboratory Station 9.8, silicon monochromator, $\lambda = 0.69230$ Å), $\mu = 0.084$ mm^{-1}, $T = 150(2)$ K. 18920 data (7604 unique, $R_{int} = 0.0348$, $2.42 < \theta < 29.30°$), were collected on a Siemens SMART CCD diffractometer using narrow frames ($0.3°$ in ω), and were corrected semiempirically for absorption and incident beam decay. The structure was solved by direct methods and refined by full-matrix least-squares on F^2 values of all data (G. M. Sheldrick, SHELXTL manual, Siemens Analytical X-ray Instruments, Madison WI, USA, 1994, version 5) to give $wR = \{\Sigma[w(F_o^2-F_c^2)^2]/\Sigma[w(F_o^2)^2]\}^{1/2} = 0.1361$, conventional $R = 0.0541$ for F values of 7604 reflections with $F_o^2 > 2\sigma(F_o^2)$, $S = 1.070$ for 384 parameters. Residual electron density extremes were 0.429 and -0.411 eÅ^{-3}. Amide hydrogen atoms were refined isotropically with the remainder constrained; anisotropic displacement parameters were used for all non-hydrogen atoms.

Crystals of rotaxane grown in DMSO/H$_2$O, 32: $C_{70}H_{80}N_6O_{10}S_2$, $M = 1229.52$, crystal size $0.15 \times 0.12 \times 0.10$ mm, triclinic $P-1$, $a = 11.6401(3)$, $b = 16.6666(5)$, $c = 18.7274(4)$ Å, $\alpha = 102.8950(10)$, $\beta = 108.0990(10)$, $\gamma = 110.3350(10)°$, $V = 3006.38(14)$ A^3, $Z = 2$, $\rho_{calcd} = 1.358$ Mg m^{-3}; Mo$_{K\alpha}$ radiation (graphite monochromator, $\lambda = 0.71073$ Å), $\mu = 0.157$ mm^{-1}, $T = 180(2)$ K. 19537 data (13964 unique, $R_{int} = 0.0149$, $1.40 < \theta < 29.24°$), were collected on a Siemens SMART CCD diffractometer using narrow frames ($0.3°$ in ω), and were corrected semiempirically for absorption and incident beam decay. The structure was solved by direct methods and refined by full-matrix least-squares on F^2 values of all data (G. M. Sheldrick, SHELXTL manual, Siemens Analytical X-ray Instruments, Madison WI, USA, 1994, version 5) to give $wR = \{\Sigma[w(F_o^2-F_c^2)^2]/\Sigma[w(F_o^2)^2]\}^{1/2} = 0.2495$, conventional $R = 0.0772$ for F values of 13964 reflections with $F_o^2 > 2\sigma(F_o^2)$, $S = 1.046$ for 817 parameters. Residual electron density extremes were 0.674 and -1.096 eÅ^{-3}. Amide hydrogen atoms were refined isotropically with the remainder constrained; anisotropic displacement parameters were used for all non-hydrogen atoms.

([2](1,7,14,20-Tetraaza-2,6,15,19-tetraoxo-3,5,9,12,16,18,22,25

tetrabenzocyclohexacosane)-(*N,N'-bis*-(2,2-diphenylethyl)pimelamide)-rotaxane,

(33)

Selected data for ([2](1,7,14,20-Tetraaza-2,6,15,19-tetraoxo-3,5,9,12,16,18,22,25

tetrabenzocyclohexacosane)-(*N,N'-bis*-(2,2-diphenylethyl)pimelamide)-rotaxane,

33: Yield 284 mg (14 %); m.p. 140 °C; ^{1}H NMR (400 MHz, CDCl$_3$): δ = 8.09 (s, 2H,

ArH$_C$), 8.07 (br m, 4H, ArH$_B$), 7.54 (br t, 4H, NH$_D$), 7.47 (t, 2H, J = 8.1 Hz, ArH$_A$),

7.33-7.21 (m, 20H, ArH-stopper), 7.03 (s, 8H, ArH$_F$), 5.95 (br t, 2H, NH$_c$), 4.49 (d,

8H, J = 5.6 Hz, CH$_E$), 4.06 (t, 2H, J = 7.6 Hz, CH$_a$), 3.65 (dd, 4H, J = 7.6 Hz, J = 5.6

Hz, CH$_b$), 0.86-0.76 (m, 4H, CH$_d$), 0.47-0.36 (m, 4H, CH$_e$), 0.26-0.23 (m, 2H, CH$_f$);

^{13}C NMR (100 MHz, CDCl$_3$): δ = 173.8 (s, NHCO), 166.5 (s, NH$_D$CO), 142.0 (s,

ArC-ipso-stopper), 137.6 (s, ArC-ipso-xylylene), 134.0 (s, ArC-ipso-isophthaloyl),

131.3 (d, ArC$_B$), 129.0 (d, ArC$_F$), 128.8 (d, ArC$_A$), 128.1 (d, ArC-stopper), 127.5 (d,

ArC-stopper), 127.0 (d, ArC-stopper), 124.7 (d, ArC$_C$), 50.2 (d, CH$_a$), 44.2 (t, CH$_b$),

43.9 (t, CH$_E$), 34.9 (t, CH$_d$), 27.6 (t, CH$_e$), 23.3 (t, CH$_f$); HRMS (FAB+ THIOG

matrix): calcd for C$_{67}$H$_{67}$N$_6$O$_6$ [(M+H)$^+$] 1051.5124. Found 1051.5122.

Crystals of rotaxane grown in CHCl$_3$/MeOH, 33: C$_{69}$H$_{69}$N$_6$O$_6$Cl$_5$, M = 1255.55,

crystal size 0.08 × 0.03 × 0.03 mm, monoclinic, $C2/c$, a = 18.6031(9), b =

23.8302(12), c = 29.7448(14) Å, $β$ = 103.876(10)°, Z = 8, $ρ_{calcd}$ = 1.227 Mg m^{-3};

synchrotron radiation (CCLRC Daresbury Laboratory Station 9.8, silicon monochromator, $\lambda = 0.69230$ Å), $\mu = 0.24$ mm^{-1}, $T = 150(2)$ K. 32135 data (26166 unique, $R_{int} = 0.0840$, $2.97 < \theta < 25.63°$), were collected on a Siemens SMART CCD diffractometer using narrow frames (0.3° in ω), and were corrected semiempirically for absorption and incident beam decay (transmission 1.00–0.65). The structure was solved by direct methods and refined by full-matrix least-squares on F^2 values of all data (G. M. Sheldrick, SHELXTL manual, Siemens Analytical X-ray Instruments, Madison WI, USA, 1994, version 5) to give $wR = \{\Sigma[w(F_o^2-F_c^2)^2]/\Sigma[w(F_o^2)^2]\}^{1/2} = 0.4326$, conventional $R = 0.2057$ for F values of 26166 reflections with $F_o^2 > 2\sigma(F_o^2)$, $S = 2.443$ for 717 parameters. Residual electron density extremes were 2.40 and -1.30 eÅ^{-3}. Amide hydrogen atoms were refined isotropically with the remainder constrained; anisotropic displacement parameters were used for all non-hydrogen atoms.

([2](1,7,14,20-Tetraaza-2,6,15,19-tetraoxo-3,5,9,12,16,18,22,25 tetrabenzocyclohexacosane)-(*N,N'-bis*-(2,2-diphenylethyl)suberamide)-rotaxane, (34)

Selected data for ([2](1,7,14,20-Tetraaza-2,6,15,19-tetraoxo-3,5,9,12,16,18,22,25 tetrabenzocyclohexacosane)-(*N,N'-bis*-(2,2-diphenylethyl)suberamide)-rotaxane, 34: Yield 331 mg (17 %); m.p. 242 °C; ^{1}H NMR (400 MHz, CDCl$_3$): $\delta = 8.13$ (s, 2H, Ar$\underline{H}_C$), 8.11-8.08 (m, 4H, Ar$\underline{H}_B$), 7.55 (br t, 4H, N$\underline{H}_D$), 7.52 (t, $J = 8.1$ Hz, 2H,

Ar$\underline{H}_A$), 7.32-7.21 (m, 20H, Ar$\underline{H}$-stopper), 7.04 (s, 8H, Ar$\underline{H}_F$), 5.97 (br t, 2H, N$\underline{H}_c$), 4.50 (d, 8H, J = 5.6 Hz, C$\underline{H}_E$), 4.10 (t, 2H, J = 7.8 Hz, C$\underline{H}_a$), 3.67-3.60 (m, 4H, C$\underline{H}_b$), 1.02 (t, 4H, J = 7.6 Hz, C$\underline{H}_d$), 0.65-0.55 (m, 4H, C$\underline{H}_e$), 0.36-0.22 (m, 4H, C$\underline{H}_f$); ^{13}C NMR (100 MHz, CDCl$_3$): δ = 174.2 (s, NH$\underline{C}$O), 166.5 (s, NH$_D\underline{C}$O), 142.0 (s, Ar$\underline{C}$-ipso-stopper), 137.6 (s, Ar$\underline{C}$-ipso-xylylene), 133.9 (s, Ar$\underline{C}$-ipso-isophthaloyl), 131.4 (d, Ar$\underline{C}_B$), 129.1 (d, Ar$\underline{C}_F$), 128.8 (d, Ar$\underline{C}_A$), 128.1 (d, Ar$\underline{C}$-stopper), 126.9 (d, Ar$\underline{C}$-stopper), 124.7 (d, Ar$\underline{C}_C$), 50.2 (d, $\underline{C}$H$_a$), 44.3 (t, $\underline{C}$H$_b$), 44.0 (t, $\underline{C}$H$_E$), 35.4 (t, $\underline{C}$H$_d$), 27.6 (t, $\underline{C}$H$_e$), 24.0 (t, $\underline{C}$H$_f$); HRMS (FAB+ THIOG matrix): calcd for C$_{68}$H$_{69}$N$_6$O$_6$ [(M+H)$^+$] 1065.5266. Found 1065.5280.

X-ray crystallographic structure determination, crystals of rotaxane grown in CDCl$_3$/ether, 34: C$_{68}$H$_{68}$N$_6$O$_6$, M = 1065.28, crystal size 0.15 × 0.12 × 0.10 mm, monoclinic, $P2_1/c$, a = 10.10930(10), b = 24.2595(4), c = 22.8433(2) Å, β = 90.0710(10)°, V = 5602.24(12) Å^3, Z = 4, ρ_{calcd} = 1.263 Mg m^{-3}; Mo$_{K\alpha}$ radiation (graphite monochromator, λ = 0.71073 Å), μ = 0.081 mm^{-1}, T = 150(2) K. 55201 data (15270 unique, R_{int} = 0.0366, 1.78 < θ < 30.18°), were collected on a Siemens SMART CCD diffractometer using narrow frames (0.3° in ω), and were corrected semiempirically for absorption and incident beam decay. The structure was solved by direct methods and refined by full-matrix least-squares on F^2 values of all data (G. M. Sheldrick, SHELXTL manual, Siemens Analytical X-ray Instruments, Madison WI, USA, 1994, version 5) to give wR = $\{\Sigma[w(F_o^2-F_c^2)^2]/\Sigma[w(F_o^2)^2]\}^{1/2}$ = 0.1866, conventional R = 0.0699 for F values of 15270 reflections with $F_o^2 > 2\sigma(F_o^2)$, S = 1.078 for 763 parameters. Residual electron density extremes were 0.403 and –0.508 eÅ^{-3}. Amide hydrogen atoms were refined isotropically with the remainder constrained; anisotropic displacement parameters were used for all non-hydrogen atoms.

([2](1,7,14,20-Tetraaza-2,6,15,19-tetraoxo-3,5,9,12,16,18,22,25

tetrabenzocyclohexacosane)-(*N*,*N'*-*bis*-(2,2-diphenylethyl)azelamide)-rotaxane,

(35)

Selected data for ([2](1,7,14,20-Tetraaza-2,6,15,19-tetraoxo-3,5,9,12,16,18,22,25

tetrabenzocyclohexacosane)-(*N*,*N'*-*bis*-(2,2-diphenylethyl)azelamide)-rotaxane,

35: Yield 296 mg (15 %); m.p. 204 °C; ^{1}H NMR (400 MHz, CDCl$_3$): δ = 8.13 (d,

4H, J = 7.8 Hz, Ar$\underline{H}_B$), 8.10 (s, 2H, Ar$\underline{H}_C$), 7.52-7.45 (br m, 6H, N$\underline{H}_D$ & Ar$\underline{H}_A$),

7.33-7.21 (m, 20H, Ar$\underline{H}$-stopper), 7.03 (s, 8H, Ar$\underline{H}_F$), 6.06 (br t, 2H, N$\underline{H}_c$), 4.49 (d,

8H, J = 5.3 Hz, C$\underline{H}_E$), 4.10 (t, 2H, J = 7.8 Hz, C$\underline{H}_a$), 3.65 (dd, 4H, J = 7.8 Hz, J =5.6

Hz, C$\underline{H}_b$), 1.12 (t, 4H, J = 8.1 Hz, C$\underline{H}_d$), 0.78-0.72 (m, 4H, J = 8.1 Hz, C$\underline{H}_e$), 0.53-

0.46 (m, 4H, C$\underline{H}_f$), 0.34-0.24 (m, 2H, C$\underline{H}_g$); ^{13}C NMR (100 MHz, CDCl$_3$): δ = 174.2

(s, NH$\underline{C}$O), 166.4 (s, NH$_D\underline{C}$O), 142.1 (s, Ar$\underline{C}$-ipso-stopper), 137.6 (s, Ar$\underline{C}$-ipso-

xylylene), 133.8 (s, Ar$\underline{C}$-ipso-isophthaloyl), 131.3 (d, Ar$\underline{C}_B$), 129.1 (d, Ar$\underline{C}_F$), 128.8

(d, Ar$\underline{C}_A$), 128.7 (d, Ar$\underline{C}$-stopper) 128.1 (d, Ar$\underline{C}$-stopper), 126.9 (d, Ar$\underline{C}$-stopper),

124.8 (d, Ar$\underline{C}_C$), 50.1 (d, $\underline{C}$H$_a$), 44.4 (t, $\underline{C}$H$_b$), 44.1 (t, $\underline{C}$H$_E$), 35.2 (t, $\underline{C}$H$_d$), 27.5 (t, -

$\underline{C}$H$_2$-), 26.7 (t, -$\underline{C}$H$_2$-), 23.9 (t, -$\underline{C}$H$_2$-); HRMS (FAB+ THIOG matrix): calcd for

C$_{69}$H$_{71}$N$_6$O$_6$ [(M+H)$^+$] 1079.5439. Found 1079.5435.

X-ray crystallographic structure determination, crystals of rotaxane grown in

CHCl$_3$/ether, 35: C$_{69}$H$_{70}$N$_6$O$_6$, M = 1079.31, crystal size 0.20 × 0.18 × 0.15 mm,

monoclinic, $P2_1/c$, a = 10.2440(2), b = 24.234, c = 23.2044(5) Å, β = 92.4800(10)°,

$V = 5755.19(17)$ A^3, $Z = 4$, $\rho_{calcd} = 1.246$ Mg m^{-3}; Mo$_{K\alpha}$ radiation (graphite monochromator, $\lambda = 0.71073$ Å), $\mu = 0.080$ mm^{-1}, $T = 180(2)$ K. 34761 data (13923 unique, $R_{int} = 0.01673$, $1.76 < \theta < 29.09°$), were collected on a Siemens SMART CCD diffractometer using narrow frames ($0.3°$ in ω), and were corrected semiempirically for absorption and incident beam decay. The structure was solved by direct methods and refined by full-matrix least-squares on F^2 values of all data (G. M. Sheldrick, SHELXTL manual, Siemens Analytical X-ray Instruments, Madison WI, USA, 1994, version 5) to give $wR = \{\Sigma[w(F_o^2-F_c^2)^2]/\Sigma[w(F_o^2)^2]\}^{1/2} = 0.2355$, conventional $R = 0.1247$ for F values of 13923 reflections with $F_o^2 > 2\sigma(F_o^2)$, $S = 1.012$ for 754 parameters. Residual electron density extremes were 0.425 and -0.309 eÅ^{-3}. Amide hydrogen atoms were refined isotropically with the remainder constrained; anisotropic displacement parameters were used for all non-hydrogen atoms.

([2](1,7,14,20-Tetraaza-2,6,15,19-tetraoxo-3,5,9,12,16,18,22,25 tetrabenzocyclohexacosane)-(N,N'-bis-(2,2-diphenylethyl)sebacamide)-rotaxane, (36)
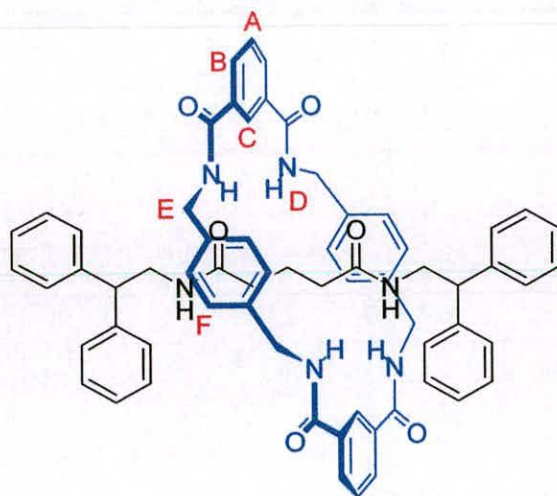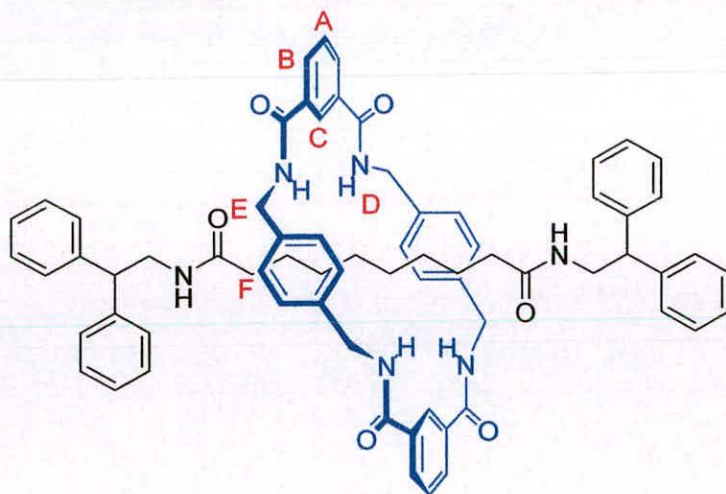

Selected data for ([2](1,7,14,20-Tetraaza-2,6,15,19-tetraoxo-3,5,9,12,16,18,22,25 tetrabenzocyclohexacosane)-(N,N'-bis-(2,2-diphenylethyl)sebacamide)-rotaxane, 36: Yield 351 mg (18 %); m.p. 249 °C; ^{1}H NMR (400 MHz, C$_2$D$_2$Cl$_4$): $\delta = 8.14$ (br s,

2H, Ar$\underline{H}_C$), 8.12 (br s, 4H, Ar$\underline{H}_B$), 7.59 (br s, 4H, N$\underline{H}_D$), 7.55 (br t, 4H, J = 7.8 Hz, Ar$\underline{H}_B$), 7.33-7.22 (m, 20H, Ar$\underline{H}$-stopper), 7.04 (s, 8H, Ar$\underline{H}_F$), 6.21 (br t, 2H, N$\underline{H}_c$), 4.48 (d, 8H, J = 5.3 Hz, C$\underline{H}_E$), 4.10 (t, 2H, J = 7.8 Hz, C$\underline{H}_a$), 3.66 (m, 4H, C$\underline{H}_b$), 1.21-1.10 (m, 4H, C$\underline{H}_d$), 0.85-0.76 (m, 4H, C$\underline{H}_e$), 0.63-0.54 (m, 4H. C$\underline{H}_f$), 0.51-0.46 (m, 4H, C$\underline{H}_g$); ^{13}C NMR (100 MHz, CDCl$_3$): δ = 174.2 (s, NH$\underline{C}$O) 166.4 (s, NH$_D\underline{C}$O), 142.1 (s, Ar$\underline{C}$-ipso-stopper), 137.6 (s, Ar$\underline{C}$-ipso-xylylene), 133.9 (s, Ar$\underline{C}$-ipso-isophthaloyl), 131.3 (d, Ar$\underline{C}_B$), 129.1 (d, Ar$\underline{C}_F$), 128.8 (d, Ar$\underline{C}_A$), 128.7 (d, Ar$\underline{C}$-stopper), 128.3 (d, Ar$\underline{C}$-stopper), 126.9 (d, Ar$\underline{C}$-stopper), 124.8 (d, Ar$\underline{C}_C$), 50.1 (d, $\underline{C}$H$_a$), 44.4 (t, $\underline{C}$H$_b$), 44.1 (t, $\underline{C}$H$_E$), 35.2 (t, $\underline{C}$H$_d$), 27.6 (t, -$\underline{C}$H$_2$-), 26.8 (t, -$\underline{C}$H$_2$-), 24.0 (t, -$\underline{C}$H$_2$-); HRMS (FAB+ THIOG matrix): calcd for C$_{67}$H$_{67}$N$_6$O$_6$ [(M+H)$^+$] 1093.5580. Found 1093.5592.

X-ray crystallographic structure determination, crystals of rotaxane 36 grown in C$_2$H$_2$Cl$_4$/ether: C$_{70}$H$_{72}$N$_6$O$_6$, M = 1093.34, crystal size 0.08 × 0.07 × 0.05 mm, triclinic, P-1, a = 8.1440(8), b = 10.5732(10), c = 17.8480(17) Å, α = 105.545(2), β = 98.001(2), γ = 99.427(2)°, V = 1433.3(2) Å^3, Z = 1, ρ_{calcd} = 1.267 Mg m^{-3}; synchrotron radiation (CCLRC Daresbury Laboratory Station 9.8, silicon monochromator, λ = 0.68950 Å), μ = 0.081 mm^{-1}, T = 150(2) K. 11416 data (5454 unique, R_{int} = 0.0471, 1.98 < θ < 25.00°), were collected on a Siemens SMART CCD diffractometer using narrow frames (0.3° in ω), and were corrected semiempirically for absorption and incident beam decay (transmission 1.00–0.77). The structure was solved by direct methods and refined by full-matrix least-squares on F^2 values of all data (G. M. Sheldrick, SHELXTL manual, Siemens Analytical X-ray Instruments, Madison WI, USA, 1994, version 5) to give wR = $\{\Sigma[w(F_o^2-F_c^2)^2]/\Sigma[w(F_o^2)^2]\}^{1/2}$ = 0.2176, conventional R = 0.1001 for F values of 5454 reflections with $F_o^2 > 2\sigma(F_o^2)$, S = 1.200 for 382 parameters. Residual electron density extremes were 0.740 and –0.387 eÅ^{-3}. Amide hydrogen atoms were refined isotropically with the remainder constrained; anisotropic displacement parameters were used for all non-hydrogen atoms.
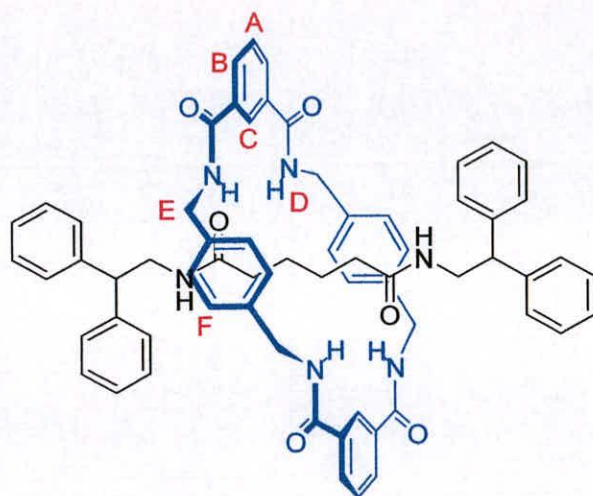
([2](1,7,14,20-Tetraaza-2,6,15,19-tetraoxo-3,5,9,12,16,18,22,25 tetrabenzocyclohexacosane)-(*N,N'-bis*-(2,2-diphenylethyl)decanamide)-rotaxane, (37)
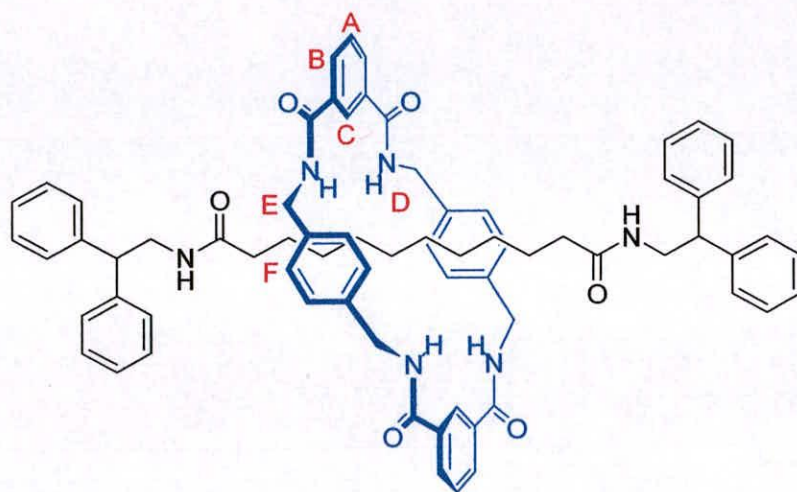
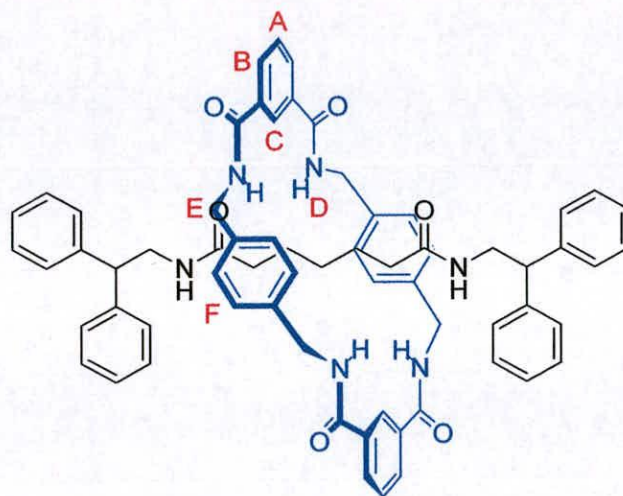**Selected data for ([2](1,7,14,20-Tetraaza-2,6,15,19-tetraoxo-3,5,9,12,16,18,22,25 tetrabenzocyclohexacosane)-(*N,N'-bis*-(2,2-diphenylethyl)decanamide)-rotaxane, 37:** Yield 229 mg (12 %). m.p. 218-219 °C; ^{1}H NMR (400 MHz, d_6-DMSO): δ = 8.91 (t, 4H, J = 5.8 Hz, N$\underline{H}_D$), 8.12 (s, 2H, Ar$\underline{H}_C$), 7.94 (dd, 4H, J = 7.8 Hz, J = 1.3 Hz, Ar$\underline{H}_B$), 7.57 (t, 4H, J = 5.6 Hz, Ar$\underline{H}_A$), 7.52 (t, 2H, J = 7.7 Hz, N$\underline{H}_c$), 7.34–7.19 (m, 20H, Ar$\underline{H}$-stopper), 7.01 (s, 8H, Ar$\underline{H}_F$), 4.33 (d, 8H, J = 5.7 Hz, C$\underline{H}_E$), 4.16 (t, 2H, J = 7.8 Hz, C$\underline{H}_a$), 3.67-3.63 (m, 4H, C$\underline{H}_b$), 1.34-1.30 (m, 4H, C$\underline{H}_d$), 0.75-0.72 (m, 4H, C$\underline{H}_e$), 0.39-0.32 (m, 12H, -C$\underline{H}_2$-alkyl); ^{13}C NMR (100 MHz, CDCl$_3$): δ = 173.4 (s, NH$\underline{C}$O) 165.9 (s, NH$_D\underline{C}$O), 143.2 (s, Ar$\underline{C}$-ipso-stopper), 138.2 (s, Ar$\underline{C}$-ipso-xylylene), 134.9 (s, Ar$\underline{C}$-ipso-isophthaloyl), 129.9 (d, Ar$\underline{C}_B$), 128.7 (d, Ar$\underline{C}_F$), 128.5 (d, Ar$\underline{C}_A$), 128.4 (d, Ar$\underline{C}$-stopper), 128.2 (d, Ar$\underline{C}$-stopper), 126.8 (d, Ar$\underline{C}$-stopper) 126.6 (d, Ar$\underline{C}_C$), 50.4 (d, $\underline{C}$H$_a$), 43.9 (t, $\underline{C}$H$_E$), 43.0 (t, $\underline{C}$H$_b$), 35.1 (t, $\underline{C}$H$_d$), 28.8 (t, -$\underline{C}$H$_2$-), 28.7 (t, -$\underline{C}$H$_2$-), 28.5 (t, -$\underline{C}$H$_2$-), 25.0 (t, -$\underline{C}$H$_2$-); LRMS (FAB+ mNBA matrix) m/z (rel. int.): 1122 (12.6 %) [(M+H)$^+$], HRMS (FAB, mNBA matrix): calcd for C$_{72}$H$_{77}$N$_6$O$_6$ [(M+H)$^+$] 1121.5905. Found 1121.5938.

X-ray crystallographic structure determination, crystals of rotaxane grown in CHCl₃/ether, 37: $C_{72}H_{76}N_6O_6$, $M = 1121.39$, crystal size $0.12 \times 0.05 \times 0.05$ mm, triclinic, $P\text{-}1$, $a = 8.5024(9)$, $b = 10.4249(11)$, $c = 17.5264(19)$ Å, $\alpha = 99.719(2)$, $\beta = 100.927(2)$, $\gamma = 99.733(2)°$, $V = 1470.6(3)$ Å^3, $Z = 1$, $\rho_{calcd} = 1.266$ Mg m^{-3}; synchrotron radiation (CCLRC Daresbury Laboratory Station 9.8, silicon monochromator, $\lambda = 0.68830$ Å), $\mu = 0.081$ mm^{-1}, $T = 150(2)$ K. 14617 data (7777 unique, $R_{int} = 0.0310$, $2.07 < \theta < 29.21°$), were collected on a Siemens SMART CCD diffractometer using narrow frames ($0.3°$ in ω), and were corrected semiempirically for absorption and incident beam decay (transmission 1.00–0.77). The structure was solved by direct methods and refined by full-matrix least-squares on F^2 values of all data (G. M. Sheldrick, SHELXTL manual, Siemens Analytical X-ray Instruments, Madison WI, USA, 1994, version 5) to give $wR = \{\Sigma[w(F_o^2 - F_c^2)^2]/\Sigma[w(F_o^2)^2]\}^{1/2} = 0.1435$, conventional $R = 0.0565$ for F values of 7777 reflections with $F_o^2 > 2\sigma(F_o^2)$, $S = 0.957$ for 391 parameters. Residual electron density extremes were 0.600 and -0.296 eÅ^{-3}. Amide hydrogen atoms were refined isotropically with the remainder constrained; anisotropic displacement parameters were used for all non-hydrogen atoms.

([2](1,7,14,20-Tetraaza-2,6,15,19-tetraoxo-3,5,9,12,16,18,22,25 tetrabenzocyclohexacosane)-(N,N'-bis-(2,2-diphenylethyl)dodecanamide)-rotaxane, (38)
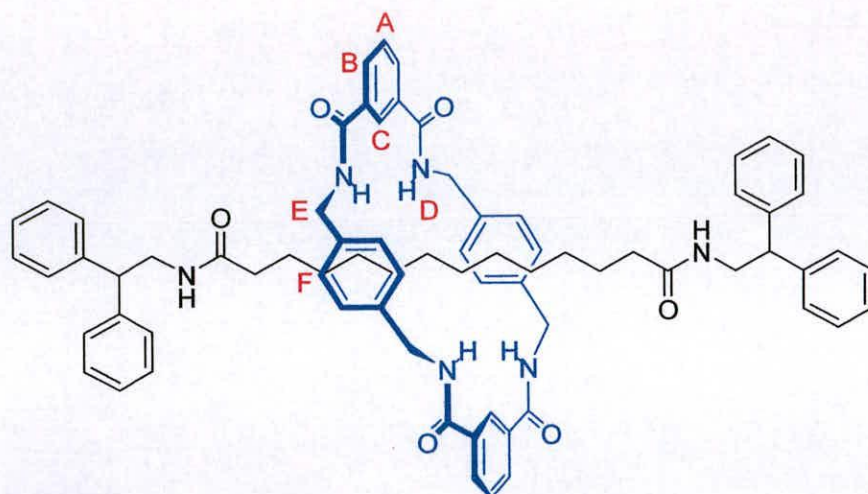
Selected data for ([2](1,7,14,20-Tetraaza-2,6,15,19-tetraoxo-3,5,9,12,16,18,22,25 tetrabenzocyclohexacosane)-(*N,N'-bis*-(2,2-diphenylethyl)dodecanamide) rotaxane, 38: Yield 186 mg (10 %); m.p. 201 °C; ^{1}H NMR (400 MHz, CDCl$_3$): δ = 8.18 (s, 2H, ArH$_C$), 8.16-8.11 (m, 4H, ArH$_B$), 7.57 (t, 2H, J = 8.1 Hz, ArH$_A$), 7.31-7.19 (m, 24H, ArH-stopper & NH$_D$), 7.01 (s, 8H, ArH$_F$), 6.11 (br t, 2H, NH$_e$), 4.49 (d, 8H, J = 5.1 Hz, CH$_E$), 4.11 (t, 2H, J = 7.8 Hz, CH$_a$), 3.63 (dd, 4H, J = 7.8 Hz, J = 5.6 Hz, CH$_b$), 1.29 (t, 4H, J = 7.6 Hz, CH$_d$), 1.03-0.92 (m, 4H, CH$_e$), 0.95 (br s, 8H, -CH$_2$-alkyl); ^{13}C NMR (100 MHz, CDCl$_3$): δ = 174.1 (s, NHCO), 166.2 (s, NH$_D$CO), 142.2 (s, ArC-ipso-stopper), 137.5 (s, ArC-ipso-xylylene), 133.8 (s, ArC-ipso-isophthaloyl), 131.0 (d, ArC$_B$), 129.2 (d, ArC$_F$), 128.7 (d, ArC$_A$), 128.6 (d, ArC-stopper), 128.1 (d, ArC-stopper), 126.8 (d, ArC-stopper), 124.9 (d, ArC$_C$), 50.0 (d, CH$_a$), 44.4 (t, CH$_b$), 44.2 (t, CH$_E$), 35.6 (t, CH$_d$), 28.6 (t, -CH$_2$-), 28.6 (t, -CH$_2$-), 28.4 (t, -CH$_2$-), 24.7 (t, -CH$_2$-); HRMS (FAB+, mNBA matrix): calcd for C$_{74}$H$_{81}$N$_6$O$_6$: [(M+H)$^+$] 1149.6218. Found 1149.6210.

X-ray crystallographic structure determination, crystals of rotaxane grown in CHCl$_3$/ether, 38: C$_{74}$H$_{80}$N$_6$O$_6$, M = 1149.44, crystal size 0.10 × 0.05 × 0.05 mm, monoclinic, $P2_1/c$, a = 11.4490(18), b = 8.8620(14), c = 31.166(5) Å, β = 94.141(4)°, V = 3153.9(9) Å^3, Z = 2, ρ_{calcd} = 1.210 Mg m^{-3}; synchrotron radiation (CCLRC

Daresbury Laboratory Station 9.8, silicon monochromator, $\lambda = 0.68950$ Å), $\mu = 0.077$ mm^{-1}, $T = 150(2)$ K. 10273 data (3210 unique, $R_{int} = 0.0846$, $2.07 < \theta < 20.00°$), were collected on a Siemens SMART CCD diffractometer using narrow frames ($0.3°$ in ω), and were corrected semi-empirically for absorption and incident beam decay. The structure was solved by direct methods and refined by full-matrix least-squares on F^2 values of all data (G. M. Sheldrick, SHELXTL manual, Siemens Analytical X-ray Instruments, Madison WI, USA, 1994, version 5) to give $wR = \{\Sigma[w(F_o^2 - F_c^2)^2]/\Sigma[w(F_o^2)^2]\}^{1/2} = 0.2654$, conventional $R = 0.1046$ for F values of 3210 reflections with $F_o^2 > 2\sigma(F_o^2)$, $S = 1.142$ for 393 parameters. Residual electron density extremes were 0.563 and -0.765 eÅ^{-3}. Amide hydrogen atoms were refined isotropically with the remainder constrained; anisotropic displacement parameters were used for all non-hydrogen atoms.

([2](1,7,14,20-Tetraaza-2,6,15,19-tetraoxo-3,5,9,12,16,18,22,25 tetrabenzocyclohexacosane)-(*N*,*N'*-bis-(2,2-diphenylethyl)tetradecanamide)- rotaxane, (39)
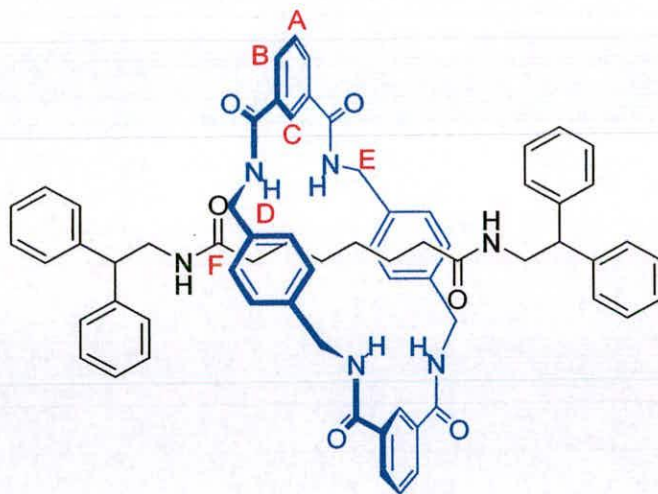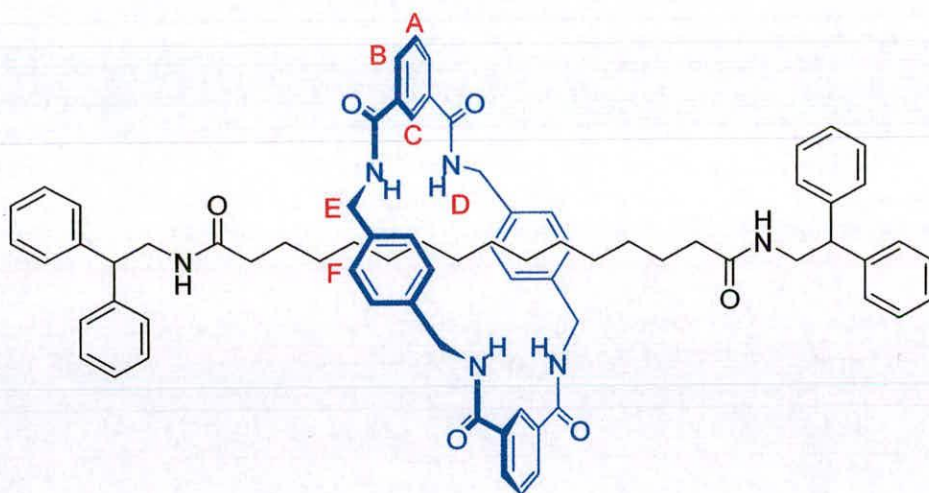

Selected data for ([2](1,7,14,20-Tetraaza-2,6,15,19-tetraoxo-3,5,9,12,16,18,22,25 tetrabenzocyclohexacosane)-(*N*,*N'*-bis-(2,2-diphenylethyl)tetradecanamide) rotaxane, 39: Yield 183 m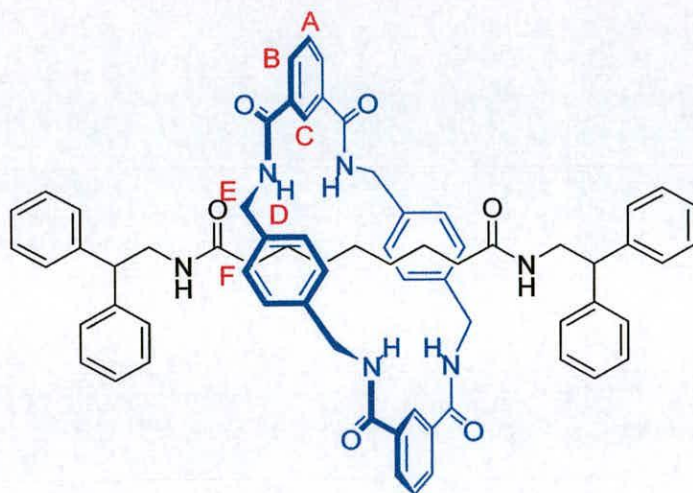g (10 %); m.p. 163 °C; ^{1}H NMR (400 MHz, CDCl$_3$): $\delta = 8.17$ (s, 2H, ArH$_C$), 8.15-8.10 (m, 4H, ArH$_B$), 7.57 (t, 2H, $J = 7.8$ Hz, ArH$_A$), 7.30-7.18 (m, 24H, ArH-stopper, & NH$_D$), 7.01 (s, 8H, ArH$_F$), 6.05 (br t, 2H, NH$_C$), 4.49

(d, 8H, J = 5.1 Hz, C$\underline{H}_E$), 4.09 (t, 2H, J = 7.8 Hz, C$\underline{H}_a$), 3.61 (dd, 4H, J = 7.8 Hz, J = 5.6 Hz, C$\underline{H}_b$), 1.29-1.20 (m, 4H, C$\underline{H}_d$), 1.12-1.10 (m, 4H, C$\underline{H}_f$), 1.02-0.92 (m, 12H, -C$\underline{H}_2$-alkyl), 0.87-0.83 (m, 4H, -C$\underline{H}_2$-alkyl), 0.77-0.73 (m, 4H, -C$\underline{H}_2$-alkyl); ^{13}C NMR (100 MHz, CDCl$_3$): δ = 174.0 (s, NH$\underline{C}$O), 166.1 (s, NH$_D\underline{C}$O), 142.2 (s, Ar$\underline{C}$-ipso-stopper), 137.5 (s, Ar$\underline{C}$-ipso-xylylene), 133.8 (s, Ar$\underline{C}$-ipso-isophthaloyl), 131.0 (d, Ar$\underline{C}_B$), 129.2 (d, Ar$\underline{C}_F$), 128.7 (d, Ar$\underline{C}_A$), 128.6 (d, Ar$\underline{C}$-stopper), 128.1 (d, Ar$\underline{C}$-stopper), 126.8 (d, Ar$\underline{C}$-stopper), 124.8 (d, Ar$\underline{C}_C$), 50.1 (d, $\underline{C}$H$_a$), 44.4 (t, $\underline{C}$H$_b$) 44.2 (t, $\underline{C}$H$_E$), 35.7 (t, $\underline{C}$H$_d$), 29.2 (t, -$\underline{C}$H$_2$-), 29.1 (t, -$\underline{C}$H$_2$-), 29.0 (t, -$\underline{C}$H$_2$-), 28.8 (t, -$\underline{C}$H$_2$-), 24.8 (t, -$\underline{C}$H$_2$-); HRMS (FAB+, mNBA matrix): calcd for C$_{76}$H$_{85}$N$_6$O$_6$: [(M+H)$^+$] 1177.6531. Found 1177.6532.

X-ray crystallographic structure determination, crystals of rotaxane grown in CHCl$_3$/ether, 39: C$_{78}$H$_{86}$Cl$_3$N$_6$O$_6$, M = 1309.88, crystal size 0.12 × 0.08 × 0.05 mm, monoclinic, $P2_1/c$, a = 20.5947(5), b = 9.2683(2), c = 19.1134(4) Å, β = 92.3500(10)°, V = 3645.26(14) A^3, Z = 2, ρ_{calcd} = 1.193 Mg m^{-3}; Mo$_{K\alpha}$ radiation (graphite monochromator, λ = 0.71073 Å), μ = 0.181 mm^{-1}, T = 180(2) K. 22137 data (8833 unique, R_{int} = 0.0607, 1.98 < θ < 29.16°), were collected on a Siemens SMART CCD diffractometer using narrow frames (0.3° in ω), and were corrected semiempirically for absorption and incident beam decay. The structure was solved by direct methods and refined by full-matrix least-squares on F^2 values of all data (G. M. Sheldrick, SHELXTL manual, Siemens Analytical X-ray Instruments, Madison WI, USA, 1994, version 5) to give wR = $\{\Sigma[w(F_o^2-F_c^2)^2]/\Sigma[w(F_o^2)^2]\}^{1/2}$ = 0.2063, conventional R = 0.0739 for F values of 8833 reflections with $F_o^2 > 2\sigma(F_o^2)$, S = 1.025 for 445 parameters. Residual electron density extremes were 0.534 and –0.549 eÅ^{-3}. Amide hydrogen atoms were refined isotropically with the remainder constrained; anisotropic displacement parameters were used for all non-hydrogen atoms.

[(2,2-Diphenyl-ethylcarbomoyl)-methyl]-carbamic acid *tert*-butyl ester (S8)
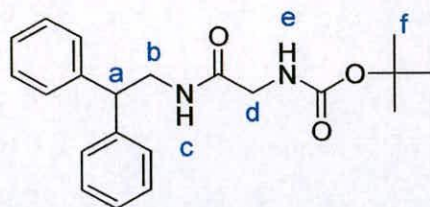
HOBt (2.32 g, 17.1 mmol) was added in one portion to a stirred solution of Boc-glycine (2.00 g, 11.4 mmol), triethylamine (3.98 mL, 28.6 mmol) in dichloromethane (120 mL) at 0 °C. The reaction mixture was stirred at 0 °C for 10 min and then EDCI (3.29 g, 17.1 mmol) was added in one portion to the reaction mixture. The reaction mixture was stirred for a further 20 min at which time 2,2-diphenylethylamine (1.74 g, 13.7 mmol) was added in one portion at 0 °C. The reaction mixture was then stirred at room temperature for 14 h. The reaction mixture was washed with 1 M aqueous hydrochloric acid (3 x 20 mL), saturated aqueous sodium hydrogen carbonate (3 x 20 mL) and saturated aqueous sodium chloride (2 x 20 mL), dried (MgSO$_4$) and concentrated under reduced pressure to give **S8** as a colorless solid. Yield 3.39 g (84 %); m.p. 130-133 °C; ^{1}H NMR (400 MHz, CDCl$_3$): δ = 7.34-7.22 (m, 10H, Ar$\underline{H}$), 5.94 (br s, 1H, N$\underline{H}_c$), 4.95 (br s, 1H, N$\underline{H}_e$), 4.18 (t, 1H, J = 7.8 Hz, C$\underline{H}_a$), 3.93 (dd, 2H, J = 5.9 Hz, J = 7.6 Hz, C$\underline{H}_b$), 3.69 (d, 2H, J = 5.9 Hz, C$\underline{H}_d$), 1.39 (s, 9H, C$\underline{H}_f$); ^{13}C NMR (100 MHz, CDCl$_3$): δ = 169.3 (s, N$\underline{H}_c$CO), 141.6 (s, Ar$\underline{C}$-ipso), 128.7 (d, Ar$\underline{C}$), 127.9 (d, Ar$\underline{C}$), 126.8 (d, Ar$\underline{C}$), 50.4 (d, $\underline{C}$H$_a$), 44.2 (s, $\underline{C}$(CH$_3$)$_3$), 43.6 (t, $\underline{C}$H$_d$), 28.2 (q, C($\underline{C}$H$_3$)$_3$); LRMS (FAB+ mNBA matrix) *m/z* (rel. int.): 355 (77.4 %) [(M+H)$^+$], HRMS (FAB+) calcd for C$_{21}$H$_{27}$N$_2$O$_3$ [(M+H)$^+$] 355.2022. Found 355.2024.

2-Amino-*N*-(2,2-diphenyl-ethyl)-acetamide (S9)
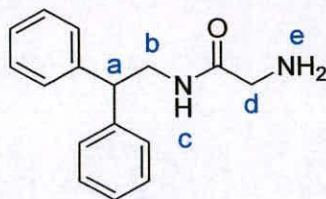
Acetyl chloride (1.20 mL, 17.0 mmol) was added dropwise to a stirred solution of **S8** (2.00 g, 5.65 mmol) in methanol (30 mL) at 0 °C. The reaction mixture was stirred at 0 °C for 2 h and at room temperature for 6 h. The reaction mixture was concentrated under reduced pressure. The remaining residue was partitioned between saturated aqueous sodium hydrogen carbonate and chloroform and stirred vigorously for 2 h and the layers were separated. The organic layer was dried (MgSO$_4$) and concentrated under reduced pressure to give **S9** as a colorless solid. Yield 1.40 g (99 %); m.p. 210-212 °C (decomp); ^{1}H NMR (400 MHz, d_6-DMSO): δ = 8.47 (t, 1H, J = 5.0 Hz, N$\underline{H}_c$), 8.00 (br s, 2H, NH$_e$), 7.32-7.20 (m, 10H, Ar$\underline{H}$), 4.19 (t, 1H, J = 7.8 Hz, C$\underline{H}_a$), 3.81-3.77 (m, 2H, C$\underline{H}_b$), 3.44 (s, 2H, CH$_d$); ^{13}C NMR (100 MHz, CDCl$_3$): δ = 166.5 (s, NH$\underline{C}$O), 143.0 (s, Ar$\underline{C}$-ipso), 128.8 (d, Ar$\underline{C}$), 128.1 (d, Ar$\underline{C}$), 126.8 (d, Ar$\underline{C}$), 50.4 (d, $\underline{C}$H$_a$), 43.6 (t, $\underline{C}$H$_d$); LRMS (FAB+ mNBA matrix) m/z (rel. int.): 255 (100 %) [(M+H)$^+$], HRMS (FAB+) calcd for C$_{16}$H$_{19}$N$_2$O [(M+H)$^+$] 255.1497. Found 255.1494.

Dodecanedioic acid *bis*-{[(2,2-diphenyl-ethylcarbamoyl)-methyl]-amide} (S10)
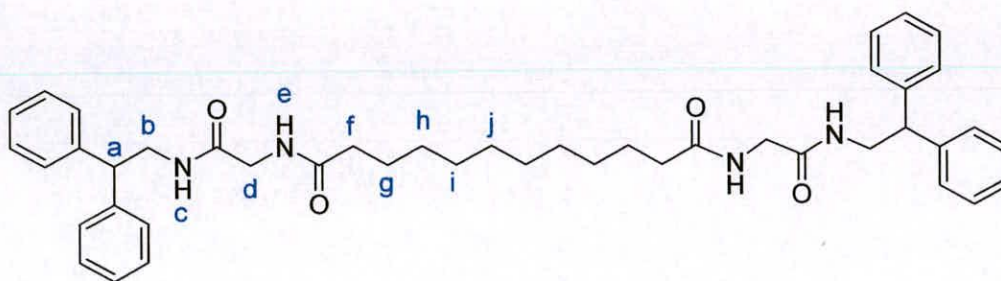
Dodecanoyl dichloride (937 µL in dichloromethane (10 mL), 3.75 mmol) was added dropwise over 10 min to a stirred solution of **S9** (2.00 g, 7.87 mmol) and triethylamine (1.65 mL, 11.8 mmol) in dichloromethane (10 mL) at 0 °C. The

reaction mixture was allowed to warm to room temperature and stirred for 16 h. The resulting mixture was washed with 1 M aqueous hydrochloric acid (2 x 10 mL), saturated aqueous sodium hydrogen carbonate (2 x 10 mL), saturated aqueous sodium chloride (10 mL), dried (MgSO$_4$) and concentrated under reduced pressure to give **S10** as a colorless solid. Yield 4.09 g (74 %); m.p. 130-131 °C; ^{1}H NMR (400 MHz, CDCl$_3$): 7.29-7.20 (m, 20H, Ar$\underline{H}$-stopper), 6.48 (t, 2H, J = 5.1 Hz, N$\underline{H}$CO), 6.37 (t, 2H, J = 5.1 Hz, N$\underline{H}$CO), 4.17 (t, 2H, J = 7.8 Hz, C$\underline{H}_a$), 3.89 (dd, 4H, J = 5.1 Hz, J = 7.8 Hz, C$\underline{H}_b$), 3.73 (d, 4H, J = 5.1 Hz, C$\underline{H}_d$), 2.15 (t, 4H, J = 7.3 Hz, C$\underline{H}_d$), 1.28 (br s, 16H, -C$\underline{H}_2$-alkyl); ^{13}C NMR (100 MHz, d_6-DMSO): δ = 172.8 (s, NH$\underline{C}$O), 169.4 (s, NH$\underline{C}$O), 143.1 (s, Ar$\underline{C}$-ipso-stopper), 128.7 (d, Ar$\underline{C}$-stopper), 128.2 (d, Ar$\underline{C}$-stopper), 126.6 (d, Ar$\underline{C}$-stopper), 50.4 (d, $\underline{C}H_a$), 43.4 (t, $\underline{C}H_b$), 42.2 (t, $\underline{C}H_d$), 35.3 (t, $\underline{C}H_f$), 29.2 (t, -$\underline{C}H_2$-), 29.1 (t, -$\underline{C}H_2$-), 29.0 (t, -$\underline{C}H_2$-), 25.4 (t, -$\underline{C}H_2$-); LRMS (FAB+ mNBA matrix) m/z (rel. int.): 703 (81.4 %) [(M+H)$^+$], HRMS (FAB+) calcd for C$_{44}$H$_{55}$N$_4$O$_4$ [(M+H)$^+$] 703.4223. Found 703.4206.

([2](1,7,14,20-Tetraaza-2,6,15,19-tetraoxo-3,5,9,12,16,18,22,25 tetrabenzocyclohexacosane)- dodecanedioic acid *bis*-{[(2,2-diphenyl-ethylcarbamoyl) - methyl] -amide} (40)
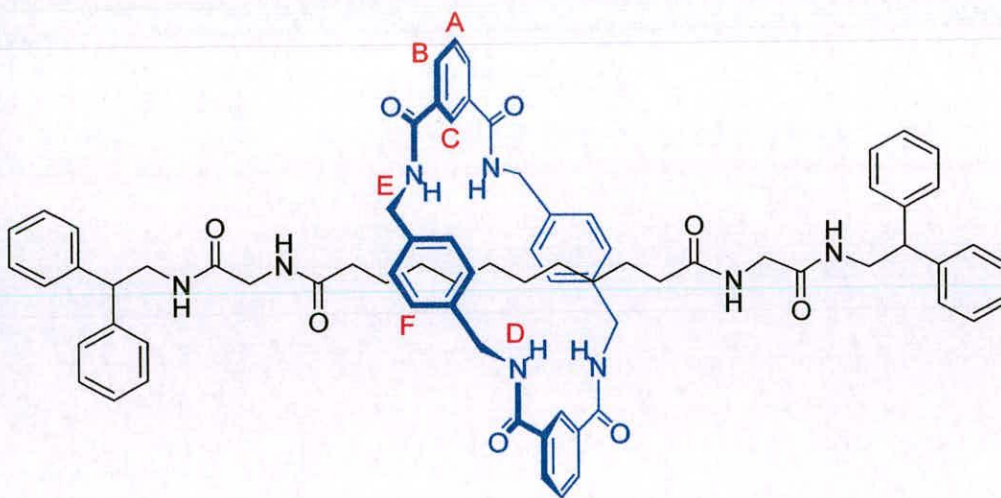
Selected data for ([2](1,7,14,20-Tetraaza-2,6,15,19-tetraoxo-3,5,9,12,16,18,22,25 tetrabenzocyclohexacosane)- dodecanedioic acid *bis*-{[(2,2-diphenyl-ethylcarbamoyl) - methyl] -amide}, (40): Yield 2.03 g (41 %); m.p. 181-182 °C;

^{1}H NMR (400 MHz, CDCl$_3$): 8.35 (s, 2H, ArH$_C$), 8.13 (dd, 4H, J = 6.6 Hz, J = 1.5 Hz, ArH$_B$), 7.60-7.55 (m, 6H, NH$_D$ & ArH$_A$), 7.31-7.15 (m, 20H, ArH-stopper), 7.02 (s, 8H, ArH$_F$), 6.78 (br s, 2H, NH$_e$), 6.49 (t, 2H, J = 5.1 Hz, NH$_e$), 6.40 (t, 2H, J = 5.1 Hz, NH$_c$), 5.97 (br s, 2H, NH$_c$), 4.49 (d, 8H, J = 5.1 Hz, CH$_E$), 4.17 (t, 2H, J = 8.0 Hz, CH$_a$), 4.12 (t, 2H, J = 8.0 Hz, CH$_a$), 3.88 (dd, 4H, J = 8.0 Hz, J = 5.8 Hz, CH$_b$), 3.79 (dd, 4H, J = 7.8 Hz, J = 5.7 Hz, CH$_b$), 3.71 (d, 4H, J = 5.1 Hz, CH$_d$), 3.15 (br s, 4H, CH$_d$), 2.14 (t, 4H, J = 7.6 Hz, CH$_f$), 1.90 (t, 4H, J = 7.6 Hz, CH$_f$), 1.35-1.28 (m, 16H, -CH$_2$- alkyl), 1.18-1.10 (m, 16 H, -CH$_2$-alkyl); ^{13}C NMR (100 MHz, d_6-DMSO): δ = 173.5 (s, NHCO), 172.8 (s, NHCO), 169.4 (s, NHCO), 165.8 (s, NH$_D$CO), 143.1 (ArC-ipso-thread), 138.0 (s, ArC-ipso-xylylene), 134.3 (s, ArC-ipso-isophthaloyl), 130.3 (d, ArC$_B$), 129.0 (d, ArC$_F$), 128.7 (d, ArC$_A$), 128.2 (d, ArC-stopper), 128.1 (d, ArC-stopper), 126.6 (d, ArC-thread), 126.3 (d, ArC$_C$), 50.41 (d, CH$_a$), 50.37 (d, CH$_a$), 43.5 (t, CH$_d$), 43.4 (t, CH$_d$), 43.3 (t, CH$_E$), 42.2 (t, CH$_E$), 35.5 (t, CH$_f$), 34.9 (t, CH$_f$), 29.2 (t, -CH$_2$-), 29.1 (t, -CH$_2$-), 29.0 (t, -CH$_2$-), 28.9 (t, -CH$_2$-), 28.8 (t, -CH$_2$-), 28.6 (t, -CH$_2$-), 25.4 (t, -CH$_2$-), 25.0 (t, -CH$_2$-); LRMS (FAB+ mNBA matrix) m/z (rel. int.): 1235 (5.6 %) [(M+H)$^+$], HRMS (FAB+) calcd for C$_{76}$H$_{83}$N$_8$O$_8$ [(M+H)$^+$] 1235.6334. Found 1235.6299.

N,N'-dimethyl-N,N'-bis-(2,2-diphenyl)succinamide (42)
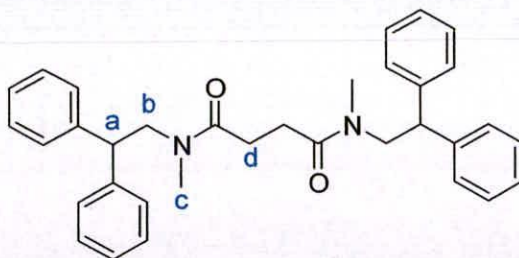
Selected data for *N,N'-dimethyl-N,N'-bis-(2,2-diphenyl)succinamide, 42*: Yield 2.00 g (76 %); m.p. 138-140 °C; ^{1}H NMR (400 MHz, CDCl$_3$): ratio *EE:EZ:ZZ*, = 2:1:1, δ = 7.31-7.19 (m, ArH-stopper), 4.29-4.22 (m, CH$_a$), 4.14-4.11 (m, CH$_a$), 4.02-3.96 (m, CH$_b$), 2.81 (s, CH$_c$), 2.75 (s, CH$_c$), 2,69 (s, CH$_c$), 2.65 (s, CH$_c$), 2.62 (s, CH$_c$), 2.31-2.21 (m, CH$_d$); ^{13}C NMR (100 MHz, CDCl$_3$): δ = 172.3 (s, CH$_c$NCO), 172.1 (s, CH$_c$NCO), 142.22 (s, ArC-ipso-stopper), 142.19 (s, ArC-ipso-stopper), 141.75 (s, ArC-stopper), 128.7 (d, ArC-stopper), 128.6 (d, ArC-stopper), 128.4 (d,

ArC-stopper), 128.22 (d, ArC-stopper), 128.15 (d, ArC-stopper), 128.1 (d, ArC-stopper), 126.9 (d, ArC-stopper), 126.55 (d, ArC-stopper), 126.53 (d, ArC-stopper), 55.2 (t, CH_b), 55.1 (t, CH_b), 53.5 (t, CH_b), 53.4 (t, CH_b), 49.9 (d, CH_a), 49.7 (d, CH_a), 49.1 (d, CH_a), 49.0 (d, CH_a), 36.4 (q, CH_c), 36.3 (q, CH_c), 34.5 (q, CH_c), 34.3 (q, CH_c), 28.9 (t, CH_d or CH_e), 28.6 (t, CH_d or CH_e), 27.8 (t, CH_d or CH_e), 27.6 (t, CH_d or CH_e); LRMS (FAB+ mNBA matrix) *m/z* (rel. int.): 505 (41.5 %) [(M+H)$^+$], HRMS (FAB+) calcd for $C_{34}H_{37}N_2O_2$ [(M+H)$^+$] 505.2855. Found 505.2873.

N,N'-dimethyl-*N,N'-bis*-(2,2-diphenyl)glutaramide (43)
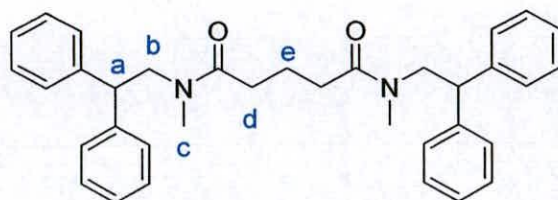
Selected data for *N,N'*-dimethyl-*N,N'-bis*-(2,2-diphenyl)glutaramide, 43: Yield 1.8 g (64%); m.p. 130-132 °C; ^{1}H NMR (400 MHz, CDCl$_3$): ratio *EE:EZ:ZZ* = 2:1:1, δ = 7.34-7.22 (m, ArH-stopper), 4.33-4.22 (m, CH_a), 4.15-4.00 (t, *J* = 7.7 Hz, CH_a), 3.95-3.75 (m, CH_b), 2.74 (s, CH_c), 2.51 (s, CH_c), 2.47 (s, CH_c), 2.05 (t, *J* = 7.6 Hz, CH_d), 1.95 (t, *J* = 7.0 Hz, CH_d), 1.70-1.68 (m, CH_e), 1.50-1.61 (m, CH_e); ^{13}C NMR (100 MHz, CDCl$_3$): δ = 172.63 (s, CH$_c$NCO), 172.58 (s, CH$_c$NCO), 172.48 (s, CH$_c$NCO), 142.0 (s, ArC-ipso-stopper), 141.6 (s, ArC-ipso-stopper), 141.5 (s, ArC-stopper), 128.5 (d, ArC-stopper), 128.2 (d, ArC-stopper), 128.0 (d, ArC-stopper), 127.9 (d, ArC-stopper), 126.8 (d, ArC-stopper), 126.7 (d, ArC-stopper), 126.4 (d, ArC-stopper), 54.8 (t, CH_b), 52.8 (t, CH_b), 52.5 (t, CH_b), 49.8 (d, CH_a), 49.6 (d, CH_a); 49.1 (d, CH_a), 36.3 (q, CH_c), 36.2 (q, CH_c), 34.0 (q, CH_c), 33.0 (t, CH_d), 32.8 (t, CH_d), 31.7 (t, CH_d), 20.6 (t, CH_e), 20.3 (t, CH_e), 20.2 (t, CH_e) LRMS (FAB+ mNBA matrix) *m/z* (rel. int.): 519 (58.2 %), [(M+H)$^+$], HRMS (FAB+) calcd for $C_{35}H_{39}N_2O_2$ [(M+H)$^+$] 519.3012. Found 519.3005.

N,N'-dimethyl-N,N'-bis-(2,2-diphenyl)adipamide (44)
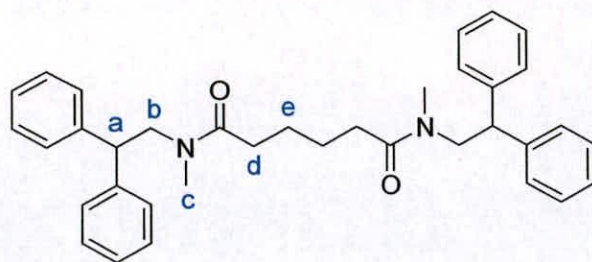
Selected data for N,N'-dimethyl-N,N'-bis-(2,2-diphenyl)adipamide, 44: Yield 1.4 g (67%); m.p. 140-142 °C; ^{1}H NMR (400 MHz, CDCl$_3$): ratio *EE:EZ:ZZ* = 2:1:1, δ = 7.35-7.17 (m, ArH-stopper), 4.39 (t, *J* = 8.0 Hz, CH$_a$), 4.17 (t, *J* = 8.0 Hz, CH$_a$), 3.96 (d, *J* = 8.0 Hz, CH$_b$), 3.90 (d, *J* = 8.0 Hz, CH$_b$), 2.85 (s, CH$_c$), 2.83 (s, CH$_c$), 2.66 (s, CH$_c$), 2.64 (s, CH$_c$), 2.17-2.11 (br m, CH$_d$), 1.87-1.80 (br m, CH$_d$), 1.40-1.35 (br m, CH$_e$), 1.30-1.25 (br m, CH$_e$); LRMS (FAB+ mNBA matrix) *m/z* (rel. int.): 533 (46.0 %), [(M+H)$^+$], HRMS (FAB+) calcd for C$_{36}$H$_{41}$N$_2$O$_2$ [(M+H)$^+$] 533.3168. Found 533.3165.

N,N'-dimethyl-N,N'-bis-(2,2-diphenyl)suberamide, (45)
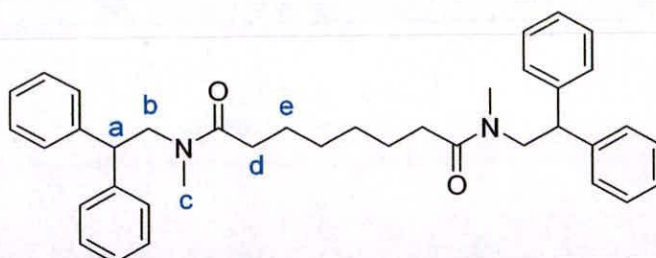
Selected data for N,N'-dimethyl-N,N'-bis-(2,2-diphenyl)suberamide, 45: Yield 2.04 g (77 %); mp 125-126 °C; ^{1}H NMR (400 MHz, CDCl$_3$): ratio *EE:EZ:ZZ* = 2:1:1, δ = 7.29–7.18 (m, ArH-stopper), 4.40 (t, *J* = 8.1 Hz, CH$_a$), 4.19 (t, *J* = 8.1 Hz, CH$_a$), 3.99 (d, *J* = 8.1 Hz, CH$_b$), 3.92 (d, *J* = 8.1 Hz, CH$_b$), 2.83 (s, CH$_c$), 2.67 (s, CH$_c$), 2.66 (s, CH$_c$), 2.18-2.12 (m, CH$_d$), 1.88-1.83 (m, CH$_d$), 1.53-1.35 (m, -CH$_2$-alkyl), 1.25-1.05 (m, -CH$_2$-alkyl); ^{13}C NMR (100 MHz, CDCl$_3$): δ = 173.2 (s, CH$_c$NCO), 142.2 (s, ArC-ipso), 141.7 (s, ArC-ipso), 128.7 (d, ArC-stopper), 128.4 (ArC-

stopper), 128.2 (d, ArC-stopper), 128.1 (d, ArC-stopper), 127.0 (d, ArC-stopper), 126.5 (d, ArC-stopper), 55.3 (t, CH$_b$), 53.0 (t, CH$_b$), 49.8 (d, CH$_a$), 49.1 (d, CH$_a$), 36.3 (q, CH$_d$), 34.1 (q, CH$_d$), 33.6 (t, CH$_d$), 32.4 (t, CH$_d$), 29.22 (t, -CH$_2$-), 29.18 (t, -CH$_2$-), 25.0 (t, -CH$_2$-), 24.9 (t, -CH$_2$-); LRMS (FAB+ mNBA matrix) *m/z* (rel. int.): 561 (30.7 %) [(M+H)$^+$], HRMS (FAB+) calcd for C$_{38}$H$_{45}$N$_2$O$_2$ [(M+H)$^+$] 561.3481. Found 561.3483.

N,N'-dimethyl-*N,N'-bis*-(2,2-diphenyl)sebacamide (46)
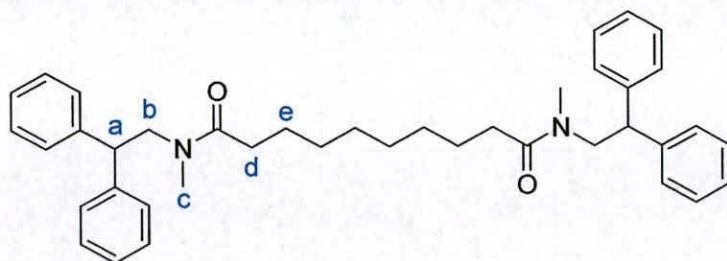
Selected data for *N,N'*-dimethyl-*N,N'-bis*-(2,2-diphenyl)sebacamide, 46: Yield 1.92 g (82%); mp 121-123 °C; ^{1}H NMR (400 MHz, CDCl$_3$): ratio *EE:EZ:ZZ* = 2:1:1, δ = 7.33-7.18 (m, ArH-stopper), 4.40 (t, *J* = 8.0 Hz, CH$_a$), 4.19 (t, *J* = 7.6 Hz, CH$_a$), 3.99 (d, *J* = 8.0 Hz, CH$_b$), 3.91 (d, *J* = 7.6 Hz, CH$_b$), 2.84 (s, CH$_c$), 2.67 (s, CH$_c$), 2.17 (t, *J* = 7.6 Hz, CH$_d$), 1.86 (t, *J* = 7.6 Hz, CH$_d$), 1.41-1.32 (m, -CH$_2$-alkyl), 1.23-1.10 (m, -CH$_2$-alkyl); ^{13}C NMR (100 MHz, CDCl$_3$): δ = 173.4 (s, CH$_c$NCO), 173.3 (s, CH$_c$NCO), 142.1 (s, ArC-ipso-stopper), 141.7 (s, ArC-ipso-stopper), 128.7 (d, ArC-stopper), 128.4 (d, ArC-stopper), 128.2 (d, ArC-stopper), 128.0 (d, ArC-stopper), 127.0 (d, ArC-stopper), 126.5 (d, ArC-stopper), 55.2 (t, CH$_b$), 53.0 (t, CH$_b$), 49.7 (d, CH$_a$), 49.0 (d, CH$_a$), 36.3 (q, CH$_c$), 34.1, (q, CH$_c$), 33.6 (t, CH$_d$), 32.4 (t, CH$_d$), 29.33 (t, -CH$_2$-), 29.30 (t, -CH$_2$-), 29.2 (t, -CH$_2$-), 25.1 (t, -CH$_2$-), 24.9 (t, -CH$_2$-); LRMS (FAB+ mNBA matrix) *m/z* (rel. int.): 589 (63.3 %) [(M+H)$^+$], HRMS (FAB+) calcd for C$_{40}$H$_{49}$N$_2$O$_2$ [(M+H)$^+$] 589.3794. Found 589.3786.

N,N'-dimethyl-N,N'-bis-(2,2-diphenyl)decanamide (47)
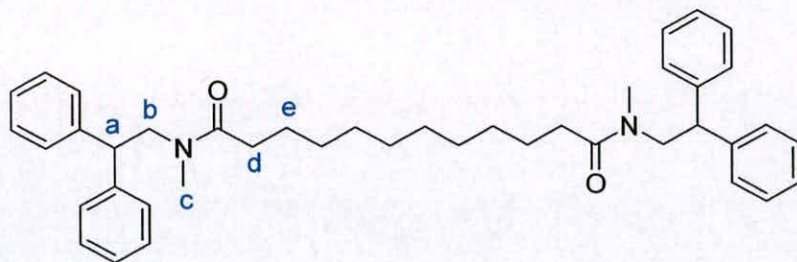
Selected data for *N,N'-dimethyl-N,N'-bis-(2,2-diphenyl)decanamide*, 47: Yield 1.54 g (79%); ^1H NMR (400 MHz, $CDCl_3$): ratio *EE:EZ:ZZ* = 2:1:1, δ = 7.31–7.20 (m, 10H, Ar$\underline{H}$-stopper), 4.40 (t, *J* = 8.0 Hz, C$\underline{H}_a$), 4.19 (t, *J* = 7.6 Hz, C$\underline{H}_a$), 3.99 (d, *J* = 8.0 Hz, C$\underline{H}_b$), 3.92 (d, *J* = 7.6 Hz, C$\underline{H}_b$), 2.84 (s, C$\underline{H}_c$), 2.67 (s, C$\underline{H}_c$), 2.17 (t, *J* = 7.6 Hz, C$\underline{H}_d$), 1.87 (t, *J* = 7.6 Hz, C$\underline{H}_d$), 1.41-1.32 (m, -C$\underline{H}_2$-alkyl), 1.23-1.10 (m, -C$\underline{H}_2$-alkyl); ^{13}C NMR (100 MHz, $CDCl_3$): δ = 173.5 (s, $CH_cN\underline{C}O$), 173.4 (s, $CH_cN\underline{C}O$), 142.1 (s, Ar$\underline{C}$-ipso-stopper), 141.7 (s, Ar$\underline{C}$-ipso-stopper), 128.7 (d, Ar$\underline{C}$-stopper), 128.4 (d, Ar$\underline{C}$-stopper), 128.2 (d, Ar$\underline{C}$-stopper), 128.1 (d, Ar$\underline{C}$-stopper), 128.0 (d, Ar$\underline{C}$-stopper), 127.0 (d, Ar$\underline{C}$-stopper), 126.6 (d, Ar$\underline{C}$-stopper), 126.4 (d, Ar$\underline{C}$-stopper), 55.3 (t, $\underline{C}H_b$), 53.0 (t, $\underline{C}H_b$), 49.8 (d, $\underline{C}H_a$), 49.1 (d, $\underline{C}H_a$), 36.4 (q, $\underline{C}H_c$), 34.2, (q, $\underline{C}H_c$), 33.7 (t, $\underline{C}H_d$), 32.4 (t, $\underline{C}H_d$), 29.43 (t, -$\underline{C}H_2$-), 29.40 (t, -$\underline{C}H_2$-), 29.37 (t, -$\underline{C}H_2$-), 29.35 (t, -$\underline{C}H_2$-), 25.1 (t, -$\underline{C}H_2$-), 25.0 (t, -$\underline{C}H_2$-); LRMS (FAB+ mNBA matrix) *m/z* (rel. int.): 617 (63.9 %) [(M+H)$^+$], HRMS (FAB+) calcd for $C_{42}H_{53}N_2O_2$ [(M+H)$^+$] 617.4107. Found 617.4110.

N,N'-dimethyl-N,N'-bis-(2,2-diphenyl)dodecanamide (48)
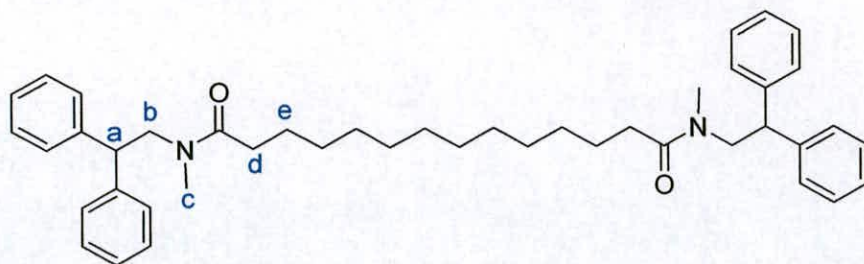
Selected data for *N,N'*-dimethyl-*N,N'*-*bis*-(2,2-diphenyl)dodecanamide, 48: Yield 1.88 g (90%); ^{1}H NMR (400 MHz, CDCl$_3$): ratio *EE:EZ:ZZ* = 2:1:1, δ = 7.32–7.16 (m, ArH-stopper), 4.40 (t, J = 8.3 Hz, CH$_a$) 4.18 (t, J = 7.5 Hz, CH$_a$), 3.98 (d, J = 8.3 Hz, CH$_b$), 3.90 (d, J = 7.5 Hz, CH$_b$), 2.82 (s, CH$_c$), 2.64 (s, CH$_c$), 2.16 (t, J = 7.6 Hz, CH$_d$), 1.87 (t, J = 7.6 Hz, CH$_d$), 1.52-1.37 (m, -CH$_2$-alkyl), 1.24-1.11 (m, -CH$_2$-alkyl); ^{13}C NMR (100 MHz, CDCl$_3$): δ = 173.3 (s, CH$_c$NCO), 173.2 (s, CH$_c$NCO), 142.0 (s, ArC-ipso-stopper), 141.6 (s, ArC-ipso-stopper), 128.6 (d, ArC-stopper), 128.3 (d, ArC-stopper), 128.1 (d, ArC-stopper), 127.9 (d, ArC-stopper), 126.8 (d, ArC-stopper), 126.4 (d, ArC-stopper), 55.1 (t, CH$_b$), 52.9 (t, CH$_b$), 49.7 (d, CH$_a$), 48.9 (d, CH$_a$), 36.2 (q, CH$_c$), 34.0, (q, CH$_c$), 33.5 (t, CH$_d$), 32.3 (t, CH$_d$), 29.5 (t, -CH$_2$-), 29.37 (t, -CH$_2$-), 29.32 (t, -CH$_2$-), 29.25 (t, -CH$_2$-), 29.21 (t, -CH$_2$-), 25.0 (t, -CH$_2$-), 24.9 (t, -CH$_2$-); LRMS (FAB+ mNBA matrix) *m/z* (rel. int.): 645 (59.7 %), (M+H)$^+$), HRMS (FAB+) calcd for C$_{44}$H$_{57}$N$_2$O$_2$ (M + H)$^+$ 645.4420. Found 645.4421.

N,N'-dimethyl-N,N'-bis-(2,2-diphenyl)tetradecanamide, (49)
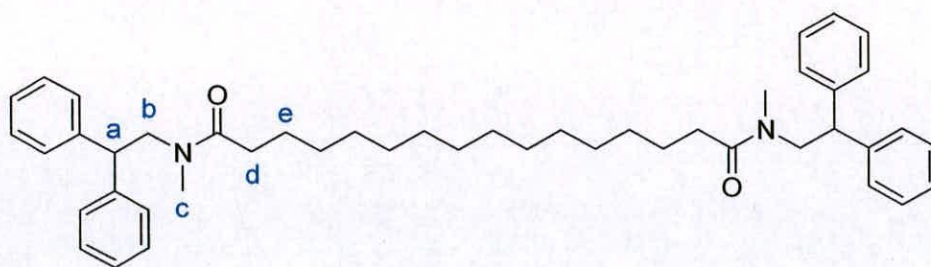
Selected data for N,N'-dimethyl-N,N'-bis-(2,2-diphenyl)tetradecanamide, 49:
Yield 1.34 g (74%); ^{1}H NMR (400 MHz, CDCl$_3$): ratio *EE:EZ:ZZ* = 2:1:1, δ = 7.31-
7.17 (m, Ar$\underline{H}$-stopper), 4.40 (t, *J* = 8.1 Hz, C$\underline{H}_a$), 4.19 (t, *J* = 7.3 Hz, C$\underline{H}_b$), 3.99 (d, *J*
= 8.0 Hz, C$\underline{H}_b$), 3.93 (d, *J* =7.3 Hz, C$\underline{H}_b$), 2.84 (s, C$\underline{H}_c$), 2.67 (s, C$\underline{H}_c$), 2.17 (t, *J* = 7.6
Hz, C$\underline{H}_d$), 1.87 (t, *J* = 7.6 Hz, C$\underline{H}_d$), 1.44-1.11 (m, -C$\underline{H}_2$-alkyl); ^{13}C NMR (100 MHz,
CDCl$_3$): δ = 173.5 (s, CH$_3$N$\underline{C}$O), 173.4 (s, CH$_3$N$\underline{C}$O), 142.1 (s, Ar$\underline{C}$-ipso-stopper),
141.7 (s, Ar$\underline{C}$-ipso-stopper), 128.7 (d, Ar$\underline{C}$-stopper), 128.4 (d, Ar$\underline{C}$-stopper), 128.2
(d, Ar$\underline{C}$-stopper), 128.1 (d, Ar$\underline{C}$-stopper), 128.0 (d, Ar$\underline{C}$-stopper), 127.0 (d, Ar$\underline{C}$-
stopper), 126.6 (d, Ar$\underline{C}$-stopper), 126.4 (d, Ar$\underline{C}$-stopper), 55.3 (t, $\underline{C}$H$_b$), 53.0 (t, $\underline{C}$H$_b$),
49.8 (d, $\underline{C}$H$_a$), 49.1 (d, $\underline{C}$H$_a$), 36.4 (q, $\underline{C}$H$_c$), 34.2, (q, $\underline{C}$H$_c$), 33.7 (t, $\underline{C}$H$_d$), 32.4 (t,
$\underline{C}$H$_d$), 29.43 (t, -$\underline{C}$H$_2$-), 29.40 (t, -$\underline{C}$H$_2$-), 29.37 (t, -$\underline{C}$H$_2$-), 29.35 (t, -$\underline{C}$H$_2$-), 25.1 (t, -
$\underline{C}$H$_2$-), 25.0 (t, -$\underline{C}$H$_2$-); LRMS (FAB+ mNBA matrix) *m/z* (rel. int.): 674 (73.1 %)
[(M+H)$^+$], HRMS (FAB+) calcd for C$_{46}$H$_{61}$N$_2$O$_2$ [(M+H)$^+$] 673.4733. Found
673.4734.

([2](1,7,14,20-Tetraaza-2,6,15,19-tetraoxo-3,5,9,12,16,18,22,25 tetrabenzocyclohexacosane)-*(N,N′-dimethyl-N,N′-bis*-(2,2-diphenyl) succinamide) rotaxane, (50)
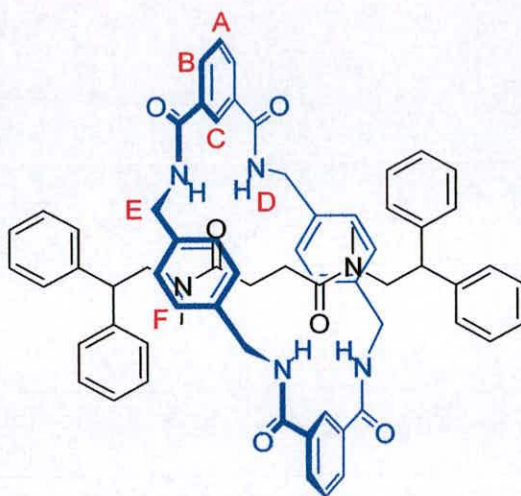
Selected data for ([2](1,7,14,20-Tetraaza-2,6,15,19-tetraoxo-3,5,9,12,16,18,22,25 tetrabenzocyclohexacosane)-*(N,N′-dimethyl-N,N′-bis*-(2,2-diphenyl) succinamide)-rotaxane, 50: Yield 0.26 g (26%); m.p. 174-177 °C; ^{1}H NMR (400 MHz, d_6-DMSO): δ = 9.00 (br t, N$\underline{H}_D$), 8.64 (br s, Ar$\underline{H}_C$), 8.58 (br s, Ar$\underline{H}_C$), 8.55 (br s, Ar$\underline{H}_C$) 8.41 (t, J = 5.1 Hz, N$\underline{H}_D$), 8.28 (t, J = 5.1 Hz, N$\underline{H}_D$), 8.22 (d, J = 8.0 Hz, Ar$\underline{H}_B$), 8.12 (d, J = 8.0 Hz, Ar$\underline{H}_B$), 8.07 (d, J = 8.0 Hz, Ar$\underline{H}_B$), 7.64 (t, J = 7.8 Hz, ArC$\underline{H}_A$), 7.46 (t, J = 7.7 Hz, Ar$\underline{H}_A$), 7.30-7.18 (m, Ar$\underline{H}$-stopper,), 6.93 (s, Ar$\underline{H}_F$), 6.88 (s, Ar$\underline{H}_F$), 6.85 (s, Ar$\underline{H}_F$), 4.51 (br t, C$\underline{H}_a$), 4.40 (dd, J = 5.8 Hz, J = 14.0 Hz, C$\underline{H}_E$), 4.35 (d, J = 5.1 Hz, C$\underline{H}_E$), 4.17 (t, J = 7.5 Hz, C$\underline{H}_a$), 3.82 (d, J = 7.1 Hz, C$\underline{H}_b$) 3.72 (d, J = 7.2 Hz, C$\underline{H}_a$), 3.49 (d, J = 7.8 Hz, C$\underline{H}_b$), 2.79 (s, C$\underline{H}_c$) 2.73 (s, C$\underline{H}_c$), 2.17 (s, C$\underline{H}_c$), 1.00-0.89 (br m, C$\underline{H}_d$ & C$\underline{H}_e$); ^{13}C NMR (100 MHz, d_6-DMSO): δ = 173.0, 166.3, 143.1, 137.3, 134.8, 131.5, 129.3, 129.1, 128.8, 128.1, 126.8, 125.9, 50.4, 43.7, 29.1; LRMS (FAB+ mNBA matrix) m/z (rel. int.): 1037 (78.2 %) [(M+H)$^+$], HRMS calcd for $C_{66}H_{65}N_6O_6$ [(M+H)$^+$] 1037.4966. Found 1037.4956.

***X*-ray crystallographic structure determination, 50**: $C_{68}H_{68}Cl_4N_6O_6$, M = 1207.08, colourless prism, crystal size 0.08 × 0.10 × 0.14 mm, monoclinic, $P2_1/c$, a = 11.3792(10), b = 15.2413(14), c = 18.545(2) Å, β = 107.346(2)°, V = 3070.1(5) Å^3, Z

= 2, ρ_{calcd} = 1.306 mg m^{-3}; Mo$_{K\alpha}$ radiation (graphite monochromator, λ = 0.71073 Å), μ = 0.251 mm^{-1}, T = 293(2) K. 12859 data (4398 unique, R_{int} = 0.1786, 1.76 < θ < 23.26°), were collected on a Siemens SMART CCD diffractometer using narrow frames (0.3° in ω), and were corrected semiempirically for absorption and incident beam decay. The structure was solved by direct methods and refined by full-matrix least-squares on F^2 values of all data (G. M. Sheldrick, SHELXTL manual, Siemens Analytical X-ray Instruments, Madison WI, USA, 1994, version 5) to give wR = $\{\Sigma[w(F_o^2-F_c^2)^2]/\Sigma[w(F_o^2)^2]\}^{1/2}$ = 0.1839, conventional R = 0.0649 for F values of 4348 reflections with $F_o^2 > 2\sigma F_o^2$), S = 0.858 for 388 parameters. Residual electron density extremes were 0.271 and -0.242 eÅ^{-3}. Amide hydrogen atoms were refined isotropically with the remainder constrained; anisotropic displacement parameters were used for all non-hydrogen atoms.
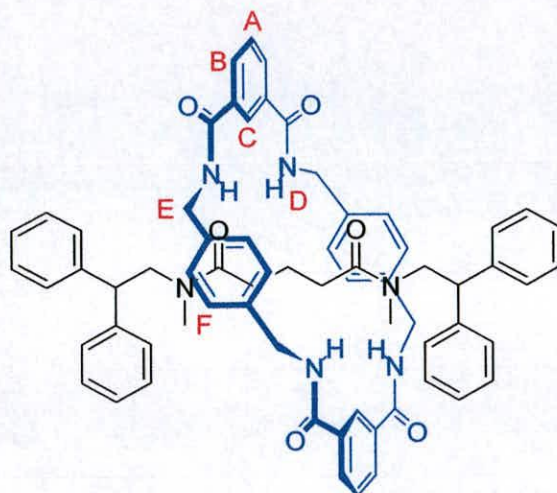
([2](1,7,14,20-Tetraaza-2,6,15,19-tetraoxo-3,5,9,12,16,18,22,25 tetrabenzocyclohexacosane-*N,N'*-dimethyl-*N,N'*-bis-(2,2-diphenyl)glutaramide, (51)

Selected data for ([2](1,7,14,20-Tetraaza-2,6,15,19-tetraoxo-3,5,9,12,16,18,22,25 tetrabenzocyclohexacosane-*N,N'*-dimethyl-*N,N'*-bis-(2,2-diphenyl)glutaramide,

51: Yield 6 mg (0.2 %); ^{1}H NMR (400 MHz, CDCl$_3$): δ = 8.57 (s, Ar$\underline{H}_C$) 8.54 (s, Ar$\underline{H}_C$), 8.33 (dd, J = 1.4 Hz, J = 7.8 Hz, Ar$\underline{H}_B$), 7.67 (t, J = 8.1 Hz, Ar$\underline{H}_A$), 7.64 (t, J =5.3 Hz, N$\underline{H}_D$), 7.34-7.12 (m, Ar$\underline{H}$-stopper), 6.90 (s, Ar$\underline{H}_F$), 6.88 (s, Ar$\underline{H}_F$), 4.61 (dd, J = 5.1 Hz, C$\underline{H}_E$), 4.49 (d, J = 5.3 Hz, C$\underline{H}_E$), 4.36 (dd, J = 5.1 Hz, C$\underline{H}_E$), 4.21-4.13 (m, C$\underline{H}_a$), 3.97 (d, J = 7.8 Hz, C$\underline{H}_b$), 3.89 (d, J = 7.8 Hz, C$\underline{H}_b$) 3.80 (d, J = 7.8 Hz, C$\underline{H}_b$), 2.92 (s, C$\underline{H}_c$), 2.61 (s, C$\underline{H}_c$), 2.40 (s, C$\underline{H}_c$), 0.90-0.78 (m, -C$\underline{H}_2$-alkyl), 1.10 (t, J = 7.6 Hz, C$\underline{H}_d$), 0.34-0.20 (m, -C$\underline{H}_2$-alkyl); LRMS (FAB+ mNBA matrix) *m/z* (rel. int.): 1052 (15.2 %) [(M+H)$^+$], HRMS calcd for C$_{67}$H$_{67}$N$_6$O$_6$ (M + H)$^+$ 1051.5122, Found 1051.5130.

([2](1,7,14,20-Tetraaza-2,6,15,19-tetraoxo-3,5,9,12,16,18,22,25 tetrabenzocyclohexacosane)-*N,N'*-dimethyl-*N,N'*-*bis*(2,2-diphenyl)adipamide, (52)
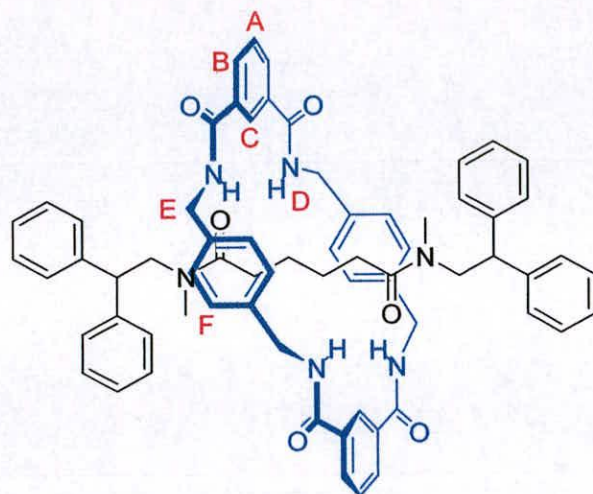
Selected data for ((([2](1,7,14,20-Tetraaza-2,6,15,19-tetraoxo-3,5,9,12,16,18,22,25tetrabenzocyclohexacosane)-*N,N'*-dimethyl-*N,N'*-*bis*(2,2-diphenyl)adipamide rotaxane, 52: Yield 7 mg (0.4 %); ^{1}H NMR (400 MHz, CDCl$_3$): δ= 8.35 (s, ArH$_C$), 8.28-8.23 (m, ArH$_B$ & NH$_D$), 7.69-7.60 (m, ArH$_A$), 7.29-7.18 (m, ArH-stopper), 7.01 (s, ArH$_F$), 6.98 (s, ArH$_F$), 4.44 (d, J = 5.6 Hz, CH$_E$), 4.25 (t, J = 8.0 Hz, CH$_a$), 4.07 (t, J = 8.0 Hz, CH$_a$), 4.01 (d, J = 8.0 Hz, CH$_b$), 3.76 (d, J = 8.0 Hz, CH$_b$), 2.93 (s, CH$_c$), 2.89 (s, CH$_c$), 2.69 (s, CH$_c$), 2.59 (s, CH$_c$), 1.51-0.97 (m, -CH$_2$-alkyl), 0.90-0.80 (m, -CH$_2$-alkyl), 0.42-0.20 (m, -CH$_2$-alkyl); LRMS (FAB+ mNBA matrix) *m/z* (rel. int.): 1066 (14.0 %) [(M+H)$^+$], HRMS calcd for C$_{68}$H$_{69}$N$_6$O$_6$ [(M+H)$^+$] 1065.5279. Found 1065.5263.

([2](1,7,14,20-Tetraaza-2,6,15,19-tetraoxo-3,5,9,12,16,18,22,25

cetrabenzocyclohexacosane)-(N,N'-bis(2,2-diphenylethyl)suberamide)-rotaxane,
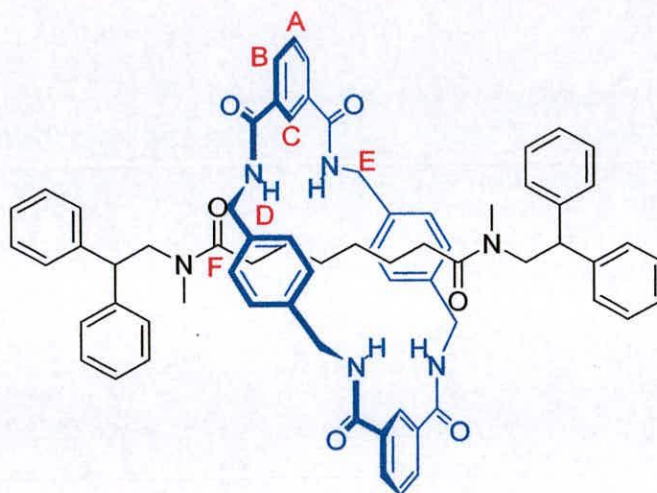
53

Selected data for ([2] (1,7,14,20- Tetraaza 2,6,15,19-tetraoxo-3,5,9,12,16,18,22,25tetrabenzocyclohexacosane) (*N,N'bis*- (2,2diphenylethyl-*N,N*-methyl)suberamide) rotaxane, 53: Yield 15 mg (1.2 %); m.p. 242 °C; ^{1}H NMR (400 MHz, CDCl$_3$): δ = 8.57 (s, Ar$\underline{H}_C$), 8.54 (s, Ar$\underline{H}_C$), 8.33 (d, *J* = 7.9 Hz, ArC$\underline{H}_B$), 7.67-7.61 (m, Ar$\underline{H}_A$ & N$\underline{H}_D$), 7.33-7.16 (m, Ar$\underline{H}$-stopper), 6.90 (s, C$\underline{H}_c$), 6.87 (s, C$\underline{H}_c$), 4.61 (dd, *J* = 14.1 Hz, *J* = 5.3 Hz, C$\underline{H}_E$), 4.49 (d, *J* = 5.3 Hz, C$\underline{H}_E$), 4.35 (dd, *J* = 14.1 Hz, *J* = 5.3 Hz, C$\underline{H}_E$), 4.21-4.15 (m, C$\underline{H}_a$), 3.97 (d, *J* = 7.8 Hz, C$\underline{H}_b$), 3.89 (d, *J* = 7.8 Hz, C$\underline{H}_b$) 3.80 (d, *J* = 7.8 Hz, C$\underline{H}_b$), 2.92 (s, C$\underline{H}_c$), 2.58 (s, C$\underline{H}_c$), 2.40 (s, C$\underline{H}_c$), 1.34-1.15 (m, -C$\underline{H}_2$-alkyl), 0.90-0.77 (m, -C$\underline{H}_2$-alkyl), 0.36-0.31 (m, -C$\underline{H}_2$-alkyl); LRMS (FAB+ mNBA matrix) *m/z* (rel. int.): 1093 (12.7 %) [(M+H)$^+$], HRMS (FAB+) calcd for C$_{70}$H$_{73}$N$_6$O$_6$ [(M+H)$^+$] 1093.5592. Found 1093.5605.

([2](1,7,14,20-Tetraaza-2,6,15,19-tetraoxo-3,5,9,12,16,18,22,25 tetrabenzocyclohexacosane)-(*N,N'-bis*-(2,2-diphenylethyl)sebacamide) rotaxane, 54
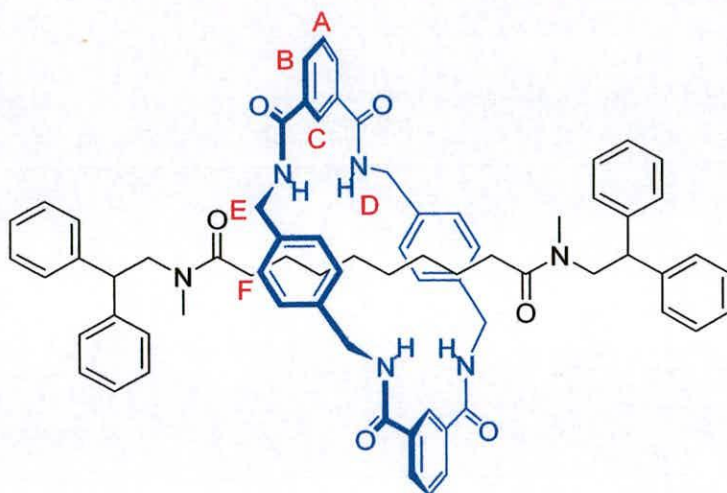
Selected data for ([2](1,7,14,20-Tetraaza-2,6,15,19-tetraoxo-3,5,9,12,16,18,22,25 tetrabenzocyclohexacosane)-(*N,N'-bis*-(2,2-diphenylethyl)sebacamide)-rotaxane, 54: Yield 13 mg (0.8 %); m.p. 194-196 °C; ^{1}H NMR (400 MHz, CHCl$_3$): δ = 8.36 (s, ArCH$_C$), 8.27-8.24 (m, ArH$_B$), 7.68-7.61 (m, ArH$_A$), 7.28-7.18 (m, ArH-stopper), 7.04 (s, 8H, ArH$_F$), 7.01 (s, ArH$_F$), 6.99 (s, ArH$_F$), 4.51-4.44 (m, CH$_E$), 4.26 (t, *J* = 8.0 Hz, CH$_a$) 4.10 (t, *J* = 7.8 Hz, CH$_a$), 4.01 (d, *J* = 8.0 Hz, CH$_b$), 2.93 (s, CH$_c$), 2.89 (s, CH$_c$), 2.69 (s, CH$_c$), 2.59 (s, CH$_c$), 2.34 (t, *J* = 7.6 Hz, CH$_d$), 2.19 (t, *J* = 7.6 Hz, CH$_d$), 1.34-1.21 (m, -CH$_2$-alkyl), 0,97-0.85 (m, -CH$_2$-alkyl), 0.42-0.28 (m, -CH$_2$-alkyl); LRMS (FAB+ mNBA matrix) *m/z* (rel. int.): 1121 (5.8 %) [(M+H)$^+$], HRMS (FAB+) calcd for C$_{72}$H$_{77}$N$_6$O$_6$ [(M+H)$^+$] 1121.5905. Found 1121.5908.

([2](1,7,14,20-Tetraaza-2,6,15,19-tetraoxo-3,5,9,12,16,18,22,25 tetrabenzocyclohexacosane)-(*N,N'-bis*-(2,2-diphenylethyl)decanamide) rotaxane, (55)
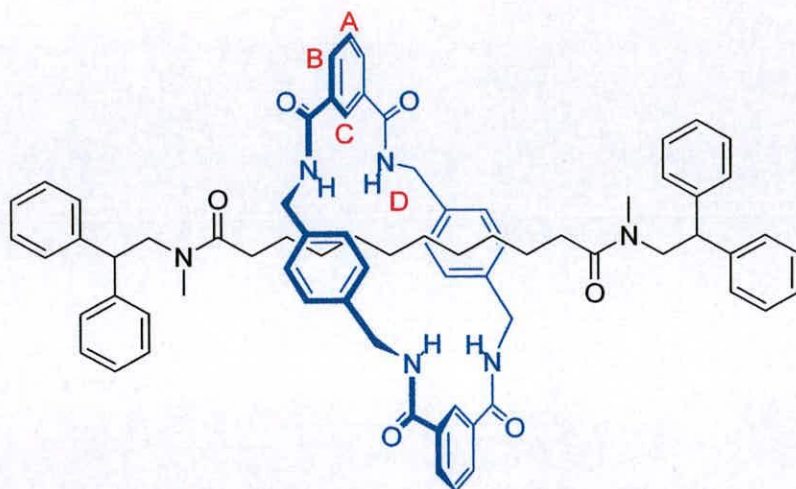
Selected data for ([2](1,7,14,20-Tetraaza-2,6,15,19-tetraoxo-3,5,9,12,16,18,22,25 tetrabenzocyclohexacosane)-(*N,N'-bis*-(2,2-diphenylethyl)decanamide)-rotaxane, 55: Yield 9 mg (0.5 %). ^{1}H NMR (400 MHz, CHCl$_3$): δ = 8.28 (s, Ar$\underline{H}_C$), 8.23 (s, Ar$\underline{H}_C$), 8.13 (d, J = 7.8 Hz, Ar$\underline{H}_B$), 7.75 (t, J = 5.6 Hz, Ar$\underline{H}_A$), 7.33-7.23 (m, ArH-stopper), 7.10 (s, 8H, Ar$\underline{H}_F$), 7.07 (s, Ar$\underline{H}_F$), 4.59 (dd, J = 6.0 Hz, J = 14.9 Hz, C$\underline{H}_E$), 4.48 (d, J = 5.3 Hz, C$\underline{H}_E$), 4.43-4.36 (m, C$\underline{H}_a$, C$\underline{H}_E$), 4.20 (t, J = 7.8 Hz, C$\underline{H}_a$), 4.05 (d, J = 8.0 Hz, C$\underline{H}_b$), 4.00 (d, J = 8.0 Hz, C$\underline{H}_b$), 2.87 4.26 (t, J = 8.0 Hz, C$\underline{H}_a$), 4.10 (t, J = 7.8 Hz, C$\underline{H}_a$), 4.01 (d, J = 8.0 Hz, C$\underline{H}_b$), 2.86 (s, C$\underline{H}_c$), 2.77 (s, C$\underline{H}_c$), 2.67 (s, C$\underline{H}_c$), 2.34 (t, J = 7.6 Hz, C$\underline{H}_d$), 2.19 (t, J = 7.6 Hz, C$\underline{H}_d$), 1.64-1.43 (m, -C$\underline{H}_2$-alkyl), 0,93-0.82 (m, -C$\underline{H}_2$-alkyl), 0.63-0.50 (m, -C$\underline{H}_2$-alkyl); LRMS (FAB+ mNBA matrix) m/z (rel. int.): 1150 (9.0 %) [(M+H)$^+$], HRMS (FAB+) calcd for C$_{74}$H$_{81}$N$_6$O$_6$ [(M+H)$^+$] 1149.6218. Found 1149.6219.

CHAPTER THREE

A First Generation Mechanically Interlocking Auxiliary

"All good things come to those who know how to wait"

Wolfgang Pauli

3.0 Introduction

As well as being prototypical design elements for various types of molecular machines,[1-5] rotaxanes (molecules in which one or more rings are held on one or more threads by bulky stoppers[6]) often dramatically change their components' properties (including solubility,[7] fluorescence,[8] electroluminescence[9] and membrane transport[10]) and can protect encapsulated regions of threaded substrates from chemical attack[11] and degradation[12]. Interestingly, since they are molecular compounds - *not* supramolecular[13] complexes (i.e. the atoms cannot be separated without breaking covalent bonds) - rotaxane architectures also, in principle, circumvent patents that only claim derivatives that branch out from a principal structure through continuous sequences of covalent bonds. Despite such attractive characteristics, practical exploitation of the property-changing and patent-breaking features of rotaxanes have been slow to develop. This is probably because most efficient strategies for rotaxane synthesis require specific recognition elements to be built into each noncovalently-linked unit,[14,15] thus limiting the types of chemical structures that can be interlocked. In other words, up to now it has not been possible to make a mechanically interlocked derivative of any particular pharmaceutical, dye, chromophore, catalyst or reagent that one might choose.

3.1 Results and Discussion

Here we describe a practical rotaxane synthesis which has the potential to be more general than previous methods because it does not depend upon a strong recognition motif existing between the ultimately interlocked components. A synthetic auxiliary is used to mechanically interlock a macrocycle around a suitable template, followed by translation of the ring to a position over the desired substrate and, finally, cleavage of the auxiliary to leave a rotaxane (e.g. **1**) with no designed noncovalent interactions between macrocycle and thread (Scheme 3.1). As well as providing a synthetic route to otherwise difficult or impossible to obtain structures, a consequence of forcing such unnatural geometries upon molecular fragments is seen in the X-ray crystal

structure of rotaxane **1**, which features the first example of an *NH*-amide-to-*alkyl-O*-ester hydrogen bond.
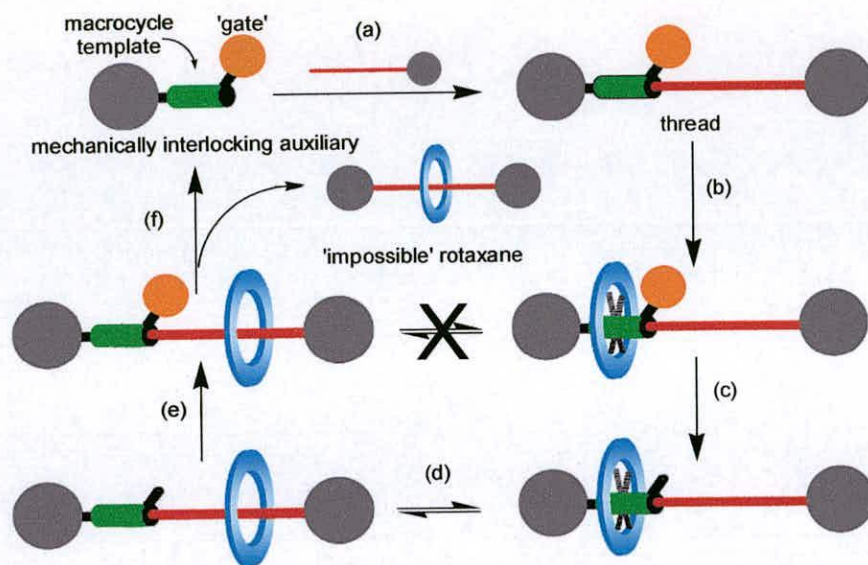
Scheme 3.1. Schematic preparation of an otherwise difficult or impossible to obtain rotaxane using a mechanically interlocking auxiliary. (a) attach substrate to auxiliary; (b) formation of rotaxane about template; (c) open gate; (d) shuttle macrocycle from template to substrate; (e) close gate; (f) cleave auxiliary.

Switching the position of a macrocycle between nonequivalent sites in a rotaxane can be achieved using a variety of stimuli in bistable "molecular shuttles".[1,6] In one such system, a benzylic amide macrocycle is assembled around a glycine-containing peptide template through intercomponent hydrogen bonding in nonpolar solvents.[11,16,17] The macrocycle can subsequently be decomplexed from the peptide by changing to a highly polar medium which solvates the peptide and macrocycle hydrogen bonding sites more strongly than they bind to each other.[18,19] We decided to investigate whether this solvent effect could be used to move the macrocycle from its template site to a desired substrate during synthesis, providing a means to a 'mechanically interlocking auxiliary' (Scheme 3.2).[20]
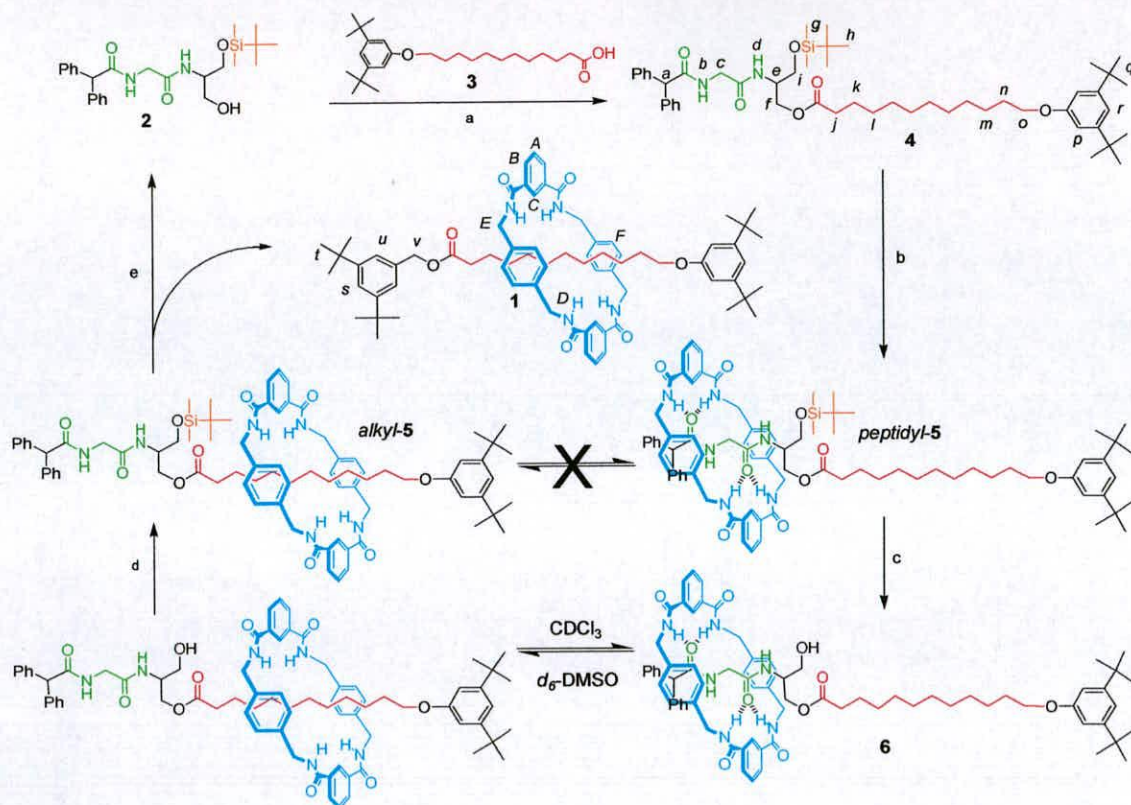
Scheme 3.2. Synthesis of rotaxane **1**. (a) 1-(3-dimethylaminopropyl)-3-ethyl-carbodiimide hydrochloride, 4-dimethylaminopyridine (4-DMAP), CH$_2$Cl$_2$, 87%; (b) isophthaloyl dichloride, *p*-xylylenediamine, Et$_3$N, CHCl$_3$, 25%; (c) tetrabutylammonium fluoride, THF, 95%; (d) *tert*-butyldimethylsilyl chloride, imidazole, 4-DMAP, DMSO, 85%; (e) di-*tert*-butylbenzyl alcohol, potassium *tert*-butoxide (5 mol %), 78%. Full experimental procedures can be found in the Section 3.4.

The mechanically interlocking auxiliary, **2**, consists of an *N*-stoppered glycine residue and a mono-silylated serinol derivative. The role of the serinol is two-fold; the free hydroxyl group provides a site for attachment of a carboxylic acid-terminated substrate (and eventual cleavage of the auxiliary) *via* an ester linkage, while the bulky *tert*-butyldimethylsilyl ether acts as a closed "gate" through which the macrocycle cannot pass. Coupling of **2** to the dodecanoic acid **3** gave the composite thread **4**, which was subjected to standard[16-19] hydrogen bond-directed rotaxane forming conditions to give the [2]rotaxane *peptidyl*-**5**.[21] Since the xylylene rings of the macrocycle shield the encapsulated region of the thread, the position of the macrocycle in the rotaxane could be unambiguously determined by comparing the nuclear magnetic resonance (NMR) chemical shifts of the thread and rotaxane protons. The ^{1}H NMR spectra in CDCl$_3$ (Figure 3.1a and b) and d_6-DMSO (Figure

3.2a and b) shows that the closed gate means the macrocycle resides solely on the peptide station in both solvents (for example, the rotaxane H_c glycine protons are shielded by -1.26 ppm in CDCl$_3$ and by -1.30 ppm in d_6-DMSO with respect to H_c in the thread).
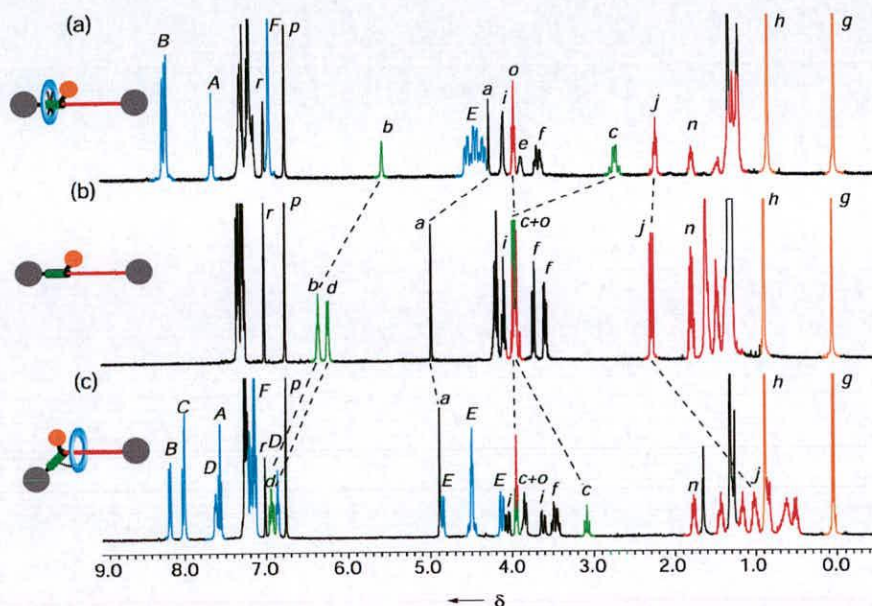
Figure 3.1. 400 MHz ^{1}H NMR spectra of (a) *peptidyl*-5, (b) 4, and (c) *alkyl*-5 in CDCl$_3$ at 298K. The color coding and lettering correspond to the assignments shown in Scheme 3.2.

Cleavage of the silyl group of *peptidyl*-5 with tetrabutylammonium fluoride afforded [2]rotaxane **6**. In **6** the macrocycle can move through the open gate to get to either the peptide or substrate side of the thread and ^{1}H NMR confirms its location is determined by the nature of the solvent. Accordingly, **6** was dissolved in anhydrous DMSO and the silyl ether reattached with *tert*-butyldimethylsilyl chloride.[22] A new rotaxane was isolated in 85% yield together with <2% of *peptidyl*-5. ^{1}H NMR confirms the new rotaxane to be *alkyl*-5, a translational diastereoisomer (identical covalent connectivity but a different spatial arrangement[23]) of *peptidyl*-5 with the macrocycle locked on the alkyl chain side of the closed gate irrespective of the solvent the rotaxane is dissolved in (Figures 3.1c and 3.2c).[24]
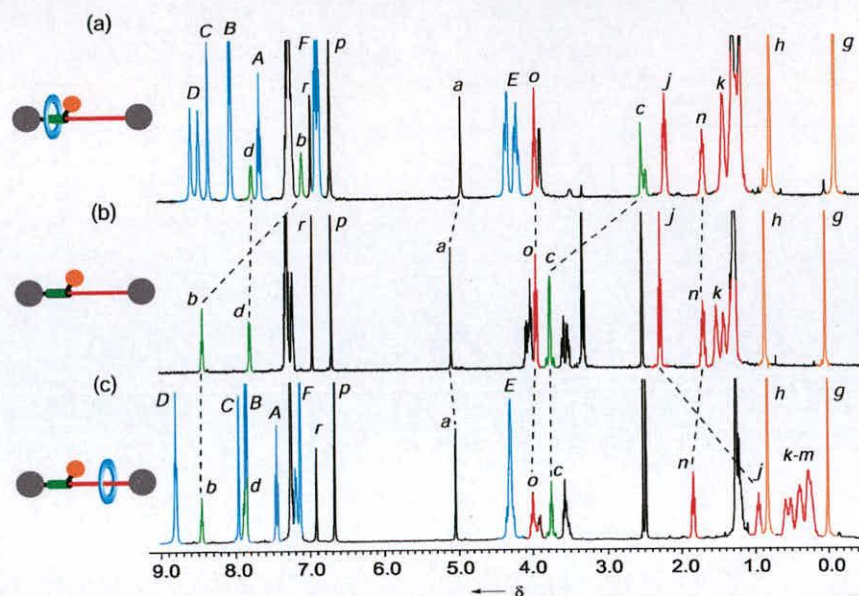
Figure 3.2. 400 MHz ^{1}H NMR spectra of (a) *peptidyl-5*, (b) **4**, and (c) *alkyl-5* in d_6-DMSO at 298K.

Since there are no strong binding interactions between the macrocycle and thread in *alkyl-5*, maintaining the rotaxane architecture whilst cleaving the mechanically interlocking auxiliary requires a reaction that does not permit unstoppering at any stage.[25] Transesterification with di-*tert*-butylbenzyl alcohol in the presence of catalytic potassium *tert*-butoxide,[26] afforded the desired [2]rotaxane **1** in 78% yield with complete recovery of the regenerated auxiliary and no evidence of any accompanying dethreading.[27] The shielding of all the alkyl chain protons in the ^{1}H NMR spectrum of **1** (Figure 3.3) shows that the macrocycle is delocalized over the entire length of the substrate, although the greater shielding of H$_j$ indicates that it spends more time nearer the ester end of the molecule in CDCl$_3$.
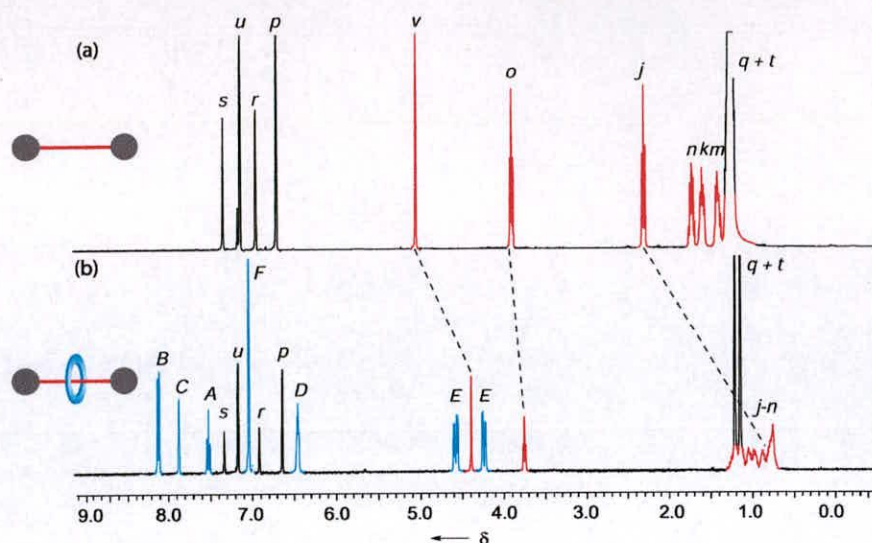
Figure 3.3. 400 MHz ^{1}H NMR spectra of (a) thread and (b) rotaxane **1** in CDCl$_3$ at 298K.

Small single crystals of the rotaxane suitable for X-ray crystallography using a synchrotron source were obtained by slow evaporation of a solution of **1** in acetonitrile. The X-ray crystal structure (Figure 3.4) confirms the interlocked nature of the rotaxane and shows a remarkable consequence of forcing such unnatural spatial arrangements on submolecular fragments. Although ester groups are normally poor hydrogen bonding groups,[28] the ester in the thread is the best acceptor available to the macrocycle amide hydrogen bond donors. Accordingly, the rotaxane exhibits not only a rare[29] example of a solid state *NH*-amide-to-*acyl-O*-ester hydrogen bond, but also what appears to be a genuine *NH*-amide-to-*alkyl-O*-ester hydrogen bond, which is long (2.60 Å) but directional (162.2° is a typical NH···O hydrogen bond angle[30]) to one of the *sp^3*-oxygen's lone pair orbitals in what is presumably a very weak interaction.

185
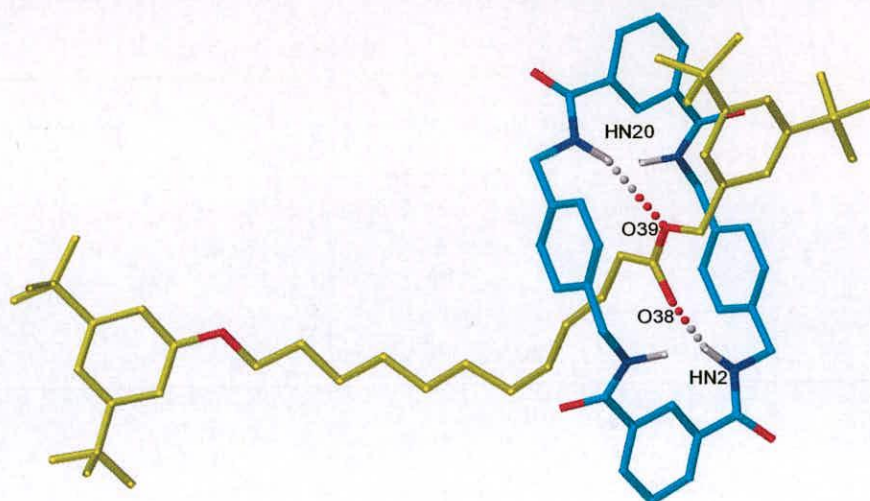
Figure 3.4. X-ray crystal structure of rotaxane **1**. Intramolecular hydrogen-bond lengths and angles: O38-HN2 1.89 Å, 161.9°; O39-HN20 2.60 Å, 162.2°.

3.2 Conclusion

In conclusion, we have synthesized a rotaxane **1** whose components bear no formal mutual recognition elements through the first example of controlled sub-molecular translational motion in organic synthesis. In principle, there is no reason why mechanically interlocking auxiliary strategies should not work with other molecular shuttle systems, including those based on cyclodextrins which already have US FDA approval for use in the pharmaceutical and food industries. In our laboratories the approach is currently being used to prepare mechanically interlocked analogues of substrates that are unavailable by conventional synthetic methods and to modify the physical and chemical properties of a range of pharmaceuticals, dyes, reagents, catalysts and components for molecular electronics.

3.3 References

1   V. Balzani, A. Credi, F. M. Raymo, J. F. Stoddart, *Angew. Chem. Int. Ed.* **2000**, *39*, 3348-3391.

2   C. P. Collier, E. W. Wong, M. Bělohradský, F. M. Raymo, J. F. Stoddart, P. J. Kuekes, R. S. Williams, J. R. Heath, *Science* **1999**, *285*, 391-394.

3   A. M. Brouwer, C. Frochot, F. G. Gatti, D. A. Leigh, L. Mottier, F. Paolucci, S. Roffia, G. W. H. Wurpel, *Science* **2001**, *291*, 2124-2128.

4   M. C. Jiménez, C. Dietrich-Buchecker, J.-P. Sauvage, *Angew. Chem. Int. Ed.* **2000**, *39*, 3284-3287.

5   P. Thordarson, E. J. A. Bijsterveld, A. E. Rowan, R. J. M. Nolte, *Nature* **2003**, *424*, 915-918.

6   J.-P. Sauvage, C. Dietrich-Buchecker (eds.), *Molecular Catenanes Rotaxanes and Knots: A Journey Through the World of Molecular Topology*, Wiley-VCH, Weinheim, **1999**.

7   A. G. Johnston, D. A. Leigh, A. Murphy, J. P. Smart, M. D. Deegan, *J. Am. Chem. Soc.* **1996**, *118*, 10662-10663.

8   S. Anderson, H. L. Anderson, *Angew. Chem. Int. Ed. Engl.* **1996**, *35*, 1956-1959.

9   F. Cacialli, J. S. Wilson, J. J. Michels, C. Daniel, C. Silva, R. H. Friend, N. Severin, P. Samori, J. P. Rabe, M. J. O'Connell, P. N. Taylor, H. L. Anderson, *Nature Mater.* **2002**, *1*, 160-164.

10   V. Dvornikovs, B. E. House, M. Kaetzel, J. R. Dedman, D. B. Smithrud, *J. Am. Chem. Soc.* **2003**, *125*, 8290-8301.

11   D. A. Leigh, A. Murphy, J. P. Smart, A. M. Z. Slawin, *Angew. Chem. Int. Ed. Engl.* **1997**, *36*, 728-732.

12   M. R. Craig, M. G. Hutchings, T. D. W. Claridge, H. L. Anderson, *Angew. Chem. Int. Ed.* **2001**, *40*, 1071-1074.

13   It has been proposed [V. Balzani, A. Credi, M. Venturi, *Chem. Eur. J.* **2002**, *8*, 5524-5532; M. Venturi, A. Credi, V. Balzani, *Molecular Devices and Machines - A Journey into the Nanoworld*, Wiley-VCH: Weinheim, **2003**] that the term 'supramolecular' be expanded from Lehn's original definition of 'chemistry

beyond the molecule' (i.e. assemblies of two or more molecules or ions held together by noncovalent forces) to include large molecules (e.g. dendrimers, rotaxanes, proteins *etc*) which feature functional intramolecular interactions or photophysics. In our view such a revision is unwarranted. When scientific language evolves it needs to retain a precise definition in order to remain useful (e.g. 'acid' to 'Lewis acid' or 'Brønsted acid'). Consider as a contrary example the term 'self-assembly', which has acquired such an imprecise meaning over recent years that it now conveys virtually nothing as a descriptor. In its currently accepted definition, 'supramolecular' – by analogy to the term 'molecular' – refers to how the atoms in a structure are held together, not their photophysical properties. It distinguishes molecules from clusters of molecules, for example pseudorotaxanes (host-guest complexes where the components are free to exchange between bound and unbound species) and rotaxanes (molecules where the components cannot exchange with outside systems without breaking covalent bonds). It does not matter that their properties can be similar nor that bond energies sometimes make it difficult to distinguish between molecular and supramolecular species, just as the timescale-dependent inversion of asymmetric nitrogen atoms does not confer on the term 'chirality' any less clear a meaning. Language – especially scientific language – needs to be precise; subject areas, e.g. 'supramolecular chemistry' or 'organometallic catalysis', on the other hand, should be as broad and inclusive as possible, and have always happily encompassed chemistry not technically suggested by their titles [J.-M. Lehn, *Supramolecular Chemistry: Concepts and Perspectives*, Wiley-VCH, Weinheim, **1995**, p. 90].

14   In addition to the rotaxane-forming methods based on specific templates for metal ion coordination, aromatic stacking and hydrogen bonding,[6] cyclodextrins [S. A. Nepogodiev, J. F. Stoddart, *Chem. Rev.* **1998**, *98*, 1959-1976] and certain cyclophanes[12] can form rotaxanes of a broad range of substrates through general hydrophobic binding. The trapping of phenolate-anions by amide macrocycles can also produce rotaxanes with no recognition elements, [C. Seel, F. Vögtle, *Chem. Eur. J.* **2000**, *6*, 21-24; R. Shukla, M. J. Deetz, B. D. Smith, *Chem. Commun.* **2000**, 2397-2398] but requires a specific

template in the stopper and is apparently of limited generality[C. A. Schalley, G. Silva, C. F. Nising, P. Linnartz, *Helv. Chim. Acta* **2002**, *85*, 1578-1596].

15 The earliest rotaxane syntheses produced rotaxanes without attractive interactions between the subunits but were carried out under 'statistical' conditions which only generates rotaxanes in low yields [I. T. Harrison, S. Harrison, *J. Am. Chem. Soc.* **1967**, *89*, 5723-5724]. Other routes to rotaxanes without noncovalent recognition elements between macrocycle and thread have been developed based on covalent bond-directed methods[G. Schill, H. Zollenkopf *Liebigs Ann. Chem.* **1969**, *721*, 53; K. Hiratani, J-I. Suga, Y. Nagawa, H. Houjou, H. Tokuhisa, M. Numata, K. Watanabe, *Tetrahedron Lett.* **2002**, *43*, 5747-5750].

16 M. Asakawa, G. Brancato, M. Fanti, D. A. Leigh, T. Shimizu, A. M. Z. Slawin, J. K. Y. Wong, F. Zerbetto, S. Zhang, *J. Am. Chem. Soc.* **2002**, *124*, 2939-2950.

17 G. Brancato, F. Coutrot, D. A. Leigh, A. Murphy, J. K. Y. Wong, F. Zerbetto, *Proc. Natl. Acad. Sci. USA* **2002**, *99*, 4967-4971.

18 A. S. Lane, D. A. Leigh, A. Murphy, *J. Am. Chem. Soc.* **1997**, *119*, 11092-11093.

19 T. Da Ros, D. M. Guldi, A. F. Morales, D. A. Leigh, M. Prato, R. Turco, *Org. Lett.* **2003**, *5*, 689-691.

20 Since hydrogen bonding of the DMSO to the peptide and macrocycle provides much of the driving force for displacement of the macrocycle from the template, this switching strategy should be largely independent of the nature of the substrate.

21 The italicised prefix refers to the position of the macrocycle on the thread.

22 Silyl ether protections of hydroxyl groups are routinely performed in DMF but DMSO is equally efficacious, a key requirement for the gate functionality with the chosen method of shuttling.

23 J. O. Jeppesen, J. Perkins, J. Becher, J. F. Stoddart, *Angew. Chem. Int. Ed.* **2001**, *40*, 1216-1221.

24 One (but not both) of the glycyl H_c protons of *alkyl*-**5** is shielded by 1.02 ppm in $CDCl_3$ indicating that the macrocycle is able to hydrogen bond to the peptide despite being locked on the substrate side of the silyl ether gate.

25   For examples of post-assembly stopper-substitution reactions in rotaxanes see a) S. J. Rowan, S. J. Cantrill, J. F. Stoddart, *Org. Lett.* **1999**, *1*, 129-132; b) S. J. Rowan, J. F. Stoddart, *J. Am. Chem. Soc.* **2000**, *122*, 164-165; c) S. J. Rowan, S. J. Cantrill, J. F. Stoddart, A. J. P. White, D. J. Williams, *Org. Lett.* **2000**, *2*, 759-762; d) D. W. Zehnder, D. B. Smithrud, *Org. Lett.* **2001**, *3*, 2485-2487; e) S. H. Chiu, S. J. Rowan, S. J. Cantrill, J. F. Stoddart, A. J. P. White, D. L. Williams, *Chem. Eur. J.* **2002**, *8*, 5170-5183.

26   M. G. Stanton, M. R. Gagné, *J. Am. Chem. Soc.* **1997**, *119*, 5075-5076.

27   The *tert*-butyloxy group is too small to act as a stopper, but tertiary alkoxides are unreactive towards esters and so 'BuOK provides a means of generating low concentrations of the reactive stopper primary alkoxide *in situ*.

28   F. G. Gatti, D. A. Leigh, S. A. Nepogodiev, A. M. Z. Slawin, S. J. Teat, J. K. Y. Wong, *J. Am. Chem. Soc.* **2001**, *123*, 5983-5989.

29   There are fewer than 30 examples of amide-ester hydrogen bonds in the Cambridge Crystallographic Database and all are of the *NH*-to-*acyl*-*O*-oxygen type[C. Alemán, J. J. Navas, S. Muñoz-Guerra, *J. Phys. Chem.* **1995**, *99*, 17653-17661 and ref. 28]

30   G. A. Jeffrey, *An Introduction to Hydrogen Bonding*, Oxford University Press: Oxford, **1997**.

3.4 Experimental
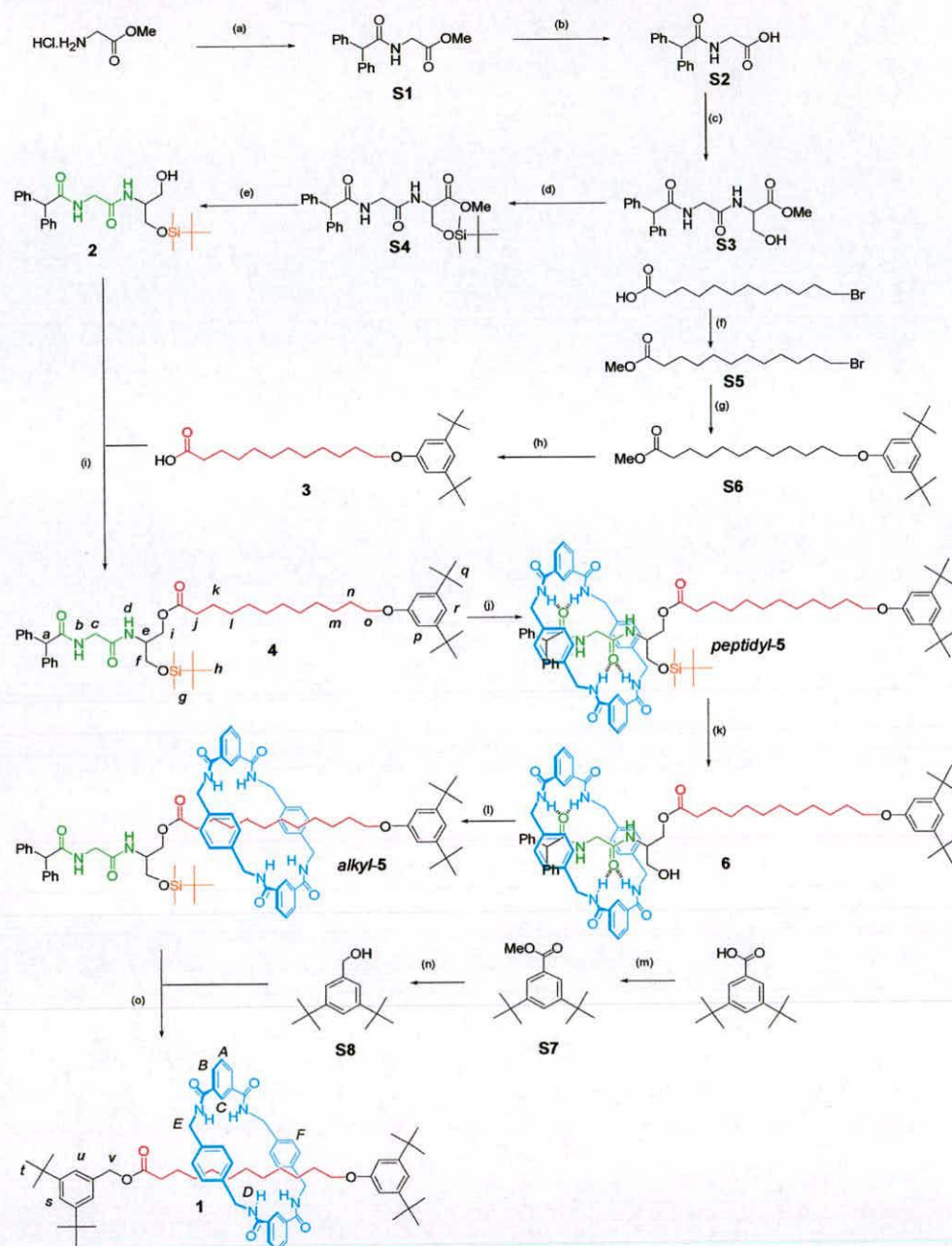
Scheme 3.3. Synthesis of Rotaxane **1**, a) diphenylacetyl chloride, Et₃N, 95 %; b) NaOH, EtOH, H₂O, 99 % c) DL-serine methyl ester hydrochloride, EDCI, HOBt, Et₃N, CH₂Cl₂, 90 %; d) *tert*-butyldimethylsilyl chloride, imidazole, 4-DMAP, CH₂Cl₂, 97%; e) NaBH₄, LiCl, MeOH, THF, 99 %; f) H₂SO₄, MeOH, Δ, 95 %; g) 3,5-di-*tert*-butylphenol, K₂CO₃, NaI, 2-butanone, 89 %; h) NaOH, THF, H₂O, 98 %; i) EDCI, DMAP, CH₂Cl₂, 87 %; j) isophthaloyl dichloride, *p*-xylylenediamine, Et₃N, CHCl₃, 25 %; k) TBAF, THF, 95 %; l) *tert*-butyldimethylsilyl chloride, imidazole, 4-DMAP, 85 %; m) H₂SO₄, MeOH, Δ, 93 %; n) DIBAL, toluene, -78 °C, 95 %; o) potassium *tert*-butoxide, 65 °C, 78 %. Full experimental procedures are described below.

Diphenylacetylglycine methyl ester (S1)[1]
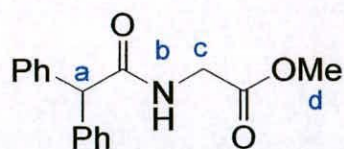
Diphenylacetyl chloride (24.0 g, 104 mmol) was added portionwise over 10 min to a stirred solution of glycine methyl ester hydrochloride (11.9 g, 94.7 mmol) and triethylamine (19.8 mL, 142 mmol) in chloroform (200 mL) under an atmosphere of nitrogen, at 0 °C. The reaction mixture was then stirred at room temperature for 16 h. The reaction mixture was washed with water (3 x 50 mL), dried (MgSO$_4$) and concentrated under reduced pressure. The remaining solid was recrystallized from toluene: hexane to give **S1** as a colorless solid. Yield 25.5 g (95 %); m.p. 112-114 °C; ^{1}H NMR (400 MHz, CDCl$_3$): δ = 7.30-7.20 (m, 10H, Ar$\underline{H}$), 6.22 (br t, 1H, N$\underline{H}_b$), 4.95 (s, 1H, C$\underline{H}_a$), 3.99 (d, 2H, J = 5.3 Hz, C$\underline{H}_c$), 3.69 (s, 3H, C$\underline{H}_d$); ^{13}C NMR (100 MHz, CDCl$_3$): δ = 172.2 (s, $\underline{C}$O$_2$CH$_d$), 170.2 (s, NH$\underline{C}$O), 139.1 (s, Ar$\underline{C}$-ipso), 128.9 (d, Ar$\underline{C}$), 128.7 (d, Ar$\underline{C}$), 127.3 (d, Ar$\underline{C}$), 58.7 (d, $\underline{C}$H$_a$), 52.2 (q, $\underline{C}$H$_d$), 41.4 (t, $\underline{C}$H$_b$); LRMS (FAB+ mNBA matrix) m/z (rel. int.): 284 (100 %), [(M+H)$^+$], HRMS (FAB+) calcd for C$_{17}$H$_{18}$NO$_3$ [(M+H)$^+$] 284.1287. Found 284.1290.

Diphenylacetylglycine (S2)
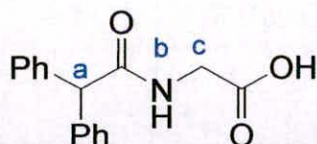
Aqueous sodium hydroxide solution (141 mL of a 1 M solution, 141 mmol) was added dropwise over 15 min to a stirred solution of **S1** (12.7 g, 47.0 mmol) in THF (200 mL) at room temperature. The reaction mixture was stirred at room temperature for 12 h. The reaction mixture was concentrated under reduced pressure and the remaining residue was diluted with water (150 mL), cooled to 0 °C and acidified to pH 1 by the dropwise addition of 1 M aqueous hydrochloric acid. The aqueous layer was extracted with chloroform (3 x 20 mL), dried (MgSO$_4$), and concentrated under reduced pressure to give

S2 as a colorless solid. Yield 12.0 g (99 %); m.p. 164-166 °C; ^{1}H NMR (400 MHz, d_6-DMSO): δ = 12.69 (br s, 1H, CO$_2$H), 8.61 (t, 1H, J = 5.6 Hz, NH$_b$), 7.38-7.23 (m, 10H, ArH), 5.11 (s, 1H, CH$_a$), 3.85 (d, 2H, J = 5.6 Hz, CH$_c$); ^{13}C NMR (100 MHz, d_6-DMSO): δ = 171.8 (s, CO$_2$H), 171.5 (s, NHCO), 140.6 (s, ArC-ipso), 128.9 (d, ArC), 128.5 (d, ArC), 126.9 (d, ArC), 56.5 (d, CH$_a$), 41.2 (t, CH$_b$); LRMS (FAB+ mNBA matrix) m/z (rel. int.): 270 (100 %) [(M+H)$^+$], HRMS (FAB+) calcd for C$_{16}$H$_{16}$NO$_3$ [(M+H)$^+$] 270.1130. Found 270.1126.

Diphenylacetylglycyl-3-hydroxy-2-amidopropionic acid methyl ester (S3)
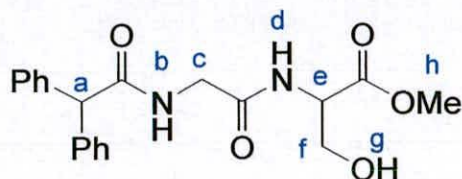
HOBt (3.27 g, 24.2 mmol) was added in one portion to a stirred solution of **S2** (5.00 g, 18.6 mmol), and triethylamine (7.77 mL, 55.8 mmol) in dichloromethane (200 mL), at 0 °C. The reaction mixture was stirred at 0 °C for 25 min then EDCI (4.63 g, 24.2 mmol) was added to the solution in one portion at 0 °C, with stirring. After 20 min DL-serine methyl ester hydrochloride (3.18 g, 20.5 mmol) was added portionwise over 10 min at 0 °C. The reaction mixture was stirred at 0 °C for 1 h and at room temperature for a further 18 h. The reaction mixture was washed with 1 M aqueous hydrochloric acid (3 x 50 mL) saturated aqueous sodium hydrogen carbonate (3 x 50 mL) and saturated aqueous sodium chloride, dried (MgSO$_4$) and concentrated under reduced pressure. The residue was purified by column chromatography on silica gel using ethyl acetate: petroleum ether 40-60 °C (4: 1) as eluent to give **S3** as a colorless solid. Yield 6.15 g (90 %); m.p. 76-77 °C; ^{1}H NMR (400 MHz, CDCl$_3$): δ = 7.35-7.24 (m, 10H, ArH), 7.18 (d, 1H, J = 7.5 Hz, NH$_d$), 6.70 (t, 1H, J = 5.5 Hz, NH$_b$), 4.98 (s, 1H, CH$_a$), 4.58-4.55 (m, 1H, CH$_e$), 3.97 (d, 2H, J = 5.5 Hz, CH$_c$), 3.85-3.75 (br m, 2H, CH$_f$), 3.74 (s, 3H, CH$_h$), 3.26 (br s, 1H, OH$_g$); ^{13}C NMR (100 MHz, CDCl$_3$): δ = 173.3 (s, CO$_2$CH$_h$), 170.7 (s, NH$_b$CO), 168.9 (s, NH$_d$CO), 138.9 (s, ArC-ipso), 128.8 (d, ArC), 128.7 (d, ArC), 127.4 (d, ArC), 62.4 (t,

C$\underline{H}_f$), 58.5 (d, $\underline{C}H_a$), 54.7 (d, $\underline{C}H_e$), 52.6 (q, $\underline{C}H_h$), 43.1 (t, $\underline{C}H_c$); LRMS (FAB+ mNBA matrix) *m/z* (rel. int.): 371 (87.7 %), [(M+H)$^+$], HRMS (FAB+) calcd for C$_{20}$H$_{23}$N$_2$O$_5$ [(M+H)$^+$] 371.1670. Found 371.1600.

Diphenylacetylglycyl-3-(dimethyl-*tert*-butylsiloxy)-2-amidopropionic acid methyl ester (S4)
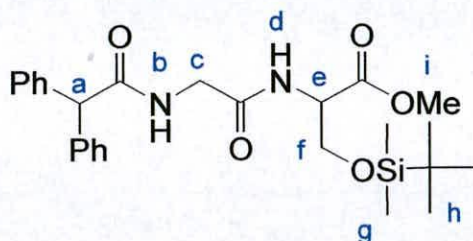
tert-Butyldimethylsilyl chloride (9.00 g, 61.0 mmol) was added portionwise over 5 min, to a stirred solution of **S3** (6.15 g, 16.7 mmol) in dichloromethane (150 mL) at room temperature, under an atmosphere of nitrogen. Imidazole (2.83 g, 41.6 mmol) was then added in one portion and the reaction mixture was then stirred at room temperature for 18 h. The reaction mixture was washed with water (3 x 20 mL), saturated aqueous sodium chloride (2 x 10 mL), dried (MgSO$_4$) and concentrated under reduced pressure. The remaining residue was purified by column chromatography on silica gel using petroleum ether 40-60 °C: ethyl acetate (10: 1) as eluent to give **S4** as a colorless oil. Yield 7.80 g (97 %); ^{1}H NMR (400 MHz, CDCl$_3$): δ = 7.35-7.21 (m, 10H, Ar$\underline{H}$), 7.14 (d, 1H, *J* = 8.0 Hz, N$\underline{H}_d$), 7.07 (t, 1H, *J* = 5.1 Hz, N$\underline{H}_b$), 4.99 (s, 1H, C$\underline{H}_a$), 4.68-4.64 (m, 1H, C$\underline{H}_e$), 4.04-4.01 (dd, 1H, *J* = 10.1 Hz, *J* = 3.0 Hz, CH$\underline{H}_f$), 3.96-3.94 (m, 2H, C$\underline{H}_c$), 3.82-3.78 (dd, 1H, *J* = 10.1 Hz, *J* = 3.0 Hz, C$\underline{H}_f$H), 0.90 (s, 9H,C$\underline{H}_h$), 0.03 (s, 3H, C$\underline{H}_g$), 0.02 (s, 3H, C$\underline{H}_g$); ^{13}C NMR (100 MHz, CDCl$_3$): δ = 172.3 (s, $\underline{C}$O$_2$CH$_i$), 170.3 (s, NH$_b\underline{C}$O), 168.8 (s, NH$_d\underline{C}$O), 139.1 (s, Ar$\underline{C}$-ipso), 128.6 (d, Ar$\underline{C}$), 128.4 (d, Ar$\underline{C}$), 126.9 (d, Ar$\underline{C}$), 63.1 (t, $\underline{C}$H$_f$), 58.0 (d, $\underline{C}$H$_a$), 54.2 (d, $\underline{C}$H$_e$), 52.0 (q, $\underline{C}$H$_i$), 43.0 (t, $\underline{C}$H$_b$), 25.5 (q, $\underline{C}$H$_h$), 17.9 (s, $\underline{C}$(CH$_h$)), -5.7 (q, $\underline{C}$H$_g$), -5.9 (q, $\underline{C}$H$_g$); LRMS (FAB+ mNBA matrix) *m/z* (rel. int.): 485 (56.7 %) [(M+H)$^+$], HRMS (FAB+) calcd for C$_{26}$H$_{37}$N$_2$O$_5$Si [(M+H)$^+$] 485.2472. Found 485.2476.

Diphenylacetylglycyl-3-(dimethyl-*tert*-butylsiloxy)-1-hydroxy-propanol (2)
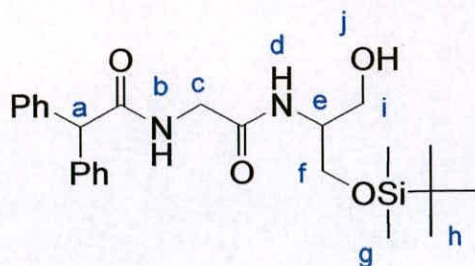
Anhydrous lithium chloride (2.72 g, 64.5 mmol) and sodium borohydride (2.46 g, 64.5 mmol) were added sequentially, both in one portion, to a stirred solution of **S4** (7.38 g, 16.2 mmol) in anhydrous THF (40 mL) at 0 °C. Ethanol (120 mL) was then at added in one portion at 0 °C. The reaction mixture was then stirred at room temperature for 16 h. The reaction mixture was cooled to 0 °C and acidified to pH 5 by the dropwise addition of 10 % aqueous citric acid solution. The reaction mixture was concentrated under reduced pressure, diluted with water (50 mL) and extracted with chloroform (3 x 50 mL), dried (MgSO$_4$) and concentrated under reduced pressure. The remaining residue was purified by column chromatography on silica gel using petroleum ether 40-60 °C: ethyl acetate (5: 1) as eluent to give **2** as a colorless viscous oil. Yield 7.35 g (99 %); ^{1}H NMR (400 MHz, CDCl$_3$): δ = 7.35-7.20 (m, 11H, Ar$\underline{H}$ & N$\underline{H}_b$), 6.92 (d, 1H, J = 8.0 Hz, N$\underline{H}_d$), 4.97 (s, 1H, C$\underline{H}_a$), 3.96-3.91 (m, 2H, CH$\underline{H}_c$ & C$\underline{H}_e$), 3.81-3.76 (m, 1H C$\underline{H}_c$H), 3.68-3.57 (m, 4H, C$\underline{H}_f$ & C$\underline{H}_i$), 3.49 (br s, 1H, O$\underline{H}_j$), 0.89 (s, 9H, C$\underline{H}_h$), 0.05 (s, 3H, C$\underline{H}_g$), 0.04 (s, 3H, C$\underline{H}_g$); ^{13}C NMR (100 MHz, CDCl$_3$): δ = 172.8 (s, NH$_b\underline{C}$O), 168.9 (s, NH$_d\underline{C}$O), 139.0 (s, Ar$\underline{C}$-ipso), 128.7 (d, Ar$\underline{C}$), 128.5 (d, Ar$\underline{C}$), 127.1 (d, Ar$\underline{C}$), 62.3 (t, $\underline{C}$H$_i$), 62.1 (t, $\underline{C}$H$_f$), 58.1 (d, $\underline{C}$H$_a$), 52.3 (d, $\underline{C}$H$_e$), 43.2 (t, $\underline{C}$H$_c$), 25.7 (q, $\underline{C}$H$_h$), 18.0 (s, $\underline{C}$(CH$_h$)), -5.6 (q, $\underline{C}$H$_g$), -5.7 (q, $\underline{C}$H$_g$); LRMS (FAB+ mNBA matrix) m/z (rel. int.): 457 (47.3 %) [(M+H)$^+$], HRMS (FAB+) calcd for C$_{25}$H$_{39}$N$_2$O$_4$Si [(M+H)$^+$] 457.2523. Found 457.2518.

Methyl-12-bromododecanoate (S5)
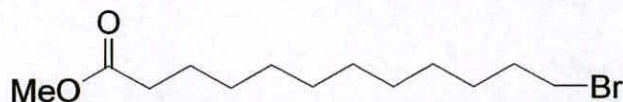
This compound was prepared as described in H. Shabany, R. Pajewski, E. Abel, A. Mukhopadhyay, G. W. Gokel, *J. Heterocyclic Chem.* **2001**, *38*, 1393-1400; and showed identical spectroscopic data to that reported therein.

Methyl-12-(3,5-di-*tert*-butylphenoxy) dodecanoate (S6)
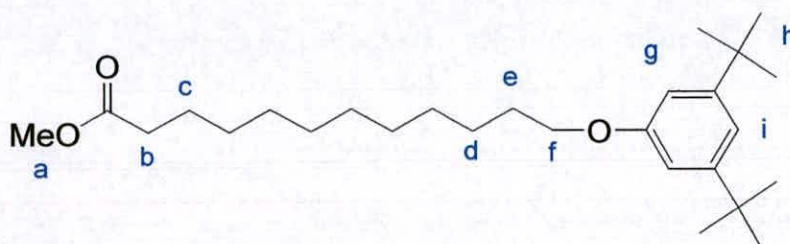
S5 (3.30 g, 11.3 mmol), 3,5-di-*tert*-butylphenol (2.44 g, 11.8 mmol), anhydrous potassium carbonate (15.6 g, 113 mmol) and sodium iodide (one crystal) in 2-butanone (120 mL) were heated under reflux for 2 days. The reaction mixture was filtered and concentrated under reduced pressure. The remaining residue was purified by column chromatography on silica gel using ethyl acetate: petroleum ether 40-60 °C (1: 1) as eluent to give S6 as a colorless oil. Yield 4.21 g (89 %); ^{1}H NMR (400 MHz, CDCl$_3$): δ = 7.03 (t, 1H, J = 1.7 Hz, C$\underline{H}_g$), 6.78 (d, 2H, J = 1.7 Hz, C$\underline{H}_i$), 3.98 (t, 2H, J = 6.5 Hz, C$\underline{H}_f$), 3.69 (s, 3H, C$\underline{H}_a$), 2.33 (t, 2H, J = 7.5 Hz, C$\underline{H}_b$), 1.82-1.79 (m, 2H, C$\underline{H}_e$), 1.74-1.63 (m, 2H, C$\underline{H}_c$), 1.55-1.49 (m, 2H, C$\underline{H}_d$), 1.47-1.31 (m, 30H, C$\underline{H}_h$ & -C$\underline{H}_2$-alkyl); ^{13}C NMR (100 MHz, CDCl$_3$): δ = 174.3 (s, $\underline{C}$O$_2$CH$_a$), 158.6 (s, Ar$\underline{C}$-ipso), 152.0 (s, Ar$\underline{C}$-meta), 114.7 (d, Ar$\underline{C}$H$_i$), 108.7 (d, Ar$\underline{C}$H$_g$), 67.7 (t, $\underline{C}$H$_f$), 51.4 (q, $\underline{C}$H$_a$), 34.9 (s, $\underline{C}$(CH$_h$)), 34.1 (t, $\underline{C}$H$_b$), 31.4 (q, $\underline{C}$H$_h$), 29.5 (t, -$\underline{C}$H$_2$-), 29.5 (t, -$\underline{C}$H$_2$-), 29.4 (t, -$\underline{C}$H$_2$-), 29.4 (t, -$\underline{C}$H$_2$-), 29.4 (t, -$\underline{C}$H$_2$-), 29.2 (t, -$\underline{C}$H$_2$-), 29.1 (t, -$\underline{C}$H$_2$-), 26.1 (t, -$\underline{C}$H$_2$-), 24.9 (t, -$\underline{C}$H$_2$-); LRMS (FAB+ mNBA matrix) *m/z* (rel.

int.): 419 (48.0 %) [(M+H)$^+$], HRMS (FAB+) calcd for C$_{27}$H$_{47}$O$_3$ [(M+H)$^+$] 419.3525. Found 419.3535.

12-(3,5-di-*tert*-butylphenoxy) dodecanoic acid (3)
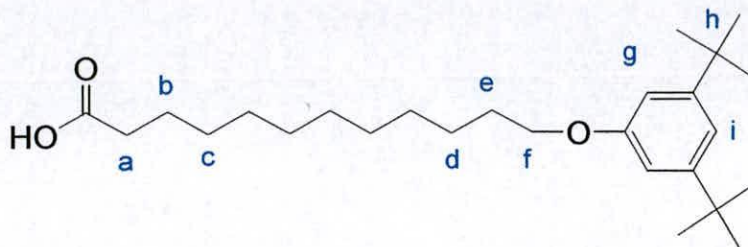
Sodium hydroxide (29.4 mL of a 1 M aqueous solution, 29.4 mmol) was added dropwise over 10 min to a stirred solution of **S6** (4.10 g, 9.81 mmol) in ethanol (50 mL) at room temperature. The reaction mixture was then heated under reflux for 16 h. The reaction mixture was concentrated under reduced pressure and diluted with water (50 mL), cooled to 0 °C and acidified to pH 1 by the dropwise addition of 1 M aqueous hydrochloric acid. The aqueous layer was extracted with ethyl acetate (3 x 20 mL), dried (MgSO$_4$), and concentrated under reduced pressure to give **3** as a colorless solid. Yield 3.90 g (98 %); m.p. 54-56 °C; ^{1}H NMR (400 MHz, CDCl$_3$): δ = 7.02 (t, 1H, J = 1.7 Hz, C$\underline{H}_g$), 6.77 (d, 2H, J = 1.7 Hz, C$\underline{H}_i$), 3.97 (t, 2H, J = 6.6 Hz, C$\underline{H}_f$), 2.36 (t, 2H, J = 7.3 Hz, C$\underline{H}_a$), 1.83-1.76 (m, 2H, C$\underline{H}_e$), 1.69-1.61 (m, 2H, C$\underline{H}_b$), 1.52-1.43 (m, 2H, C$\underline{H}_d$), 1.33-1.27 (m, 30H, -C$\underline{H}_2$-alkyl & C$\underline{H}_h$); ^{13}C NMR (100 MHz, CDCl$_3$): δ = 180.3 (s, $\underline{C}$O$_2$H), 158.6 (s, Ar$\underline{C}$-ipso), 152.1 (s, Ar$\underline{C}$-meta), 114.8 (d, Ar$\underline{C}$H$_i$), 108.8 (d, Ar$\underline{C}$H$_g$), 67.5 (t, $\underline{C}$H$_f$), 35.0 (s, $\underline{C}$(CH$_h$)), 34.3 (t, $\underline{C}$H$_a$), 31.5 (q, $\underline{C}$H$_h$), 29.7 (t, -$\underline{C}$H$_2$-), 29.6 (t, -$\underline{C}$H$_2$-), 29.5 (t, -$\underline{C}$H$_2$-), 29.4 (t, -$\underline{C}$H$_2$-), 29.3 (t, -$\underline{C}$H$_2$-), 29.2 (t, -$\underline{C}$H$_2$-), 29.3 (t, -$\underline{C}$H$_2$-), 26.2 (t, -$\underline{C}$H$_2$-), 24.9 (t, -$\underline{C}$H$_2$-); LRMS (FAB+ mNBA matrix) m/z (rel. int.): 405 (64.9 %) [(M+H)$^+$], HRMS (FAB+) calcd for C$_{26}$H$_{45}$O$_3$ [(M+H)$^+$] 405.3369. Found 405.3372.

Diphenylacetylglycyl-3-(dimethyl-*tert*-butylsiloxy)-1-(3,5-di-*tert*-butylphenoxy-1'-dodecanoxy) propanol (4)
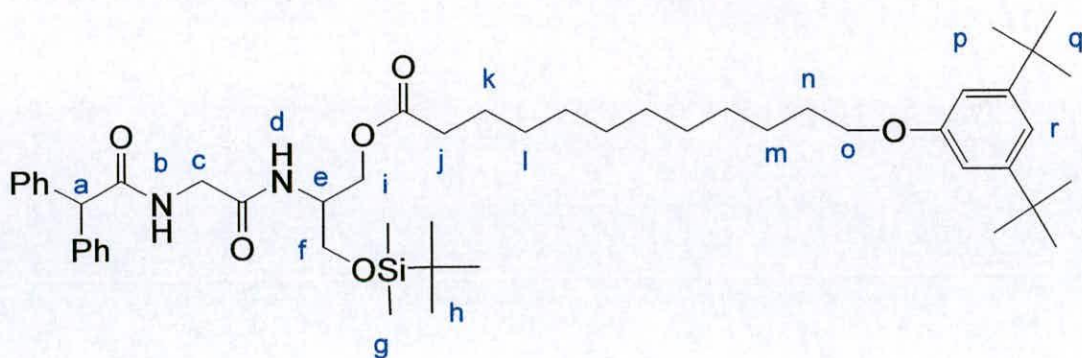
EDCI (3.20 g, 16.7 mmol) and 4-DMAP (155 mg, 1.26 mmol) were added in one portion to stirred solution of **3** (5.15 g, 12.8 mmol) and **2** (6.10 g, 13.4 mmol) in dichloromethane (100 mL) at 0 °C. The reaction mixture was then stirred at room temperature for 14 h. The reaction mixture was washed with 1 M aqueous hydrochloric acid (3 x 50 mL) saturated aqueous sodium hydrogen carbonate (3 x 50 mL) and saturated aqueous sodium chloride (2 x 20 mL), dried (MgSO$_4$) and concentrated under reduced pressure. The remaining residue was purified by column chromatography on silica gel using ethyl acetate: petroleum ether 40-60 °C (1: 1) as eluent to give **4** as a colorless oil. Yield 9.34 g (87 %); ^{1}H NMR (400 MHz, CDCl$_3$): δ = 7.37-7.26 (m, 10H, Ar$\underline{H}$-stopper), 7.16 (t, 1H, J = 5.0 Hz, N$\underline{H}_b$), 7.08 (t, 1H, J = 1.7 Hz, C$\underline{H}_r$), 6.92 (d, 1H, J = 8.3 Hz, N$\underline{H}_d$), 6.83 (d, 2H, J = 1.7 Hz, C$\underline{H}_p$), 5.02 (s, 1H, C$\underline{H}_a$), 4.21 (m, 1H, C$\underline{H}_e$), 4.18-4.13 (m, 2H, C$\underline{H}_i$), 4.03 (t, 2H, J = 6.6 Hz, C$\underline{H}_o$), 3.98 (m, 2H, C$\underline{H}_c$), 3.74-3.71 (dd, 1H, J = 9.8 Hz, J = 3.3 Hz, C$\underline{H}_f$H), 3.62- 3.57 (dd, 1H, J = 9.8 Hz, J = 3.3 Hz, CH$\underline{H}_f$), 2.31 (t, 2H, J = 7.6 Hz, C$\underline{H}_j$), 1.85- 1.81(m, 2H, C$\underline{H}_n$), 1.65-1.62 (m, 2H, C$\underline{H}_k$), 1.56-153 (m, 2H, C$\underline{H}_l$), 1.39-1.31 (m, 30H, C$\underline{H}_q$ & -C$\underline{H}_2$-alkyl), 0.89 (s, 9H, C$\underline{H}_h$), 0.05 (s, 6H, C$\underline{H}_g$); ^{13}C NMR (100 MHz, CDCl$_3$): δ = 173.3 (s, $\underline{C}$O$_2$R), 172.5 (s, NH$_b\underline{C}$O), 168.5 (s, NH$_d\underline{C}$O), 158.5 (s, Ar$\underline{C}$-ipso), 151.8 (s, Ar$\underline{C}$-meta), 139.0 (s, Ar$\underline{C}$-ipso), 128.6 (d, Ar$\underline{C}$), 128.5 (d, Ar$\underline{C}$), 127.1 (d, Ar$\underline{C}$), 114.5 (d, Ar$\underline{C}$H$_r$), 108.6 (d, Ar$\underline{C}$H$_p$), 67.5 (t, $\underline{C}$H$_o$), 62.1 (t, $\underline{C}$H$_f$), 61.2 (t, $\underline{C}$H$_i$), 58.1 (d, $\underline{C}$H$_a$), 49.5 (d, $\underline{C}$H$_e$), 43.5 (t, $\underline{C}$H$_c$), 34.8 (s, $\underline{C}$(CH$_q$)), 33.9 (t, $\underline{C}$H$_j$), 31.3 (q, $\underline{C}$H$_q$), 29.4 (t, -$\underline{C}$H$_2$-), 29.4 (t, -$\underline{C}$H$_2$-), 29.3 (t, -$\underline{C}$H$_2$-), 29.3 (t, -$\underline{C}$H$_2$-), 29.3 (t, -$\underline{C}$H$_2$-), 29.1 (t, -$\underline{C}$H$_2$-), 29.0 (t, -$\underline{C}$H$_2$-), 26.0 (t, -$\underline{C}$H$_2$-), 25.6 (q, $\underline{C}$H$_h$), 24.7 (t, -$\underline{C}$H$_2$-), 18.0 (s, $\underline{C}$(CH$_h$)), -5.7 (q, $\underline{C}$H$_g$); LRMS (FAB+ mNBA matrix) *m/z* (rel. int.): 843 (16.6 %)

[(M+H)$^+$], HRMS (FAB+) calcd for C$_{51}$H$_{79}$N$_2$O$_6$Si [(M+H)$^+$] 843.5707. Found 843.5709.

[2](1,7,14,20-Tetraaza-2,6,15,19-tetraoxo-3,5,9,12,16,18,22,25-tetrabenzocyclohexacosane)-Diphenylacetylglycyl-3-(dimethyl-*tert*-butylsiloxy)-1-(3,5-di-*tert*-butylphenoxy-1'-dodecanoxy) propanol rotaxane (*peptidyl*-5)

4 (3.00 g, 3.56 mmol) and triethylamine (9.95 mL, 71.4 mmol) were dissolved in anhydrous chloroform (360 mL) and stirred vigorously whilst solutions of *p*-xylylene diamine (3.88 g, 28.5 mmol) in anhydrous chloroform (50 mL) and isophthaloyl dichloride (5.79 g, 28.5 mmol,) in anhydrous chloroform (50 mL) were simultaneously added over a period of 4 h using motor-driven syringe pumps. After a further 2 h the resulting suspension was filtered and the filtrate was washed with 1 M aqueous hydrochloric acid (3 x 50 mL) saturated aqueous sodium hydrogen carbonate (3 x 50 mL) and saturated aqueous sodium chloride (2 x 20 mL), dried (MgSO$_4$) and concentrated under reduced pressure. The residue was purified by column chromatography on silica gel using chloroform: methanol (100: 1) as eluent to give *peptidyl*-**5** as a colorless solid. Yield 1.22 g (25 %); m.p. 224-226 °C; ^{1}H NMR (400 MHz, CDCl$_3$): δ = 8.24 (s, 2H, ArH$_C$), 8.20 (d, 4H, J = 7.7 Hz, ArH$_B$), 7.64 (t, 2H, J = 7.7 Hz, ArH$_A$), 7.31- 7.12 (m, 11H, NH$_d$ & ArH-stopper), 7.01 (t, 1H, J = 1.7 Hz, ArH$_r$), 6.95 (s, 8H, ArH$_F$), 6.76 (d, 2H, J = 1.7 Hz, ArH$_p$), 5.57 (br t, 1H, NH$_b$), 4.56-4.30 (m, 8H, CH$_E$), 4.28 (s, 1H, CH$_a$), 4.09 (m, 2H, CH$_f$), 3.96 (t, 2H, J = 6.6 Hz, CH$_o$), 3.88 (br m, 1H, CH$_e$), 3.70-3.60 (m, 2H,

C$\underline{H}_i$), 2.72-2.69 (m, 2H, C$\underline{H}_c$), 2.22 (t, 2H, J = 7.1 Hz, C$\underline{H}_j$), 1.82-1.74 (m, 2H, C$\underline{H}_n$), 1.50-1.43 (m, 2H, C$\underline{H}_k$), 1.31-1.20 (m, 50H, C$\underline{H}_h$ & C$\underline{H}_2$-alkyl), 0.84 (s, 9H, C$\underline{H}_h$), 0.03 (s, 3H, C$\underline{H}_g$), 0.02 (s, 3H, C$\underline{H}_g$); ^{13}C NMR (100 MHz, CDCl$_3$): δ = 173.4 (s, $\underline{C}$O$_2$R), 172.2 (s, NH$\underline{C}$O), 169.3 (s, NH$\underline{C}$O), 166.5 (s, NH$_E\underline{C}$O), 166.3 (s, NH$_E\underline{C}$O), 158.6 (s, Ar$\underline{C}$-ipso), 152.0 (s, Ar$\underline{C}$-meta), 138.3 (s, Ar$\underline{C}$-ipso), 137.3 (s, Ar$\underline{C}$-ipso-xylylene), 137.0 (s, Ar$\underline{C}$-ipso-xylylene), 134.2 (s, Ar$\underline{C}$-ipso-isophthaloyl), 133.2 (s, Ar$\underline{C}$-ipso-isophthaloyl), 131.8 (d, Ar$\underline{C}_B$), 131.4 (d, Ar$\underline{C}_C$), 129.2 (d, Ar$\underline{C}_A$), 129.0 (d, Ar$\underline{C}$-stopper) 128.3 (d, Ar$\underline{C}$-stopper), 128.3 (d, Ar$\underline{C}$-xylylene), 127.8 (d, Ar$\underline{C}$-stopper) 123.7 (d, Ar$\underline{C}$-xylylene), 114.7 (d, Ar$\underline{C}$H$_r$), 108.7 (d, Ar$\underline{C}$H$_p$), 67.7 (t, $\underline{C}$H$_o$), 61.8 (t, $\underline{C}$H$_f$), 61.3 (t, $\underline{C}$H$_i$), 58.3 (d, $\underline{C}$H$_a$), 50.8 (d, $\underline{C}$H$_e$), 44.1 (d, $\underline{C}$H$_E$), 42.2 (t, $\underline{C}$H$_c$), 34.9 (s, $\underline{C}$(CH$_q$)), 33.9 (t, -$\underline{C}$H$_2$-), 31.4 (q, $\underline{C}$H$_q$), 29.5 (t, -$\underline{C}$H$_2$-), 29.4 (t, -$\underline{C}$H$_2$-), 29.2 (t, -$\underline{C}$H$_2$-), 29.1 (t, -$\underline{C}$H$_2$-), 29.0 (t, -$\underline{C}$H$_2$-), 29.0 (t, -$\underline{C}$H$_2$-), 28.8 (t, -$\underline{C}$H$_2$-), 28.7 (t, -$\underline{C}$H$_2$-), 26.1 (t, -$\underline{C}$H$_2$-), 25.7 (q, $\underline{C}$H$_h$), 24.6 (t, -$\underline{C}$H$_2$-), 18.2 (s, $\underline{C}$(CH$_h$)), -5.3 (q, $\underline{C}$H$_g$); LRMS (FAB+ mNBA matrix) m/z (rel. int.): 1375 (7.6 %) [(M+H)$^+$], HRMS (FAB+) calcd for C$_{83}$H$_{107}$N$_6$O$_{10}$Si [(M+H)$^+$] 1375.7818. Found 1375.7804.

[2](1,7,14,20-Tetraaza-2,6,15,19-tetraoxo-3,5,9,12,16,18,22,25-tetrabenzocyclohexacosane)-diphenylacetylglycyl-3-hydroxy-1-(3,5-di-*tert*-butylphenoxy-1'-dodecanoxy)-propanol rotaxane (6)
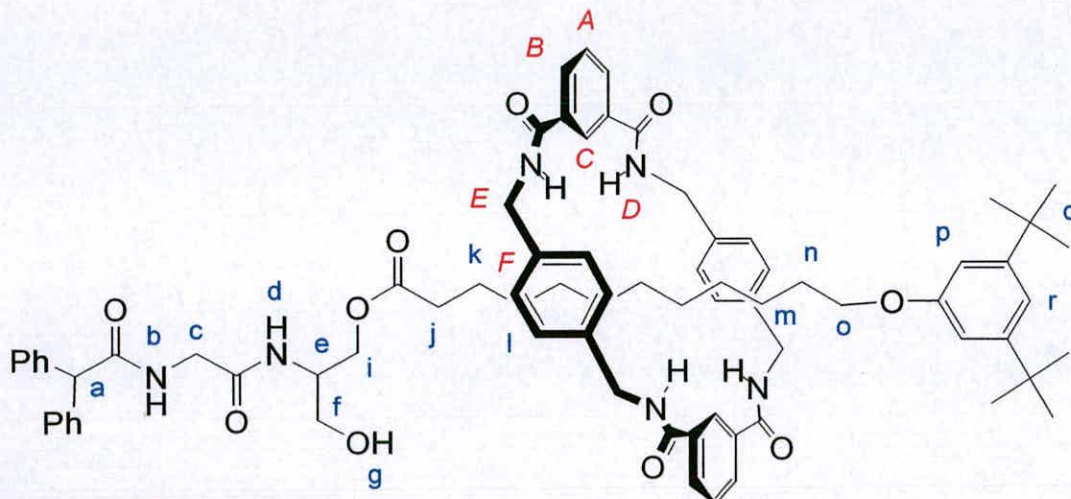
TBAF (75 mg, 0.24 mmol) was added dropwise to a stirred solution of *peptidyl*-**5** (300 mg, 0.22 mmol) in THF (2 mL) at room temperature. The reaction mixture was stirred at room temperature for 12 h. The reaction mixture was concentrated under reduced pressure and the residue was purified by column chromatography on silica gel using chloroform: methanol (99: 1) as eluent to give **6** as a colorless solid. Yield 261 mg (95 %); m.p. 250 °C (decomp); ^{1}H NMR (400 MHz, d_6-DMSO): δ = 8.74 (br t, 4H, N$\underline{H}_D$), 8.25 (br s, 1H, N$\underline{H}_b$), 8.07 (s, 2H, Ar$\underline{H}_C$), 7.94 (d, 4H, J = 7.8 Hz, Ar$\underline{H}_B$), 7.84 (d, 1H, J = 7.3 Hz, N$\underline{H}_d$), 7.52 (t, 2H, J = 7.8 Hz, Ar$\underline{H}_A$), 7.31-7.23 (m, 10H, Ar$\underline{H}$-stopper), 7.15 (s, 8H, Ar$\underline{H}_F$), 6.96 (t, 1H, J = 1.7 Hz, ArC$\underline{H}_r$), 6.72 (d, 2H, J = 1.7 Hz, ArC$\underline{H}_p$), 5.07 (s, 1H, C$\underline{H}_a$), 4.89 (t, 1H, J = 5.5 Hz, O$\underline{H}_g$), 4.43-4.28 (m, 8H, C$\underline{H}_E$), 3.97-3.85 (m, 3H, C$\underline{H}_e$ & C$\underline{H}_f$), 3.70 (t, 2H, J = 6.9 Hz, C$\underline{H}_o$), 3.64 (br s, 2H, C$\underline{H}_c$), 3.42-3.31 (m, 2H, C$\underline{H}_i$), 1.84 (t, 2H, J = 7.5 Hz, C$\underline{H}_j$), 1.36-1.26 (m, 22H, -C$\underline{H}_2$-alkyl & C$\underline{H}_q$), 1.10-0.98 (m, 2H, -C$\underline{H}_2$-alkyl), 0.85-0.78 (br m, 2H, -C$\underline{H}_2$-alkyl), 0.61 (br m, 4H, -C$\underline{H}_2$-alkyl). 0.51-0.45 (br m, 6H, -C$\underline{H}_2$-alkyl); ^{13}C (100 MHz, d_6-DMSO): δ = 173.5 (s, $\underline{C}$O$_2$R), 171.6 (s, NH$_b$$\underline{C}$O), 169.9 (s, NH$_d$$\underline{C}$O), 166.0 (s, NH$_E$$\underline{C}$O), 165.9 (s, NH$_E$$\underline{C}$O), 158.6 (s, Ar$\underline{C}$-ipso), 151.7 (s, Ar$\underline{C}$-meta), 140.5 (s, Ar$\underline{C}$-ipso), 138.2 (s, Ar$\underline{C}$-ipso-xylylene), 138.3 (s, Ar$\underline{C}$-ipso-

xylylene), 135.0 (s, Ar$\underline{C}$-ipso-isophthaloyl), 129.6 (d, Ar$\underline{C}_B$), 128.8 (d, Ar$\underline{C}_C$), 128.7 (d, Ar$\underline{C}_A$), 128.4 (d, Ar$\underline{C}$-stopper), 128.3 (d, Ar$\underline{C}$-stopper), 128.3 (d, Ar$\underline{C}$-xylylene), 127.2 (d, Ar$\underline{C}$-xylylene), 126.9 (d, Ar$\underline{C}$-stopper), 114.1 (d, Ar$\underline{C}$H$_r$), 108.9 (d, Ar$\underline{C}$H$_p$), 67.5 (t, $\underline{C}$H$_o$), 62.8 (t, $\underline{C}$H$_f$), 60.2 (t, $\underline{C}$H$_h$), 56.4 (d, $\underline{C}$H$_a$), 50.0 (d, $\underline{C}$H$_e$), 42.9 (t, $\underline{C}$H$_E$), 42.3 (t, $\underline{C}$H$_c$), 34.8 (s, $\underline{C}$(CH$_3$)$_3$), 33.4 (s, $\underline{C}$(CH$_q$)), 31.5 (q, $\underline{C}$H$_q$), 29.2 (t, -$\underline{C}$H$_2$-), 29.1 (t, -$\underline{C}$H$_2$-), 29.1 (t, -$\underline{C}$H$_2$-), 29.0 (t, -$\underline{C}$H$_2$-), 28.9 (t, -$\underline{C}$H$_2$-), 28.8 (t, -$\underline{C}$H$_2$-), 28.7 (t, -$\underline{C}$H$_2$-), 28.5 (t, -$\underline{C}$H$_2$-), 25.6 (t, -$\underline{C}$H$_2$-), 24.4 (t, -$\underline{C}$H$_2$-); LRMS (FAB+ mNBA matrix) *m/z* (rel. int.): 1261 (42.0 %) [(M+H)$^+$], HRMS (FAB+) calcd for C$_{77}$H$_{93}$N$_6$O$_{10}$ [(M+H)$^+$] 1261.6953. Found 1261.6931.

[2](1,7,14,20-Tetraaza-2,6,15,19-tetraoxo-3,5,9,12,16,18,22,25-tetrabenzocyclohexacosane)-diphenylacetylglycyl-3-(dimethyl-*tert*-butylsiloxy)-1-(3,5-di-*tert*-butylphenoxy-1'-dodecanoxy) propanol rotaxane (*alkyl*-5)
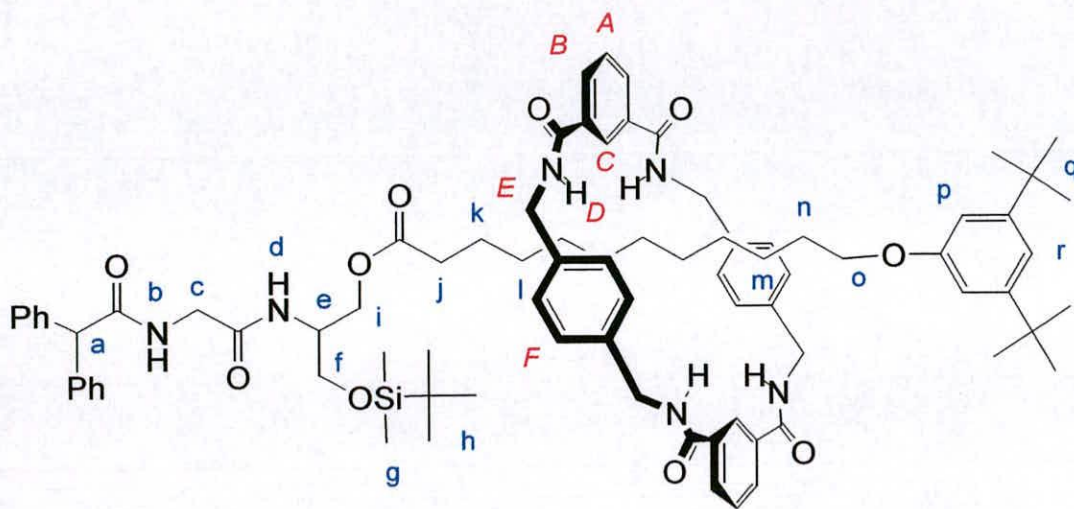
tert-Butyldimethylsilyl chloride (60 mg, 0.396 mmol) was added to a stirred solution of **6** (250 mg, 0.198 mmol) in anhydrous DMSO (3.00 mL) at room temperature, under an atmosphere of nitrogen. Imidazole (50 mg, 0.792 mmol) was then added and the reaction mixture was then stirred at room temperature for 18 h. The reaction mixture was treated with water (10 mL) and the resulting precipitate was filtered. The filtrate was purified by column chromatography on silica gel using chloroform: methanol (99: 1) as eluent to give *alkyl*-5 as a colorless solid. Yield 230 mg (85 %); m.p. 210 °C; ^{1}H NMR (400 MHz, CDCl$_3$): δ = 8.14 (d, 2H, *J* = 7.8 Hz, ArH$_B$), 7.98 (d, 2H, *J* = 7.8 Hz, ArH$_B$), 7.97 (s, 2H, ArH$_C$), 7.58 (br t, 2H, *J* = 6.3 Hz, NH$_D$), 7.55 (t, 2H, *J* = 7.8 Hz, ArH$_A$), 7.25-7.19 (m, 10H, ArH-stopper), 7.14 (d, 4H, *J* = 8.0 Hz, ArH$_F$), 7.09 (d, 4H, *J* = 8.0 Hz, ArH$_F$), 6.98 (t, 1H, *J* = 1.5 Hz, ArH$_r$), 6.93-6.88 (m, 2H, overlapping NH$_b$ & NH$_d$), 6.83 (br t, 2H, *J* = 5.5 Hz, NH$_D$), 6.73 (d, 2H, *J* = 1.5 Hz, ArCH$_p$), 4.85 (s, 1H, CH$_a$), 4.83 (dd, 2H, *J* =14.5 Hz, *J* = 6.8 Hz, CH$_E$), 4.46-4.41 (m, 4H, CH$_E$), 4.10 (dd, 2H, *J* = 14.5 Hz, *J* = 4.3 Hz, CH$_E$), 4.02 (dd, 1H, *J* = 16.6 Hz, *J* = 5.3 Hz, CH$_f$H), 3.92 (t, 2H, *J* = 6.5 Hz, CH$_o$), 3.90- 3.78 (m, 2H, CHH$_c$ & CH$_e$), 3.61- 3.55 (dd, 1H, *J* = 16.6 Hz, *J* = 5.3 Hz, CHH$_f$), 3.46-3.41 (m, 2H, CH$_i$), 3.05 (t, 1H, *J* = 11.3 Hz, CHH$_c$), 1.74-1.72 (m, 2H, CH$_n$), 1.43-1.38 (m, 2H, -CH$_2$-

alkyl), 1.38-1.23 (m, 22H, C$\underline{H}_q$ & -C$\underline{H}_2$-alkyl), 1.15-1.09 (m, 2H, -C$\underline{H}_2$-alkyl), 1.00-0.95 (m, 2H, -C$\underline{H}_2$-alkyl), 0.85 (s, 9H, C$\underline{H}_h$), 0.83-0.79 (m, 2H, -C$\underline{H}_2$-alkyl), 0.60-0.55 (m, 4H, -C$\underline{H}_2$-alkyl), 0.50- 0.47 (m, 2H, -C$\underline{H}_2$-alkyl), 0.01 (s, 3H, C$\underline{H}_g$), 0.00 (s, 3H, C$\underline{H}_g$); ^{13}C NMR (100 MHz, CDCl$_3$): δ = 176.0 (s, $\underline{C}$O$_2$R), 173.1 (s, NH$\underline{C}$O), 169.9 (s, NH$\underline{C}$O), 166.9 (s, NH$_E\underline{C}$O), 166.1 (s, NH$_E\underline{C}$O), 158.6 (s, Ar$\underline{C}$-ipso), 152.1 (s, Ar$\underline{C}$-meta), 139.0 (s, Ar$\underline{C}$-ipso), 138.2 (s, Ar$\underline{C}$-ipso-xylylene), 137.2 (s, Ar$\underline{C}$-ipso-xylylene), 134.6 (s, Ar$\underline{C}$-ipso-isophthaloyl), 134.2 (s, Ar$\underline{C}$-ipso-isophthaloyl), 131.8 (d, Ar$\underline{C}_B$), 130.4 (d, Ar$\underline{C}_C$), 129.3 (d, Ar$\underline{C}_A$), 128.8 (d, Ar$\underline{C}$-stopper) 128.7 (d, Ar$\underline{C}$-stopper), 127.8 (d, Ar$\underline{C}$-stopper) 127.4 (d, Ar$\underline{C}$-xylylene), 123.9 (d, Ar$\underline{C}$-xylylene), 114.8 (d, Ar$\underline{C}_r$), 108.8 (d, Ar$\underline{C}_p$), 67.7 (t, $\underline{C}$H$_o$), 64.6 (t, $\underline{C}$H$_i$), 62.3 (t, $\underline{C}$H$_f$), 58.6 (d, $\underline{C}$H$_a$), 50.1 (d, $\underline{C}$H$_e$), 43.9 (t, $\underline{C}$H$_c$), 43.5 (d, $\underline{C}$H$_E$), 35.0 (s, $\underline{C}$(CH$_h$)), 32.8 (t, $\underline{C}$H$_j$), 31.4 (q, $\underline{C}$H$_h$), 29.7 (t, -$\underline{C}$H$_2$-), 29.5 (t, -$\underline{C}$H$_2$-), 29.5 (t, -$\underline{C}$H$_2$-), 29.4 (t, -$\underline{C}$H$_2$-), 29.2 (t, -$\underline{C}$H$_2$-), 28.9 (t, -$\underline{C}$H$_2$-), 28.4 (t, -$\underline{C}$H$_2$-), 26.1 (t, -$\underline{C}$H$_2$-), 25.7 (q, ($\underline{C}$H$_h$)), 23.7 (t, -$\underline{C}$H$_2$-), 18.2 (s, $\underline{C}$(CH$_h$)), -5.5 (q, $\underline{C}$H$_g$); LRMS (FAB+ mNBA matrix) *m/z* (rel. int.): 1375 (4.1 %) [(M+H)$^+$], HRMS (FAB+) calcd for C$_{83}$H$_{107}$N$_6$O$_{10}$Si [(M+H)$^+$] 1375.7818. Found 1375.7811.

3,5-di-*tert*-butyl methyl benzoate (S7)
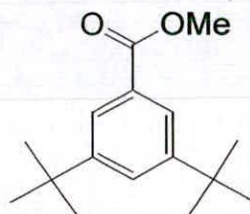
This compound was prepared as described in J. Hung, A. P. Cole, R. M. Waymouth, *Macromolecules* **2003**, *36*, 2454-2463; and showed identical spectroscopic data to that reported therein.

3,5-di-*tert*-butylbenzyl alcohol (S8)[2]
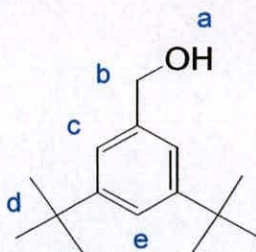
DIBAL-H (1.5 M solution in toluene, 15.3 mL, 23.0 mmol) was added dropwise over 10 min at −78 °C, under an atmosphere of nitrogen to a stirred solution of **S7** (1.90 g, 7.66 mmol) in anhydrous toluene (100 mL). The reaction was stirred at −78 °C for 3 h and then at room temperature for 10 h. The reacton mixture was cooled to 0 °C and the treated with methanol (2 mL), and 10% aqueous citric acid (50 mL). The organic layer was separated and the aqueous layer was washed with toluene (3 x 20 mL). The combined organic layers were washed with saturated aqueous sodium chloride (2 x 20 mL), dried (MgSO$_4$) and concentrated under reduced pressure to yield **S8** as a colorless solid. Yield 1.60 g (95 %); m.p. 52-53 °C (Lit: m.p. 52-53 °C); ^{1}H NMR (400 MHz, CDCl$_3$): δ = 7.43 (s, 1H, Ar<u>H</u>-para), 7.27 (s, 2H, Ar<u>H</u>-ortho), 4.69 (d, 2H, J = 5.8 Hz, C<u>H</u>$_b$), 2.24 (t, 1H, J = 5.8 Hz, O<u>H</u>$_a$), 1.39 (s, 18H, C<u>H</u>$_d$); ^{13}C NMR (100 MHz, CDCl$_3$): δ = 151.0 (s, Ar<u>C</u>-ipso), 139.9 (s, Ar<u>C</u>-meta), 121.6 (d, Ar<u>C</u>), 121.3 (d, Ar<u>C</u>), 65.9 (t, <u>C</u>H$_b$), 34.1 (s, <u>C</u>(CH$_d$)), 31.4 (q, <u>C</u>H$_d$); LRMS (FAB+ mNBA matrix) *m/z* (rel. int.): 220 (70.9 %) [(M+H)$^+$], HRMS (FAB+) calcd for C$_{15}$H$_{24}$O [(M+H)$^+$] 220.1827. Found 220.1825.

**([2](1,7,14,20-Tetraaza-2,6,15,19-tetraoxo-3,5,9,12,16,18,22,25-tetrabenzocyclohexacosane)-3,5-di-*tert*-butylbenzyl-12'-(3,5-di-*tert*-butylphenoxy)dodecanoate rotaxane (1)**
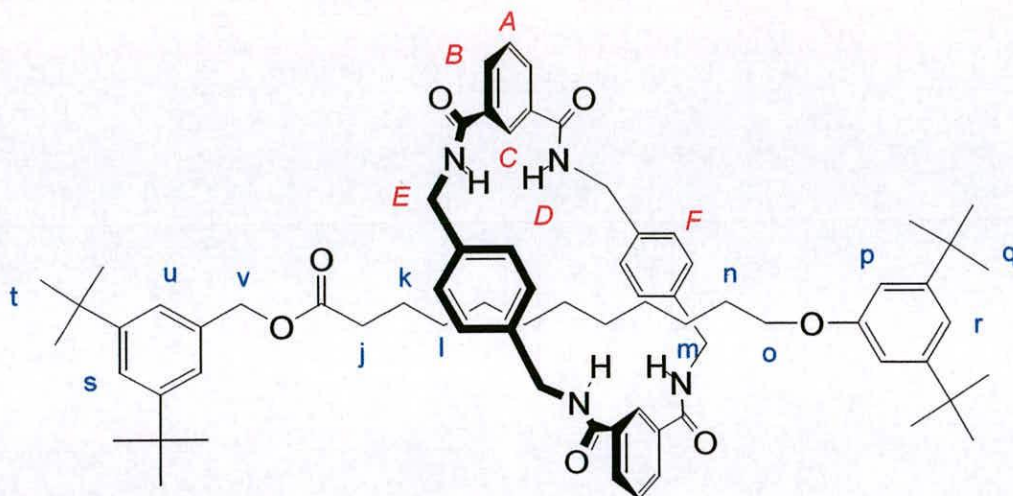
A melt of **S8** (698 mg, 3.17 mmol), *alkyl*-**5** (218 mg, 0.16 mmol), and a catalytic amount of potassium *tert*-butoxide (5 mol%) was heated with vigorous stirring at 65 °C under argon for 3 hours. The reaction was allowed to cool to room temperature and the remaining residue was purified by column chromatography on silica gel using chloroform: methanol (100: 1) as eluent to give **1** as a colorless solid. 114 mg (78 %); m.p. 150-152 °C; ^{1}H NMR (400 MHz, CDCl$_3$) δ = 8.22 (dd, 4H, J = 7.8 Hz, J = 0.9 Hz, ArH$_B$), 7.98 (s, 2H, ArH$_C$), 7.60 (t, 2H, J = 7.8 Hz, ArH$_A$), 7.41 (t, 1H, J = 1.6 Hz, ArH$_s$), 7.14 (s, 8H ArH$_F$), 7.10 (d, 2H, J = 1.6 Hz, ArH$_u$), 7.02 (t, 1H, J = 1.5 Hz, ArH$_r$), 6.74 (d, 2H, J = 1.5 Hz, ArH$_p$), 6.60 (br t, 4H, NH$_D$), 4.68 (dd, 4H, J = 14.2 Hz, J = 5.8 Hz, CH$_E$), 4.49 (s, 2H, CH$_v$), 4.34 (dd, 4H, J = 14.2 Hz, J = 5.8 Hz, CH$_E$), 3.85 (t, 2H, J = 6.6 Hz, CH$_o$), 1.71-1.67 (m, 2H, CH$_n$), 1.31-1.18 (m, 44H, CH$_q$, CH$_t$ & -CH$_2$-alkyl), 1.12-0.85 (m, 14H, -CH$_2$-alkyl); ^{13}C NMR (100 MHz, CDCl$_3$): δ = 175.2 (s, $\underline{C}$O$_2$R), 165.9 (s, NH$_E\underline{C}$O), 158.5 (s, Ar$\underline{C}$-ipso), 152.1 (s, Ar$\underline{C}$-meta), 151.8 (s, Ar$\underline{C}$-meta) 137.3 (s, Ar$\underline{C}$-ipso-xylylene), 133.9 (s, Ar$\underline{C}$-ipso-isophthaloyl), 133.4 (s, Ar$\underline{C}$-ipso-isophthaloyl), 131.8 (d, Ar$\underline{C}_B$), 129.6 (d, Ar$\underline{C}_C$), 128.9 (d, Ar$\underline{C}_A$), 123.8, (d, Ar$\underline{C}_F$), 123.2 (d, Ar$\underline{C}_s$), 122.5 (d, Ar$\underline{C}_u$), 114.8(d, Ar$\underline{C}_r$), 108.7 (d, Ar$\underline{C}_p$), 67.7 (t, $\underline{C}$H$_o$), 66.1 (t, $\underline{C}$H$_d$), 44.2 (t, $\underline{C}$H$_E$), 34.9 (s, ($\underline{C}$(CH$_q$) or ($\underline{C}$(CH$_t$)), 34.8 (s, ($\underline{C}$(CH$_q$) or ($\underline{C}$(CH$_t$)), 33.1 (t, $\underline{C}$H$_j$), 31.4 (q, $\underline{C}$H$_t$ or $\underline{C}$H$_q$), 31.3 (q, $\underline{C}$H$_t$ or $\underline{C}$H$_q$), 29.4 (t, -$\underline{C}$H$_2$-), 29.3 (t, -$\underline{C}$H$_2$-), 29.2 (t, -$\underline{C}$H$_2$-), 29.0 (t, -$\underline{C}$H$_2$-), 28.7 (t, -

$\underline{C}H_2$-), 26.1 (t, -$\underline{C}H_2$-), 24.1 (t, -$\underline{C}H_2$-); LRMS (FAB+ mNBA matrix) *m/z* (rel. int.): 1140 (3.3 %) [(M+H)$^+$], HRMS (FAB+) calcd for $C_{73}H_{95}N_4O_7$ [(M+H)$^+$] 1139.7201. Found 1139.7204.

X-ray crystallographic structure determination, crystals of rotaxane grown in MeCN, 1: $C_{77}H_{100}N_6O_7$, $M = 1221.63$, colourless prism, crystal size $0.08 \times 0.02 \times 0.01$ mm, monoclinic, C_c, $a = 10.9589(6)$, $b = 66.995(4)$, $c = 9.8620(6)$ Å, $\beta = 103.6410(10)°$, $V = 7036.3(7)$ Å^3, $Z = 4$, $\rho_{calcd} = 1.153$ mg m^{-3}; Mo$_{K\alpha}$ radiation (graphite monochromator, $\lambda = 0.68750$ Å), $\mu = 0.074$ mm^{-1}, $T = 293(2)$ K. 23039 data (13981 unique, $R_{int} = 0.1597$, $1.18 < \theta < 20.88°$), were collected on a Siemens SMART CCD diffractometer using narrow frames ($0.3°$ in ω), and were corrected semiempirically for absorption and incident beam decay. The structure was solved by direct methods and refined by full-matrix least-squares on F^2 values of all data (G. M. Sheldrick, SHELXTL manual, Siemens Analytical X-ray Instruments, Madison WI, USA, 1994, version 5) to give $wR = \{\Sigma[w(F_o^2-F_c^2)^2]/\Sigma[w(F_o^2)^2]\}^{1/2} = 0.2997$, conventional $R = 0.0991$ for F values of 13931 reflections with $F_o^2 > 2\sigma(F_o^2)$, $S = 0.796$ for 814 parameters. Residual electron density extremes were 0.314 and -0.398 eÅ^{-3}. Amide hydrogen atoms were refined isotropically with the remainder constrained; anisotropic displacement parameters were used for all non-hydrogen atoms.

3,5-di-*tert*-butylbenzyl-12'-(3,5-di-*tert*-butylphenoxy)dodecanoate (*thread*-1)
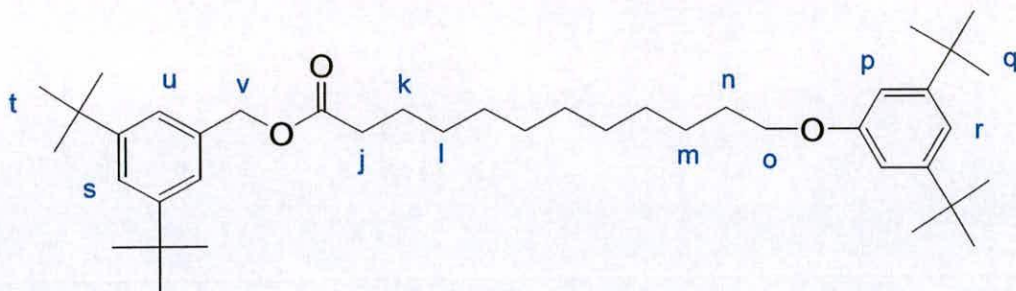
EDCI (80.0 mg, 0.417 mmol) and 4-DMAP (4 mg, 10 mol %) were added to a stirred solution of **3** (137 mg, 0.339 mmol) and **S7** (80.0 mg, 0.364 mmol) in dichloromethane (10 mL) at 0 °C. The reaction mixture was then stirred at room temperature for 14 h. The reaction mixture was then washed with 1 M aqueous hydrochloric acid (3 x 20 mL) saturated aqueous sodium hydrogen carbonate (3 x 20 mL) and saturated aqueous sodium chloride (2 x 10 mL), dried (MgSO₄) and concentrated under reduced pressure. The remaining residue was purified by column chromatography on silica gel using petroleum ether 40-60 °C: ethyl acetate (5: 1) as eluent to give *thread*-**1** as a colorless oil. Yield 200 mg (97 %); ^{1}H NMR (400 MHz, CDCl₃): δ = 7.45 (t, 1H, J = 1.7 Hz, Ar$\underline{H}_s$), 7.24 (d, 2H, J = 1.7 Hz, Ar$\underline{H}_u$), 7.05 (t, 1H, J = 1.7 Hz, Ar$\underline{H}_r$), 6.80 (d, 2H, J = 1.7 Hz, Ar$\underline{H}_p$), 5.15 (s, 2H, C$\underline{H}_v$), 3.99 (t, 2H, J = 6.5 Hz, C$\underline{H}_o$), 2.41 (t, 2H, J = 7.5 Hz, C$\underline{H}_j$), 1.86- 1.79 (m, 2H, C$\underline{H}_n$), 1.72-1.67 (m, 2H, C$\underline{H}_k$), 1.53-1.46 (m, 2H, C$\underline{H}_m$), 1.40-1.21 (m, 48H, C$\underline{H}_t$, C$\underline{H}_q$ & -C$\underline{H}_2$-alkyl); ^{13}C NMR (100 MHz, CDCl₃): δ = 173.4 (s, $\underline{C}$O₂CH₃), 158.6 (s, Ar$\underline{C}$-ipso), 152.0 (s, Ar$\underline{C}$-meta), 151.0 (s, Ar$\underline{C}$-meta), 135.1 (s, Ar$\underline{C}$-ipso), 122.5 (d, ArH_s), 122.3 (d, ArH_u), 114.7 (d, ArH_r), 108.8 (d, ArH_p), 67.7 (t, $\underline{C}H_o$), 66.8 (t, $\underline{C}H_v$), 34.9 (s, $\underline{C}$(CH$_t$) or $\underline{C}$(CH$_q$)), 34.8 (s, $\underline{C}$(CH$_t$) or $\underline{C}$(CH$_q$)), 34.4 (t, $\underline{C}H_j$), 31.4 (q, $\underline{C}H_t$ or $\underline{C}H_q$), 31.4 (q, $\underline{C}H_t$ or $\underline{C}H_q$), 29.7 (t, -$\underline{C}H_2$-), 29.5 (t, -$\underline{C}H_2$-), 29.5 (t, -$\underline{C}H_2$-), 29.4 (t, -$\underline{C}H_2$-), 29.4 (t, -$\underline{C}H_2$-), 29.3 (t, -$\underline{C}H_2$-), 29.1 (t, -$\underline{C}H_2$-), 26.1 (t, -$\underline{C}H_2$-), 25.0 (t, -$\underline{C}H_2$-); LRMS (FAB+ mNBA matrix) *m/z* (rel. int.): 607 (16.2 %) [(M+H)$^+$], HRMS (FAB+) calcd for C₄₁H₆₆O₃ [(M+H)$^+$] 606 5012. Found 606.5011.

3.5 Experimental References

1   H. Nakatomi, K. Ando, M. Kawasaki, B. Yasui, Y. Miki, S. Takemura, *Chem. Pharm. Bull.* **1979**, *27*, 1021-1029.

2   A. Thomas, G. Anikumar, V. Nair, *Tetrahedron* **1996**, *52*, 2481-2488.

CHAPTER FOUR

A Second Generation Mechanically Interlocking Auxiliary

Prepared for submission for Organic Letters as:

Controlled Submolecular Translational Motion in Synthesis: A Second Generation Mechanically Interlocking Auxiliary"

Jeffrey S. Hannam and David A Leigh.

"I have not failed I have just found 10,000 ways that won't work"

Thomas Alva Edison

4.0 Introduction

The synthesis of mechanically interlocked molecules (such as catenanes and rotaxanes) is a key goal in contemporary synthetic chemistry.[1] Rotaxanes and catenanes are desirable targets as the *mechanical* bond associated with such architectures offers potential and presents opportunities unavailable to conventional covalent structures.[2]

Early syntheses of rotaxanes relied on either directed[3] or statistical approaches,[4] but both afforded trace amounts of the requisite interlocked products. The advent of supramolecular chemistry has led to the use of template-directed synthesis, to efficiently construct rotaxanes, relying on non-covalent recognition sites between interacting components. A number of recognition motifs are currently available in the synthetic chemist's armoury, these include the use of metal ion coordination,[5] π-electron donor / π-electron acceptors[6] and hydrogen bonding,[7,8,9] to name but a few.[10] However, these strategies require recognition elements to be built into each noncovalently-linked unit to provide the intercomponent "glue" during the assembly process, thus inherently restricting both the types of structures that can be interlocked and often the chemistry that such molecules can undergo.

One of the most striking features of rotaxane architectures is that their mechanically interlocked components can move relative to one another without breaking covalent bonds. Controlling the location of a macrocycle between two or more nonequivalent sites ("stations") on a linear thread has been achieved in "molecular shuttles"[11] – molecules with moving parts which are seen as possible components of "nanoscale machinery".[12]

We recently described the principle and function of a mechanically interlocking auxiliary (Chapter 3), based on solvent dependent translational isomerism observed in a series of amphiphilic rotaxanes.[13] This strategy enabled the synthesis of a rotaxane whose components bear no formal mutual recognition elements in the first example of controlled sub-molecular translational motion in organic synthesis. A potential

weakness of the strategy is the relatively low yield for the formation of the benzylic amide macrocycle-containing rotaxane and we cogitated that the overall yield could be improved by replacement of the original hydrogen bond template (based on glycyl-serinol) with the a more efficient macrocycle template motif.

Here we report our results and observations on using a second generation mechanically interlocking auxiliary based on a fumaramide template motif[14] to prepare rotaxane **1** whose components bear no formal mutual recognition elements.

4.1 Results and Discussion

Despite the promise of an improved yield in the rotaxane formation step, the general protocol when using a fumaramide auxiliary would include an extra step (Scheme 4.1- step c). This is because the macrocycle in such systems is maintained on the template motif even in highly polar solvents, such as DMSO,[15] however, the fumaramide motif contains a photoswitchable double bond, the isomerization ($E \rightarrow Z$) of which results in a profound weakening of the interaction between macrocycle and thread. The isomerization ($E \rightarrow Z$) of the fumaramide template has been exploited in benzylic amide macrocycle-containing rotaxanes to affect large amplitude motions in such systems.[16]
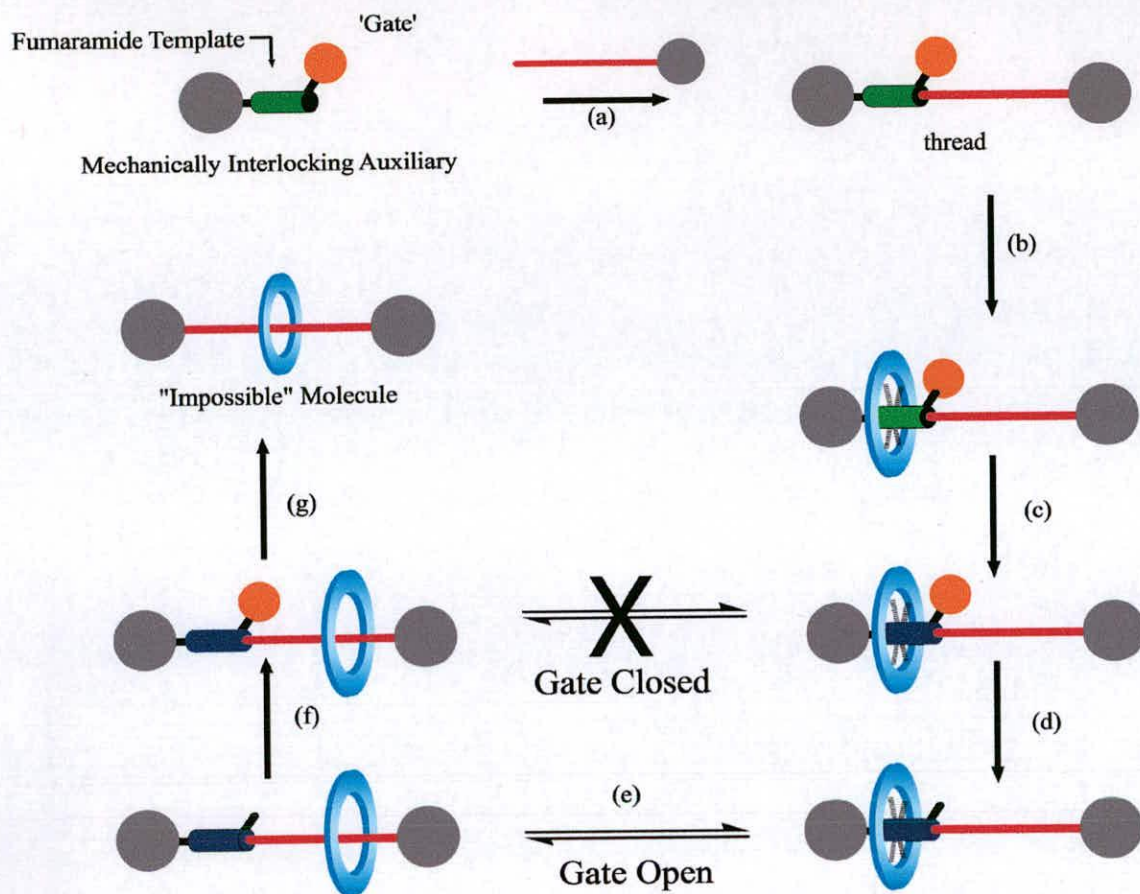
Scheme 4.1. Schematic preparation of an otherwise difficult or impossible to obtain rotaxane using a second generation mechanically interlocking auxiliary: (a) attach substrate to auxiliary; (b) formation of rotaxane about template; (c) isomerization ($E{\rightarrow}Z$); (d) open gate; (e) shuttle macrocycle from template to substrate; (f) close gate; (g) cleave auxiliary.

The second generation mechanically interlocking auxiliary **2** (Scheme 4.2) consists of a fumaramide template group appended with a mono-silylated serinol similar to that used in the original glycine-based system.[17] The coupling of the fumaramide-based auxiliary to the undecanoic acid **3** afforded composite thread **4**, which was subjected to standard hydrogen bond-directed rotaxane forming conditions to give the [2]rotaxane **5** in a 62 % yield.
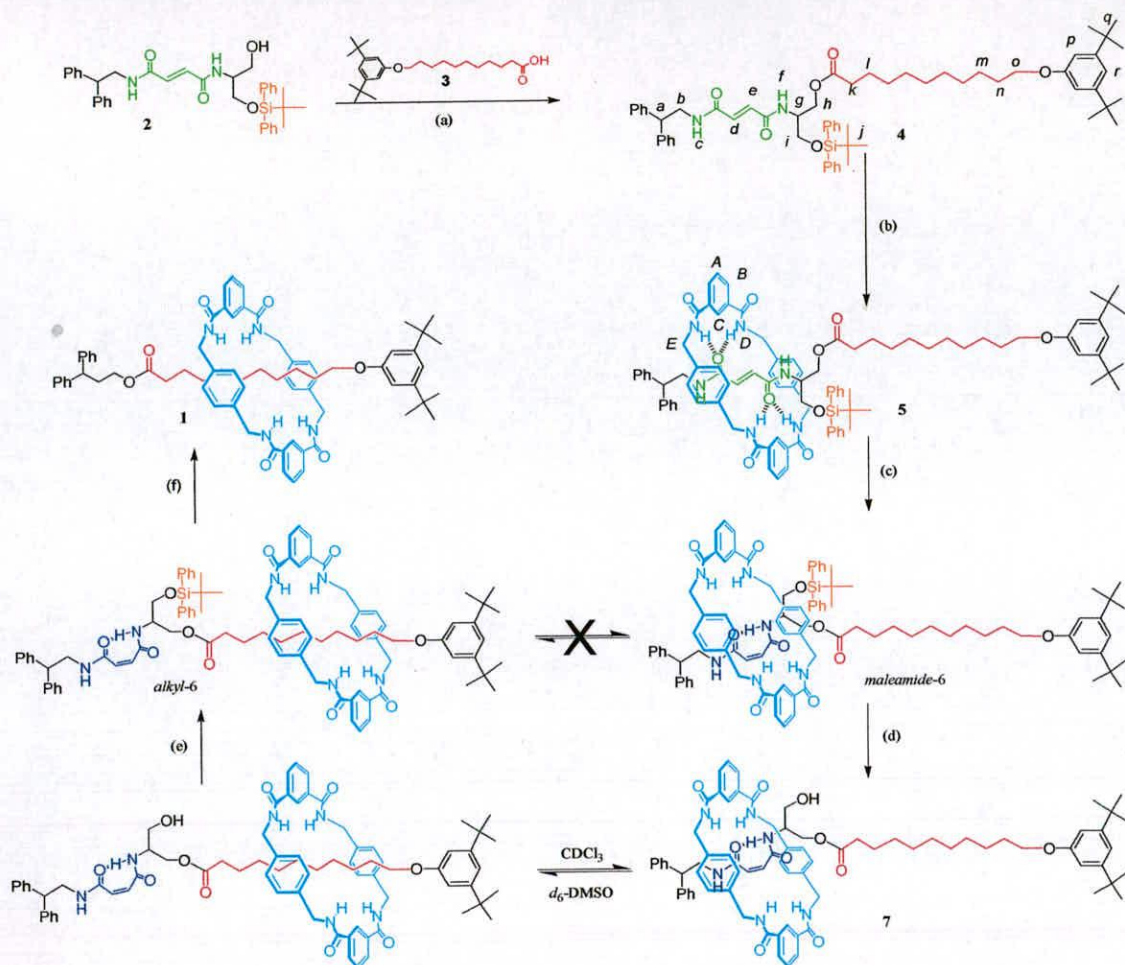
Scheme 4.2. Synthesis of rotaxane **1**: (a) 1-(3-dimethylaminopropyl)-3-ethyl-carbodiimide hydrochloride, 4-DMAP, CH_2Cl_2, 93 %; (b) isophthaloyl dichloride, *p*-xylylenediamine, Et_3N, $CHCl_3$, 62 %; (c) hυ 254nm, 20 min, 49 %; (d) tetrabutylammonium fluoride, THF, 98 %; (e) *tert*-butylphenylsilyl chloride, imidazole, 4-DMAP, DMSO, 78 %; (f) 3,3-diphenylpropanol, potassium *tert*-butoxide (5 mol %), 81 %.

The interlocked structure of **5** was confirmed by inspection of the ¹H NMR spectra of **5** in d_6-DMSO (Figure 4.1b) and $CDCl_3$ (Figure 4.1d) both show shielding (-1.32 ppm in both solvents) of the fumaryl-protons (H_d, H_e) compared to the corresponding thread **5** (Figures 4.1a and 4.1c). This is characteristic of benzylic amide macrocycle-containing [2]rotaxanes where aromatic ring currents in the *p*-xylylene rings result in significant upfield shifting ($\Delta\delta_H > 1$ ppm) of protons on the portion of the thread covered by the macrocycle.[18]
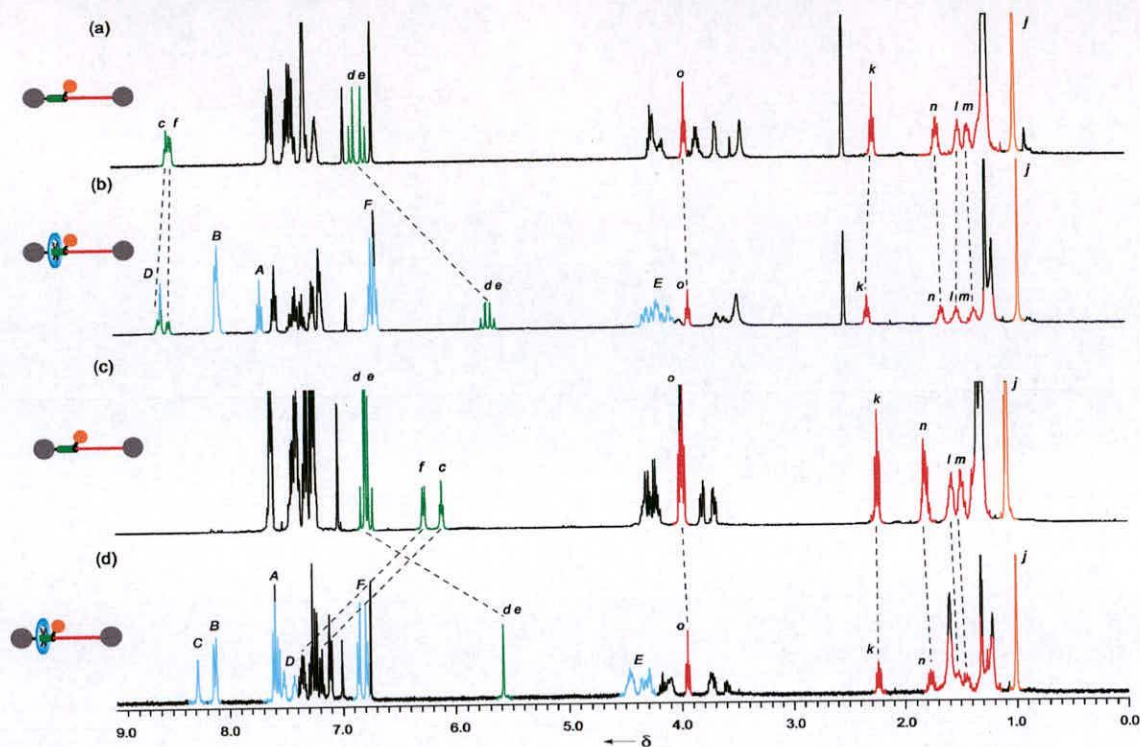
Figure 4.1. 400 MHz ^{1}H NMR spectra of (a) **4**, (b) [2]rotaxane **5** in d_6-DMSO and (c) **4**, and (d) [2]rotaxane **5** in CDCl$_3$ both at 298K. The color coding and lettering correspond to the assignments shown in Scheme 4.2.

Satisfied with the increased yield of the composite [2]rotaxane **5** derived from our fumaramide-based auxiliary **2**, we then came to the second crucial step in Scheme 4.1, i.e. the isomerization of the *E*-olefin in the fumaramide-containing [2]rotaxane to the corresponding *Z*-olefin (step (c)). Initially we attempted the direct irradiation of **5** at 254 nm in CH$_2$Cl$_2$ (20 min), which afforded *maleamide*-**6** in 49 % yield. Unfortunately attempts to affect the isomerization (*E*→*Z*) using catalytic benzophenone, irradiating at 350 nm only gave trace amounts of *maleamide*-**6**.
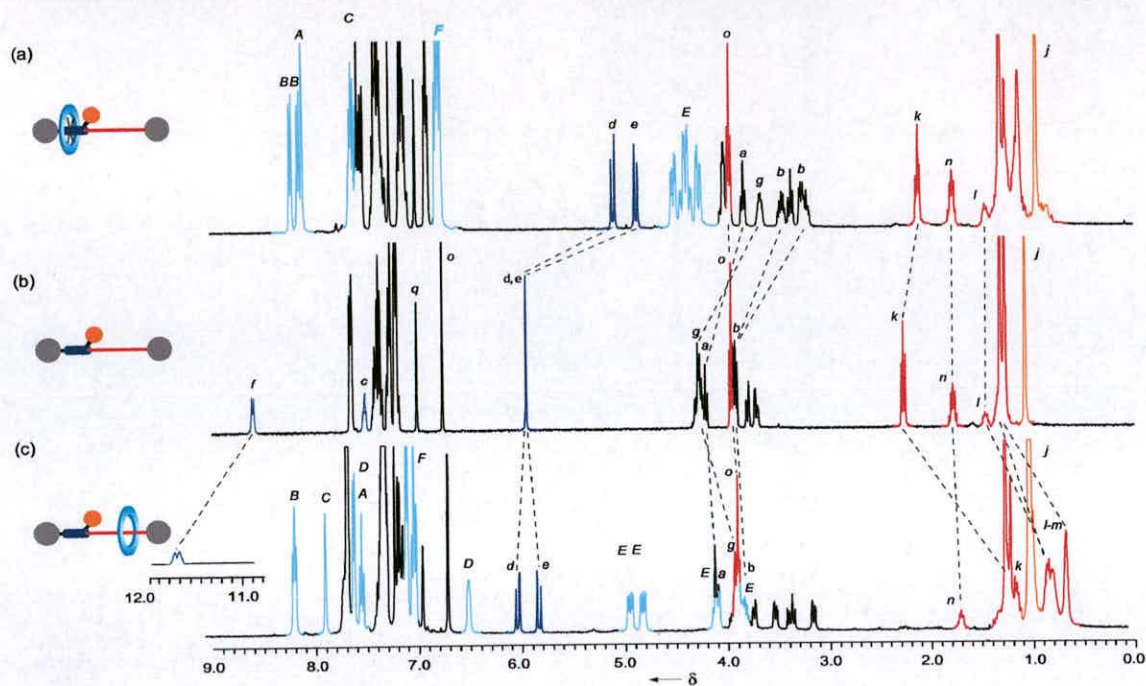
Figure 4.2. 400 MHz ^{1}H NMR spectra of (a) *maleamide*-**6**, (b) *thread*-**6**, and (c) *alkyl*-**6** in CDCl$_3$ at 298K.

Analysis of the ^{1}H NMR spectra of *maleamide*-**6** (Figure 4.2a) in CDCl$_3$ and d_6-DMSO (Figure 4.3a) again shows shielding of the double bond protons (H$_d$ and H$_e$) when compared to the thread (Figures 4.2b and 4.3b). In addition the alkyl chain protons (shown in red) suffer little or no shielding; indicating that the gate function is preventing translational motion across the thread.
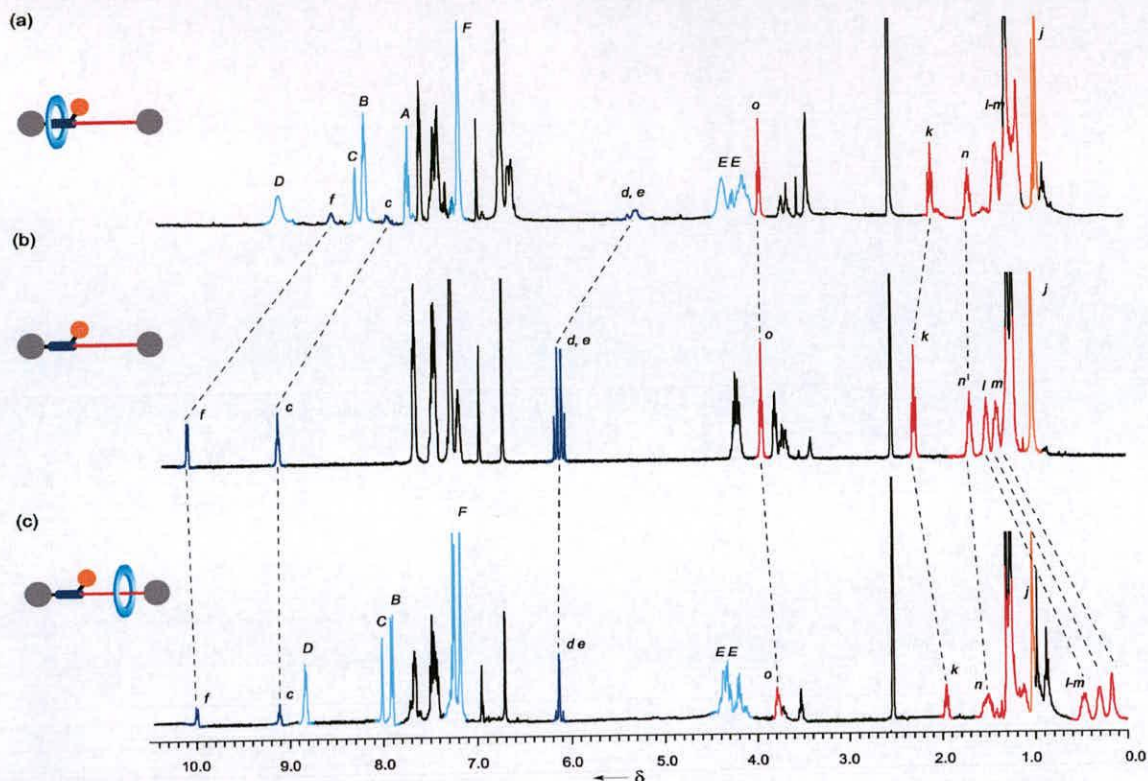
Figure 4.3. 400 MHz ^{1}H NMR spectra of (a) *maleamide-6*, (b) *thread-6*, and (c) *alkyl-6* in d_6-DMSO at 298K.

The cleavage of the silyl group of *maleamide-6* with *tetra*-butylammonium fluoride gave **7** in excellent yield. At this point, we decided to study the translational isomerism (Figure 4.1-step e) of open gate rotaxane **7** in a number of solvents, with varying hydrogen bonding abilities. Due to the shielding experienced by the portions of thread over which the macrocycle resides by comparison of the ^{1}H NMR spectra of rotaxane and corresponding thread hence ascertain the position of the macrocycle in the shuttling step/ processes. Thus, we chose to compare the difference in chemical shifts of the maleic methine protons (H_d and H_e) in rotaxane **7** in solvents of varying hydrogen bonding ability (CDCl$_3$ < d_3-MeCN < d_4-MeOD < d_7-DMF < d_6-DMSO). The first observation is that in CDCl$_3$ the methine protons (H_d and H_e) of rotaxane **7** shift only by 0.41 and 0.30 ppm respectively, suggesting that the macrocycle is spending a significant amount of time away from the maleamide station. This is confirmed by visual comparison of the ^{1}H NMR spectra of **7** in CDCl$_3$ (Figure 4.4d) and corresponding thread (*thread-7*) (Figure 4.4c) as the alkyl chain protons experience a slight upfield shift. This may be unsurprising as the maleamide motif

binds the benzylic amide macrocycle weakly; hence the energy barrier for shuttling is very low. The maleic methine protons in d_4-MeOD and d_7-DMF are shielded to lesser extent than in CDCl$_3$, and are virtually unchanged in d_6-DMSO.

This shuttling behavior can be also be observed by shielding of the alkyl chain protons in **7**, when compared to the corresponding thread (*thread*-**7**) (Figure 4.4a). These observations indicate that DMSO remains the only "synthetically useful" solvent for this mechanically interlocking auxiliary.

solvent	δ_H CH$_d$ *thread*-**7**	δ_H CH$_e$ *thread*-**7**	δ_H CH$_d$ **7**	δ_H CH$_e$ **7**	$\Delta\delta_H$ CH$_d$	$\Delta\delta_H$ CH$_e$
CDCl$_3$	6.06	5.92	5.65	5.62	-0.41	-0.30
d_3-MeCN	6.04	5.95	5.66	5.40	-0.39	-0.55
d_4-MeOD	6.12	6.07	5.95	5.60	-0.17	-0.47
d_7-DMF	6.20	6.18	6.03	5.89	-0.17	-0.29
d_6-DMSO	6.11	6.06	6.10	5.93	-0.01	-0.13

Table 4.1 Differential chemical shifts ($\Delta\delta_H$) for maleamide protons (H$_d$ and H$_e$) in **7** and *thread*-**7**
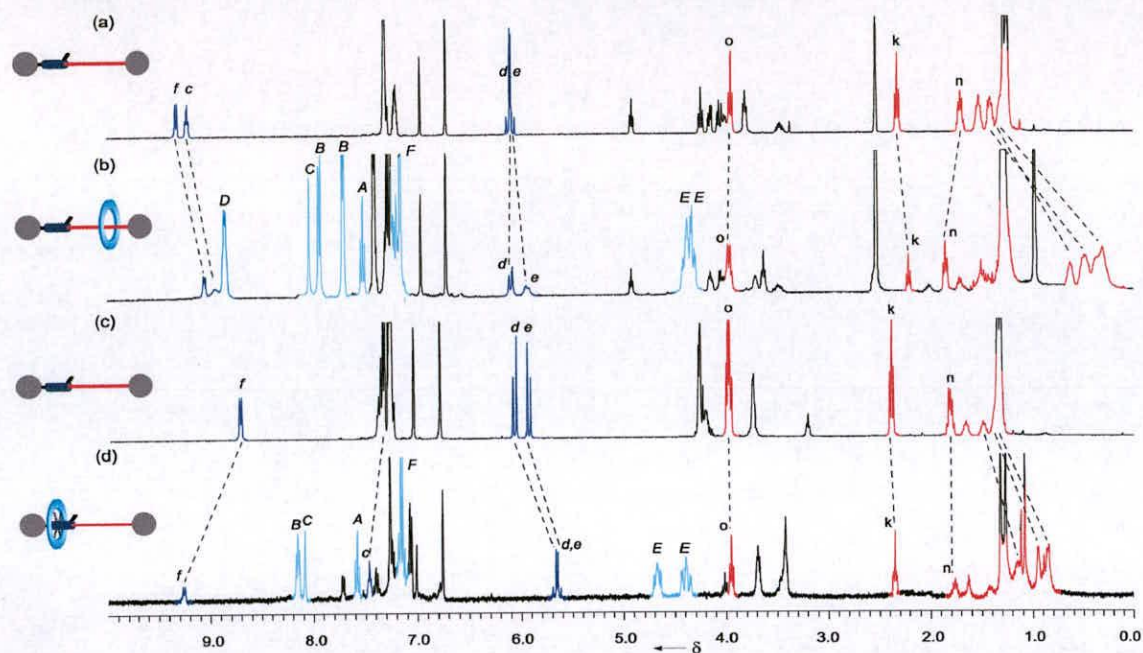
Figure 4.4. 400 MHz ^{1}H NMR spectra of (a) *thread*-**7**, (b) [2]rotaxane **7** in d_6-DMSO and (c) *thread*-**7**, and (d) [2]rotaxane **7** in CDCl$_3$ both at 298K. The color coding and lettering correspond to the assignments shown in Scheme 4.2.

Thus, **7** was dissolved in DMSO and treated with *tert*-butyldiphenylsilyl chloride to reattach the gate function. The crude ^{1}H NMR spectrum showed a small amount of the undesired diastereoisomer *maleamide*-**6** (7 %) along with the requisite diastereoisomer. Pleasingly, the diastereoisomers were readily separated by column chromatography to afford *alkyl*-**6** in 78 % yield. Analysis of the ^{1}H NMR spectrum of *alkyl*-**6** in CDCl$_3$ (Figure 4.2c) shows no shielding of the maleamide protons together with general shielding of the alkyl chain protons, providing irrefutable evidence for residency of the macrocycle on the alkyl chain. Intriguingly, the amide proton NH$_f$ of *alkyl*-**6** in CDCl$_3$ is found at 11.72 ppm. The proton NH$_f$ in the corresponding thread is already at a low field (8.75 ppm) through internal hydrogen bonding to the carbonyl of the maleic station. The proton NH$_f$ in *alkyl*-**6** now experiences an inductive effect from hydrogen bonding of the macrocycle residing on the alkyl chain in conjunction with the internal hydrogen bond to the NH$_c$-CO carbonyl, hence reducing the electron density on this proton. Immediate evidence for this general phenomena is contained in the ^{1}H NMR spectra of the thread-*maleamide*-**5** as the proton NH$_c$ resides at an 'unusually' low field (7.55 ppm) *via* an inductive effect

through the adjacent amide carbonyl, which is, in turn, hydrogen-bonded to NH$_f$. The ^{1}H NMR spectra in d_6-DMSO of *alkyl*-**6** (Figure 4.3c) shows strong shielding of the alkyl chain protons, but the protons of the maleamide station (NH$_f$ and NH$_c$) reside at an identical place as compared to the corresponding thread. This supports the hydrogen bonding hypothesis for the observation of proton NH$_f$ in *alkyl*-**6** residing at such a high field.

The mechanically interlocking auxiliary was then removed by the transesterification protocol used in Chapter 3, but on this occasion using the commercially available 3,3-diphenylpropanol in the presence of catalytic potassium *tert*-butoxide to afford the desired [2]rotaxane **1** in 81 %. The ^{1}H NMR spectra of **1** in CDCl$_3$ (Figure 4.5d) displays a general shielding of the alkyl chain protons of the thread with emphasis on H$_k$ indicating that the macrocycle is binding to the ester function, in agreement with those observations in analogous molecules (Chapter 3).
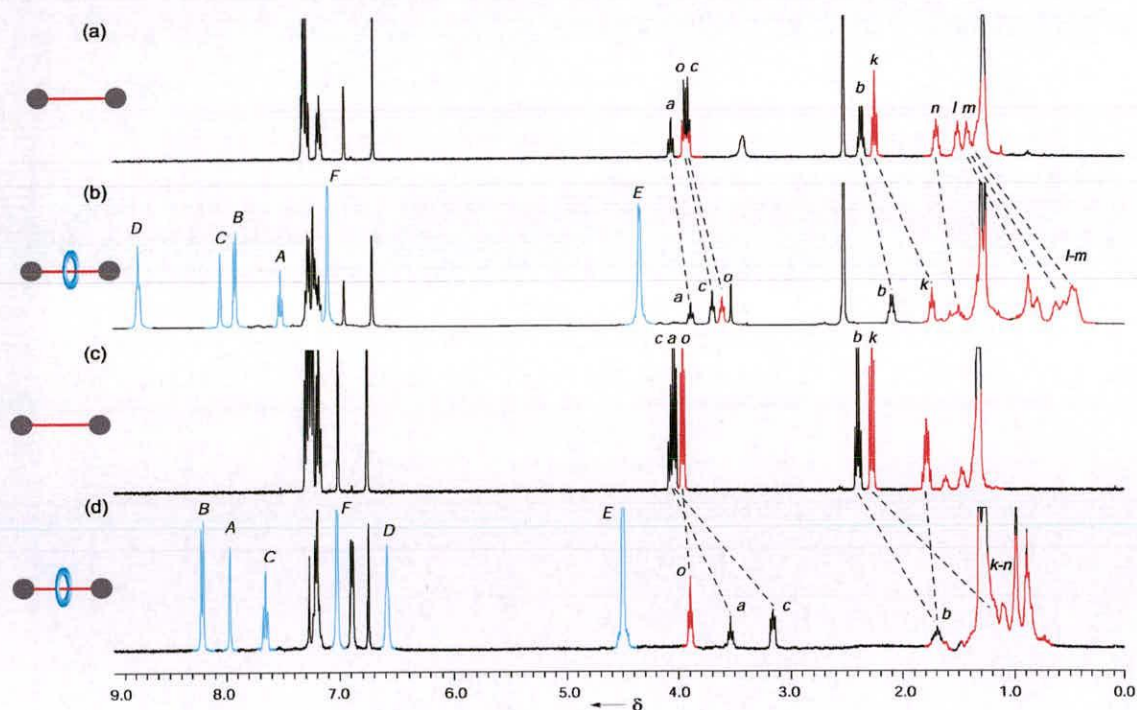
Figure 4.5. 400 MHz ^{1}H NMR spectra of (a) *thread*-**1**, (b) [2]rotaxane **1** in d_6-DMSO and (c) *thread*-**1**, and (d) [2]rotaxane **1** in CDCl$_3$ both at 298K. The color coding and lettering correspond to the assignments shown in Scheme 4.2.

4.2 Conclusions and Future Perspectives

In conclusion, we have demonstrated the use and function of a second generation mechanically interlocking auxiliary based on the photoswitchable fumaramide template group. While the low yield of the isomerization step is disappointing, we believe this is advantageously outweighed by the efficiency of the rotaxane formation step around the fumaramide template, which was previuosly the synthetic "bottle neck" in the mechanically interlocking auxiliary protocol. Also we believe we can circumvent the low yields of isomerization through removal of the fumaramide rotaxanes by trituration exploiting the enhanced solubility of maleamide-derived [2]rotaxanes.[16a] If we are to make this protocol general for the preparation of a range of mechanically interlocked molecules, then it would be desirable to have our mechanically interlocking auxiliary already appended with a macrocycle in a so-called "rotaxane-in-a-bottle" approach. This would allow attachment of this [2]rotaxane auxiliary to our substrate molecules and then enable translation of the ring to the substrate and cleavage of the auxiliary to afford the requisite rotaxane. The advantages of this approach are that substrate molecules are not attached to the auxiliary when the rotaxane forming reactions are performed. Hence, any interactions between template group and substrates, which could be detrimental to the resulting yield of the rotaxane, are negated. Also preforming the rotaxane on a template before attachment to substrate molecules means costly substrates are not involved in the low yielding rotaxane formation step and would enable the use of substrates unstable to the reaction conditions. This methodology is currently being developed using the second generation mechanically interlocking auxiliary to form novel rotaxanes unavailable to conventional hydrogen bond-directed synthesis and hence modify the physical and chemical properties of a range of commercially important materials (e.g. pharmaceuticals, dyes, *etc.*).

4.3 References

1   For general review into the synthesis of interlocked molecular architectures see: a) D. B. Amabilino, J. F. Stoddart, *Chem. Rev.* **1995**, *95*, 2725-2828; b) J.-P. Sauvage, C. Dietrich-Buchecker (Eds.), *Molecular Catenanes Rotaxanes and Knots*: *A Journey Through the World of Molecular Topology*, Wiley-VCH, Weinheim, **1999**.

2   For examples see: a) P. Thordarson, E. J. A. Bijsterveld, A. E. Rowan, R. J. M. Nolte, *Nature* **2003**, *424*, 915-918; b) A. G. Johnston, D. A. Leigh, A. Murphy, J. P. Smart, M. D. Deegan, *J. Am. Chem. Soc.* **1996**, *118*, 10662-10663; c) M. Asakawa, G. Brancato, M. Fanti, D. A. Leigh, T. Shimizu, A. M. Z. Slawin, J. K. Y. Wong, F. Zerbetto, S. W. Zhang, *J. Am. Chem. Soc.* **2002**, *124*, 2939-2950; d) S. Anderson, T. D. W. Claridge, H. L. Anderson, *Angew. Chem. Int. Ed. Engl.* **1997**, *36*, 1310-1313; e) F. Cacialli, J. S. Wilson, J. J. Michels, C. Daniel, C. Silva, R. H. Friend, N. Severin, P. Samori, J. P. Rabe, M. J. O'Connell, P. N. Taylor, H. L. Anderson, *Nature Mater.* **2002**, *1*, 160-164.

3   G. Schill, *Catenanes, Rotaxanes and Knots*; Academic Press, New York, **1971**.

4   a) I. T. Harrison, S. Harrison, *J. Am. Chem. Soc.* **1967**, *89*, 5723-5724 b) I. T. Harrison, *J. Chem. Soc. Perkin Trans. 1* **1974**, 301-304.

5   For a representative example see: N. Armaroli, V. Balzani, J. P. Collin, P. Gaviña, J. P. Sauvage, B. Ventura, *J. Am. Chem. Soc.* **1999**, *121*, 4397-4408.

6   For a representative example see: P. L. Anelli, P. R. Ashton, R. Ballardini, V. Balzani, M. Delgado, M. T. Gandolfi, T. T. Goodknow, A. E. Kaifer, D. Philp, M. Pietraszkiewicz, L. Prodi, M. V. Reddington, A. M. Z. Slawin, N. Spencer, J. F. Stoddart, C. Vicent, D. J. Williams, *J. Am. Chem. Soc.* **1992**, *114*, 193-218.

7   For examples of rotaxanes assembled through hydrogen bonding between neutral amide functions see: a) D. A. Leigh, A. Murphy, J. P. Smart, A. M. Z. Slawin, *Angew. Chem. Int. Ed. Engl.* **1997**, *36*, 728-732; b) F. G. Gatti, D. A. Leigh, S. A. Nepogodiev, A. M. Z. Slawin, S. J. Teat, J. K. Y. Wong, *J. Am.*

Chem. Soc. **2001**, *123*, 5983-5989; c) R. Jäger, F. Vögtle, *Angew. Chem. Int. Ed. Engl.* **1997**, *36*, 930-944.

8 For examples of rotaxanes assembled through hydrogen bonding to anions see: a) J. A. Wisner, P. D. Beer, M. G. B. Drew, M. R. Sambrook, *J. Am. Chem. Soc.* **2002**, *124*, 12469-12476; b) G. M. Hübner, J. Gläser, C. Seel, F. Vögtle, *Angew. Chem. Int. Ed.* **1999**, *38*, 383-386; c) P. Ghosh, O. Mermagen, C. A. Schalley, *Chem. Commun.* **2002**, 2628-2629.

9 For examples of rotaxanes assembled through ammonium ion/ crown ether hydrogen bonds see: a) A. G. Kolchinski, D. H. Busch, N. W. Alcock, *J. Chem. Soc. Chem. Commun.* **1995**, 1289-1291; b) P. R. Ashton, P. T. Glink, J. F. Stoddart, P. A. Tasker, A. J. P. White, D. J. Williams, *Chem. Eur. J.* **1996**, *2*, 729-736.c) P. T. Glink, A. I. Oliva, J. F. Stoddart, A. J. P. White, D. J. Williams, *Angew. Chem. Int. Ed.* **2001**, *40*, 1870-1875.

10 Alternative "template" primarily include utilizing the hydrophobic effect predominant in binding organic molecules in aqueous solutions of cyclodextrins. For representative examples see: a) H. Ogino, *J. Am. Chem. Soc.* **1981**, *103*, 1303; b) T. Ventaka, S. Rao, D. S. Lawrence, *J. Am. Chem. Soc.* **1990**, *112*, 3614; c) P. N. Taylor, M. J. O' Connell, L. A. McNeill, M. J. Hall, R. T. Aplin, H. L. Anderson, *Angew. Chem. Int. Ed.* **2000**, *39*, 3456.

11 For representative examples see a) R. A. Bissell, E. Córdova, A. E. Kaifer, J. F. Stoddart, *Nature* **1994**, *369*, 133-137; b) N. Armaroli, V. Balzani, J.-P. Collin, P. Gaviña, J.-P. Sauvage, B. Ventura, *J. Am. Chem. Soc.* **1999**, *121*, 4397-4408; c) H. Murakami, A. Kawabuchi, K. Kotoo, M. Kunitake, N. Nakashima, *J. Am. Chem. Soc.* **1997**, *119*, 7605-7606; d) A. M. Brouwer, C. Frochot, F. G. Gatti, D. A. Leigh, L. Mottier, F. Paolucci, S. Roffia, G. W. H. Wurpel, *Science* **2001**, *291*, 2124-2128.

12 For recent reviews see: a) V. Balzani, A. Credi, F. M. Raymo, J. F. Stoddart, *Angew. Chem. Int. Ed.* **2000**, *39*, 3349-3391; b) Special Issue on Molecular Machines: *Acc. Chem. Res.* **2001**, *34*, 409-522; c) J.-P. Sauvage Molecular Machines and Motors; Ed. Struct. Bonding (Berlin) **2001**, *99*.

13 A. S. Lane, D. A. Leigh, A. Murphy, *J. Am. Chem. Soc.* **1997**, *119*, 11092-11093.

14   F. G. Gatti, D. A. Leigh, S. A. Nepogodiev, A. M. Z. Slawin, S. J. Teat, J. K. Y. Wong, *J. Am. Chem. Soc.* **2001**, *123*, 5983-5989.

15   David Leigh and Gleb Priimov - Unpublished results

16   a) F. G. Gatti, S. Lent, J. K. Y. Wong, G. Bottari, A. Altieri, M. A. F. Morales, S. J. Teat, C. Frochot, D. A. Leigh, A. M. Brouwer, F. Zerbetto, *Proc. Natl. Acad. Sci. U. S. A.* **2003**, *100*, 10-14; b) A. Altieri, G. Bottari, F. Dehez, D. A. Leigh, J. K. Y. Wong, F. Zerbetto, *Angew. Chem. Int. Ed.* **2003**, *42*, 2296-2300.

17   The *tert*-butyldimethyl silyl group used in the original mechanically interlocking auxiliary system was replaced by *tert*-butyldiphenyl silyl function in the second generation mechanically interlocking auxiliary for its increased bulk as it can independently act as a stopper to maintain the macrocycle on the thread in the absence of other blocking groups. It was hoped that this additional property would be useful in future systems and it was reasonable to assume similar behavior in the operation of the second generation auxiliary system to the first, hence we chose to change the gate function.

4.4 Experimental
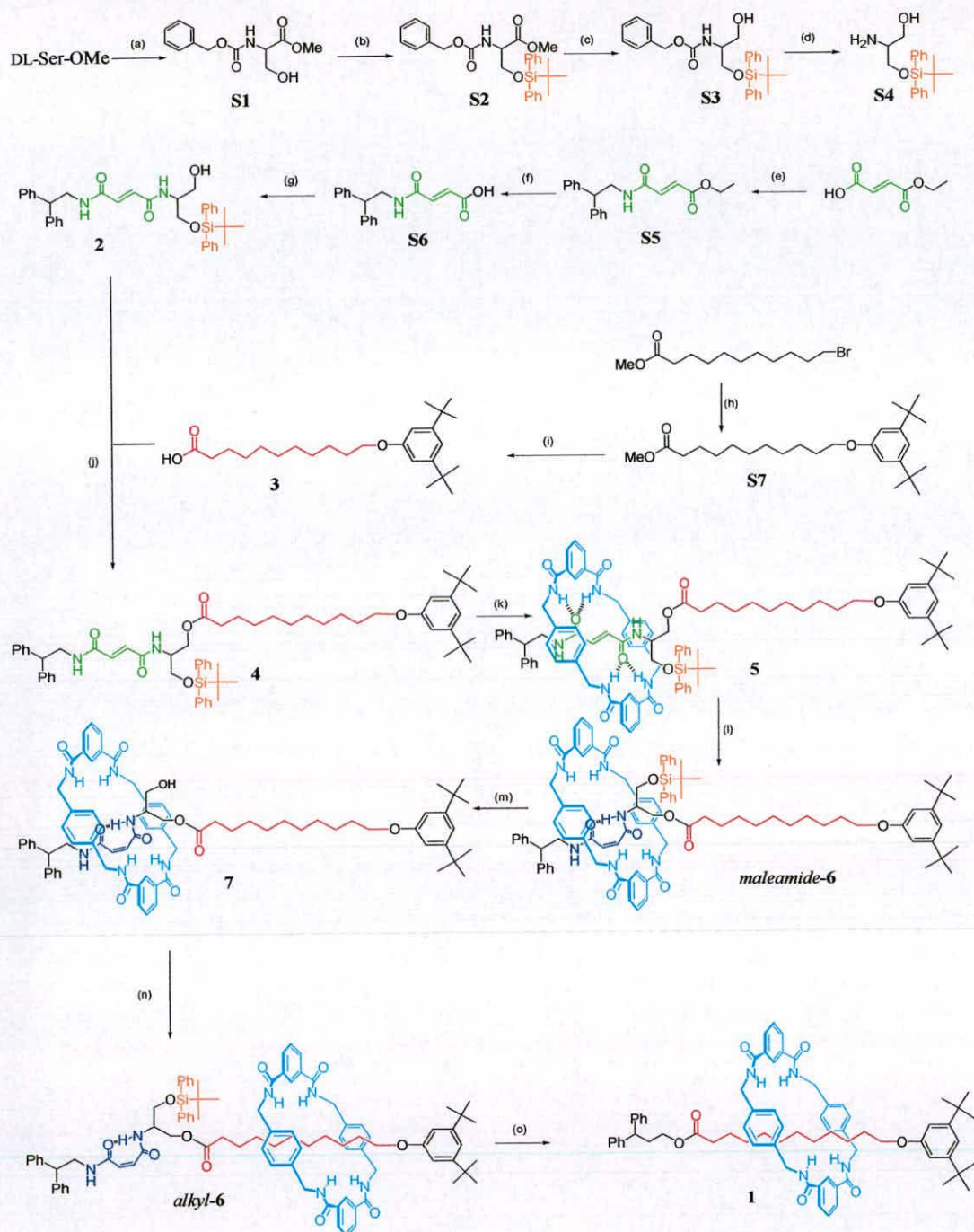
Scheme 4.3. Preparation of Rotaxane **1**. a) benzyl chloroformate, Et$_3$N, CH$_2$Cl$_2$, 70 %; b) *tert*-butyldiphenysilyl chloride, imidazole, 4-DMAP, CH$_2$Cl$_2$, 91%; c) NaBH$_4$, LiCl, MeOH, THF, 99 %; d) 5 % Pd/C, NH$_4$HCO$_2$, MeOH, 98 %; e) 2,2-diphenylethylamine, EDCI, HOBt, Et$_3$N, CH$_2$Cl$_2$, 93 %; f) NaOH, THF, H$_2$O, 98 %; g) **S4**, EDCI, HOBt, Et$_3$N, CH$_2$Cl$_2$, 93 %; h) 3,5-di-*tert*-butylphenol, K$_2$CO$_3$, NaI, 2-butanone, 91 %; i) NaOH, EtOH, H$_2$O, 96 %; j) **3**, EDCI, DMAP, CH$_2$Cl$_2$, 87 %; k) isophthaloyl dichloride, *p*-xylylene diamine, Et$_3$N, CHCl$_3$, 62 %; l) hυ 254nm, 20 min, 49 %; m) TBAF, THF, 98 %; n) *tert*-butylphenylsilyl chloride, imidazole, 4-DMAP, DMSO, 74 %; o) 3,3-diphenylpropanol, potassium *tert*-butoxide (5 mol %), 81 %.. Full experimental procedures are described below.

(2*RS*)-2[*N*-(Benzyloxycarbonyl)amino]-3-hydroxypropanoic acid methyl ester (S1)[1]
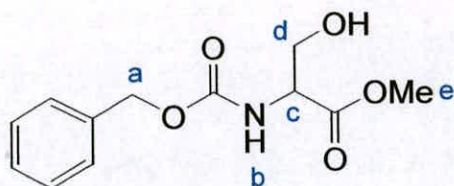
Benzylchloroformate (20.2 mL, 141 mmol) was added dropwise over 10 min to a stirred solution of DL-serine methyl ester hydrochloride (20.0 g, 129 mmol), sodium hydrogen carbonate (32.4 g, 387 mmol) in ethyl acetate (1500 mL) and water (1000 mL) at 0 °C. The reaction mixture was then stirred at room temperature for 3h. The reaction mixture was separated and the aqueous layer was extracted with ethyl actetate (2 x 100 mL) and the combined organic layers were washed with 1M hydrochloric acid (3 x 100 mL), and saturated sodium chloride (2 x100 mL) and dried (MgSO$_4$) and concentrated under reduced pressure to give a clear oil. The remaining oil was subjected to kugelrohr distillation to leave a clear oil. Yield 32.5 g (100 %); ^{1}H NMR (400 MHz, CDCl$_3$): δ = 7.42-7.30 (m, 5H, Ar<u>H</u>), 5.73 (br s, 1H, N<u>H</u>$_b$), 5.13 (s, 2H, C<u>H</u>$_a$), 4.49-4.45 (m, 1H, C<u>H</u>$_c$), 4.10 (br m, 1H, CH<u>H</u>$_d$), 3.92 (br m, 1H, C<u>H</u>$_d$H), 3.72 (s, 3H, C<u>H</u>$_e$);

(2*RS*)-2[*N*-(Benzyloxycarbonyl)amino]-3-(*tert*-butyl-diphenylsilanyloxy) propanoic acid methyl ester (S2)
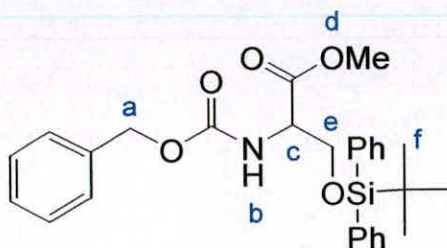
tert-Butyldimethylsilyl chloride (36.7 mL, 128 mmol) was added portionwise over 5 min, to a stirred solution of **S1** (32.5 g, 128 mmol) in dichloromethane (500 mL) at

room temperature, under an atmosphere of nitrogen. Imidazole (6.80 g, 99.9 mmol) was then added in one portion and the reaction mixture was then stirred at room temperature for 18 h. The reaction mixture was washed with water (3 x 20 mL), saturated aqueous sodium chloride (2 x 10 mL), dried (MgSO$_4$) and concentrated under reduced pressure. The residue was triturated with methanol to give **S2** as a colorless solid. Yield 17.7 g (91 %); ^{1}H NMR (400 MHz, CDCl$_3$): δ = 7.63-7.60 (m, 4H, SiArC$\underline{H}$-ortho), 7.42-7.30 (m, 11H, ArC$\underline{H}$ & SiArC$\underline{H}$-meta & para), 5.73 (d, 1H, J = 8.6 Hz, N$\underline{H}_b$), 5.13 (s, 2H, C$\underline{H}_a$), 4.49-4.45 (m, 1H, C$\underline{H}_c$), 4.10 (dd, 1H, J = 10.2 Hz, J = 2.8 Hz, C$\underline{H}$H$_e$), 3.92 (dd, 1H, J = 10.2 Hz, J = 2.8 Hz, CH$\underline{H}_e$), 3.73 (s, 3H, C$\underline{H}_d$), 1.05 (s, 9H, C$\underline{H}_f$); ^{13}C NMR (100 MHz, CDCl$_3$): δ = 170.7 (s, $\underline{C}$OCH$_d$), 155.7 (s, NH$\underline{C}$O), 136.2 (s, Ar$\underline{C}$-ipso), 135.2 (d, SiAr$\underline{C}$H-ortho), 132.6 (s, SiAr$\underline{C}$-ipso), 129.8 (Ar$\underline{C}$H), 128.4 (d, Ar$\underline{C}$H), 128.0 (d, Ar$\underline{C}$H), 127.9 (d, Ar$\underline{C}$H), 127.6 (d, Ar$\underline{C}$H), 66.8 (t, $\underline{C}$H$_a$), 64.3 (t, $\underline{C}$H$_e$), 55.8 (d, $\underline{C}$H$_c$), 52.2 (q, $\underline{C}$H$_d$), 26.6 (q, ($\underline{C}$H$_f$)), 19.1 (s, $\underline{C}$(CH$_f$)); LRMS (FAB+ mNBA matrix) *m/z* (rel. int.): 492 (18.5 %), [(M+H)$^+$], HRMS (FAB+) calcd for C$_{28}$H$_{33}$NO$_5$Si [(M+H)$^+$] 492.2206. Found 492.2201.

(2*RS*)-2[*N*-(Benzyloxycarbonyl)amino]-3-(*tert*-butyl-diphenylsilanyloxy) propan-1-ol (S3)
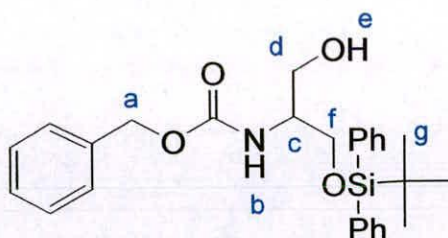
Anhydrous lithium chloride (22.4 g, 540 mmol) and sodium borohydride (20.4 g, 540 mmol) were added sequentially, both in one portion, to a stirred solution of **S2** (52.0 g, 106 mmol) in anhydrous THF (300 mL) at 0 °C. Ethanol (1.5 L) was then at added in one portion at 0 °C. The reaction mixture was then stirred at room temperature for 16 h. The reaction mixture was cooled to 0 °C and acidified to pH 5 by the dropwise

addition of 10% aqueous citric acid solution. The reaction mixture was concentrated under reduced pressure, diluted with water (500 mL) and extracted with chloroform (3 x 200 mL), dried (MgSO$_4$) and concentrated under reduced pressure. The residue was recrystallized from hexane to give **S3** as a colorless solid. Yield 49.0 g (99 %); mp 85-86 °C; ^{1}H NMR (400 MHz, CDCl$_3$): δ = 7.66-7.63 (m, 4H, SiArC$\underline{H}$-ortho), 7.46-7.34 (m, 11H, ArC$\underline{H}$ & SiArC$\underline{H}$-meta & para), 5.35 (br s, 1H, N$\underline{H}_b$), 5.11 (s, 2H, C$\underline{H}_a$), 3.87- 3.71 (m, 5H, C$\underline{H}_c$, C$\underline{H}_d$ & C$\underline{H}_f$), 2.40 (br s, 1H, O$\underline{H}_e$), 1.09 (s, 9H, C$\underline{H}_g$); ^{13}C NMR (100 MHz, CDCl$_3$): δ = 156.4 (s, Ar$\underline{C}$-ipso), 136.4 (s, Ar$\underline{C}$-ipso), 135.2 (d, SiAr$\underline{C}$H-ortho), 132.7 (s, SiAr$\underline{C}$-ipso), 129.9 (d, Ar$\underline{C}$H), 129.8 (Ar$\underline{C}$H), 128.5 (d, Ar$\underline{C}$H), 128.1 (d, Ar$\underline{C}$H), 128.0 (d, Ar$\underline{C}$H), 127.8 (d, Ar$\underline{C}$H), 66.8 (t, $\underline{C}$H$_a$), 63.9 (t, $\underline{C}$H$_d$), 63.1 (t, $\underline{C}$H$_f$), 53.5 (d, $\underline{C}$H$_c$), 26.8 (q, C($\underline{C}$H$_g$)), 19.2 (s, $\underline{C}$(CH$_g$)); LRMS (FAB+ mNBA matrix) *m/z* (rel. int.): 464 (42.5 %), [(M+H)$^+$], HRMS (FAB+) calcd for C$_{27}$H$_{33}$N$_2$O$_4$Si [(M+H)$^+$] 464.2257. Found 464.2257.

(2*RS*)-2-Amino-3-(*tert*-butyl-diphenylsilanyloxy)-propan-1-ol (S4)
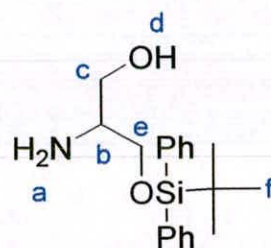
Ammonium formate (0.273 g, 4.32 mmol) was added in one portion to a stirred solution of **S3** (1.00 g, 2.16 mmol), 10 % palladium on carbon (0.10 g, 10 % w/w) in methanol (20 mL) at room temperature. The reaction mixture was stirred at room temperature for 1 h, filtered through Celite® and the filtrate was concentrated under reduced pressure. The residue was dissolved in ethyl acetate (100 mL) and washed with water (1 x 20 mL), saturated aqueous sodium chloride (2 x 30 mL), dried (MgSO$_4$) and concentrated under reduced pressure to give **S4** as a colorless oil. Yield 0.690 g (98 %); ^{1}H NMR (400 MHz, CDCl$_3$): δ = 7.66-7.63 (m, 4H, SiArC$\underline{H}$-ortho), 7.40-7.35 (m, 6H, SiArC$\underline{H}$-meta & para), 3.86-3.73 (m, 4H, C$\underline{H}_c$ & C$\underline{H}_e$), 3.63-3.55 (br m, 1H, C$\underline{H}_b$) 1.05 (s, 9H, C$\underline{H}_f$); ^{13}C NMR (100 MHz, CDCl$_3$): δ = 135.2 (d,

SiArCH-ortho), 132.7 (d, ArCH), 132.6 (s, ArC-ipso), 129.8 (d, ArCH), 63.9 (t, CH$_c$), 63.1 (t, CH$_e$), 53.5 (d, CH$_c$), 26.8 (q, C(CH$_f$)), 19.2 (s, C(CH$_f$)); LRMS (FAB+ mNBA matrix) *m/z* (rel. int.): 329 (81.4 %), [(M+H)$^+$], HRMS (FAB+) calcd for C$_{19}$H$_{27}$NO$_2$Si [(M+H)$^+$] 329.1811. Found 329.1818.

N-(2,2-Diphenylethyl)-fumaric acid ethyl ester (S5)
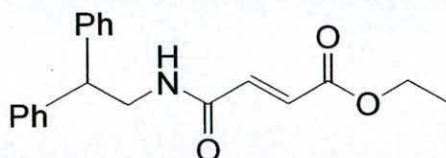
This compound was prepared as described in A. Altieri, G. Bottari, F. Dehez, D. A. Leigh, J. K. Y. Wong, F. Zerbetto, *Angew. Chem. Int. Edit.* **2003**, *42*, 2296-2300; and showed identical spectroscopic data to that reported therein.

N-(2,2-Diphenylethyl)-fumaramide acid (S6)
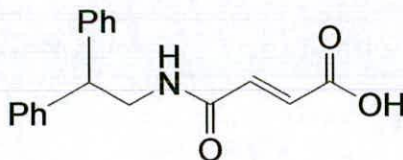
This compound was prepared as described in A. Altieri, G. Bottari, F. Dehez, D. A. Leigh, J. K. Y. Wong, F. Zerbetto, *Angew. Chem. Int. Edit.* **2003**, *42*, 2296-2300; and showed identical spectroscopic data to that reported therein.

(*E*)-But-2-enedioic acid [(2,2-diphenylethyl)-amide-2-(*tert*-butyl-diphenyl-siloxy)propan-1-oxy] amide (2)
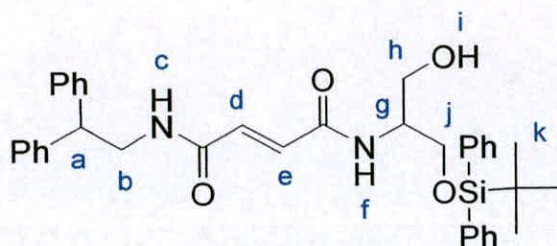
HOBt (0.691 g, 5.08 mmol) was added to a stirred solution of **S6** (1.00 g, 3.39 mmol), and triethylamine (1.18 mL, 8.47 mmol) in dichloromethane (30 mL), at 0 °C. The reaction mixture was stirred at 0 °C for 25 min then EDCI (0.975 g, 5.08 mmol) was added to the solution in one portion at 0 °C, with stirring. After 20 min **S4** (1.34 g, 4.07 mmol) was added at 0 °C. The reaction mixture was stirred at 0 °C for 1 h and at room temperature for a further 18 h. The reaction mixture was washed with 1 M aqueous hydrochloric acid (3 x 50 mL) saturated aqueous sodium bicarbonate (3 x 50 mL) and saturated aqueous sodium chloride (1 x 20 mL), dried (MgSO$_4$) and concentrated under reduced pressure. The residue was purified by column chromatography on silica gel using ethyl acetate: petroleum ether 40-60 °C (4: 1) as eluent to give **2** as a colorless solid. Yield 1.83 g (89 %); m.p. 120-121 °C; ^{1}H NMR (400 MHz, CDCl$_3$): 7.64-7.61 (m, 4H, SiArC$\underline{H}$-ortho), 7.46-7.24 (m, 16H, ArC$\underline{H}$ & SiArC$\underline{H}$-meta & para), 6.77 (d, 1H, J = 14.9 Hz, C$\underline{H}_d$), 6.65 (d, 1H, J = 14.9 Hz, C$\underline{H}_e$), 6.29 (d, 1H, J = 7.6 Hz, N$\underline{H}_f$), 5.70 (t, 1H, J = 5.7 Hz, N$\underline{H}_c$), 4.23 (t, 1H, J = 7.8 Hz, C$\underline{H}_a$), 4.07-4.00 (m, 3H, C$\underline{H}_g$ & C$\underline{H}_b$), 3.87, (dd, 2H, J = 10.6 Hz, J = 3.8 Hz, C$\underline{H}_h$), 3.79 (dd, 1H, J = 10.6 Hz, J = 4.3 Hz, C$\underline{H}_j$H), 3.71-3.65 (br m, 1H, CH$\underline{H}_j$), 2.52 (br s, 1H O$\underline{H}_i$), 1.08 (s, 9H, C$\underline{H}_k$); ^{13}C NMR (100 MHz, CDCl$_3$): δ = 164.5 (s, NH$\underline{C}$O), 164.2 (s, NH$\underline{C}$O), 141.6 (s, Ar$\underline{C}$-ipso), 135.5 (d, SiAr$\underline{C}$H-ortho), 135.4 (d, SiAr$\underline{C}$H-ortho), 133.2 (d, $\underline{C}$H$_e$ or $\underline{C}$H$_d$), 132.8 (d, $\underline{C}$H$_e$ or $\underline{C}$H$_d$), 132. 7 (s, SiAr$\underline{C}$-ipso), 132.6 (s, SiAr$\underline{C}$-ipso), 130.0 (d, Ar$\underline{C}$H), 129.9 (d, Ar$\underline{C}$H), 128.7 (d, Ar$\underline{C}$H), 127.9 (d, Ar$\underline{C}$H), 127.85 (d, Ar$\underline{C}$H), 127.85 (d, Ar$\underline{C}$H), 126.9 (d, Ar$\underline{C}$H), 63.1 (t, $\underline{C}$H$_h$), 62.4 (t, $\underline{C}$H$_j$), 52.6 (d, $\underline{C}$H$_g$), 50.3 (d, $\underline{C}$H$_a$), 44.2 (t, $\underline{C}$H$_b$), 26.8 (q, C($\underline{C}$H$_k$)), 19.2 (s, $\underline{C}$(CH$_k$)); LRMS (FAB+ mNBA matrix) *m/z* (rel. int.): 607 (28.2 %),

[(M+H)$^+$], HRMS (FAB+) calcd for C$_{37}$H$_{43}$N$_2$O$_4$Si [(M+H)$^+$] 607.2992. Found 607.2995.

Methyl-11-(3,5-di-*tert*-butylphenoxy) undecanoate (S7)
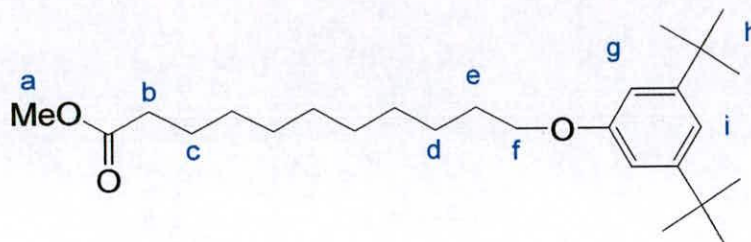
Methyl-11-bromoundecanoate (10.0 g, 35.8 mmol), 3,5-di-*tert*-butylphenol (7.76 g, 37.6 mmol), anhydrous potassium carbonate (49.5 g, 358 mmol) and sodium iodide (one crystal) in 2-butanone (350 mL) were heated under reflux for 2 days. The reaction mixture was filtered and concentrated under reduced pressure. The residue was purified by column chromatography on silica gel using petroleum ether 40-60 °C: ethyl acetate (10: 1) as eluent to give S7 as a colorless oil. Yield 13.2 g (91 %); ^{1}H NMR (400 MHz, CDCl$_3$): δ = 7.02 (t, 1H, *J* = 1.6 Hz, CH$_i$), 6.77 (d, 2H, *J* = 1.6 Hz, CH$_g$), 3.98 (t, 2H, *J* = 6.6 Hz, CH$_f$), 3.68 (s, 3H, CH$_a$), 2.32 (t, 2H, *J* = 7.4 Hz, CH$_b$), 1.83-1.76 (m, 2H, CH$_e$), 1.65-1.60 (m, 2H, CH$_c$), 1.51-1.42 (m, 2H, CH$_d$), 1.40-1.30 (m, 28H, CH$_h$ & -CH$_2$-alkyl); ^{13}C NMR (100 MHz, CDCl$_3$): δ = 174.3 (s, CO$_2$CH$_a$), 158.6 (s, ArC-ipso), 152.1 (s, ArC-meta), 114.7 (d, ArCH$_i$), 108.8 (d, ArCH$_g$), 67.7 (t, CH$_f$), 51.4 (q, CO$_2$CH$_a$), 35.0 (s, C(CH$_h$)), 34.1 (t, CH$_b$), 31.4 (q, C(CH$_h$)), 29.5 (t, -CH$_2$-), 29.5 (t, -CH$_2$-), 29.4 (t, -CH$_2$-), 29.4 (t, -CH$_2$-), 29.2 (t, -CH$_2$-), 29.1 (t, -CH$_2$-), 26.1 (t, -CH$_2$-), 24.9 (t, -CH$_2$-); LRMS (FAB+ mNBA matrix) *m/z* (rel. int.): 405 (60.1 %) [(M+H)$^+$], HRMS (FAB+): calcd for C$_{26}$H$_{44}$O$_3$ [(M+H)$^+$] 404.3291. Found 404.3295.

11-(3,5-di-*tert*-butylphenoxy) undecanoic acid (3)
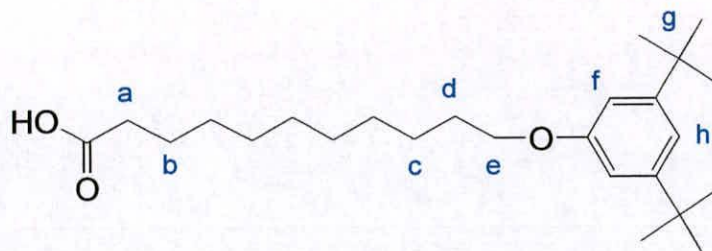
Aqueous sodium hydroxide solution (111 mL of a 1 M solution, 111 mmol) was added to a stirred solution of **S7** (15.0 g, 37.1 mmol) in ethanol (370 mL) at room temperature. The reaction mixture was then heated under reflux for 16 h. The reaction mixture was concentrated under reduced pressure and diluted with water (500 mL), cooled to 0 °C and acidified to pH 1 by the dropwise addition of 1 M aqueous hydrochloric acid solution. The aqueous layer was extracted with ethyl acetate (3 x 50 mL), dried (MgSO$_4$), and concentrated under reduced pressure to give **3** as a colorless solid. Yield 13.9 g (96 %); m.p. 71-73 °C; ^{1}H NMR (400 MHz, CDCl$_3$): δ = 7.03 (t, 1H, J = 1.6 Hz, C$\underline{H}_h$), 6.77 (d, 2H, J = 1.6 Hz, C$\underline{H}_f$), 3.98 (t, 2H, J = 6.6 Hz, C$\underline{H}_e$), 2.37 (t, 2H, J = 7.6 Hz, C$\underline{H}_a$), 1.84-1.76 (m, 2H, C$\underline{H}_d$), 1.67-1.62 (m, 2H, C$\underline{H}_b$), 1.50-1.42 (m, 2H, C$\underline{H}_c$), 1.40-1.25 (m, 28H, -C$\underline{H}_2$-alkyl & C$\underline{H}_g$); ^{13}C NMR (100 MHz, CDCl$_3$): δ = 179.9 (s, $\underline{C}O_2H$), 158.7 (s, Ar$\underline{C}$-ipso), 152.1 (s, Ar$\underline{C}$-meta), 114.8 (d, Ar$\underline{C}H_h$), 108.8 (d, Ar$\underline{C}H_f$), 67.8 (t, $\underline{C}H_e$), 35.0 (s, $\underline{C}(CH_g)$), 34.0 (t, $\underline{C}H_a$), 31.5 (q, C($\underline{C}H_g$)), 29.5 (t, -$\underline{C}H_2$-), 29.4 (t, -$\underline{C}H_2$-), 29.4 (t, -$\underline{C}H_2$-), 29.2 (t, -$\underline{C}H_2$-), 29.0 (t, -$\underline{C}H_2$-), 26.1 (t, -$\underline{C}H_2$-), 24.7 (t, -$\underline{C}H_2$-); LRMS (FAB+ mNBA matrix) *m/z* (rel. int.): 390 (62.8 %) [(M+H)$^+$], HRMS (FAB+): calcd for C$_{25}$H$_{42}$O$_3$ [(M+H)$^+$] 390.3134. Found 390.3134.

(*E*)-But-2-enedioic acid [(2,2-diphenylethyl)-amide-3-(diphenyl-*tert*-butylsiloxy)-11-(3,5-di-*tert*-butylphenoxy undecanoate) propan-1-oxy] amide (4)
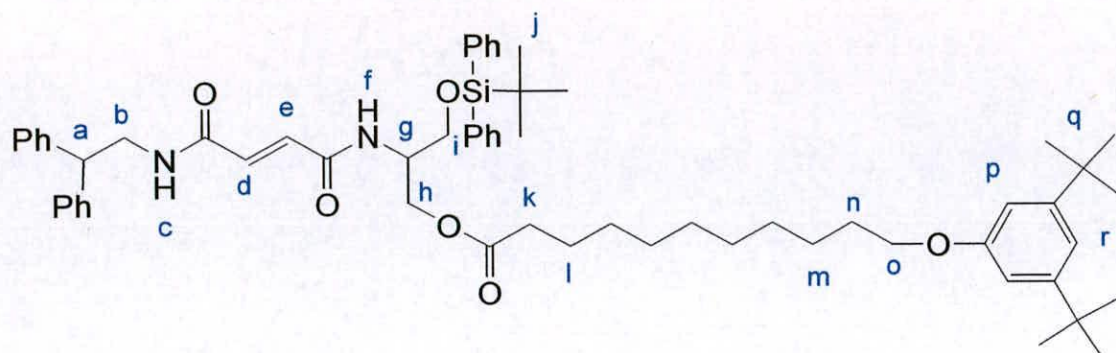
EDCI (0.553 g, 2.88 mmol) and a catalytic amount of 4-DMAP were added to stirred solution of **3** (750 mg, 1.92 mmol) and **2** (1.22 g, 2.01 mmol) at 0 °C. The reaction mixture was then stirred at room temperature for 14 h. The reaction mixture was washed with 1 M aqueous hydrochloric acid (3 x 50 mL) saturated aqueous sodium hydrogen carbonate (3 x 50 mL) and saturated aqueous sodium chloride (2 x 20 mL), dried (MgSO₄) and concentrated under reduced pressure. The residue was purified by column chromatography on silica gel using ethyl acetate: petroleum ether 40-60 °C (1: 1) as eluent to give **4** as a colorless oil. Yield 1.75 g (93 %); ^{1}H NMR (400 MHz, CDCl₃): 7.61 (d, 4H, *J* = 7.8 Hz, SiArC$\underline{H}$-ortho,), 7.46-7.24 (m, 16H, ArC$\underline{H}$-stopper & SiArC$\underline{H}$-meta & para), 7.01 (t, 1H, *J* = 1.6 Hz, ArC$\underline{H}_r$), 6.76 (d, 2H, *J* = 1.6 Hz, ArC$\underline{H}_p$), 6.75 (d, 1H, *J* = 14.7 Hz, C$\underline{H}_d$), 6.65 (d, 1H, *J* = 14.7 Hz, C$\underline{H}_e$), 6.03 (d, 1H, *J* = 8.3 Hz, N$\underline{H}_f$), 5.72 (t, 1H, *J* = 5.7 Hz, N$\underline{H}_c$), 4.35-4.15 (m, 4H, C$\underline{H}_a$, C$\underline{H}_g$ & C$\underline{H}_h$), 4.01 (t, 2H, *J* = 7.6 Hz, C$\underline{H}_b$), 3.96 (t, 2H, *J* = 6.6 Hz, C$\underline{H}_o$), 3.87, (dd, 1H, *J* = 10.5 Hz, *J* = 2.7 Hz, C$\underline{H}$H$_i$), 3.69 (dd, 1H, *J* = 10.5 Hz, *J* = 2.7 Hz, C$\underline{H}_i$H), 2.23 (t, 2H, *J* = 7.6 Hz, C$\underline{H}_k$), 1.82-1.75 (m, 2H, C$\underline{H}_n$), 1.45-1.20 (m, 32H, -C$\underline{H}_2$-alkyl, C$\underline{H}_q$) 1.07 (s, 9H, C$\underline{H}_j$); ^{13}C NMR (100 MHz, CDCl₃): δ = 173.5 (s, $\underline{C}$O₂R), 163.8 (s, NH$\underline{C}$O), 163.7 (s, NH$\underline{C}$O), 158.6 (s, Ar$\underline{C}$-ipso), 152.0 (s, Ar$\underline{C}$-meta), 141.5 (s, Ar$\underline{C}$-ipso), 135.5 (d, SiAr$\underline{C}$H-ortho), 135.4 (d, SiAr$\underline{C}$H-ortho), 133.4 (d, Ar$\underline{C}$H), 132.7 (s, SiAr$\underline{C}$-ipso), 132.6 (d, Ar$\underline{C}$H), 132.6 (s, SiAr$\underline{C}$-ipso), 130.0 (d, Ar$\underline{C}$H), 129.9 (d, Ar$\underline{C}$H), 128.8 (d, Ar$\underline{C}$H), 127.9 (d, Ar$\underline{C}$H), 127.85 (d, Ar$\underline{C}$H), 127.8 (d, Ar$\underline{C}$H), 126.9 (d, Ar$\underline{C}$H), 114.7 (d, Ar$\underline{C}$H$_r$), 108.7 (d, Ar$\underline{C}$H$_p$), 67.7 (t, $\underline{C}$H$_o$), 62.2 (t, $\underline{C}$H$_h$), 62.1 (t, $\underline{C}$H$_i$), 50.3 (d, $\underline{C}$H$_a$), 49.7 (d, $\underline{C}$H$_g$), 44.1 (t, $\underline{C}$H$_b$), 34.9 (s, $\underline{C}$(CH₃)₃), 34.0 (t,

$\underline{C}H_k$), 31.4 (q, C($\underline{C}H_q$)), 29.5 (t, -$\underline{C}H_2$-), 29.4 (t, -$\underline{C}H_2$-), 29.4 (t, -$\underline{C}H_2$-), 29.4 (t, -$\underline{C}H_2$-), 29.2 (t, -$\underline{C}H_2$-), 29.1 (t, -$\underline{C}H_2$-), 26.8 (q, SiC($\underline{C}H_3$)$_3$), 26.1 (t, -$\underline{C}H_2$-), 24.7 (t, -$\underline{C}H_2$-), 19.2 (s, Si$\underline{C}$(CH$_3$)$_3$); LRMS (FAB+ mNBA matrix) *m/z* (rel. int.): 979 (3.2 %), [(M+H)$^+$], HRMS (FAB+) calcd for C$_{62}$H$_{83}$N$_2$O$_6$Si [(M+H)$^+$] 979.6020. Found 979.6017.

[2](1,7,14,20-Tetraaza-2,6,15,19-tetraoxo-3,5,9,12,16,18,22,25-tetrabenzocyclohexacosane)-(*E*)-But-2-enedioic acid (2,2-diphenylethyl)-amide-3-(*tert*-butyl-diphenyl-silanyloxy)-11-(3,5-di-*tert*-butylphenoxy undecanoate propan-1-oxy) amide rotaxane (5)

4 (3.00 g, 3.56 mmol) and triethylamine (9.95 mL, 71.4 mmol) were dissolved in anhydrous chloroform (360 mL) and stirred vigorously whilst solutions of *p*-xylylene diamine (3.88 g, 28.5 mmol) in anhydrous chloroform (50 mL) and isophthaloyl dichloride (5.79 g, 28.5 mmol) in anhydrous chloroform (50 mL) were simultaneously added over a period of 4 h using motor-driven syringe pumps. After a further 2 h the resulting suspension was filtered and the filtrate was washed with 1 M aqueous hydrochloric acid (3 x 50 mL) saturated aqueous sodium hydrogen carbonate (3 x 50 mL) and saturated aqueous sodium chloride (2 x 20 mL), dried

(MgSO$_4$) and concentrated under reduced pressure. The residue was purified by column chromatography on silica gel using chloroform: methanol (100: 1) as eluent to give **5** as a colorless solid. Yield 1.32 g (62 %); m.p. 171-172 °C; ^{1}H NMR (400 MHz, CDCl$_3$): 8.29 (s, 2H, ArC$\underline{H}_C$), 8.13 (d, 4H, J = 7.8 Hz, ArC$\underline{H}_B$), 7.62-7.56 (m, 6H, ArC$\underline{H}_A$ & SiArC$\underline{H}$-ortho), 7.53 (t, 2H, J = 5.1 Hz, N$\underline{H}_D$), 7.43 (t, 2H, J = 5.1 Hz, N$\underline{H}_D$), 7.39-7.16 (m, 18H, N$\underline{H}_D$, N$\underline{H}_c$, N$\underline{H}_f$, ArC$\underline{H}$-stopper & SiArC$\underline{H}$-meta), 7.11 (d, J = 7.0 Hz, SiArC$\underline{H}$-para), 7.01 (t, 1H, J = 1.5 Hz, ArC$\underline{H}_r$), 6.86 (d, 4H, J = 7.8 Hz, ArC$\underline{H}_F$), 6.77 (d, 4H, J =7.8 Hz, ArC$\underline{H}_F$), 6.75 (d, 2H, J = 1.5Hz, C$\underline{H}_p$), 5.58 (s, 2H, C$\underline{H}_e$ & C$\underline{H}_d$), 4.45-4.40 (m, 4H, C$\underline{H}_E$), 4.38-4.28 (m, 4H, C$\underline{H}_E$), 4.18 (t, 1H, J = 7.8 Hz, C$\underline{H}_a$), 4.12-4.05 (m, 3H, C$\underline{H}_h$ & C$\underline{H}_g$), 3.96 (t, 2H, J = 6.6 Hz, C$\underline{H}_o$), 3.77-3.70 (m, 3H, C$\underline{H}_b$ & C$\underline{H}_i$H), 3.60 (dd, 1H, J = 9.8 Hz, J = 7.1 Hz, CH$\underline{H}_i$), 2.24 (t, 2H, J = 7.6 Hz, C$\underline{H}_k$), 1.80-1.75 (m, 2H, C$\underline{H}_n$), 1.47-1.39 (m, 8H, -C$\underline{H}_2$-alkyl), 1.31-1.21 (m, 24H, -C$\underline{H}_2$-alkyl & C$\underline{H}_q$), 1.07 (s, 9H, C$\underline{H}_j$); ^{13}C NMR (100 MHz, CDCl$_3$): δ = 173.5 (s, $\underline{C}$O$_2$R), 166.5 (s, NH$_D\underline{C}$O), 166.4 (s, NH$_D\underline{C}$O), 165.8 (s, NH$\underline{C}$O), 165.6 (s, NH$\underline{C}$O), 158.6 (s, Ar$\underline{C}$-ipso), 152.0 (s, Ar$\underline{C}$-meta), 141.4 (s, Ar$\underline{C}$-ipso), 135.5 (d, SiAr$\underline{C}$H-ortho), 135.4 (d, SiAr$\underline{C}$H-ortho), 133.4 (d, $\underline{C}$H$_e$ or $\underline{C}$H$_d$), 132.7 (s, SiAr$\underline{C}$-ipso), 132.6 (d, Ar$\underline{C}$H), 132.6 (s, Ar$\underline{C}$-ipso), 130.0 (d, $\underline{C}$H$_e$ or $\underline{C}$H$_d$), 129.9 (d, Ar$\underline{C}$H), 128.8 (d, Ar$\underline{C}$H), 127.9 (d, Ar$\underline{C}$H), 127.85 (d, Ar$\underline{C}$H), 127.8 (d, Ar$\underline{C}$H),126.9 (d, Ar$\underline{C}$H), 114.7 (d, Ar$\underline{C}$H$_r$), 108.7 (d, Ar$\underline{C}$H$_p$), 67.7 (t, $\underline{C}$H$_o$), 62.2 (t, $\underline{C}$H$_h$), 62.1 (t, $\underline{C}$H$_i$), 50.3 (d, $\underline{C}$H$_a$), 49.7 (d, $\underline{C}$H$_g$), 44.1 (t, $\underline{C}$H$_b$), 34.9 (s, $\underline{C}$(CH$_q$)), 34.0 (t, $\underline{C}$H$_k$), 31.4 (q, $\underline{C}$H$_q$), 29.5 (t, -$\underline{C}$H$_2$-), 29.4 (t, -$\underline{C}$H$_2$-), 29.4 (t, -$\underline{C}$H$_2$-), 29.4 (t, -$\underline{C}$H$_2$-), 29.2 (t, -$\underline{C}$H$_2$-), 29.1 (t, -$\underline{C}$H$_2$-), 26.8 (q, $\underline{C}$H$_j$), 26.1 (t, -$\underline{C}$H$_2$-), 24.7 (t, -$\underline{C}$H$_2$-), 19.2 (s, $\underline{C}$(CH$_j$)); LRMS (FAB+ mNBA matrix) m/z (rel. int.): 1512 (100 %), [(M+H)$^+$], HRMS (FAB+) calcd for C$_{94}$H$_{111}$N$_6$O$_{10}$Si [(M+H)$^+$] 1512.8165. Found 1512.8185.

[2](1,7,14,20-Tetraaza-2,6,15,19-tetraoxo-3,5,9,12,16,18,22,25-tetrabenzocyclohexacosane)-(*Z*)-But-2-enedioic acid 2,2-diphenylethylamide-3-(*tert*-butyl-diphenyl-silanyloxy)-11-(3,5-di-*tert*-butylphenoxyundecanoate propan-1-oxy) amide rotaxane (*maleamide*-6)
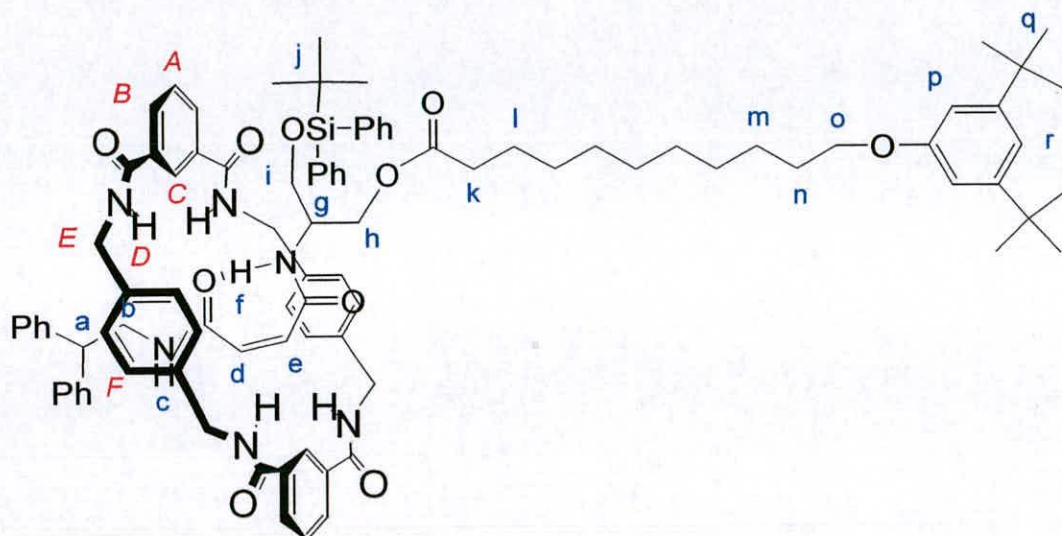
5 (600 mg, 0.397 mmol) was dissolved in dichloromethane (100 mL) in a quartz vessel. The solution was directly irradiated at 254 nm using a multilamp photo-reactor. Different photostationary states were reached in 20 min, after which the reaction mixture was concentrated under reduced pressure to afford the crude product. The residue was purified by column chromatography on silica gel using chloroform: methanol (99: 1) as eluent to give *maleamide*-6 as a colorless solid. Yield 290 g, (49 %); m.p. 141-144 °C; ^{1}H NMR (400 MHz, CDCl$_3$): δ = 8.22 (d, J = 7.6 Hz, ArCH$_B$), 8.15 (d, J = 7.6 Hz, ArCH$_B$), 8.11 (s, 2H, ArCH$_C$), 7.65-7.53 (m, 8H, SiArCH-ortho, NH$_D$, ArCH$_A$ & NH$_c$), 7.45-7.31 (m, 11H, ArCH-stopper & NH$_f$), 7.18-7.10 (m, 6H, SiArCH-meta & para), 7.02 (t, 1H, J =1.6 Hz, CH$_r$), 6.96 (d, 2H, J =1.6 Hz, CH$_p$), 6.90 (t, 2H, J = 5.4 Hz, NH$_D$), 6.81 (d, 4H, J = 7.8 Hz, ArCH$_F$), 6.77 (d, 4H, J = 7.8 Hz, ArCH$_F$), 5.09 (d, 1H, J = 12.8 Hz, CH$_d$), 4.88 (d, 1H, J = 12.8 Hz, CH$_e$), 4.53-4.24 (m, 8H, CH$_E$), 4.06-4.00 (m, 2H, CH$_h$), 3.97 (t, 2H, J = 6.6 Hz, CH$_o$), 3.83 (t, 1H, J = 8.0 Hz, CH$_a$), 3.68-3.65 (m, 1H, CH$_g$), 3.49-3.42 (m, 1H, CHH$_b$), 3.39-3.34 (m, 1H, CHH$_i$), 3.28-3.18 (m, 2H, CH$_i$H & CH$_b$H), 2.12 (t, 2H, J = 7.8 Hz, CH$_k$), 1.82-1.74 (m, 2H, CH$_n$), 1.51-1,13 (m, 32H, -CH$_2$-alkyl & CH$_q$), 0.95 (s, 9H, CH$_j$); ^{13}C NMR (100 MHz, CDCl$_3$): δ = 174.5 (s, $\underline{C}$O$_2$R), 166.6 (s, NH$_D$$\underline{C}$O),

166.1 (s, $NH_D\underline{C}O$), 164.9 (s, $NH\underline{C}O$), 164.4 (s, $NH\underline{C}O$), 158.6 (s, $Ar\underline{C}$-ipso), 152.1 (s, $Ar\underline{C}$-meta), 141.6 (s, $Ar\underline{C}$-ipso-stopper), 141.5 (s, $Ar\underline{C}$-ipso-stopper), 137.1 (s, $Ar\underline{C}$-ipso-xylylene), 136.7 (s, $Ar\underline{C}$-ipso-xylylene), 135.5 (d, $SiAr\underline{C}H$-ortho), 135.4 (d, $SiAr\underline{C}H$-ortho), 134.3 (s, $Ar\underline{C}$-ipso-isophthaloyl), 133.6 (s, $Ar\underline{C}$-ipso-isophthaloyl), 133.4 (d, $\underline{C}H_e$ or $\underline{C}H_d$), 132.8 (s, $SiAr\underline{C}$-ipso), 132.5 (s, $SiAr\underline{C}$-ipso), 131.8 (d, $Ar\underline{C}H$), 130.1 (d, $Ar\underline{C}H$), 129.9 (d, $Ar\underline{C}H$), 129.3 (d, $Ar\underline{C}H$), 129.0 (d, $Ar\underline{C}H$), 128.7 (d, $Ar\underline{C}H$), 128.6 (d, $Ar\underline{C}H$), 128.5 (d, $Ar\underline{C}H$), 128.1 (d, $\underline{C}H_e$ or $\underline{C}H_d$), 128.0 (d, $Ar\underline{C}H$), 127.8 (d, $Ar\underline{C}H$), 127.7 (d, $Ar\underline{C}H$), 127.6 (d, $Ar\underline{C}H$), 126.9 (d, $Ar\underline{C}H$), 126.8 (d, $Ar\underline{C}H$), 124.6 ($Ar\underline{C}H$), 114.8 (d, $Ar\underline{C}H_r$), 108.8 (d, $Ar\underline{C}H_p$), 67.7 (t, $\underline{C}H_o$), 61.5 (t, $\underline{C}H_h$), 61.0 (t, $\underline{C}H_i$), 50.2 (d, $\underline{C}H_a$), 50.0 (d, $\underline{C}H_g$), 44.7 (t, $\underline{C}H_E$) 44.1 (t, $\underline{C}H_E$), 43.8 (t, $\underline{C}H_b$), 35.0 (s, $\underline{C}(CH_q)$), 34.0 (t, $\underline{C}H_k$), 31.4 (q, $C(\underline{C}H_3)_3$), 29.5 (t, $-\underline{C}H_2-$), 29.4 (t, $-\underline{C}H_2-$), 29.3 (t, $-\underline{C}H_2-$), 29.2 (t, $-\underline{C}H_2-$), 29.0 (t, $-\underline{C}H_2-$), 26.6 (q, $\underline{C}H_j$), 26.1 (t, $-\underline{C}H_2-$), 24.4 (t, $-\underline{C}H_2-$), 19.1 (s, $\underline{C}(CH_j)$); LRMS (FAB+ mNBA matrix) *m/z* (rel. int.): 1512 (100 %), $[(M+H)^+]$, HRMS (FAB+) calcd for $C_{94}H_{111}N_6O_{10}Si$ $[(M+H)^+]$ 1511.8131. Found 1511.8142.
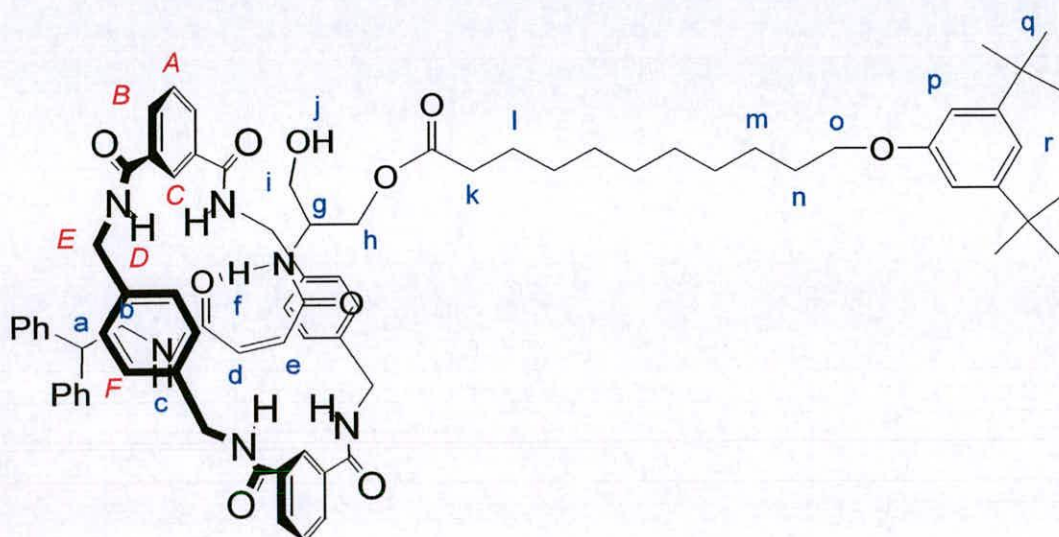
[2](1,7,14,20-Tetraaza-2,6,15,19-tetraoxo-3,5,9,12,16,18,22,25-tetrabenzocyclohexacosane)- (*Z*)-But-2-enedioic acid (2,2-diphenylethyl)-amide-3-hydroxy-11-(3,5-di-*tert*-butylphenoxy undecanoate propan-1-oxy) amide rotaxane (7).

TBAF (128 mg, 0.407 mmol) was added in one portion to a stirred solution of *maleamide*-**6** (205 mg, 0.136 mmol) in THF (5 mL) at room temperature. The reaction mixture was stirred at room temperature for 3 h. The reaction mixture was concentrated under reduced pressure and the residue was purified by column chromatography on silica gel using chloroform: methanol (50: 1) as eluent to give **7** as a colorless solid. Yield 170 mg (98 %); mp 210-211 °C; ^{1}H NMR (400 MHz, CDCl$_3$): δ = 9.27 (d, 1H, J = 7.3 Hz, C$\underline{H}_f$), 8.15-8.13 (m, 2H, N$\underline{H}_D$), 8.10 (s, 2H, ArC$\underline{H}_C$), 7.72 (dd, 4H, J = 7.6Hz, J = 2.7 Hz, ArC$\underline{H}_B$), 7.57 (t, 2H, J = 7.8 Hz, ArC$\underline{H}_A$), 7.42-7.36 (m, 4H, SiArC$\underline{H}$-ortho), 7.25-7.11 (m, 22H, ArC$\underline{H}$-stopper, SiArC$\underline{H}$-meta & para, N$\underline{H}_D$ & ArC$\underline{H}_F$), 7.04 (d, 4H, J = 7.8 Hz, ArC$\underline{H}_F$) 7.02 (t, 1H, J = 1.5 Hz, C$\underline{H}_r$), 6.76 (d, 2H, J = 1.5 Hz, C$\underline{H}_p$), 5.66 (d, 1H, J = 13.4 Hz, C$\underline{H}_d$), 5.62 (d, 1H, J = 13.4 Hz, C$\underline{H}_e$), 4.69-4.62 (m, 4H, C$\underline{H}_E$), 4.43-4.34 (m, 4H, C$\underline{H}_E$), 4.02-3.93 (m, C$\underline{H}_a$ & C$\underline{H}_o$), 3.68-3.63 (m, 4H, C$\underline{H}_g$, C$\underline{H}_i$H & C$\underline{H}_b$), 3.49-3.44 (m, 3H, C$\underline{H}_h$ & CH$\underline{H}_i$), 2.34 (t, 2H, J = 7.6 Hz, C$\underline{H}_k$), 1.78-1.74 (m, 2H, C$\underline{H}_n$), 1.42-0.80 (m, 34H, -C$\underline{H}_2$-alkyl & C$\underline{H}_q$); ^{13}C NMR (400 MHz, d_6-DMSO): δ = 173.6 (s, $\underline{C}$O$_2$R), 165.9 (s, NH$\underline{C}$O), 165.9 (s, NH$\underline{C}$O), 164.1 (s, NH$\underline{C}$O), 163.2 (s, NH$\underline{C}$O), 157.7 (s, Ar$\underline{C}$-ipso),

151.7 (s, ArC-meta), 143.0 (s, ArC-ipso-stopper), 138.3 (s, ArC-ipso-xylylene), 136.6 (s, ArC-ipso-xylylene), 135.1 (s, ArC-ipso-isophthaloyl), 134.9 (s, ArC-ipso-isophthaloyl), 134.3 (d, CH=CH$_d$), 129.5 (d, CH$_e$=CH), 129.4 (d, ArCH), 128.7 (d, ArCH), 128.4 (d, ArCH), 128.3 (d, ArCH), 128.0 (d, ArCH), 127.8 (d, ArCH), 126.6 (d, ArCH), 114.0 (d, ArCH$_r$), 108.9 (d, ArCH$_p$), 67.6 (t, CH$_k$), 50.2 (d, CH$_a$), 49.8 (d, CH$_g$), 42.8 (t, CH$_b$), 40.1 (t, CH$_E$), 34.9 (s, C(CH$_q$)), 34.0 (t, CH$_k$) 31.6 (q, CH$_q$), 29.1 (t, -CH$_2$-), 29.0 (t, -CH$_2$-), 28.7 (t, -CH$_2$-), 28.6 (t, -CH$_2$-), 28.5 (t, -CH$_2$-), 28.1 (t, -CH$_2$-), 28.0 (t, -CH$_2$-), 26.8 (t, -CH$_2$-); LRMS (FAB+ mNBA matrix) *m/z* (rel. int.): 1279 (3.2 %),

[2](1,7,14,20-Tetraaza-2,6,15,19-tetraoxo-3,5,9,12,16,18,22,25-tetrabenzocyclohexacosane)-(*Z*)-But-2-enedioic acid 2,2-diphenylethylamide-3-(*tert*-butyl-diphenyl-silanyloxy)-11-(3,5-di-*tert*-butylphenoxy undecanoate propan-1-oxy) amide rotaxane (*alkyl*-6)
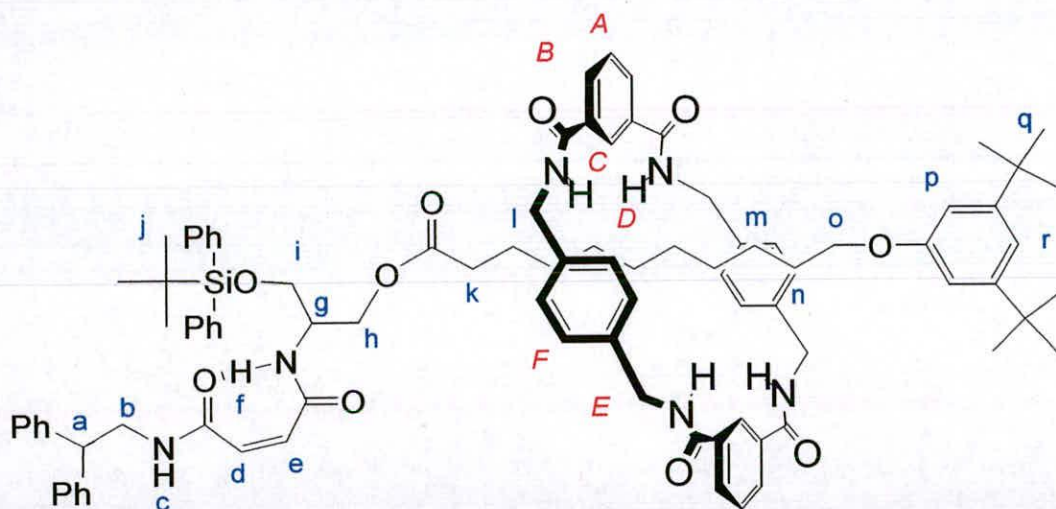
tert-Butyldiphenylsilyl chloride (203 μL, 0.780 mmol) was added to a stirred solution of **7** (200 mg, 0.156 mmol) in anhydrous DMSO (3.00 mL) at room temperature, under an atmosphere of nitrogen. Imidazole (50 mg, 0.792 mmol) was then added and the reaction mixture was then stirred at room temperature for 18 h. The reaction mixture was treated with water (10 mL) and the aqueous layer was extracted with ethyl acetate (3 x 20 mL), dried (MgSO$_4$) and concentrated under

reduced pressure. The residue was purified by column chromatography on silica gel using chloroform: methanol (99: 1) as eluent to give *alkyl*-**6** as a colorless solid. Yield 175 mg (74 %); ^{1}H NMR (400 MHz, CDCl$_3$): δ = 11.74 (d, 1H, J = 10.3 Hz, N$\underline{H}_f$), 8.16-8.11 (m, 4H, ArC$\underline{H}_B$), 7.83 (s, 2H, ArC$\underline{H}_C$), 6.95 (t, 1H, J = 1.5 Hz, C$\underline{H}_r$), 6.64 (d, 2H, J = 1.5 Hz, C$\underline{H}_p$), 6.45 (br s, 2H, N$\underline{H}_D$), 5.97 (d, 1H, J = 13.4 Hz, C$\underline{H}$=CH), 5.77 (d, 1H, J = 13.4 Hz, $\underline{C}H_e$ or C$\underline{H}_d$), 4.88 (dd, 2H, J = 14.0 Hz, J = 6.8 Hz, C$\underline{H}_E$), 4.75 (dd, 2H, J = 14.0 Hz, J = 6.8 Hz, C$\underline{H}_E$), 4.07-4.01 (m, 3H, C$\underline{H}_E$ & C$\underline{H}_a$), 3.90-3.73 (m, 7H, C$\underline{H}_E$, C$\underline{H}_o$, C$\underline{H}_g$ & C$\underline{H}_b$), 3.66 (dd, 1H, J = 3.0 Hz, J = 10.3 Hz, C$\underline{H}_h$H), 3.48-3.46 (m, 1H, CH$\underline{H}_h$), 3.34-3.31 (m, 1H, C$\underline{H}_i$H), 3.10-3.07 (m, 1H, CH$\underline{H}_i$), 1.67-1.61 (m, 2H, C$\underline{H}_n$), 1.20-0.97 (m, 26H, -C$\underline{H}_2$-alkyl, C$\underline{H}_q$), 0.95 (s, 9H, C$\underline{H}_j$), 0.80-0.71 (m, 4H, -C$\underline{H}_2$-alkyl), 0.60 (br s, 2H, -C$\underline{H}_2$-alkyl); ^{13}C NMR (100 MHz, CDCl$_3$): δ = 174.5 (s, $\underline{C}$O$_2$R), 166.6 (s, NH$_D\underline{C}$O), 166.1 (s, NH$_D\underline{C}$O), 164.9 (s, NH$\underline{C}$O), 164.4 (s, NH$\underline{C}$O), 158.6 (s, Ar$\underline{C}$-ipso), 152.1 (s, Ar$\underline{C}$-meta), 141.6 (s, Ar$\underline{C}$-ipso-stopper), 141.5 (s, Ar$\underline{C}$-ipso-stopper), 137.1 (s, Ar$\underline{C}$-ipso-xylylene), 136.7 (s, Ar$\underline{C}$-ipso-xylylene), 135.5 (d, SiAr$\underline{C}$H-ortho), 135.4 (d, SiAr$\underline{C}$H-ortho), 134.3 (s, Ar$\underline{C}$-ipso-isophthaloyl), 133.6 (s, Ar$\underline{C}$-ipso-isophthaloyl), 133.4 (d, $\underline{C}$H=CH), 132.8 (s, SiAr$\underline{C}$-ipso), 132.5 (s, SiAr$\underline{C}$-ipso), 131.8 (d, Ar$\underline{C}$H), 130.1 (d, Ar$\underline{C}$H), 129.9 (d, Ar$\underline{C}$H), 129.3 (d, Ar$\underline{C}$H), 129.0 (d, Ar$\underline{C}$H), 128.7 (d, Ar$\underline{C}$H), 128.6 (d, Ar$\underline{C}$H), 128.5 (d, Ar$\underline{C}$H), 128.1 (d, CH=$\underline{C}$H), 128.0 (d, Ar$\underline{C}$H), 127.8 (d, Ar$\underline{C}$H), 127.7 (d, Ar$\underline{C}$H), 127.6 (d, Ar$\underline{C}$H), 126.9 (d, Ar$\underline{C}$H), 126.8 (d, Ar$\underline{C}$H), 124.6 (Ar$\underline{C}$H), 114.8 (d, Ar$\underline{C}$H$_r$), 108.8 (d, Ar$\underline{C}$H$_p$), 67.7 (t, $\underline{C}$H$_o$), 61.5 (t, $\underline{C}$H$_h$), 61.0 (t, $\underline{C}$H$_i$), 50.2 (d, $\underline{C}$H$_a$), 50.0 (d, $\underline{C}$H$_g$), 44.7 (t, $\underline{C}$H$_E$) 44.1 (t, $\underline{C}$H$_E$), 43.8 (t, $\underline{C}$H$_b$), 35.0 (s, $\underline{C}$(CH$_q$)), 34.0 (t, $\underline{C}$H$_k$), 31.4 (q, $\underline{C}$H$_q$), 29.5 (t, -$\underline{C}$H$_2$-), 29.4 (t, -$\underline{C}$H$_2$-), 29.3 (t, -$\underline{C}$H$_2$-), 29.2 (t, -$\underline{C}$H$_2$-), 29.0 (t, -$\underline{C}$H$_2$-), 26.6 (q, $\underline{C}$H$_j$), 26.1 (t, -$\underline{C}$H$_2$-), 24.4 (t, -$\underline{C}$H$_2$-), 19.1 (s, $\underline{C}$(CH)$_j$); LRMS (FAB+ mNBA matrix) m/z (rel. int.): 1512 (92 %), [(M+H)$^+$], HRMS (FAB+) calcd for ^{13}C$_1$C$_{93}$H$_{111}$N$_6$O$_{10}$Si [(M+H)$^+$] 1512.8160. Found 1511.8142.

[2](1,7,14,20-Tetraaza-2,6,15,19-tetraoxo-3,5,9,12,16,18,22,25-tetrabenzocyclohexacosane)-3,3-diphenylpropyl-11-(3,5-di-*tert*-butylphenoxy)undecanoate rotaxane (1)
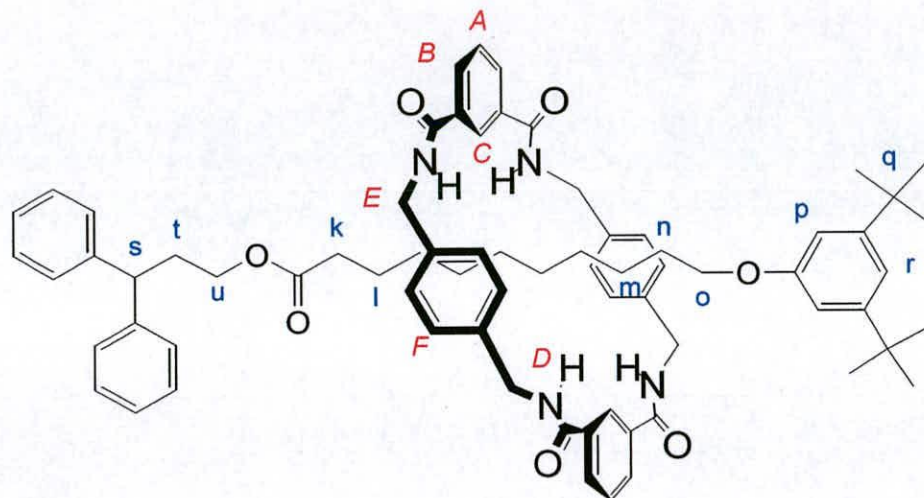
A melt of 3,3-diphenylpropanol (491 mg, 2.31 mmol), *alkyl*-**6** (175 mg, 0.116 mmol), and a catalytic amount of potassium *tert*-butoxide (5 mol %) was heated with vigorous stirring at 65 °C under argon for 3 h. The reaction was allowed to cool to room temperature and the residue was purified by column chromatography on silica gel using chloroform: methanol (100: 1) as eluent to give **1** as a colorless solid. Yield 108 mg (85 %); mp 157-160 °C; ^{1}H NMR (400 MHz, CDCl$_3$): δ = 8.22 (dd, 4H, J = 1.5 Hz, J = 7.8 Hz, ArC$\underline{H}_B$), 7.97 (s, 2H, ArC$\underline{H}_C$), 7.66 (t, 2H, J = 7.8 Hz, ArC$\underline{H}_A$), 4.55-4.46 (m, 8H, C$\underline{H}_E$), 3.90 (t, 2H, J = 6.6 Hz, C$\underline{H}_o$), 3.54 (t, 1H, J = 7.6 Hz, C$\underline{H}_s$), 3.16 (t, 2H, J = 7.8 Hz, C$\underline{H}_u$), 1.67-1.58 (m, 4H, C$\underline{H}_t$ & C$\underline{H}_k$), 1.45-1.26 (m, 30H, -C$\underline{H}_2$-alkyl & C$\underline{H}_q$), 1.09-0.82 (m, 6H, -C$\underline{H}_2$-alkyl); ^{13}C NMR (100 MHz, CDCl$_3$): δ = 175.3 (s, $\underline{C}$O$_2$R), 166.0 (s, NH$_D\underline{C}$O), 158.5 (s, Ar$\underline{C}$-ipso), 152.1 (s, Ar$\underline{C}$-meta), 143.3 (s, Ar$\underline{C}$-ipso-stopper), 137.3 (s, Ar$\underline{C}$-ipso-xylylene), 134.1 (s, Ar$\underline{C}$-ipso-isophthaloyl), 131.4 (d, Ar$\underline{C}$H$_B$), 129.6 (d, Ar$\underline{C}$H$_C$), 128.8 (d, Ar$\underline{C}$H$_A$), 128.7 (d, Ar$\underline{C}$H), 127.3 (d, Ar$\underline{C}$H), 126.8 (d, Ar$\underline{C}$H), 123.2, (d, Ar$\underline{C}$H$_F$) 114.8 (d, Ar$\underline{C}$H$_r$), 108.7 (d, Ar$\underline{C}$H$_p$), 67.7 (t, $\underline{C}$H$_o$), 63.9 (t, $\underline{C}$H$_u$), 47.2 (d, $\underline{C}$H$_s$), 44.1 ($\underline{C}$H$_E$), 35.0 (s, $\underline{C}$(CH$_3$)$_3$), 34.0 (t, $\underline{C}$H$_k$), 34.2 (t, $\underline{C}$H$_t$), 31.4 (q, C($\underline{C}$H$_3$)$_3$), 29.4 (t, -$\underline{C}$H$_2$-), 29.4 (t, -$\underline{C}$H$_2$-), 29.3 (t, -$\underline{C}$H$_2$-), 29.1 (t, -$\underline{C}$H$_2$-), 28.9 (t, -$\underline{C}$H$_2$-), 26.1 (t, -$\underline{C}$H$_2$-), 24.1 (t, -$\underline{C}$H$_2$-), 22.7 (t, -$\underline{C}$H$_2$-); LRMS (FAB+ mNBA matrix) *m/z* (rel. int.): 1117 (5.7 %),

[(M+H)$^+$], HRMS (FAB+) calcd for C$_{72}$H$_{85}$N$_4$O$_7$ [(M+H)$^+$] 1117.6418. Found 1117.6411.

(*Z*)-But-2-enedioic acid 2,2-diphenylethylamide-3-(diphenyl-*tert*-butylsiloxy)-11-(3,5-di-tert-butylphenoxy undecanoate propan-1-oxy) amide *thread*-6
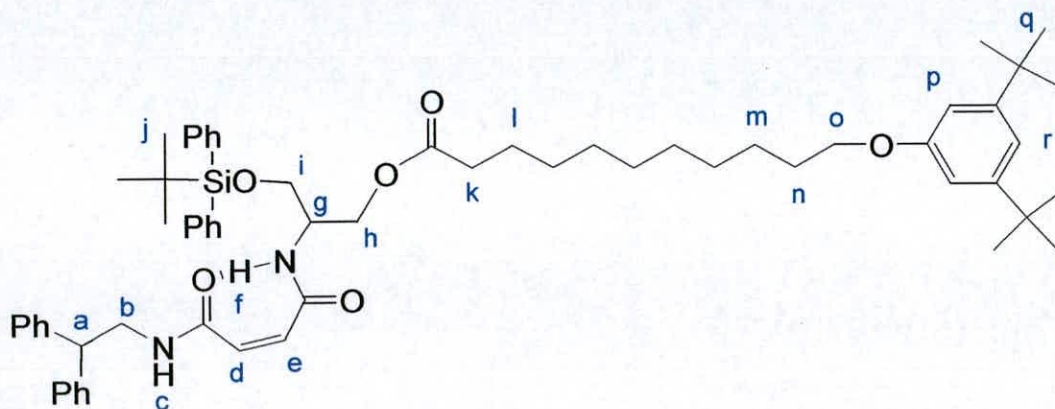
4 (150 mg, 0.153 mmol) was dissolved in dichloromethane (30 mL) in a quartz vessel. The solution was directly irradiated at 254 nm using a multilamp photo-reactor. Different photostationary states were reached in 20 min, after which the reaction mixture was concentrated under reduced pressure to afford the crude product. The residue was purified by column chromatography on silica gel using ethyl acetate: petroleum ether 40-60 °C (1: 1) as eluent to give *thread*-6 as a colorless oil. Yield 81 mg (53 %); ^{1}H NMR (400 MHz, CDCl$_3$): δ = 8.61 (d, 1H, *J* = 7.1 Hz, NH$_f$), 7.67-7.64 (m, 4H, SiArCH-ortho), 7.52 (t, 1H, *J* = 5.2 Hz, NH$_c$), 7.44-7.19 (m, 16H, ArCH-stopper & SiArCH-meta & para), 7.02 (t, 1H, *J* = 1.6 Hz, ArCH$_r$), 6.76 (d, 2H, *J* = 1.6 Hz, ArCH$_p$), 5.95 (s, 2H, CH$_d$ & CH$_e$), 4.33-4.25 (m, 3H, CH$_g$ & CH$_h$), 4.21 (t, 1H, *J* = 8.3 Hz, CH$_a$), 3.96 (t, 2H, *J* = 6.6 Hz, CH$_o$), 3.93-3.90 (m, 2H, CH$_b$), 3.80 (dd, 2H, *J* = 10.5 Hz, *J* = 3.0 Hz, CH$_i$), 2.27 (t, 2H, *J* = 7.8 Hz, CH$_k$), 1.82-1.75 (m, 2H, CH$_n$), 1.61-1.55 (m, 2H, CH$_l$), 1.48-1.44 (m, 2H, CH$_m$), 1.37-1.22 (m, 30H, -CH$_2$-alkyl & CH$_q$), 1.07 (s, 9H, CH$_j$); ^{13}C NMR (100 MHz, CDCl$_3$): δ = 173.5 (s, $\underline{C}$O$_2$R), 164.5 (s, NH$\underline{C}$O), 164.2 (s, NH$\underline{C}$O), 158.6 (s, Ar$\underline{C}$-ipso), 152.0 (s, Ar$\underline{C}$-meta), 141.7 (s, Ar$\underline{C}$-ipso-stopper), 135.5 (d, SiAr$\underline{C}$H-ortho), 135.5 (d, SiAr$\underline{C}$H-ortho), 133.1 (d, $\underline{C}$H=CH), 133.0 (s, SiAr$\underline{C}$-ipso), 132.9 (s, SiAr$\underline{C}$-ipso), 131.7 (d,

CH=$\underline{C}$H), 129.8 (d, Ar$\underline{C}$H), 129.7 (d, Ar$\underline{C}$H), 128.6 (d, Ar$\underline{C}$H), 127.9 (d, Ar$\underline{C}$H), 127.7 (d, Ar$\underline{C}$H), 126.7 (d, Ar$\underline{C}$H), 114.7 (d, Ar$\underline{C}$H$_r$), 108.8 (d, Ar$\underline{C}$H$_p$), 67.7 (t, $\underline{C}$H$_o$), 62.1 (t, $\underline{C}$H$_i$), 61.0 (t, $\underline{C}$H$_h$), 50.2 (d, $\underline{C}$H$_g$), 49.9 (d, $\underline{C}$H$_a$), 44.1 (t, $\underline{C}$H$_b$), 34.9 (s, $\underline{C}$(CH$_3$)$_3$), 34.1 (t, $\underline{C}$H$_k$), 31.4 (q, C($\underline{C}$H$_3$)$_3$), 29.5 (t, -$\underline{C}$H$_2$-), 29.4 (t, -$\underline{C}$H$_2$-), 29.4 (t, -$\underline{C}$H$_2$-), 29.4 (t, -$\underline{C}$H$_2$-), 29.2 (t, -$\underline{C}$H$_2$-), 29.1 (t, -$\underline{C}$H$_2$-), 26.8 (t, q, $\underline{C}$H$_j$), 24.7 (t, $\underline{C}$H$_2$-), 19.2 (s, $\underline{C}$(CH$_j$)); LRMS (FAB+ mNBA matrix) m/z (rel. int.): 979 (27.5 %), [(M+H)$^+$], HRMS (FAB+) calcd for C$_{62}$H$_{83}$N$_2$O$_6$Si [(M+H)$^+$] 979.6020. Found 979.6019.
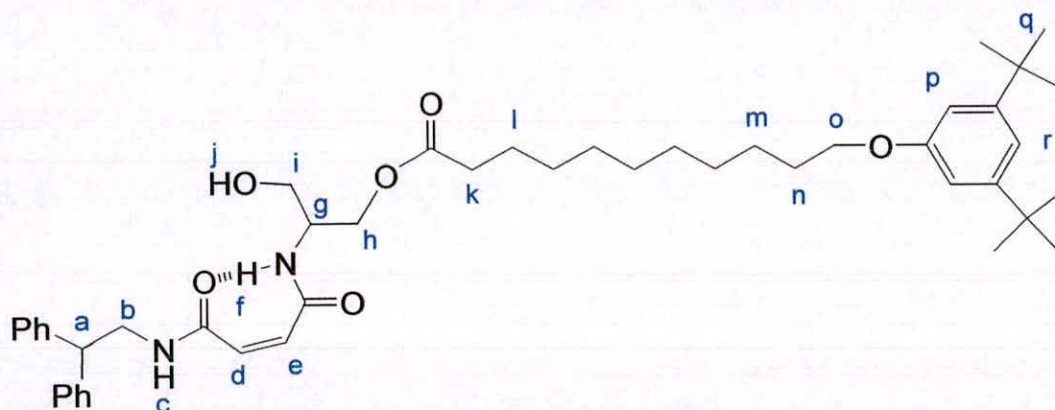
(Z)-But-2-enedioic acid 2,2-diphenylethylamide-3-hydroxy-11-(3,5-di-*tert*-butylphenoxy undecanoate propan-1-oxy) amide *thread*-7

TBAF (85 mg, 0.270 mmol) was added in one portion to a stirred solution of *thread-6* (100 mg, 0.135 mmol) in THF (5 mL) at room temperature. The reaction mixture was stirred at room temperature for 3 h. The reaction mixture was concentrated under reduced pressure. The residue was purified by column chromatography on silica gel using hexane: ethyl acetate (1: 1) as eluent to give *thread-7* as a colorless solid. Yield 72 mg (95 %); m.p. 99-101 °C; ^{1}H NMR (400 MHz, CDCl$_3$): δ = 8.70 (d, 1H, J = 7.6 Hz, N$\underline{H}_f$), 7.35-7.24 (m, 11H, ArCH-stopper &, N$\underline{H}_c$), 7.04 (t, 1H, J = 1.6 Hz, C$\underline{H}_r$), 6.78 (d, 2H, J = 1.6 Hz, C$\underline{H}_p$), 6.06 (d, 1H, J = 13.2 Hz, C$\underline{H}_d$), 5.92 (d, 1H, J = 13.2 Hz, C$\underline{H}_e$), 4.28-4.16 (m, 3H, C$\underline{H}_g$ & C$\underline{H}_h$), 3.99-3.94 (m, 4H, C$\underline{H}_o$ & C$\underline{H}_b$), 3.74-3.71 (m, 2H, C$\underline{H}_i$), 3.19 (t, 1H, J = 5.1 Hz, O$\underline{H}_j$), 2.38 (t, 2H, J = 7.6 Hz, C$\underline{H}_k$), 1.84-1.77 (m, 2H, C$\underline{H}_n$), 1.66-1.63 (m, 2H, C$\underline{H}_l$), 1.49-1.46 (m, 2H, C$\underline{H}_m$), 1.33-1.26 (m, 28H, -CH$_2$-alkyl & C$\underline{H}_q$); ^{13}C NMR (100 MHz, CDCl$_3$): δ = 174.1 (s, $\underline{C}$O$_2$R), 165.1 (s,

NH$\underline{C}$O), 164.7 (s, NH$\underline{C}$O), 158.6 (s, Ar$\underline{C}$-ipso), 152.1 (s, Ar$\underline{C}$-meta), 141.5 (s, Ar$\underline{C}$-ipso-stopper), 133.7 (d, CH=$\underline{C}$H), 130.7 (d, $\underline{C}$H=CH), 128.7 (d, Ar$\underline{C}$H), 128.0 (d, Ar$\underline{C}$H), 126.9 (d, Ar$\underline{C}$H), 114.6 (d, Ar$\underline{C}$H$_r$), 108.8 (d, Ar$\underline{C}$H$_p$), 67.7 (t, $\underline{C}$H$_o$), 62.3 (t, $\underline{C}$H$_h$), 61.7 (t, $\underline{C}$H$_i$), 51.0 (d, $\underline{C}$H$_a$), 50.2 (d, $\underline{C}$H$_g$), 44.1 (t, $\underline{C}$H$_b$), 34.9 (s, $\underline{C}$(CH$_3$)$_3$), 34.1 (t, $\underline{C}$H$_k$), 31.4 (q, C($\underline{C}$H$_3$)$_3$), 29.5 (t, -$\underline{C}$H$_2$-), 29.5 (t, -$\underline{C}$H$_2$-), 29.4 (t, -$\underline{C}$H$_2$-), 29.4 (t, -$\underline{C}$H$_2$-), 29.2 (t, -$\underline{C}$H$_2$-), 29.1 (t, -$\underline{C}$H$_2$-), 26.1 (t, -$\underline{C}$H$_2$-), 24.8 (t, $\underline{C}$H$_2$-); LRMS (FAB+ mNBA matrix) m/z (rel. int.): 741 (82.6 %), [(M+H)$^+$], HRMS (FAB+) calcd for C$_{46}$H$_{65}$N$_2$O$_6$ [(M+H)$^+$] 741. 4843. Found 741.4843.

3,3-diphenylpropyl-11'-(3,5-di-*tert*-butylphenoxy)undecanoate *thread*-1
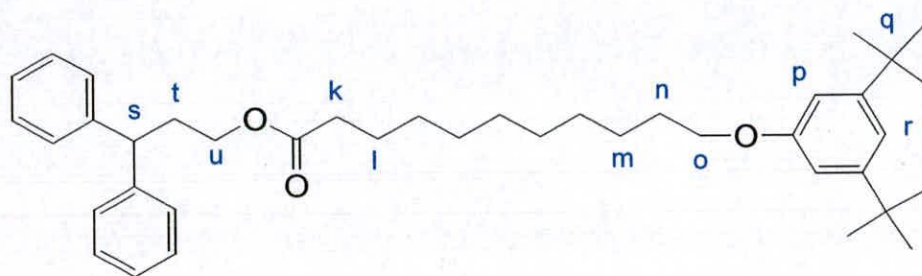
EDCI (147 mg, 0.770 mmol) and a catalytic amount of 4-DMAP were added in one portion to a stirred solution of **3** (200 mg, 0.513 mmol), 3,3-diphenylpropanol (114 mg, 0.538 mmol) in dichloromethane (10 mL) at 0 °C. The reaction mixture was stirred at 0 °C for 1 h and at room temperature for 13 h. The reaction mixture was washed with 1 M aqueous hydrochloric acid solution (2 x 20 mL), saturated aqueous sodium hydrogen carbonate (2 x 20 mL), dried (MgSO$_4$) and concentrated under reduced pressure. The residue was purified by column chromatography on silica gel using hexane: ethyl acetate (5: 1) as eluent to give *thread*-1 as a colorless oil. Yield 279 mg (93 %); ^{1}H NMR (400 MHz, CDCl$_3$): δ = 7.31-7.17 (m, 10H, Ar$\underline{CH}$-stopper), 7.01 (t, 1H, J = 1.6 Hz, Ar$\underline{CH}_r$), 6.76 (d, 2H, J = 1.6 Hz, Ar$\underline{CH}_p$), 4.05 (t, 1H, J = 7.4 Hz, $\underline{CH}_s$), 4.03 (t, 2H, J = 6.6 Hz, $\underline{CH}_u$), 3.96 (t, 2H, J = 7.6 Hz, $\underline{CH}_o$), 2.42-2.37 (m, 2H, $\underline{CH}_t$), 2.27 (t, 2H, J = 7.6 Hz, $\underline{CH}_k$), 1.81-1.75 (m, 2H, $\underline{CH}_n$), 1.62-1.57 (m, 2H, $\underline{CH}_l$), 1.50-1.41 (m, 2H, $\underline{CH}_m$), 1.39-1.27 (m, 28H, -$\underline{CH}_2$-alkyl & $\underline{CH}_q$); ^{13}C NMR (100 MHz, CDCl$_3$): δ = 173.6 (s, $\underline{C}$O$_2$R), 158.6 (s, Ar$\underline{C}$-ipso), 151.9 (s, Ar$\underline{C}$-meta), 143.9 (s, Ar$\underline{C}$-ipso-stopper), 128.5 (d, Ar$\underline{C}$H), 127.7 (d, Ar$\underline{C}$H), 126.3 (d,

Ar$\underline{C}$H), 114.6 (d, Ar$\underline{C}$H$_r$), 108.7 (d, Ar$\underline{C}$H$_p$), 67.6 (t, $\underline{C}$H$_o$), 62.5 (t, $\underline{C}$H$_u$), 47.6 (d, $\underline{C}$H$_a$), 34.9 (s, $\underline{C}$(CH$_q$)), 34.3 (t, $\underline{C}$H$_k$), 34.2 (t, $\underline{C}$H$_t$), 31.4 (q, C($\underline{C}$H$_q$)), 29.4 (t, -$\underline{C}$H$_2$-), 29.4 (t, -$\underline{C}$H$_2$-), 29.3 (t, -$\underline{C}$H$_2$-), 29.3 (t, -$\underline{C}$H$_2$-), 29.2 (t, -$\underline{C}$H$_2$-), 29.1 (t, -$\underline{C}$H$_2$-), 26.1 (t, -$\underline{C}$H$_2$-), 24.9 (t, -$\underline{C}$H$_2$-); LRMS (FAB+ mNBA matrix) m/z (rel. int.): 585 (89.2 %), [(M+H)$^+$], HRMS (FAB+) calcd for C$_{40}$H$_{57}$O$_3$ [(M+H)$^+$] 585.4309. Found 585.4317.

4.5 Experimental References

1   L. D. Arnold, T. H. Kalantar, J. C. Vederas, *J. Am. Chem. Soc.* **1985**, *107*, 7105-7109

Appendix

5.0 Publications and Presentations

Poster Presentation: J. S. Hannam, D. A. Leigh, "Mechanically Interlocking Auxiliaries: Rotaxanes Made to Order", 16th International Conference on Physical-Organic Chemistry, University of California, San Diego (UCSD), La Jolla, California, USA, August 4-9th, 2002.

Oral Presentation: "Mechanically Interlocking Auxiliaries: Rotaxanes Made to Order", 14th SCI Postgraduate Symposium on Novel Organic Chemistry (Scotland), University of Aberdeen, Aberdeen, UK, 9th April 2003. 1st Prize

Poster Presentation: J. S. Hannam, D. A. Leigh, "Mechanically Interlocking Auxiliaries: Rotaxanes Made to Order", 1st University of Glasgow-Organon Symposium on Synthetic Chemistry, University of Glasgow, Glasgow, UK, 22nd Sept, 2003. 1st Prize

J.S. Hannam, T. J. Kidd, D. A. Leigh, A. J. Wilson, *Org. Lett.* **2003**, *5*, 1907-1910.

J.S. Hannam, S. M. Lacy, D. A. Leigh, C. G. Saiz, A. M. Z. Slawin, S. G. Stitchell, *Angew. Chem. Int. Ed. Engl.* **2004**, *43*, 3260-3264.

"Magic Rod" Rotaxanes: The Hydrogen Bond-Directed Synthesis of Molecular Shuttles under Thermodynamic Control
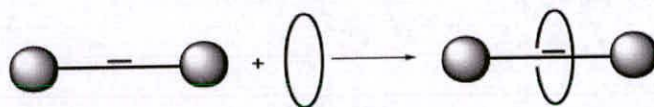
Jeffrey S. Hannam, Timothy J. Kidd, David A. Leigh,* and Andrew J. Wilson

School of Chemistry, University of Edinburgh, The Kings Buildings, West Mains Road, Edinburgh EH9 3JJ, United Kingdom

david.leigh@ed.ac.uk

Received March 21, 2003

ABSTRACT

Peptide [2]- and [3]rotaxanes are assembled in high yields under thermodynamic control using hydrogen bonding interactions and reversible cross olefin metathesis.

While the use of noncovalent interactions to direct the synthesis of rotaxanes[1] often leads to greatly improved yields over statistical methods, the final step in the rotaxane-forming reaction ("clipping" or "capping", Scheme 1) is generally

Scheme 1. Common Noncovalent Bond-Directed Strategies for Rotaxane Synthesis[a]
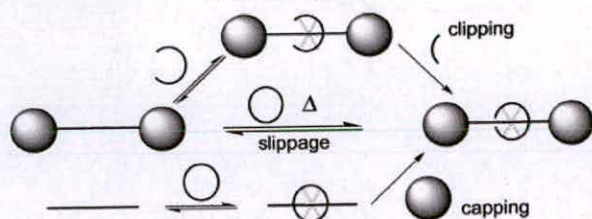
[a] Clipping and capping steps are usually irreversible, so "errors" in the synthesis (i.e., noninterlocked byproducts) cannot be corrected.

under kinetic control. Consequently, noninterlocked products formed during the reaction cannot be recycled even if

the rotaxane is the most energetically favored structure because of the built in favorable noncovalent interactions between the components. So-called "slippage" strategies[2] *are* under thermodynamic control,[3] but the necessary elevated temperatures reduce the strength of noncovalent interactions and therefore also the efficiency of rotaxane formation. Accordingly, novel approaches to the efficient synthesis of rotaxanes are still desirable.

Thermodynamic control over mechanical bond formation is particularly amenable to the principles of dynamic combinatorial chemistry (DCC).[4] The kinetic lability of metal–ligand coordination bonds and disulfide exchange reactions have both been employed to shift equilibria between interlocked and non-interlocked products.[5–7] Imine exchange, together with post-assembly covalent modification,[3] allows the high-yielding synthesis of rotaxanes by both clipping and

(1) (a) Schill, G. *Catenanes, Rotaxanes and Knots*; Academic Press: New York, 1971. (b) Amabilino, D. B.; Stoddart, J. F. *Chem. Rev.* **1995**, *95*, 2725–2828. (c) Sauvage, J.-P., Dieterich-Buchecker, C. O., Eds. *Molecular Catenanes Rotaxanes and Knots*; Wiley-VCH: Weinheim, Germany, 1999.

(2) (a) Raymo, F. M.; Houk, K. N.; Stoddart, J. F. *J. Am. Chem. Soc.* **1998**, *120*, 9318–9322. (b) Heim, C.; Affeld, A.; Nieger, M.; Vögtle, F. *Helv. Chim. Acta* **1999**, *82*, 746–759.

(3) (a) Lindsey, J. S. *New J. Chem.* **1991**, *15*, 153–180. (b) Philp, D.; Stoddart, J. F. *Angew. Chem., Int. Ed. Engl.* **1996**, *35*, 1154–1196.

(4) (a) Lehn, J.-M. *Chem Eur. J.* **1999**, *5*, 2455–2463. (b) Rowan, S. J.; Cantrill, S. J.; Cousins, G. R. L.; Sanders, J. K. M.; Stoddart, J. F. *Angew. Chem., Int. Ed.* **2002**, *41*, 898–952.

(5) (a) Fujita, M.; Ibukuro, F.; Hagihara, H.; Ogura, K. *Nature* **1994**, *367*, 720–723. (b) Fujita, M.; Aoyagi, M.; Ibukuro, F.; Ogura, K.; Yamaguchi, K. *J. Am. Chem. Soc.* **1998**, *120*, 611–612. (c) Try, A. C.; Harding, M. M.; Hamilton, D. G.; Sanders, J. K. M. *Chem. Commun.* **1998**, 723–724. (d) Padilla-Tosta, M. E.; Fox, O. D.; Drew, M. G. B.; Beer, P. D. *Angew. Chem., Int. Ed.* **2001**, *40*, 4235–4239.
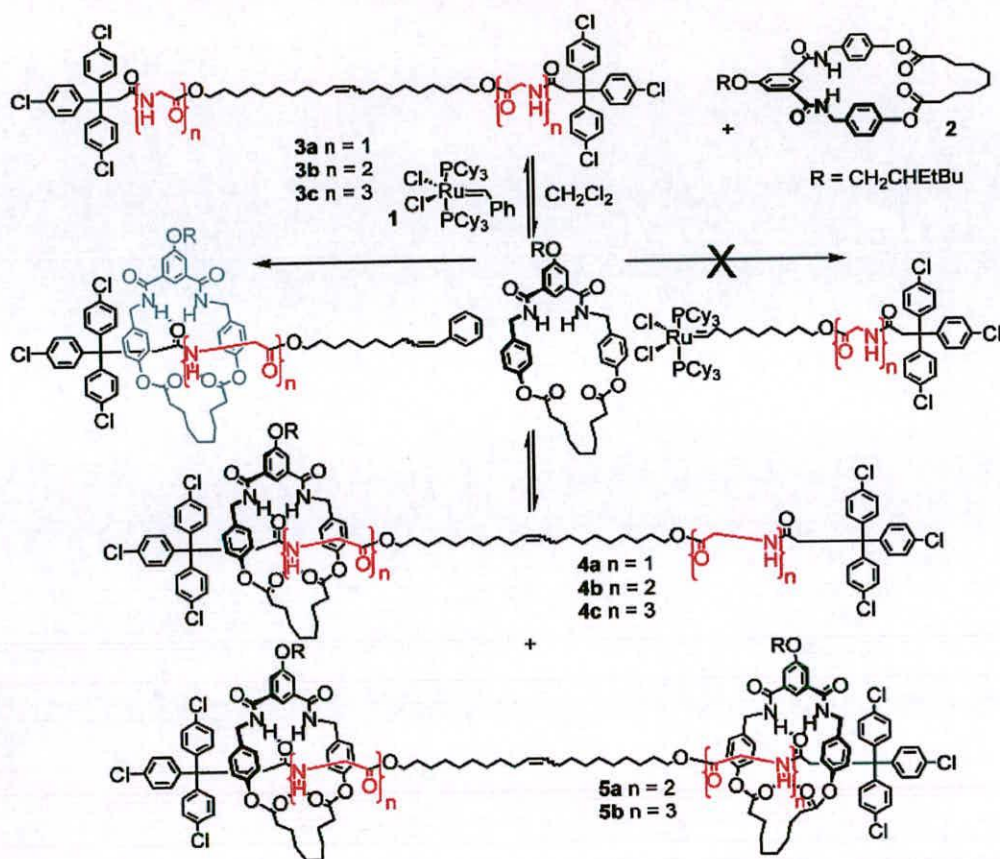
capping[8] and has also been used to achieve catenane synthesis under thermodynamic control.[9] Of the remaining synthetic transformations previously used in DCC, olefin metathesis is advantageous because removal of a reaction-specific catalyst (e.g., **1**) is all that is required to "lock" the product distribution. Indeed, olefin metathesis has been used to synthesize catenanes,[9,10] rotaxanes[11] and knots[12] under kinetic control and cantenanes and catenates under thermody-

namic[9,13] control. In our own laboratories, reversible ring-opening metathesis combined with the hydrogen bond-directed assembly of self-complementary macrocycles allowed the synthesis of kinetically robust catenanes in near quantitative yields.[14] Here we report the extension of this concept to the synthesis of hydrogen bond-assembled rotaxanes under thermodynamic control.

Schematically, when benzylic amide macrocycle **2** and a rod **3a–c** containing two bulky stoppers, peptide-based template sites, and a "magic"[14] olefin are exposed to Grubbs first-generation metathesis catalyst **1**, the rod is opened and the macrocycle binds to the template through four-point hydrogen bonding. Upon reformation of the carbon–carbon double bond, the macrocycle is trapped on the thread producing a [2]rotaxane (**4a–c**, Scheme 2). The [2]rotaxane

(6) For capping, see: (a) Chichak, K.; Walsh, M. C.; Branda, N. R. *Chem. Commun.* **2000**, 847–848. (b) Baer, A. J.; Macartney, D. H. *Inorg. Chem.* **2000**, *39*, 1410–1417. (c) Gunter, M. J.; Bampos, N.; Johnstone, K. D.; Sanders, J. K. M. *New J. Chem.* **2001**, *25*, 166–173. For clipping, see: (d) Hunter, C. A.; Low, C. M. R.; Packer, M. J.; Spey, S. E.; Vinter, J. G.; Vysotsky, M. O.; Zonta, C. *Angew. Chem., Int. Ed.* **2001**, *40*, 2678–2682. (e) Chang, S.-Y.; Choi, J. S.; Jeong, K.-S. *Chem. Eur. J.* **2001**, *7*, 2687–2697.

(7) (a) Furusho, Y.; Hasegawa, T.; Tsuboi, A.; Kihara, N.; Takata, T. *Chem. Lett.* **2000**, 18–19. (b) The kinetically controlled crystallization of a potentially dynamic system appears to have been used to advantage in a high-yielding preparation of a [3]rotaxane: Kolchinski, A. G.; Alcock, N. W.; Roesner, R. A.; Busch, D. H. *Chem. Commun.* **1998**, 1437–1438.

(8) (a) Cantrill, S. J.; Rowan, S. J.; Stoddart, J. F. *Org. Lett.* **1999**, *1*, 1363–1366. (b) Rowan, S. J.; Stoddart, J. F. *Org. Lett.* **1999**, *1*, 1913–1916. (c) Glink, P. T.; Oliva, A. I.; Stoddart, J. F.; White, A. J. P.; Williams, D. J. *Angew. Chem., Int. Ed.* **2001**, *40*, 1870–1875.

(9) Leigh, D. A.; Lusby, P. J.; Teat, S. J.; Wilson, A. J. *Angew. Chem., Int. Ed.* **2001**, *40*, 1538–1543.

(10) (a) Mohr, B.; Weck, M.; Sauvage, J.-P.; Grubbs, R. H. *Angew. Chem., Int. Ed. Engl.* **1997**, *36*, 1308–1310. (b) Weck, M.; Mohr, B.; Sauvage, J.-P. Grubbs, R. H. *J. Org. Chem.* **1999**, *64*, 5463–5471.

(11) (a) Wisner, J. A.; Beer, P. D.; Drew, M. G. B.; Sambrook, M. R. *J. Am. Chem. Soc.* **2002**, *124*, 12469–12476. (b) Coumans, R. G. E.; Elemans, J. A. A. W.; Thordarson, P.; Nolte, R. J. M.; Rowan, A. E. *Angew. Chem., Int. Ed.* **2003**, *42*, 650–654.

(12) Dietrich-Buchecker, C. O.; Rapenne, G.; Sauvage, J.-P. *Chem. Commun.* **1997**, 2053–2054.

(13) Hamilton, D. G.; Feeder, N.; Teat, S. J.; Sanders, J. K. M. *New J. Chem.* **1998**, 1019–1021.

(14) For organic "magic" rings—macrocycles that interlock without any final net change to their covalent structure, see: Kidd, T. J.; Leigh, D. A.; Wilson, A. J. *J. Am. Chem. Soc.* **1999**, *121*, 1599–1600. For the original magic rings based on coordination chemistry, see ref 5a.

Table 1. Yields of Magic Rod Rotaxanes **4a**−**c** and **5a**−**b** from Olefin Metathesis of Magic Rods **3a**−**c**

reactants	concn	[2]rotaxane **4a**−**c**	[3]rotaxane **5a**−**b**	interlocked products
1 equiv of **2** and **3a**	0.2 M	15%	0%	15%
1 equiv of **2** and **3b**	0.2 M	36%	20%	56%
1 equiv of **2** and **3c**	0.2 M	34%	24%	58%
5 equiv of **2** and **3b**	0.2 M	52%	43%	95%
1 equiv of **2** and **3b**	0.05 M	29%	11%	40%
5a	0.05 M	29%	11%	40%
1 equiv of **2** and **3b**	0.0002 M	1%	0%	1%

can subsequently become a [3]rotaxane (**5a**, **5b**) through another round of metathesis (models show that the ruthenium carbene acts as a stopper in the first round preventing direct assembly of the [3]rotaxane).

The synthesis of macrocycle **2** has previously been reported,[14] while the syntheses of threads **3a**−**c** were carried out in four steps using simple amide and ester bond-forming reactions and cross olefin metathesis in the final step. The long C_{20} threads were used because we found shorter chains (C_{10}) to react poorly, either because of steric hindrance or the formation of metal chelates with the Grubbs catalyst as proposed in the literature[15]. A triphenylmethine stopper was used as smaller groups allowed the macrocycle to de-thread.[16,17] Metathesis experiments were carried out in CH_2Cl_2 (the noncompeting solvent maximizes the strength of the intercomponent hydrogen bonding) using Grubbs catalyst **1**.[18] As the metathesis reaction is reversible (although care needs to be taken to ensure this[14]), the product distribution is determined only by the relative stabilities of the products; at high concentrations, predominantly threaded species are obtained that can, if desired, be converted back to the uninterlocked components by simply diluting the reaction mixture (but *only* in the presence of active catalyst). The rather spectacular results (overall yields of interlocked products ranging from 1 to 95% merely by changing the concentration) of the metathesis reactions of "magic rods" **3a**−**c** at different concentrations are shown in Table 1. Decomposition of the catalyst (for example, by adding *n*-propylamine) or simply sequestering it from the reaction mixture with poly(divinylbenzene) fixes the product distribution unless, and until, additional catalyst is added. Trifluoroacetylation (($CF_3CO)_2O$) of the amide groups of the rotaxane removes the intramolecular hydrogen bonding interactions and allows disassembly of the rotaxane into its components at any concentration (but *only* in the presence of **1**).[14]

The yields imply that at least two amides are necessary in each template for rotaxane assembly to be effective. How-ever, this is probably because the N-terminal amide is sterically hindered by the stopper and therefore cannot bind efficiently to the macrocycle. The reactions were shown to be under true thermodynamic control by the identical product distributions obtained from the metathesis of different starting materials containing the same overall proportions of thread and macrocycle (for example [3]rotaxane **4b** and a 1:2 mixture of thread **3b** and macrocycle **2**).

Representative ^{1}H NMR spectra of the glycylglycine magic rod rotaxanes **4b**, **5a**, and thread **3b** in $CDCl_3$ at 50 °C are shown in Figure 1. The resonances of the thread H_e and H_g protons appear at the normal chemical shifts for glycine residues (Figure 1a). The same signals in the [2]rotaxane **4b** (Figure 1b), however, display the characteristic upfield shifts[19] of a threaded species as a result of shielding by the aromatic rings of the macrocycle (note, each peptide station is only occupied at most 50% of the time in the [2]rotaxane). The amide protons, H_D, of the macrocycle appear downfield due to hydrogen bonding. Only one thread amide (H_f) undergoes an appreciable change in chemical shift and is shifted upfield, suggesting that the effects of hydrogen bonding are mostly offset by the shielding effect of the macrocycle and/or the thread amide groups intramolecularly hydrogen bonding in **3b**. Only one set of signals is seen for each glycylglycine station, indicating that shuttling of the macrocycle along the axis of the thread is fast on the NMR time scale. The [3]rotaxane (Figure 1c) experiences changes in chemical shift similar to the [2]rotaxane, although these are somewhat more pronounced (because each peptide station is occupied nearly 100% of the time in the [3]rotaxane). Finally, in the case of the [3]rotaxane, an ABX system is observed for the H_E protons of macrocycle **2**. This arises because the faces of the macrocycle experience different environments in the [3]rotaxane (one points toward the other macrocycle, the other toward the nearest stopper), while in the analogous [2]rotaxane, the two faces of the fast-shuttling macrocycle effectively experience identical environments.

In a manner similar to previously described peptide-based molecular shuttles,[19] this class of rotaxanes exhibit solvent-dependent translational isomerism; that is, in d_6-DMSO, the hydrogen bonding between the thread and the macrocycle is disrupted and the macrocycle(s) sit(s) predominantly on the alkyl chain of the thread shielding it from the polar solvent.

(15) Fürstner, A.; Langemann, K. *J. Am. Chem. Soc.* **1997**, *119*, 9130−9136.

(16) Experiments (Supporting Information) reveal that macrocycle **2** and glycylglycine threads bearing diphenyl stoppers form complexes (pseudorotaxanes, K_a = 300 M^{-1}) only slowly at room temperature. This could be considered "slow slippage" rotaxane formation.

(17) The trischlorophenyl derivative was readily available in larger and cheaper quantities than other alternatives.

(18) For a detailed description of the experimental procedure, see Supporting Information.

(19) Lane, A. S.; Leigh, D. A.; Murphy, A. *J. Am. Chem. Soc.* **1997**, *119*, 11092−11093.
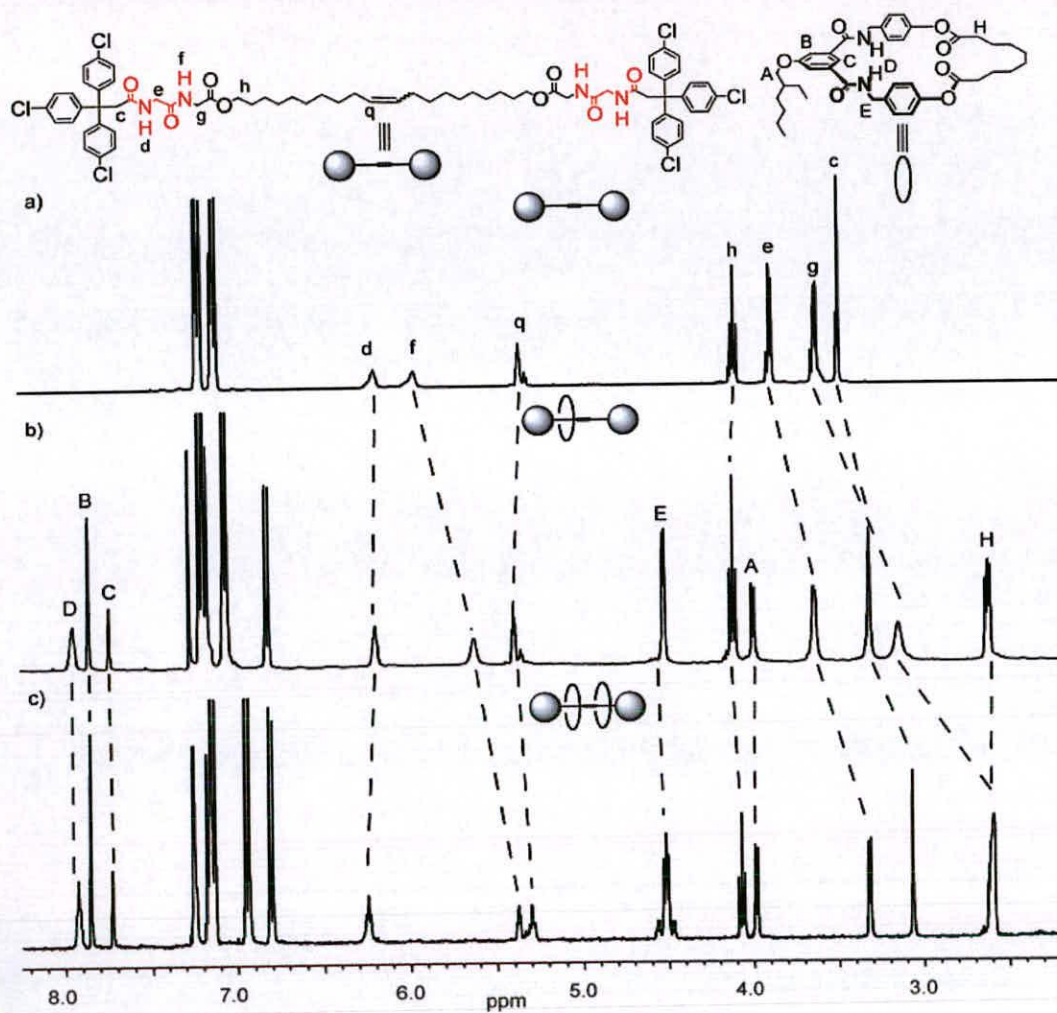
Figure 1. ^{1}H NMR spectra in CDCl$_3$ at 50 °C of (a) bis-glycylglycine thread **3b**, (b) [2]rotaxane **4b**, and (c) [3]rotaxane **5a**.

In conclusion, the combination of directed hydrogen bonding and cross olefin metathesis provides a powerful tool for the assembly (or disassembly) of rotaxanes through built in recycling of nonpreferred byproducts; a useful quality in developing "engineering up" approaches to large functional supermolecules. Significantly, since the reversible reaction involves breaking a strong C=C bond and only occurs in the presence of a specific catalyst, molecules assembled in this way are not inherently labile. Furthermore, this technique can be carried out at room temperature and below, so the programmed noncovalent interactions can be maximized. The result is the best possible kind of synthetic strategy: a thermodynamically controlled, noncovalent bond-directed assembly of a kinetically robust final superstructure.

Communications

Controlled Submolecular Translational Motion in Synthesis: A Mechanically Interlocking Auxiliary[**]

Jeffrey S. Hannam, Stephen M. Lacy, David A. Leigh,* Carlos G. Saiz, Alexandra M. Z. Slawin, and Sheila G. Stitchell

In memory of Norma A. Stoddart

As well as being prototypical design elements for various types of molecular machines,[1–5] rotaxanes (molecules in which one or more rings are held on one or more threads by bulky stoppers[6]) often dramatically change the properties of their components (including solubility,[7] fluorescence,[8] electroluminescence,[9] and membrane transport[10]) and can protect encapsulated regions of threaded substrates from chemical attack[11] and degradation.[12] Interestingly, since they are molecular compounds—not supramolecular[13] complexes (i.e., the atoms cannot be separated without breaking covalent bonds)—rotaxane architectures also, in principle, circumvent patents that only claim derivatives that branch out from a principal structure through continuous sequences of covalent bonds. Despite such attractive characteristics, practical exploitation of the property-changing and patent-breaking features of rotaxanes have been slow to develop. This is probably because most efficient strategies for rotaxane synthesis require specific recognition elements to be built into each noncovalently linked unit,[14,15] thus limiting the types of chemical structures that can be interlocked. In other words, up to now it has not been possible to make a mechanically interlocked derivative of any particular pharmaceutical, dye, chromophore, catalyst, or reagent that one might choose. Herein we describe a practical rotaxane synthesis that has the potential to be more general than previous methods because it does not depend on a strong recognition motif existing between the ultimately interlocked components. A synthetic auxiliary is used to mechanically interlock a macrocycle around a suitable template, followed by translation of the ring to a position over the desired substrate and, finally, cleavage of the auxiliary to leave a rotaxane (e.g. **1**) with no designed noncovalent interactions
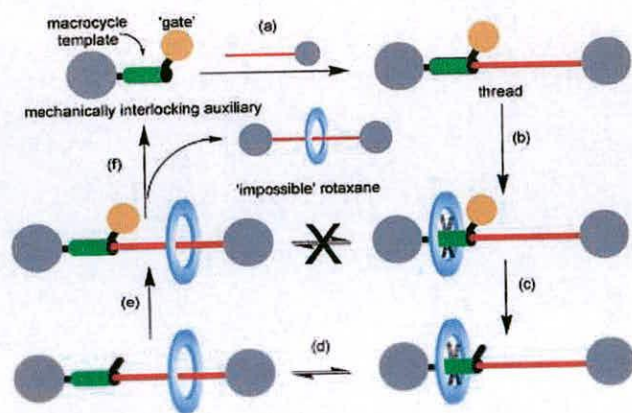
[*] J. S. Hannam, Dr. S. M. Lacy, Prof. D. A. Leigh, Dr. S. G. Stitchell
School of Chemistry
University of Edinburgh
The King's Buildings, West Mains Road, Edinburgh EH9 3JJ (UK)
Fax: (+44) 131-667-9085
E-mail: david.leigh@ed.ac.uk

Dr. C. G. Saiz, Dr. A. M. Z. Slawin
Department of Chemistry
University of St. Andrews
St Andrews, Fife KY16 9AJ (UK)

between macrocycle and thread (Scheme 1). As well as providing a synthetic route to otherwise difficult or impossible to obtain structures, a consequence of such unnatural
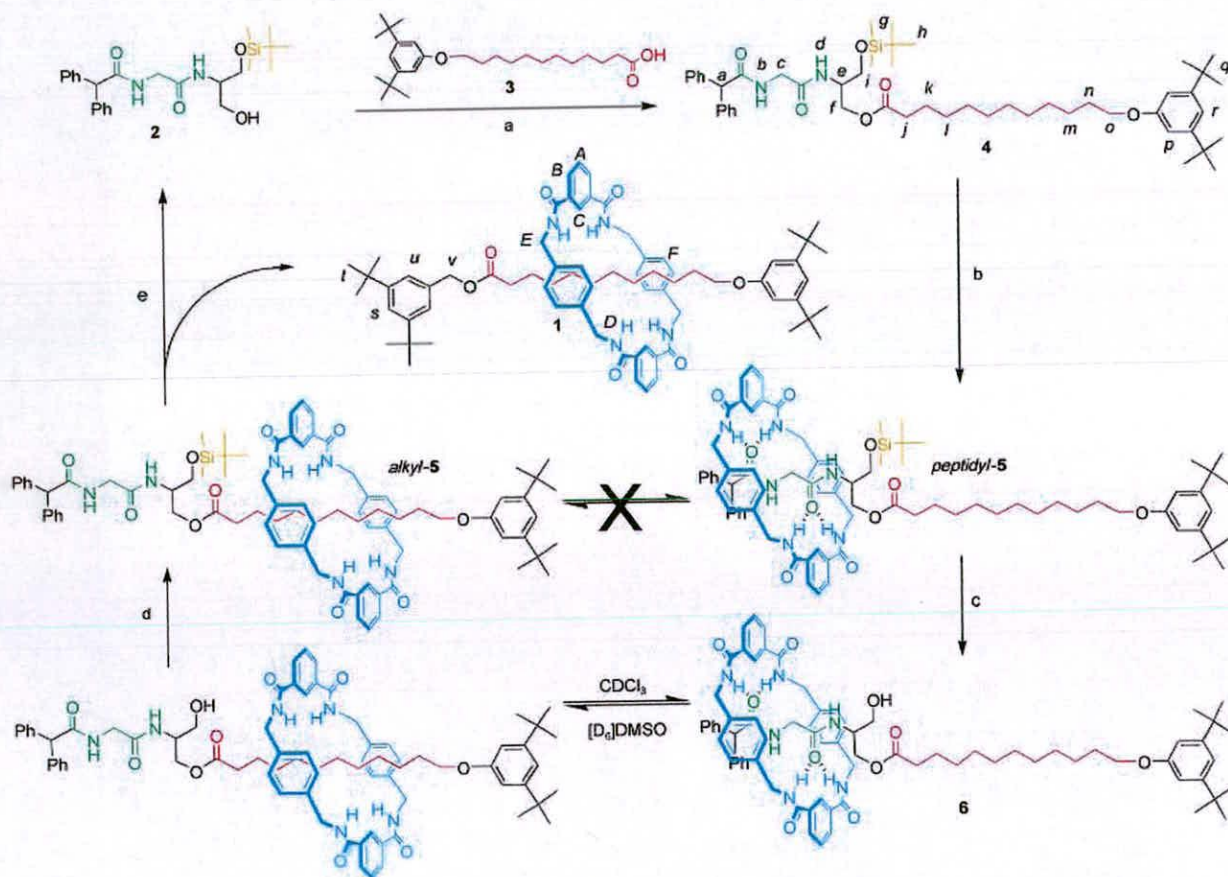
geometries upon molecular fragments is seen in the X-ray crystal structure of rotaxane **1**, which features the first example of an NH amide to *alkyl* O ester hydrogen bond.

Switching of the position of a macrocycle between nonequivalent sites in a rotaxane can be achieved by using a variety of stimuli in bistable "molecular shuttles".[1,6] In one such system, a benzylic amide macrocycle is assembled around a glycine-containing peptide template through intercomponent hydrogen bonding in nonpolar solvents.[11,16,17] The macrocycle can be subsequently decomplexed from the peptide by changing to a highly polar medium, which solvates the peptide and macrocycle hydrogen-bonding sites more strongly than they bind to each other.[18,19] We decided to investigate whether this solvent effect could be used to move the macrocycle from its template site to a desired substrate during synthesis, thus providing a means to a "mechanically interlocking auxiliary" (Scheme 2).[20]

The mechanically interlocking auxiliary, **2**, consists of an *N*-stoppered glycine residue and a monosilylated serinol derivative. The role of the serinol is twofold: the free hydroxy group provides a site for the attachment of a carboxylic acid-terminated substrate (and eventual cleavage of the auxiliary) through an ester linkage, while the bulky *tert*-butyldimethyl-silyl ether acts as a closed "gate" through which the macro-

Scheme 1. Schematic preparation of a rotaxane that is otherwise difficult or impossible to obtain by using a mechanically interlocking auxiliary. a) Attach substrate to auxiliary; b) formation of rotaxane about template; c) open gate; d) shuttle macrocycle from template to substrate; e) close gate; f) cleave auxiliary.

Scheme 2. Synthesis of rotaxane **1**. a) 1-(3-dimethylaminopropyl)-3-ethyl-carbodiimide hydrochloride, 4-dimethylaminopyridine (4-DMAP), CH$_2$Cl$_2$, 87%; b) isophthaloyl dichloride, *p*-xylylenediamine, Et$_3$N, CHCl$_3$, 25%; c) tetrabutylammonium fluoride, THF, 95%; d) *tert*-butyldimethylsilyl chloride, imidazole, 4-DMAP, DMSO, 85%; e) di-*tert*-butylbenzyl alcohol, potassium *tert*-butoxide (5 mol%), 78%. Full experimental procedures can be found in the Supporting Information.

cycle cannot pass. Coupling of **2** to the dodecanoic acid **3** gave the composite thread **4**, which was subjected to standard[16-19] hydrogen-bond-directed rotaxane-forming conditions to give the [2]rotaxane *peptidyl*-**5**.[21] Since the xylylene rings of the macrocycle shield the encapsulated region of the thread, the position of the macrocycle in the rotaxane could be unambiguously determined by comparing the nuclear magnetic resonance (NMR) chemical shifts of the thread and rotaxane protons. The ^{1}H NMR spectra in CDCl$_3$ (Figure 1a and b) and
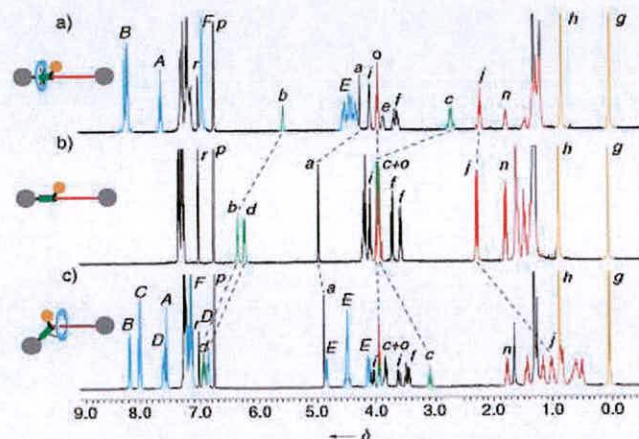

Figure 1. 400 MHz ^{1}H NMR spectra of a) *peptidyl*-**5**, b) **4**, and c) *alkyl*-**5** in CDCl$_3$ at 298 K. The color coding and lettering correspond to the assignments shown in Scheme 2.

[D$_6$]DMSO (Figure 2a and b) shows that the closed gate means the macrocycle resides solely on the peptide station in both solvents (for example, the rotaxane H$_c$ glycine protons are shielded by $\delta = -1.26$ ppm in CDCl$_3$ and by $\delta = -1.30$ ppm in [D$_6$]DMSO with respect to H$_c$ in the thread).

Cleavage of the silyl group of *peptidyl*-**5** with tetrabutylammonium fluoride afforded [2]rotaxane **6**. In **6**, the macrocycle can move through the open gate to get to either the peptide or substrate side of the thread and ^{1}H NMR spectros-
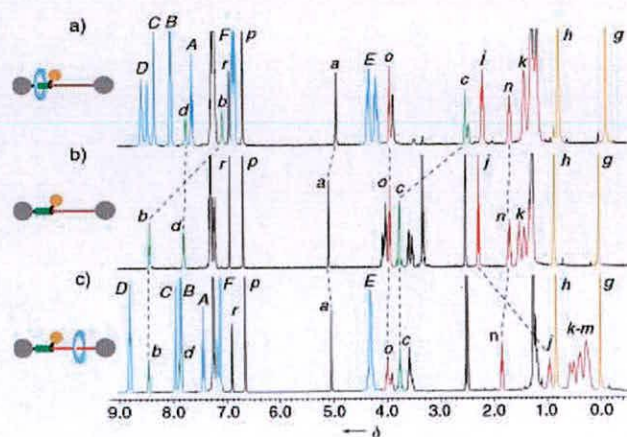

Figure 2. 400 MHz ^{1}H NMR spectra of a) *peptidyl*-**5**, b) **4**, and c) *alkyl*-**5** in [D$_6$]DMSO at 298 K.

copy confirms that its location is determined by the nature of the solvent. Accordingly, **6** was dissolved in anhydrous DMSO and the silyl ether reattached with *tert*-butyldimethylsilyl chloride.[22] A new rotaxane was isolated in 85% yield together with <2% of *peptidyl*-**5**. ^{1}H NMR spectroscopy confirms the new rotaxane to be *alkyl*-**5**, a translational diastereoisomer (identical covalent connectivity but a different spatial arrangement[23]) of *peptidyl*-**5** with the macrocycle locked on the alkyl-chain side of the closed gate, irrespective of the solvent the rotaxane is dissolved in (Figure 1c and Figure 2c).[24]

Since there are no strong binding interactions between the macrocycle and thread in *alkyl*-**5**, maintenance of the rotaxane architecture whilst cleaving the mechanically interlocking auxiliary requires a reaction that does not permit unstoppering at any stage.[25] Transesterification with di-*tert*-butylbenzyl alcohol in the presence of catalytic potassium *tert*-butoxide,[26] afforded the desired [2]rotaxane **1** in 78% yield with complete recovery of the regenerated auxiliary and no evidence of any accompanying dethreading.[27] The shielding of all the alkyl chain protons, as revealed in the ^{1}H NMR spectrum of **1** (Figure 3), indicates that the macrocycle is delocalized over the entire length of the substrate, although the greater shielding of H$_j$ indicates that it spends more time nearer the ester end of the molecule in CDCl$_3$.
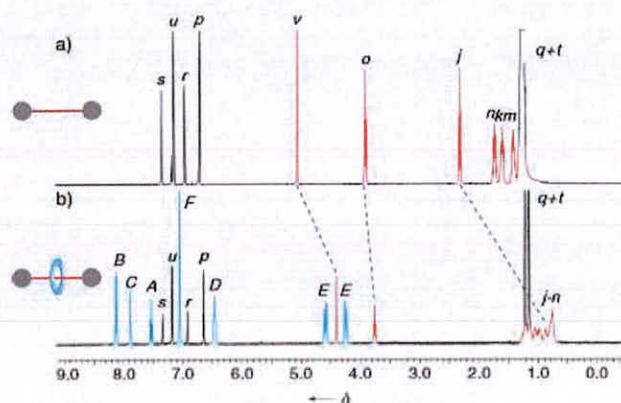

Figure 3. 400 MHz ^{1}H NMR spectra of a) thread and b) rotaxane **1** in CDCl$_3$ at 298 K.

Small single crystals of the rotaxane suitable for X-ray crystallography with a synchrotron source were obtained by slow evaporation of a solution of **1** in acetonitrile. The X-ray crystal structure (Figure 4) confirms the interlocked nature of the rotaxane and shows a remarkable consequence of forcing such unnatural spatial arrangements on submolecular fragments. Although ester groups are normally poor hydrogen-bonding groups,[28] the ester in the thread is the best acceptor available to the macrocycle amide hydrogen-bond donors. Accordingly, the rotaxane exhibits not only a rare[29] example of a solid-state hydrogen bond from the NH group of an amide to an acyl–O atom of an ester but also what appears to be a genuine hydrogen bond from the NH group of an amide to an alkyl–O atom of an ester, which is long (2.60 Å) but
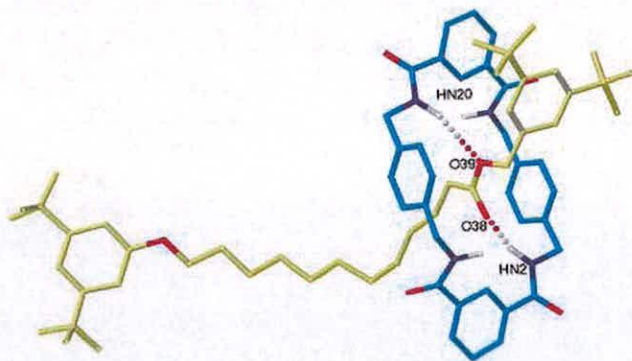
Figure 4. X-ray crystal structure of rotaxane **1**. Intramolecular hydrogen-bond lengths (Å) and angles: O38-HN2 1.89, 161.9°; O39-HN20 2.60, 162.2°. Carbon atoms of the macrocycle are shown in blue and those of the thread in yellow; oxygen atoms are red, nitrogen atoms dark blue and amide hydrogen atoms white. Non-amide hydrogen atoms are omitted for clarity. CCDC-127612 contains the supplementary crystallographic data for this paper. These data can be obtained free of charge via www.ccdc.cam.ac.uk/conts/retrieving.html (or from the Cambridge Crystallographic Data Centre, 12, Union Road, Cambridge CB21EZ, UK; fax: (+44) 1223-336-033; or deposit@ccdc.cam.ac.uk).

directional (162.2° is a typical NH⋯O hydrogen bond angle[30]) to a lone pair of an sp³-hybridized orbital of an oxygen atom, in what is presumably a very weak interaction.

In conclusion, we have synthesized rotaxane **1**, whose components bear no formal mutual recognition elements through the first example of controlled submolecular translational motion in organic synthesis. In principle, there is no reason why mechanically interlocking auxiliary strategies should not work with other molecular-shuttle systems, including those based on cyclodextrins, which already have US FDA approval for use in the pharmaceutical and food industries. In our laboratories the approach is currently being used to prepare mechanically interlocked analogues of substrates that are unavailable by conventional synthetic methods and to modify the physical and chemical properties of a range of pharmaceuticals, dyes, reagents, catalysts, and components for molecular electronics.

[1] V. Balzani, A. Credi, F. M. Raymo, J. F. Stoddart, *Angew. Chem.* **2000**, *112*, 3484–3530; *Angew. Chem. Int. Ed.* **2000**, *39*, 3348–3391.

[2] C. P. Collier, E. W. Wong, M. Bělohradský, F. M. Raymo, J. F. Stoddart, P. J. Kuekes, R. S. Williams, J. R. Heath, *Science* **1999**, *285*, 391–394.

[3] A. M. Brouwer, C. Frochot, F. G. Gatti, D. A. Leigh, L. Mottier, F. Paolucci, S. Roffia, G. W. H. Wurpel, *Science* **2001**, *291*, 2124–2128.

[4] M. C. Jiménez, C. Dietrich-Buchecker, J.-P. Sauvage, *Angew. Chem.* **2000**, *112*, 3422–3425; *Angew. Chem. Int. Ed.* **2000**, *39*, 3284–3287.

[5] P. Thordarson, E. J. A. Bijsterveld, A. E. Rowan, R. J. M. Nolte, *Nature* **2003**, *424*, 915–918.

[6] *Molecular Catenanes Rotaxanes and Knots: A Journey Through the World of Molecular Topology* (Eds.: J.-P. Sauvage, C. Dietrich-Buchecker), Wiley-VCH, Weinheim, **1999**.

[7] A. G. Johnston, D. A. Leigh, A. Murphy, J. P. Smart, M. D. Deegan, *J. Am. Chem. Soc.* **1996**, *118*, 10662–10663.

[8] S. Anderson, H. L. Anderson, *Angew. Chem.* **1996**, *108*, 2075–2078; *Angew. Chem. Int. Ed. Engl.* **1996**, *35*, 1956–1959.

[9] F. Cacialli, J. S. Wilson, J. J. Michels, C. Daniel, C. Silva, R. H. Friend, N. Severin, P. Samori, J. P. Rabe, M. J. O'Connell, P. N. Taylor, H. L. Anderson, *Nat. Mater.* **2002**, *1*, 160–164.

[10] V. Dvornikovs, B. E. House, M. Kaetzel, J. R. Dedman, D. B. Smithrud, *J. Am. Chem. Soc.* **2003**, *125*, 8290–8301.

[11] D. A. Leigh, A. Murphy, J. P. Smart, A. M. Z. Slawin, *Angew. Chem.* **1997**, *109*, 752–756; *Angew. Chem. Int. Ed. Engl.* **1997**, *36*, 728–732.

[12] M. R. Craig, M. G. Hutchings, T. D. W. Claridge, H. L. Anderson, *Angew. Chem.* **2000**, *112*, 1105–1108; *Angew. Chem. Int. Ed.* **2001**, *40*, 1071–1074.

[13] Within the context of a recent book and paper (V. Balzani, A. Credi, M. Venturi, *Chem. Eur. J.* **2002**, *8*, 5524–5532; V. Balzani, A. Credi, M. Venturi, *Molecular Devices and Machines—A Journey into the Nanoworld*, Wiley-VCH, Weinheim, **2003**) it was proposed that the term "supramolecular" be expanded from Lehn's original definition of "chemistry beyond the molecule" (i.e., assemblies of two or more molecules or ions held together by noncovalent forces) to include large molecules (e.g., dendrimers, rotaxanes, proteins etc.) which feature functional intramolecular interactions or photophysics. In our view such a revision is unwarranted. When scientific language evolves it needs to retain a precise definition to remain useful (e.g., "acid" to "Lewis acid" or "Brønsted acid"). Consider as a contrary example the term "self-assembly", which has acquired such an imprecise meaning over recent years that it now conveys virtually nothing as a descriptor. In its currently accepted definition, "supramolecular"—by analogy to the term "molecular"—refers to how the atoms in a structure are held together, not their photophysical properties. It distinguishes molecules from clusters of molecules, for example pseudorotaxanes (host–guest complexes in which the components are free to exchange between bound and unbound species) and rotaxanes (molecules in which the components cannot exchange with outside systems without breaking covalent bonds). It does not matter that their properties can be similar or that bond energies sometimes make it difficult to distinguish between molecular and supramolecular species, just as the timescale-dependent inversion of asymmetric nitrogen atoms does not confer on the term "chirality" any less clear a meaning. Language—especially scientific language—needs to be precise; subject areas, for example, "supramolecular chemistry" or "organometallic catalysis", on the other hand, should be as broad and inclusive as possible, and have always happily encompassed chemistry not technically suggested by their titles (J.-M. Lehn, *Supramolecular Chemistry: Concepts and Perspectives*, Wiley-VCH, Weinheim, **1995**, p. 90).

[14] In addition to the rotaxane-forming methods based on specific templates for metal-ion coordination, aromatic stacking and hydrogen bonding,[6] cyclodextrins (S. A. Nepogodiev, J. F. Stoddart, *Chem. Rev.* **1998**, *98*, 1959–1976), and certain cyclophanes[12] can form rotaxanes of a broad range of substrates through general hydrophobic binding. The trapping of phenolate anions by amide macrocycles can also produce rotaxanes with no recognition elements (C. Seel, F. Vögtle, *Chem. Eur. J.* **2000**, *6*, 21–24; R. Shukla, M. J. Deetz, B. D. Smith, *Chem. Commun.* **2000**, 2397–2398), but requires a specific template in the stopper and is apparently of limited generality (C. A. Schalley, G. Silva, C. F. Nising, P. Linnartz, *Helv. Chim. Acta* **2002**, *85*, 1578–1596).

[15] The earliest rotaxane syntheses produced rotaxanes without attractive interactions between the subunits but were carried out under "statistical" conditions, which only generates rotaxanes in low yields (I. T. Harrison, S. Harrison, *J. Am. Chem. Soc.* **1967**, *89*, 5723–5724). Other routes to rotaxanes without noncovalent recognition elements between macrocycle and thread have been developed based on covalent bond-directed methods (G. Schill, H. Zollenkopf, *Justus Liebigs Ann. Chem.* **1969**, *721*, 53; K. Hiratani, J.-I. Suga, Y. Nagawa, H. Houjou, H. Tokuhisa, M. Numata, K. Watanabe, *Tetrahedron Lett.* **2002**, *43*, 5747–5750).

[16] M. Asakawa, G. Brancato, M. Fanti, D. A. Leigh, T. Shimizu, A. M. Z. Slawin, J. K. Y. Wong, F. Zerbetto, S. Zhang, *J. Am. Chem. Soc.* **2002**, *124*, 2939–2950.

[17] G. Brancato, F. Coutrot, D. A. Leigh, A. Murphy, J. K. Y. Wong, F. Zerbetto, *Proc. Natl. Acad. Sci. USA* **2002**, *99*, 4967–4971.

[18] A. S. Lane, D. A. Leigh, A. Murphy, *J. Am. Chem. Soc.* **1997**, *119*, 11092–11093.

[19] T. Da Ros, D. M. Guldi, A. F. Morales, D. A. Leigh, M. Prato, R. Turco, *Org. Lett.* **2003**, *5*, 689–691.

[20] Since hydrogen bonding of the DMSO to the peptide and macrocycle provides much of the driving force for displacement of the macrocycle from the template, this switching strategy should be largely independent of the nature of the substrate.

[21] The prefix refers to the position of the macrocycle on the thread.

[22] Silyl ether protections of hydroxyl groups are routinely performed in DMF but DMSO is equally efficacious, a key requirement for the gate functionality with the chosen method of shuttling.

[23] J. O. Jeppesen, J. Perkins, J. Becher, J. F. Stoddart, *Angew. Chem.* **2001**, *113*, 1256–1261; *Angew. Chem. Int. Ed.* **2001**, *40*, 1216–1221.

[24] One (but not both) of the glycyl H_c protons of *alkyl-5* is shielded by $\delta = 1.02$ ppm in $CDCl_3$, which indicates that the macrocycle is able to hydrogen bond to the peptide despite being locked on the substrate side of the silyl ether gate.

[25] For examples of postassembly stopper-substitution reactions in rotaxanes see a) S. J. Rowan, S. J. Cantrill, J. F. Stoddart, *Org. Lett.* **1999**, *1*, 129–132; b) S. J. Rowan, J. F. Stoddart, *J. Am. Chem. Soc.* **2000**, *122*, 164–165; c) S. J. Rowan, S. J. Cantrill, J. F. Stoddart, A. J. P. White, D. J. Williams, *Org. Lett.* **2000**, *2*, 759–762; d) D. W. Zehnder, D. B. Smithrud, *Org. Lett.* **2001**, *3*, 2485–2487; e) S. H. Chiu, S. J. Rowan, S. J. Cantrill, J. F. Stoddart, A. J. P. White, D. L. Williams, *Chem. Eur. J.* **2002**, *8*, 5170–5183.

[26] M. G. Stanton, M. R. Gagné, *J. Am. Chem. Soc.* **1997**, *119*, 5075–5076.

[27] The *tert*-butyloxy group is too small to act as a stopper, but tertiary alkoxides are unreactive towards esters and so *t*BuOK provides a means of generating low concentrations of the reactive stopper primary alkoxide in situ.

[28] F. G. Gatti, D. A. Leigh, S. A. Nepogodiev, A. M. Z. Slawin, S. J. Teat, J. K. Y. Wong, *J. Am. Chem. Soc.* **2001**, *123*, 5983–5989.

[29] There are fewer than 30 examples of amide–ester hydrogen bonds in the Cambridge Crystallographic Database and all are from the NH group to the ester carbonyl oxygen atom (C. Alemán, J. J. Navas, S. Muñoz-Guerra, *J. Phys. Chem.* **1995**, *99*, 17653–17661 and ref. [28]).

[30] G. A. Jeffrey, *An Introduction to Hydrogen Bonding*, Oxford University Press, Oxford, **1997**.